

University of Warwick institutional repository: <http://go.warwick.ac.uk/wrap>

A Thesis Submitted for the Degree of PhD at the University of Warwick

<http://go.warwick.ac.uk/wrap/60739>

This thesis is made available online and is protected by original copyright.

Please scroll down to view the document itself.

Please refer to the repository record for this item for information to help you to cite it. Our policy information is available from the repository home page.

Library Declaration and Deposit Agreement

1. STUDENT DETAILS

Please complete the following:

Full name:

University ID number:

2. THESIS DEPOSIT

2.1 I understand that under my registration at the University, I am required to deposit my thesis with the University in BOTH hard copy and in digital format. The digital version should normally be saved as a single pdf file.

2.2 The hard copy will be housed in the University Library. The digital version will be deposited in the University's Institutional Repository (WRAP). Unless otherwise indicated (see 2.3 below) this will be made openly accessible on the Internet and will be supplied to the British Library to be made available online via its Electronic Theses Online Service (EThOS) service.

[At present, theses submitted for a Master's degree by Research (MA, MSc, LL.M, MS or MMedSci) are not being deposited in WRAP and not being made available via EThOS. This may change in future.]

2.3 In exceptional circumstances, the Chair of the Board of Graduate Studies may grant permission for an embargo to be placed on public access to the hard copy thesis for a limited period. It is also possible to apply separately for an embargo on the digital version. (Further information is available in the *Guide to Examinations for Higher Degrees by Research*.)

2.4 If you are depositing a thesis for a Master's degree by Research, please complete section (a) below. For all other research degrees, please complete both sections (a) and (b) below:

(a) Hard Copy

I hereby deposit a hard copy of my thesis in the University Library to be made publicly available to readers (please delete as appropriate) EITHER immediately OR after an embargo period of months/years as agreed by the Chair of the Board of Graduate Studies.

I agree that my thesis may be photocopied. YES / NO (Please delete as appropriate)

(b) Digital Copy

I hereby deposit a digital copy of my thesis to be held in WRAP and made available via EThOS.

Please choose one of the following options:

EITHER My thesis can be made publicly available online. YES / NO (Please delete as appropriate)

OR My thesis can be made publicly available only after.....[date] (Please give date)
YES / NO (Please delete as appropriate)

OR My full thesis cannot be made publicly available online but I am submitting a separately identified additional, abridged version that can be made available online.
YES / NO (Please delete as appropriate)

OR My thesis cannot be made publicly available online. YES / NO (Please delete as appropriate)

3. **GRANTING OF NON-EXCLUSIVE RIGHTS**

Whether I deposit my Work personally or through an assistant or other agent, I agree to the following:

Rights granted to the University of Warwick and the British Library and the user of the thesis through this agreement are non-exclusive. I retain all rights in the thesis in its present version or future versions. I agree that the institutional repository administrators and the British Library or their agents may, without changing content, digitise and migrate the thesis to any medium or format for the purpose of future preservation and accessibility.

4. **DECLARATIONS**

(a) I DECLARE THAT:

- I am the author and owner of the copyright in the thesis and/or I have the authority of the authors and owners of the copyright in the thesis to make this agreement. Reproduction of any part of this thesis for teaching or in academic or other forms of publication is subject to the normal limitations on the use of copyrighted materials and to the proper and full acknowledgement of its source.
- The digital version of the thesis I am supplying is the same version as the final, hard-bound copy submitted in completion of my degree, once any minor corrections have been completed.
- I have exercised reasonable care to ensure that the thesis is original, and does not to the best of my knowledge break any UK law or other Intellectual Property Right, or contain any confidential material.
- I understand that, through the medium of the Internet, files will be available to automated agents, and may be searched and copied by, for example, text mining and plagiarism detection software.

(b) IF I HAVE AGREED (in Section 2 above) TO MAKE MY THESIS PUBLICLY AVAILABLE DIGITALLY, I ALSO DECLARE THAT:

- I grant the University of Warwick and the British Library a licence to make available on the Internet the thesis in digitised format through the Institutional Repository and through the British Library via the EThOS service.
- If my thesis does include any substantial subsidiary material owned by third-party copyright holders, I have sought and obtained permission to include it in any version of my thesis available in digital format and that this permission encompasses the rights that I have granted to the University of Warwick and to the British Library.

5. **LEGAL INFRINGEMENTS**

I understand that neither the University of Warwick nor the British Library have any obligation to take legal action on behalf of myself, or other rights holders, in the event of infringement of intellectual property rights, breach of contract or of any other right, in the thesis.

Please sign this agreement and return it to the Graduate School Office when you submit your thesis.

Student's signature: Date:

**The synthesis and ring-opening
polymerisation of functionalised chiral *O*-
carboxyanhydrides and cyclic carbonates.**

by

Michael John Bennison

A thesis submitted in partial fulfilment of the requirements for the
degree of

Doctor of Philosophy in Chemistry

Department of Chemistry

University of Warwick

September 2013

Table of Contents

Table of Contents	ii
List of Figures	vii
List of Schemes	xiii
List of Tables	xvii
Abbreviations	xix
Acknowledgements	xxiii
Declaration	xxiv
Abstract	xxv
Chapter 1 Introduction to the Synthesis and Functionalisation of Poly(ester)s and Poly(carbonate)s	1
1.1 Introduction	2
1.2 Synthesis	3
1.2.1 Poly(ester)s	3
1.2.2 Poly(carbonate)s	5
1.3 Ring-Opening Polymerisation	7
1.3.1 Metal-Catalysed ROP	8
1.3.2 Organocatalysed ROP	9
1.4 Functionalisation	18
1.4.1 Poly(ester)s	19
<i>O</i> -Carboxyanhydrides	22
1.4.2 Poly(carbonate)s	25
1.5 Conclusions	31

Chapter 2 Synthesis and Ring-Opening Polymerisation of Functional <i>O</i> -Carboxyanhydride Monomers Derived from <i>L</i> -Malic Acid.....	32
2.1 Introduction.....	33
2.2 Results and Discussion	34
2.2.1 Synthesis of Functionalised <i>O</i> -Carboxyanhydrides from <i>L</i> -Malic Acid.....	34
2.2.2 Ring-opening polymerisation of (<i>S</i>)-2,2,2-trichloroethyl 2-(2,5-dioxo-1,3-dioxolan-4-yl)acetate	38
2.2.3 Ring-opening polymerisation of (<i>R</i>)-2-nitrobenzyl 2-(2,5-dioxo-1,3-dioxolan-4-yl)acetate.....	54
2.4 Conclusions and Future Work.....	66
Chapter 3 Synthesis and ring-opening polymerisation of functional chiral cyclic carbonates derived from <i>L</i> -leucine	67
3.1 Introduction.....	68
3.2 Results and Discussion	70
3.2.1 Synthesis of (<i>S</i>)-Benzyl 4-methyl-2-(5-methyl-2-oxo-1,3-dioxane-5-carboxamido)pentanoate	70
3.2.2 Ring-Opening Polymerisation of <i>O</i> -benzyl- <i>L</i> -leucine amido carbonate, BLAC	73
3.2.3 Synthesis of <i>O</i> -benzyl- <i>L</i> -leucinic ester carbonate, BLEC.....	77
3.2.4 Ring-Opening Polymerisation of <i>O</i> -benzyl- <i>L</i> -leucinic ester carbonate, BLEC - Catalyst screening.....	81
3.2.5 Ring-Opening Polymerisation of BLEC - Investigation of polymerisation control	97
3.3 Conclusions and Future Work.....	107

Chapter 4	The Synthesis, Ring-Opening Polymerisation and Post-Polymerisation Functionalisation of an Epoxide-Functional Cyclic Carbonate	109
4.1	Introduction.....	110
4.2	Results and Discussion	112
4.2.1	Synthesis of 5-Ethyl-5-((oxiran-2-ylmethoxy)methyl)-1,3-dioxan-2-one, TMOC	112
4.2.2	Ring-opening polymerisation of TMOC - Catalyst screening	114
4.2.3	Ring-opening polymerisation of TMOC - Investigation of polymerisation control	129
4.2.4	Functionalisation of P(TMOC)	136
4.2.5	Functionalisation of P(TMOC) - Preliminary condition screening.....	137
4.2.6	Functionalisation of P(TMOC) - Amine variation.....	147
4.3	Conclusions and Future Work.....	156
Chapter 5	Conclusions and Future Work.....	158
5.1	Functionalised <i>O</i> -Carboxyanhydrides from <i>L</i> -Malic Acid.....	159
5.2	Chiral Functionalised Cyclic Carbonates and Poly(carbonate)s from <i>L</i> -Leucine	160
5.3	Polymerisation of Epoxide-Functionalised Cyclic Carbonate	161
Chapter 6	Experimental	163
6.1	Materials	164
6.2	General Considerations	164
6.3	Experimental Details for Chapter 2	167
6.3.1	(<i>S</i>)-2-(2,2-Dimethyl-5-oxo-1,3-dioxolan-4-yl)acetic acid	167
6.3.2	(<i>S</i>)-2,2,2-Trichloroethyl 2-(2,2-dimethyl-5-oxo-1,3-dioxolan-4-yl)acetate.	168

6.3.3	(<i>S</i>)-2-Nitrobenzyl 2-(2,2-dimethyl-5-oxo-1,3-dioxolan-4-yl)acetate.....	169
6.3.4	(<i>S</i>)-2-Hydroxy-4-oxo-4-(2,2,2-trichloroethoxy)butanoic acid.....	171
6.3.5	(<i>S</i>)-2-Hydroxy-4-(2-nitrobenzyloxy)-4-oxobutanoic acid	171
6.3.6	Dicyclohexylammonium (<i>S</i>)-2-hydroxy-4-oxo-4-(2,2,2-trichloroethoxy) butanoate	172
6.3.7	Dicyclohexylammonium (<i>S</i>)-2-hydroxy-4-(2-nitrobenzyloxy)-4-oxobutanoate 173	173
6.3.8	(<i>S</i>)-2,2,2-Trichloroethyl 2-(2,5-dioxo-1,3-dioxolan-4-yl)acetate	175
6.3.9	(<i>S</i>)-2-Nitrobenzyl 2-(2,5-dioxo-1,3-dioxolan-4-yl)acetate	176
6.3.10	General procedure for the polymerisation of (<i>S</i>)-2,2,2-Trichloroethyl 2-(2,5- dioxo-1,3-dioxolan-4-yl)acetate.....	177
6.3.11	General procedure for the polymerisation of (<i>S</i>)-2-Nitrobenzyl 2-(2,5-dioxo- 1,3-dioxolan-4-yl)acetate	178
6.4	Experimental Details for Chapter 3	180
6.4.1	2,2,5-Trimethyl-1,3-dioxane-5-carboxylic acid.....	180
6.4.2	(<i>S</i>)-1-(Benzyloxy)-4-methyl-1-oxopentan-2-aminium 4-methylbenzene sulfonate	181
6.4.3	(<i>S</i>)-Benzyl 4-methyl-2-(2,2,5-trimethyl-1,3-dioxane-5- carboxamido)pentanoate	182
6.4.4	(<i>S</i>)-Benzyl 2-(3-hydroxy-2-(hydroxymethyl)-2-methylpropanamido)-4- methyl pentanoate	184
6.4.5	(<i>S</i>)-Benzyl 4-methyl-2-(5-methyl-2-oxo-1,3-dioxane-5- carboxamido)pentanoate	185
6.4.6	(<i>S</i>)-2-hydroxy-4-methylpentanoic acid.....	186

6.4.7	(<i>S</i>)-Benzyl 2-hydroxy-4-methylpentanoate.....	187
6.4.8	(<i>S</i>)-1-(Benzyloxy)-4-methyl-1-oxopentan-2-yl 2,2,5-trimethyl-1,3-dioxane-5-carboxylate.....	189
6.4.9	(<i>S</i>)-Benzyl 2-(3-hydroxy-2-(hydroxymethyl)-2-methylpropanoyloxy)-4-methyl pentanoate	190
6.4.10	(<i>S</i>)-1-(Benzyloxy)-4-methyl-1-oxopentan-2-yl 5-methyl-2-oxo-1,3-dioxane-5-carboxylate.....	191
6.4.11	3,9-Diphenyl-2,4,8,10-tetraoxaspiro[5.5]undecane	193
6.4.12	2,2- <i>bis</i> ((Benzyloxy)methyl)propane-1,3-diol	194
6.4.13	General procedure for the polymerisation of (<i>S</i>)-1-(Benzyloxy)-4-methyl-1-oxopentan-2-yl 5-methyl-2-oxo-1,3-dioxane-5-carboxylate ($[M]_0/[I]_0 = 20$)	195
6.5	Experimental Details for Chapter 4	197
6.5.1	5-((Allyloxy)methyl)-5-ethyl-1,3-dioxan-2-one	197
6.5.2	5-Ethyl-5-((oxiran-2-ylmethoxy)methyl)-1,3-dioxan-2-one.....	198
6.5.3	General procedure for the polymerisation of Ethyl-5-((oxiran-2-ylmethoxy)methyl)-1,3-dioxan-2-one ($[M]_0/[I]_0 = 20$)	199
6.5.5	2,4-Bis(hydroxymethyl)pentane-1,5-diol.....	201
6.5.6	1,5-Dibromo-2,4-bis(bromomethyl)pentane	202
6.5.7	(1 <i>S</i> ,5 <i>S</i>)-3,7-Dibenzyl-3,7-diazabicyclo[3.3.1]nonane.....	203
6.5.8	(<i>S</i>)-benzyl 2-amino-4-methylpentanoate.....	204
6.5.9	(<i>R</i>)-1-(benzyloxy)-4-methyl-1-oxopentan-2-aminium 4-methylbenzene sulfonate	205
6.5.10	(<i>R</i>)-benzyl 2-amino-4-methylpentanoate	206
Chapter 7 References		208

List of Figures

Figure 1.1 - Proposed modes of activation in <i>N</i> -heterocyclic carbene-catalysed ROP.....	17
Figure 1.2 - Disubstituted cyclic diesters reported by Baker <i>et al.</i>	20
Figure 1.3 - Asymmetrically substituted 1,4-dioxane-2,5-diones reported by Weck et al.....	20
Figure 2.1 - Comparison of ¹ H NMR spectra of TCEMal diol and TCEMalOCA.....	36
Figure 2.2 - Comparison of ¹ H NMR spectra of NBMal diol and NBMalOCA.....	37
Figure 2.3 - Comparison of ¹ H NMR spectra of TCEMalOCA and P(TCEMA)	38
Figure 2.4 - GPC traces of P(TCEMA) obtained using 1 equivalent of 4-(dimethylamino)pyridine, 4-methoxypyridine and pyridine.....	40
Figure 2.5 - MALDI ToF mass spectrum of P(TCEMA) obtained using 1 equivalent of 4-(dimethylamino)pyridine	41
Figure 2.6 - MALDI ToF mass spectrum of P(TCEMA) obtained using 1 equivalent of 4-methoxypyridine	44
Figure 2.7 - MALDI-ToF mass spectra of P(TCEMA) obtained using 1 equivalent of 4-methylpyridine	45
Figure 2.8 - MALDI ToF mass spectrum of P(TCEMA) obtained using 1 equivalent of pyridine	46
Figure 2.9 - GPC traces of P(TCEMA) obtained using 1,3 and 5 equivalents of 4-methoxypyridine	47
Figure 2.10 - MALDI ToF mass spectrum of P(TCEMA) obtained using 0.5 equivalents of 4-methoxypyridine	48
Figure 2.11 - MALDI ToF mass spectrum of P(TCEMA) obtained using 3 equivalents of 4-methoxypyridine	49
Figure 2.12 - MALDI ToF mass spectrum of P(TCEMA) obtained using 5 equivalents of 4-methoxypyridine	51
Figure 2.13 - GPC traces of P(TCEMA) obtained using 1 equivalent of 4-methoxypyridine with targeted degrees of polymerisation of 20, 50, 75 and 100	53

Figure 2.14 - Comparison of ¹ H NMR spectra of NBMA/OCA and P(NBMA)	54
Figure 2.15 - GPC traces of P(NBMA) obtained using 1 equivalent of 4-(dimethylamino)pyridine, 4-methoxypyridine, 4-methylpyridine and pyridine	56
Figure 2.16 - MALDI ToF mass spectrum of P(NBMA) obtained using 1 equivalent of 4-(dimethylamino)pyridine	57
Figure 2.17 - MALDI ToF mass spectrum of P(NBMA) obtained using 1 equivalent of 4-methoxypyridine	58
Figure 2.18 - MALDI ToF mass spectrum of P(NBMA) obtained using 1 equivalent of 4-methylpyridine	59
Figure 19 - MALDI ToF mass spectrum of P(NBMA) obtained using 1 equivalent of pyridine	60
Figure 2.20 - GPC traces of P(NBMA) obtained using 0.5, 1, 3 and 5 equivalents of 4-methoxypyridine	61
Figure 2.21 - MALDI ToF mass spectrum of P(NBMA) obtained using 0.5 equivalents of 4-methoxypyridine	62
Figure 2.22 - MALDI ToF mass spectrum of P(NBMA) obtained using 3 equivalents of 4-methoxypyridine	63
Figure 2.23 - MALDI ToF mass spectrum of P(NBMA) obtained using 5 equivalents of 4-methoxypyridine	63
Figure 2.24 - GPC traces of P(NBMA) obtained targeting degrees of polymerisation of 20, 50 and 75.....	65
Figure 3.1 - Cyclic carbonates functionalised with pendant sugar moieties.....	68
Figure 3.2 - Selection of reported amino- and amido-functionalised cyclic carbonates.....	69
Figure 3.3 - Comparison of ¹ H NMR spectra for amido diol and amido carbonate (BLAC)	72
Figure 3.4 - Comparison of ¹ H NMR spectra for diol and carbonate (BLEC).	80
Figure 3.5 - Comparison of ¹ H NMR spectra for BLEC and p(BLEC).....	82
Figure 3.6 - GPC traces for P(BLEC) obtained using 10 mol% DBU.....	83

Figure 3.7 - MALDI-ToF mass spectrum of P(BLEC) obtained using 10 mol% DBU at 0.25 M.....	85
Figure 3.8 - Comparison of ¹ H NMR spectra showing 4-methoxybenzyl alcohol present in the crude reaction mixture (top) and absent following acidic workup to yield pure polymer (bottom)	86
Figure 3.9 - Comparison of ¹ H NMR spectra of crude BLEC polymerisation (black) and 4-methoxybenzyl alcohol (red)	86
Figure 3.10 - GPC traces of P(BLEC) obtained using 10 mol% DBU at 2.0 M and 5 mol% DBU at 0.25 M.....	89
Figure 3.11 - MALDI-ToF mass spectrum of P(BLEC) obtained using 10 mol% DBU at 2.0 M.....	90
Figure 3.12 - MALDI-ToF mass spectrum of P(BLEC) obtained from using 5 mol% of DBU	91
Figure 3.13 - GPC traces of P(BLEC) obtained using 10 mol% DBU with 10 mol% thiourea and 10 mol% triflic acid.....	92
Figure 3.14 - MALDI ToF mass spectrum of P(BLEC) obtained using 10 mol% DBU with 10 mol% thiourea co-catalyst.....	93
Figure 3.15 - MALDI-ToF mass spectrum of P(BLEC) obtained using 10 mol% trifluoromethane sulfonic acid	95
Figure 3.16 - $[M]_0/[I]_0$ vs. M_n for P(BLEC) initiated from 4-methoxybenzyl alcohol with trendlines inclusive (—) and exclusive (—) of P(BLEC) ₂₄₃	98
Figure 3.17 - GPC traces of P(BLEC) obtained using 10 mol% DBU with targeted degrees of polymerisation of 24, 53, 98 and 243	99
Figure 3.18 - Plot of monomer conversion vs. time for P(BLEC) ₅₀	99
Figure 3.19 - Plot of Molecular weight (M_n) and dispersity (M_w/M_n , D_M) vs. monomer conversion.....	101

Figure 3.20 - P(BLEC) initiated from 1,4-butanediol with target degrees of polymerisation of 98 and 223	103
Figure 3.21 - GPC traces of P(BLEC) initiated from <i>bis</i> BMPD with targeted degrees of polymerisation of 97 and 216	106
Figure 3.22 - Proposed methodology for accessing bifunctional poly(carbonate)s bearing differing α - and ω - chain ends	108
Figure 4.1 - Comparison of ^1H NMR spectra for allyl-functionalised diol, carbonate (TMAC,) and epoxide-functionalised carbonate (TMOC)	113
Figure 4.2 - Comparison of ^1H NMR spectra for TMOC and P(TMOC)	115
Figure 4.3 - GPC traces of P(TMOC) obtained using 10 mol% DBU at 0.5 M & 1.0 M and 5 mol% DBU at 1.0 M	117
Figure 4.4 - MALDI-ToF MS spectrum of P(TMOC) ₁₀ obtained using 10 mol% DBU at 0.5 M	118
Figure 4.5 - Expansion of MALDI-ToF MS spectrum of P(TMOC) ₁₀ obtained using 10 mol% DBU at 0.5 M	119
Figure 4.6 - MALDI-ToF MS spectrum of P(TMOC) ₁₀ obtained using 10 mol% DBU at 1.0 M	120
Figure 4.7 - MALDI-ToF MS spectrum of P(TMOC) ₁₆ obtained using 5 mol% DBU at 1.0M	122
Figure 4.8 - GPC traces of P(TMOC) obtained using 10 mol% DBU / 5 mol% TU and 5 mol% DBU / 5 mol% TU at 1.0 M	123
Figure 4.9 - MALDI-ToF MS spectrum of P(TMOC) ₁₄ obtained using 10 mol% DBU and 5 mol% thiourea at 1.0 M	124
Figure 4.10 - GPC traces of P(TMOC) obtained using 5 mol% TBD at 1.0 & 0.5 M and 1 mol% at 1.0 M	126
Figure 4.11 - MALDI-ToF MS spectrum of P(TMOC) ₁₉ obtained using 1 mol% TBD at 1.0 M	128

Figure 4.12 - GPC traces of P(TMOC) initiated from 4-methoxybenzyl alcohol with target DPs of 20, 53, 72, 95 and 228.....	131
Figure 4.13 - GPC traces of P(TMOC) initiated from bisBMPD with target DPs of 46, 72, 106 and 237.....	134
Figure 4.14 - $[M]_0/[I]_0$ vs. $M_{n(\text{GPC})}$ for P(TMOC) initiated from <i>bis</i> BMPD with trendlines inclusive (—) and exclusive (—) of P(TMOC) ₁₁₇	135
Figure 4.15 - GPC traces of P(TMOC) ₂₀ and P(TMOC) ₆₄	137
Figure 4.16 - ¹ H NMR spectra of crude functionalisation test mixtures. Highlighted signals show residual epoxide and ethyl chain, with the ratio used to calculate conversion	140
Figure 4.17 - GPC traces of functionalisation tests on P(TMOC) ₂₀ using 3 & 5 equivalents of benzylamine with 20 mol% LiBr in acetonitrile at room temperature.....	142
Figure 4.18 - GPC traces of functionalisation tests on P(TMOC) ₂₀ using 1, 3 & 5 equivalents of benzylamine with 50 mol% Ca(OTf) ₂ in acetonitrile at room temperature.....	143
Figure 4.19 - Expansion of ¹ H NMR spectra for thermal addition of benzylamine to P(TMOC) ₂₀	144
Figure 4.20 - GPC traces of functionalisation tests on P(TMOC) ₂₀ using 3 & 5 equivalents of benzylamine in acetonitrile at 85 °C.....	146
Figure 4.21 - Amines used in functionalisation tests of P(TMOC) ₂₀ and P(TMOC) ₆₄	147
Figure 4.22 - GPC traces for the attempted functionalisations of P(TMOC) ₂₀	149
Figure 4.23 - GPC traces for the attempted functionalisations of P(TMOC) ₆₄	151
Figure 4.24 - GPC traces for the attempted addition of <i>O</i> -benzyl leucines to P(TMOC) ₂₀ and P(TMOC) ₆₄	153
Figure 4.25 - Tentative ¹ H NMR spectral assignments of P(TMOC) ₆₄ functionalised with <i>O</i> -benzyl leucine	154
Figure 5.1 - Proposed chiral methylation of l-malic acid to eliminate autoinitiation of functionalised MalOCAs	159

Figure 5.2 - Proposed methodology for accessing bifunctional poly(carbonate)s bearing differing α - and ω - chain ends 161

Figure 5.3 Proposed asymmetric epoxidation allows for expansion of functionalisation methodology whilst retaining chiral nature of the polymer. 162

List of Schemes

Scheme 1.1 – Poly(ester) formation <i>via</i> polycondensation reactions	3
Scheme 1.2 - Poly(ester) formation <i>via</i> ring-opening polymerisation of cyclic esters	4
Scheme 1.3 - Poly(carbonate) formation <i>via</i> polycondensation reaction.....	5
Scheme 1.4 - Industrial synthesis of LEXAN® from bis-phenol A and phosgene.....	5
Scheme 1.5 - Copolymerisation of carbon dioxide with epoxides and oxetanes	6
Scheme 1.6 - Poly(carbonate) formation <i>via</i> ring-opening polymerisation (ROP) of cyclic carbonates	7
Scheme 1.7 - Proposed mechanism for metal-catalysed anionic ring-opening polymerisation	8
Scheme 1.8 - Proposed metal-catalysed co-ordination/insertion ROP mechanism	9
Scheme 1.9 - DMAP-catalysed ROP of lactide	10
Scheme 1.10 - Proposed mechanism for the ROP of cyclic esters with DMAP	11
Scheme 1.11 - Nitrogen-containing bicyclic catalysts for the ROP of lactide.....	12
Scheme 1.12 - Comparison of mechanisms for the ROP of cyclic esters and carbonates using TBD or DBU/MTBD	13
Scheme 1.13 - ROP of cyclic esters with DBU/thiourea co-catalysts	13
Scheme 1.14 - ROP of cyclic diesters with thiourea-tertiary amine catalyst.....	14
Scheme 1.15 - ROP of cyclic carbonates with thiourea/(-)-sparteine co-catalysts	14
Scheme 1.16 - Cationic ROP of lactide	15
Scheme 1.17 - <i>N</i> -Heterocyclic carbene-catalysed ROP of cyclic esters and carbonates	16
Scheme 1.18 - Route to disubstituted cyclic diesters utilised by Baker et al.....	19
Scheme 1.19 - Enantiomerically pure bifunctional monomers by Hillmyer and Jing	21
Scheme 1.20 - Comparative ROP of lactide XIII and L-lacOCA XIV using neo-pentanol and DMAP	22
Scheme 1.21 - Proposed Mechanisms for ROP of OCAs.....	23

Scheme 1.22 - Bourissou and co-workers' synthesis of BnzGluOCA XVI	24
Scheme 1.23 - ROP of novel OCA XVII with hydroxyl-containing frug XVIII.....	25
Scheme 1.24 - Cyclic carbonates formed from pentaerythritol XIX	26
Scheme 1.25 - First known report of cyclic carbonates formed from <i>bis</i> MPA	26
Scheme 1.26 Synthesis of cyclic carbonates via a common intermediate as reported by Hedrick <i>et al.</i>	27
Scheme 1.27 - Synthesis of cyclic carbonates via an activated pentafluorophenyl ester XXI reported by Hedrick <i>et al.</i>	28
Scheme 1.28 - Synthesis of a styrene-functionalised cyclic carbonate XXIII from trimethylolpropane XXII	29
Scheme 1.29 - Synthesis of novel cyclic carbonates XXV from amino-1,3-propane diols XXIV reported by Hedrick, Yang and co-workers	30
Scheme 2.1 - Synthesis of BnMalOCA	33
Scheme 2.2 - Synthesis of O-Carboxyanhydrides from L-Malic Acid.....	35
Scheme 2.3 - Ring-opening polymerisation of TCeMalOCA with substituted pyridine catalysts.....	39
Scheme 2.4 - Desired base-catalysed ring-opening polymerisation mechanism of TCeMalOCA	42
Scheme 2.5 - Activated monomer mechanism of autoinitiated ring-opening polymerisation of O-carboxyanhydrides.....	43
Scheme 2.6 - Ring-opening of O-carboxyanhydrides at the alternative carbonyl leads to carboxylate terminated polymer species	50
Scheme 2.7 - Ring-opening polymerisation of NBMalOCA from 4-methoxybenzyl alcohol with substituted pyridine catalysts	55
Scheme 2.8 - Proposed chiral methylation of l-malic acid to eliminate autoinitiation of functionalised MalOCAs	66

Scheme 3.1 - Synthesis of cyclic carbonates derived from <i>L</i> -serine and <i>L</i> -threonine as reported by Endo and co-workers	69
Scheme 3.2 – Synthesis of <i>O</i> -benzyl- <i>L</i> -leucine carbonate (BLAC).....	71
Scheme 3.3 - "Free" diol species and hydrogen-bond stabilised bicyclic diol species	72
Scheme 3.4 - Attempted polymerisation of BLAC with a selection of organocatalysts.....	74
Scheme 3.5 - Synthesis of benzyl bispidine.....	75
Scheme 3.6 - Hydrogen bonding between the amide proton and hydroxyl lone-pair, preventing further propagation of the polymer chain	77
Scheme 3.7 - Synthesis of <i>O</i> -benzyl- <i>L</i> -leucinic ester carbonate, BLEC.....	78
Scheme 3.8 - Diazotisation of amines and α -amino acids	79
Scheme 3.9 - General ring-opening polymerisation of BLEC and catalysts employed in the condition screening	81
Scheme 3.10 - Initiation of BLEC from water with the loss of carbon dioxide leading to formal initiation from the corresponding diol.....	84
Scheme 3.11 - Proposed mechanism for the cleavage of 4-methoxybenzylic end-group to give 4-methoxytoluene and hydroxyl-terminated telechelic P(BLEC).....	88
Scheme 3.12 - Intended activated monomer mechanism for the cationic ring-opening polymerisation of cyclic carbonates.....	95
Scheme 3.13 - Synthesis of telechelic poly(carbonate) <i>via</i> joint activated chain-end and activated monomer mechanisms	96
Scheme 3.14 - Synthesis of P(BLEC) initiating from 1,4-butanediol.....	102
Scheme 3.15 - Synthesis of <i>bis</i> BMPD from pentaerythritol.....	104
Scheme 3.16 - Synthesis of P(BLEC) initiated from <i>bis</i> BMPD using 10 mol% DBU.....	105
Scheme 4.1 - Möller and co-workers use of TMOOC in the synthesis of poly(urethanes) and the proposed use of TMOOC in this work to access amino-functional poly(carbonates)	110
Scheme 4.2 - Synthesis of TMOOC	112

Scheme 4.3 - Catalysts employed in the screening of ring-opening polymerisation conditions for TMOC	114
Scheme 4.4 - TBD-catalysed initiation of TMOC from residual water to yield telechelic P(TMOC)	132
Scheme 4.5 - Homopolymerisation of TMOC from <i>bis</i> BMPD using 1 mol% TBD	133
Scheme 4.6 - Test functionalisation of P(TMOC) ₂₀ with benzylamine	138
Scheme 4.7 - Crosslinking of P(TMOC) through epoxide ring-opening by benzyl- primary and secondary amines	141
Scheme 4.8 - Aminolysis of P(TMOC) by benzylamine	145
Scheme 4.9 - Amine screening for addition to P(TMOC) ₂₀ and P(TMOC) ₆₄	147
Scheme 4.10 - Functionalisation of P(TMOC) with O-Benzyl Leucine	152
Scheme 4.11 - Asymmetric epoxidation allows for expansion of functionalisation methodology whilst retaining chiral nature of the polymer.	157

List of Tables

Table 2.1 - Catalyst screening for the polymerisation of TCEMalOCA ($[M]_0/[I]_0 = 20$).....	39
Table 2.2 - Catalyst equivalent screening for the polymerisation of TCEMalOCA ($[M]_0/[I]_0 = 20$).....	47
Table 2.3 - Attempted variation of molecular weight for the polymerisation of TCEMalOCA	52
Table 2.4 - Catalyst screening for the polymerisation of NBMalOCA ($[M]_0/[I]_0 = 20$).....	55
Table 2.5 - Catalyst equivalent screening for the polymerisation of NBMalOCA ($[M]_0/[I]_0 = 20$)	61
Table 2.6 - Attempted variation of molecular weight for the polymerisation of NBMalOCA	64
Table 3.1 - Catalyst screening for the attempted polymerisation of BLAC.....	74
Table 3.2 - Catalyst screening for polymerisation of BLEC.....	82
Table 3.3 - Polymerisation of BLEC initiated from 4-methoxybenzyl alcohol using 10mol% DBU	97
Table 3.4 - Polymerisation of BLEC targeting DP50 and analysed at certain conversions.	100
Table 3.5 - Higher molecular weight P(BLEC) initiated from 1,4-butanediol	102
Table 3.6 - Higher molecular weight P(BLEC) initiated from <i>bis</i> BMPD	104
Table 4.1 - Catalyst screening for polymerisation of TMOC ($[M]_0/[I]_0 = 20$).....	116
Table 4.2 - Polymerisation of TMOC initiating from 4-methoxybenzyl alcohol using 1 mol% TBD	130
Table 4.3 - Polymerisation of TMOC initiating from <i>bis</i> BMPD using 1 mol% TBD.....	133
Table 4.4 - Gram-scale synthesis of P(TMOC) initiating from <i>bis</i> BMPD using 1 mol% TBD	136
Table 4.5 - Catalyst screen for benzylamine addition to P(TMOC) ₂₀	139
Table 4.6 - Reanalysis of P(TMOC) ₁₀ and P(TMOC) ₆₄	141

Table 4.7 - Functionalisation of P(TMOC) ₂₀ with various amines	148
Table 4.8 - Functionalisation of P(TMOC) ₆₄ with various amines	150
Table 4.9 - Functionalisation of P(TMOC) ₂₀ and P(TMOC) ₆₄ with <i>O</i> -benzyl leucine at elevated temperature	152

Abbreviations

1,4-BD	1,4-Butanediol
<i>bis</i> BMPD	2,2- <i>bis</i> ((Benzyloxy)methyl)propane-1,3-diol
<i>bis</i> MPA	2,2- <i>bis</i> -(hydroxymethyl)propionic acid
BLAC	<i>O</i> -benzyl- <i>L</i> -leucine amido carbonate
BLEC	<i>O</i> -benzyl- <i>L</i> -leucinic ester carbonate
Bn	Benzyl
Boc	<i>tert</i> -Butoxycarbonyl
Calc.	Calculated
Cat	Catalyst
COSY	Correlation spectroscopy
d	Doublet
DBU	1,8-Diazabicyclo[5.4.0]undec-7-ene
DCC	<i>N,N'</i> -Dicyclohexylcarbodiimide
DCHA	Dicyclohexylamine
DCM	Dichloromethane
DIBAL	Diisobutylaluminium hydride
DIPEA	<i>N,N'</i> -Diisopropylethylamine
\bar{D}_M	Dispersity

DMAP	4-Dimethylaminopyridine
DMF	<i>N,N</i> -Dimethylformamide
DMSO	Dimethylsulfoxide
DP	Degree of polymerisation
EDAC	<i>N</i> -(3-Dimethylaminopropyl)- <i>N'</i> -ethylcarbodiimide hydrochloride
eq.	Equivalent(s)
ESI MS	Electrospray ionisation mass spectrometry
EtOAc	Ethyl acetate
FT-IR	Fourier transform infrared
GPC	Gel permeation chromatography
HMBC	Heteronuclear multiple-bond correlation spectroscopy
HMQC	Heteronuclear multiple-quantum correlation spectroscopy
HRMS	High resolution mass spectrometry
<i>i</i> Bu	iso-butyl
IR	Infra-red
L-Ser	L-Serine
L-Thr	L-Threonine
m	Multiplet
MALDI-ToF MS	Matrix-assisted laser desorption and ionisation time-of-flight mass spectrometry

<i>m</i> CPBA	<i>m</i> -Chloroperoxybenzoic acid
MHz	Megahertz
M_n	Number-averaged molecular weight
MTBD	7-Methyl-1,5,7-triazabicyclo[4.4.0]dec-5-ene
M_w	Weight-averaged molecular weight
<i>m/z</i>	Mass to charge ratio
NHC	<i>N</i> -Heterocyclic carbene
NMR	Nuclear magnetic resonance
Obs.	Observed
OCA	<i>O</i> -Carboxyanhydride
Opt.	Optional
<i>p</i> TSA	<i>para</i> -Toluenesulfonic acid
PDI	Polydispersity index
PGA	Poly(glycidyl acrylate)
PGMA	Poly(glycidyl methacrylate)
PMMA	Poly(methyl methacrylate)
ppm	Parts per million
PPY	4-Pyrrolidinopyridine
q	Quartet

R _f	Retention factor
ROMP	Ring-opening metathesis polymerisation
ROP	Ring-opening polymerisation
RT	Room temperature
s	Singlet
t	Triplet
TBD	1,5,7-Triazabicyclo[4.4.0]dec-5-ene
<i>t</i> Bu	<i>tert</i> -Butyl
THF	Tetrahydrofuran
TLC	Thin layer chromatography
TMAC	5-((Allyloxy)methyl)-5-ethyl-1,3-dioxan-2-one
TMOC	5-Ethyl-5-(oxiran-2-ylmethoxyl)methyl-1,3-dioxane-2-one
TU	1-(3,5- <i>bis</i> (Trifluoromethyl)phenyl)-3-cyclohexylthiourea
UV	Ultraviolet

Acknowledgements

Firstly, I would like to thank Dr Andrew Dove for allowing me the opportunity to conduct the research presented in this thesis, for his help and advice throughout the last four years as well as having put up with me for that long. Thanks also to the EPSRC for providing the funding for this research.

Immense thanks to all members of the Dove group, past and present, particularly Sarah, Richard, Robin, Danny and Vinh, all of whom I've loved having around to annoy me and be annoyed by me in equal measures.

Finally my biggest thanks go to my loving fiancé Becky, you've put up with so much from me over the years, without you I couldn't have gotten through this rollercoaster of a PhD.

Declaration

Experimental work contained in this thesis is original research carried out by the author, unless otherwise stated, in the Department of Chemistry at the University of Warwick, between October 2009 and September 2013. No material contained herein has been submitted for any other degree, or at any other institution.

Results from other authors are referenced in the usual manner throughout the text.

_____ **Date:** _____

Michael John Bennison

Abstract

This thesis presents the synthesis of two novel O-carboxyanhydrides derived from *L*-malic acid bearing 2,2,2-trichloroethyl- and 2-nitrobenzyl esters, followed by investigation of their ring-opening polymerisation to furnish chiral, functionalised poly(malic acid)s.

A further report is made of the synthesis of two novel chiral cyclic carbonates bearing leucine derivatives coupled with amide and ester linkages, the ring-opening polymerisation is investigated and leads to the controlled synthesis of dihydroxyl telechelic poly(carbonate)s with inherent chirality.

Finally, the synthesis of a cyclic carbonate bearing pendant glycidyl ether functionality is reported, followed by investigation of the homopolymerisation to yield a poly(carbonate) bearing pendant epoxide functionality, the first known report for a degradable polymer. The post-polymerisation functionalisation of this homopolymer by the addition of amines is investigated to allow a variety of functional groups to be incorporated.

Chapter 1

Introduction to the Synthesis and Functionalisation of Poly(ester)s and
Poly(carbonate)s

1.1 Introduction

Poly(ester)s and poly(carbonate)s possess many desirable and useful properties and have found numerous applications based upon both their ability to degrade under physiological conditions and the biologically-compatible nature of the products of such degradation. Due to the advantages offered by such biodegradation and biocompatibility, these applications encompass a large number of products which range from environmentally-friendly packaging materials to surgical applications or as potential vehicles for drug delivery.¹⁻⁴

This thesis discusses the synthesis and polymerisation of novel cyclic monomers, both cyclic anhydrides and cyclic carbonates, in an attempt to provide chiral homopolymers which allow for the incorporation of a desired functionality into the resulting material. The strategy adopted was two-fold: the first involving the synthesis and polymerisation of novel chiral monomers with the inclusion of a functional handle already incorporated. The second approach involved the synthesis and polymerisation of an achiral cyclic carbonate in which the incorporated functionality allows for the obtained material to in itself act as a potential substrate for a wide selection of post-polymerisation transformations, including the introduction of chirality at this stage. Both approaches were envisioned to provide novel cyclic monomers which could undergo ring-opening polymerisation, and further functionalisation if required, to obtain chiral poly(ester)s and poly(carbonate)s not previously investigated in the literature.

This introduction gives an overview of the synthesis and incorporation of functionality for both poly(ester)s and poly(carbonate)s, with an emphasis on synthesis *via* ring-opening polymerisation.

1.2 Synthesis

1.2.1 Poly(ester)s

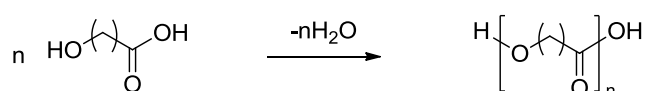
Poly(ester)s may be synthesised by a number of methods, these may be generally summarised as either polycondensation or ring-opening polymerisation (ROP) methodologies.

Polycondensation reactions have been employed in poly(ester) production for over 150 years, with Lourenco reporting the synthesis of Poly(butylene succinate) in 1863.⁵ However it wasn't until the early 20th century that poly(ester)s were thoroughly investigated, most prominently by Carothers.^{6,7} Polycondensation reactions utilise either a diacid and diol (Method A, Scheme 1.1) or a single molecule containing both acid and alcohol functionalities (Method B, Scheme 1.1). It should be noted that for polymerisations relying on the reaction between a diacid and a diol (Method A) the stoichiometry of the two reagents must be very carefully controlled as an imbalance in one of the reagents will lead to early termination of the reaction and the formation of only oligomeric material. This reliance on perfect stoichiometry may be overcome by the incorporation of both alcohol and acid on the same monomer.

Method A:



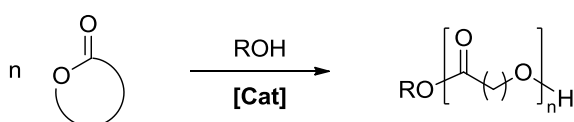
Method B:



Scheme 1.1 – Poly(ester) formation *via* polycondensation reactions

Upon heating, the reaction proceeds *via* step-growth kinetics, leading to an exponential increase in molecular weight with increasing conversion. However, the resulting polymers are very poorly controlled, generally possessing broad dispersities. The final, major problematic requirement for employing this method is that monomers require arduous purification to allow the reaction to reach the high conversions required for obtaining polymeric material of significantly high molecular weight.

Ring-opening polymerisation (ROP) however, offers a controlled alternative route to poly(ester)s, typically from cyclic esters, such as lactones or diesters, including glycolide and lactide, (Scheme 1.2) with the reaction proceeding through controlled polymerisation kinetics leading to a linear increase in the molecular weight with conversion. This, coupled with high end-group fidelity and direct control of molecular weight, based on the ratio of monomer to initiator in the starting reaction mixture, leads to ROP being regarded as a living polymerisation system. Overall this means that by varying the monomer to initiator ratio of the reaction, the resulting molecular weight may be very tightly controlled and the living nature of ROP also means that the resulting poly(ester)s possess narrow polydispersities, giving rise to well-defined properties in the bulk material.



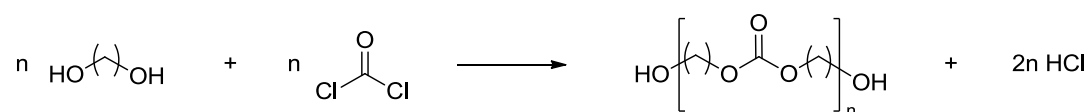
Scheme 1.2 - Poly(ester) formation *via* ring-opening polymerisation of cyclic esters

Ring-opening polymerisation in the formation of poly(ester)s can be catalysed by a range of catalysts which may be split into the following categories: simple metal alkoxides,⁸⁻¹² metal-ligand species,¹³⁻²⁰ and more recently, organocatalysts,²¹⁻²⁵ which have received greatly increased interest over the last several years. These catalytic systems and their use in the formation of poly(ester)s *via* ROP will be discussed later in this chapter (Section 1.3).

1.2.2 Poly(carbonate)s

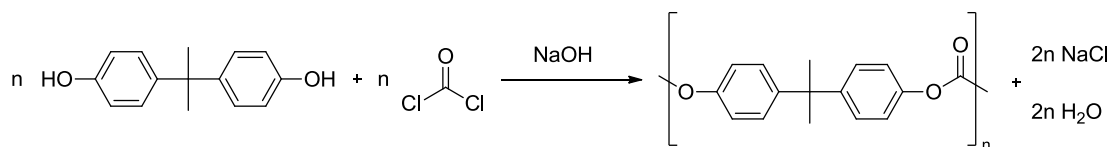
There are three significant methods for the synthesis of poly(carbonate)s; polycondensation,²⁶ the copolymerisation of carbon dioxide with either epoxides or oxetanes and the ring-opening polymerisation of cyclic carbonates.

The polycondensation reaction for the formation of poly(carbonate)s uses phosgene (or an equivalent) and a diol (Scheme 1.3).



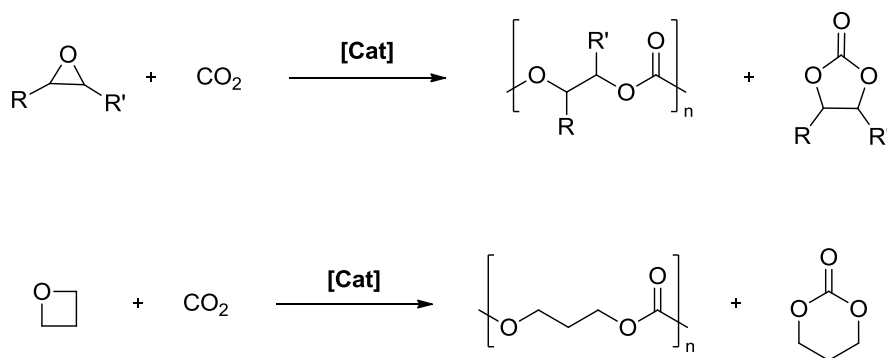
Scheme 1.3 - Poly(carbonate) formation via polycondensation reaction

As with all polycondensation reactions, the process proceeds *via* step-growth kinetics and as such suffers from the same limitations as the formation of poly(ester)s, with the use of hazardous reagents adding a particularly unfavourable drawback. However, despite the apparent disadvantages, it still remains a commercially successful, and widely applied, technique for obtaining low-cost, high volume poly(carbonate)s. A significant example of this is the production of LEXAN[®], resulting from the reaction of *bis*-phenol A and phosgene in the presence of sodium hydroxide (Scheme 1.4).²⁷



Scheme 1.4 - Industrial synthesis of LEXAN[®] from bis-phenol A and phosgene

An alternative method in the synthesis of poly(carbonate)s is the copolymerisation of carbon dioxide with both epoxides and oxetanes (Scheme 1.5). The copolymerisation of carbon dioxide and an epoxide was first reported in 1969 by Inoue *et al.*²⁸ but has since seen continuous development, with a range of catalysts being utilised (typically metal catalysts based on zinc, chromium or cobalt and using salen-type ligands) and continues to receive interest from the research community, as recently reviewed by Williams and co-workers.²⁹ This interest has recently been driven by the pressure to find a commercially viable application for carbon dioxide, making the production of poly(carbonate)s by this methodology environmentally relevant.

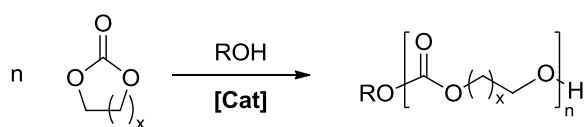


Scheme 1.5 - Copolymerisation of carbon dioxide with epoxides and oxetanes

This copolymerisation strategy has also been applied to oxetanes to synthesise an analogous series of poly(carbonate)s as to those obtained when utilising an epoxide.³⁰ However, this reaction has not received the same amount of attention, with the first report in 1977 by Koinuma *et al.* utilising triethylaluminium, water and acetylacetone as the catalyst system³¹ and Matsuda *et al.* later successfully reporting the use of Bu₃SnI and PBU₃ as an alternative catalyst system.³² It is likely that the synthesis of poly(carbonate)s *via* the copolymerisation of CO₂ has seen greater popularity using epoxides over oxetanes, mainly due to their wider availability. It is also worth noting that, typically, the copolymerisation strategy of carbon

dioxide and cyclic ethers produces a mixture of both the poly(carbonate) and the corresponding cyclic carbonate.

Finally, the ring-opening polymerisation of cyclic carbonates may be conducted in a similar manner to that used in the formation of poly(ester)s, offering all the benefits of control and high-end group fidelity as previously discussed (Scheme 1.6), whilst avoiding the inherent difficulties associated with step-growth polycondensation and the formation of a mixture of products as well as the often high pressures required with the copolymerisation method.



Scheme 1.6 - Poly(carbonate) formation via ring-opening polymerisation (ROP) of cyclic carbonates

The ROP of cyclic carbonates in the formation of poly(carbonate)s can be catalysed in a similar manner to the cyclic esters using related catalysts, which is described in the next section.

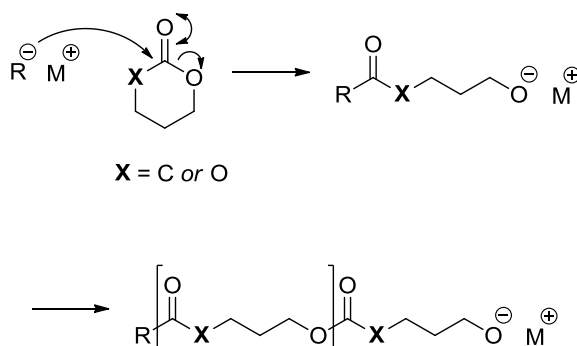
1.3 Ring-Opening Polymerisation

The ring-opening polymerisation of both cyclic esters and cyclic carbonates can be catalysed a number of ways with a range of catalysts which can be split into the following categories: simple metal alkoxides, metal-ligand species and more recently, organocatalysts, which have received increased interest in recent years.

1.3.1 Metal-Catalysed ROP

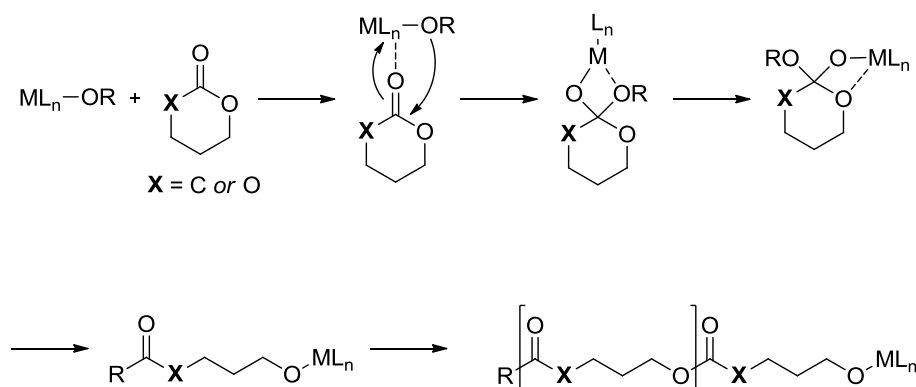
A large selection of catalyst-initiator systems have been developed for use in the ROP of cyclic esters and cyclic carbonates with the majority of these systems having been based on the use of a metal species, the first of which were simple metal alkoxides⁸⁻¹⁰ or alkyl-alkali metal complexes.^{11,12} A wide range of catalyst-initiator systems have also been reported consisting of main group,^{13-15,33} transition^{16,18,34} or rare earth^{19,20} metal alkoxides and a variety of ligands.

These metal-catalysed ROPs can proceed by one of two mechanisms, with the alkali and earth-alkali alkoxides proceeding *via* an anionic polymerisation mechanism in which the anion attacks the ester (or carbonate) carbonyl, leading to the subsequent ring-opening and formation of a new alkoxide end group which goes on to propagate in the same manner (Scheme 1.7).



Scheme 1.7 - Proposed mechanism for metal-catalysed anionic ring-opening polymerisation

Alternatively, for rare-earth and transition metal catalyst-initiator systems, a co-ordination-insertion mechanism occurs, in which initial co-ordination of the carbonyl oxygen to the catalyst's metal centre is followed by attack of the alkoxide upon the carbonyl bond, cleaving the acyl oxygen bond and leading to ring-opening of the monomer, resulting in a chain-extended alkoxide (Scheme 1.8).



Scheme 1.8 - Proposed metal-catalysed co-ordination/insertion ROP mechanism

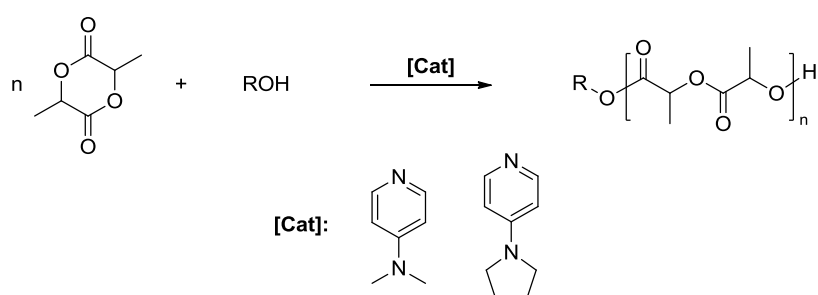
Whilst there has been a considerable amount of research conducted on the metal-catalysed ROP of cyclic esters and carbonates, with many highly effective and efficient metal-based catalyst-initiator systems being reported, it can often be difficult to fully remove the metal species during the purification of the resulting polymers. With the development of both poly(ester)s and poly(carbonate)s for use in metal-sensitive fields such as biomedical or microelectronics applications being highly desirable, this problem of removing any residual metal-catalyst can be problematic as it renders them unusable for such applications.

1.3.2 Organocatalysed ROP

In an attempt to counter this contamination and enable the use of poly(ester)s and poly(carbonate)s in these sensitive applications, there has been a significant amount of increased interest in the development of metal-free organocatalysed systems for ROPs. Such systems allow for the fine control of polymer properties made possible by ROP (i.e. molecular weight, narrow polydispersity and end group fidelity) without the subsequent problematic, and expensive, removal of metal contaminants which would disrupt the use of poly(ester)s and poly(carbonate)s for such applications.

A range of metal-free systems have been investigated and developed for the synthesis of poly(ester)s and poly(carbonate)s by ROP including simple organic nucleophiles, “superbases”, bifunctional catalyst systems, acids in cationic ROP, *N*-heterocyclic carbenes and enzymatic catalysis.

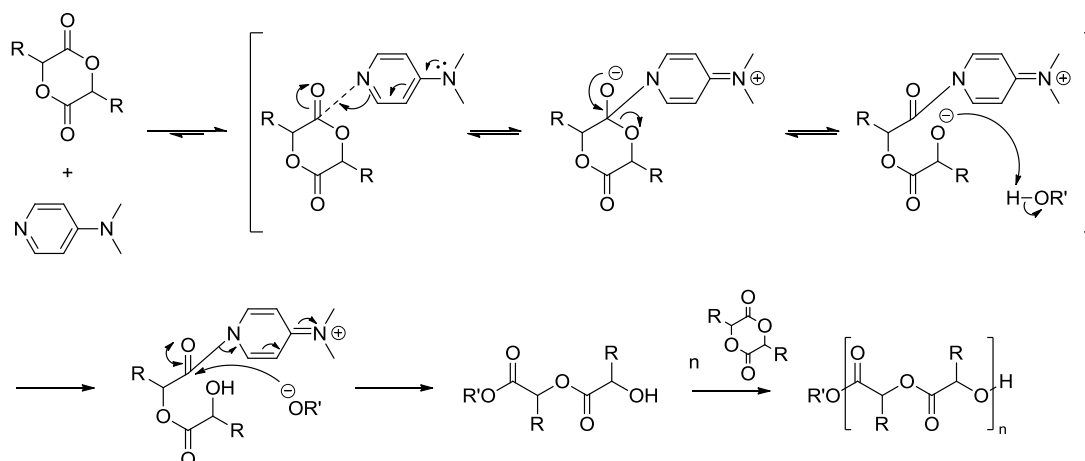
Simple organic nucleophiles have been demonstrated to be particularly effective as catalysts with a number of such molecules having been investigated, including a selection of phosphines and pyridines.^{35,36} Amongst the systems investigated, both 4-pyrrolidinopyridine (PPY) and 4-(dimethylamino)pyridine (DMAP) have shown considerable activity and control in the ROP of cyclic esters, with the first report in 2001 by Hedrik *et al.*, who demonstrated the ability of DMAP to act as a transesterification catalyst in the ROP of lactide with alcohol nucleophiles as the actual initiator (Scheme 1.9).³⁷ It is interesting to note that DMAP, in the presence of excess alcohol, has been shown to actively catalyse the depolymerisation of poly(lactic acid) in a highly efficient manner.³⁸ The methodology was later applied to cyclic carbonates, with Endo *et al.* reporting that the ROP of trimethylene carbonate and 2,2-dimethyltrimethylene carbonate could also be conducted in the presence of a nucleophilic base, in 2006.^{39,40}



Scheme 1.9 - DMAP-catalysed ROP of lactide

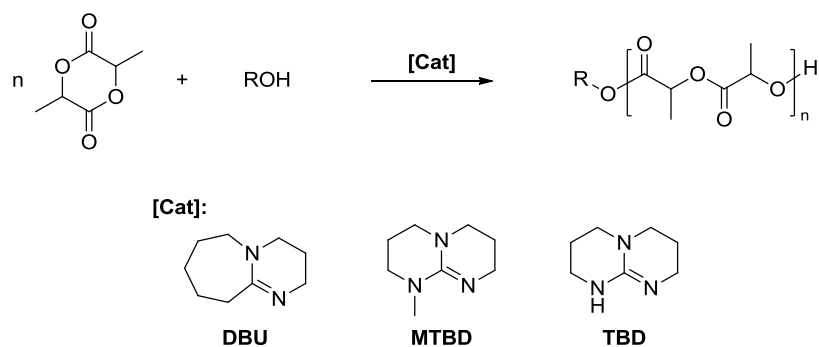
The proposed mechanism for a pyridine-based organocatalyst in ROP, such as DMAP, is thought to proceed *via* a monomer-activated mechanism (Scheme 1.10).^{37,41} First,

nucleophilic attack by DMAP on the diester leads to formation of a zwitterion, which after deprotonation of the initiating or propagating alcohol and subsequent alkoxide displacement, regenerates DMAP and yields the hydroxyl-terminated ring-opened monomer which goes onto propagate further, forming poly(ester)s.



Scheme 1.10 - Proposed mechanism for the ROP of cyclic esters with DMAP

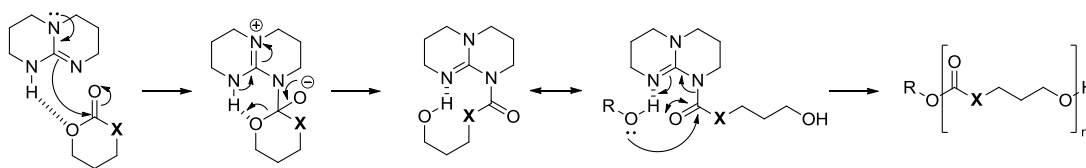
Hedrick and co-workers have demonstrated the viability of using several different organic “superbases” such as 1,8-diazabicyclo[5.4.0]undec-7-ene (DBU), 1,5,7-triazabicyclo[4.4.0]dec-5-ene (TBD) and 7-methyl-1,5,7-triazabicyclo[4.4.0]dec-5-ene (MTBD) in the ROP of lactide leading to poly(ester)s with good control of molecular weight and dispersity (Scheme 1.11).^{24,42}



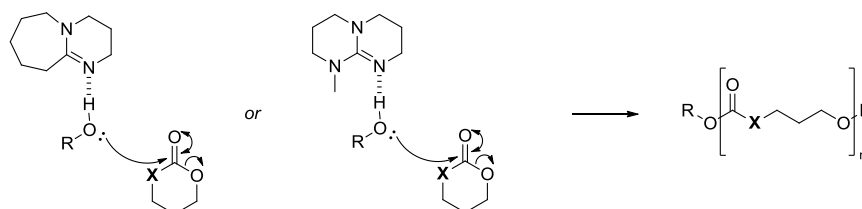
Scheme 1.11 - Nitrogen-containing bicyclic catalysts for the ROP of lactide

It is worth noting that the same group also found TBD to be efficient in the ring-opening polymerisation of δ -valerolactone and ϵ -caprolactone, whereas DBU and MTBD were unsuccessful. This was proposed to be due to the differing mechanisms for TBD *versus* DBU and MTBD (Scheme 1.12). The proposed mechanism for the ROP of cyclic esters with TBD is thought to involve bifunctional activation of both the monomer and the alcohol, whilst DBU and MTBD only activate the alcohol. Whilst the activation of the alcohol is sufficient to allow the ROP of lactide, it is not sufficient for the polymerisation of δ -valerolactone and ϵ -caprolactone to occur due to the decreased ring-strain of the cyclic monoesters compared to the ring-strain of lactide as a result of the presence of two planar ester groups.

TBD dual activation:

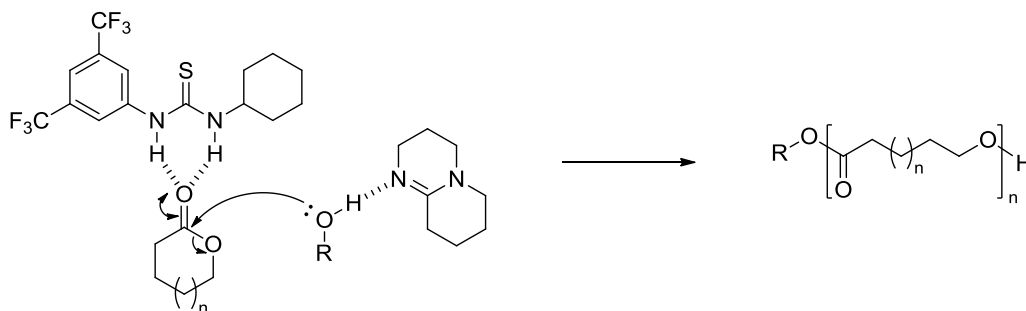


DBU and MTBD activation:



Scheme 1.12 - Comparison of mechanisms for the ROP of cyclic esters and carbonates using TBD or DBU/MTBD

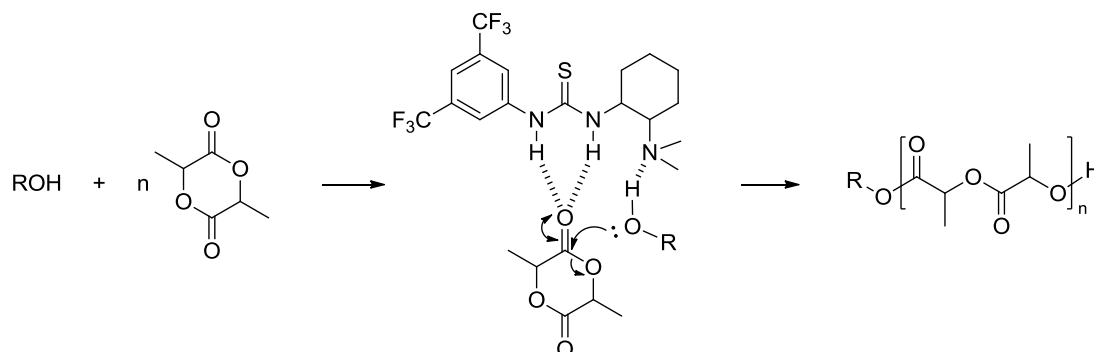
However, it was found that by introducing a thiourea co-catalyst with DBU and MTBD the ROP of both δ -valerolactone and ϵ -caprolactone could be realised *via* a dual-activation approach (Scheme 1.13).⁴²



Scheme 1.13 - ROP of cyclic esters with DBU/thiourea co-catalysts

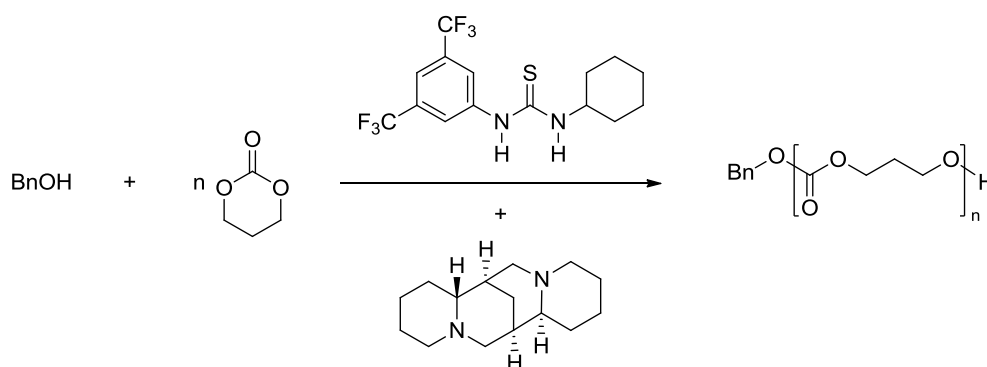
The same research team also led the development of a bifunctional organocatalytic system based on the use of thiourea-tertiary amines, whereby dual-activation *via* hydrogen-bonding

leads the lactide carbonyl to be activated towards electrophilic addition, and the initiating or propagating alcohols are activated as nucleophiles (Scheme 1.14).²⁵



Scheme 1.14 - ROP of cyclic diesters with thiourea-tertiary amine catalyst

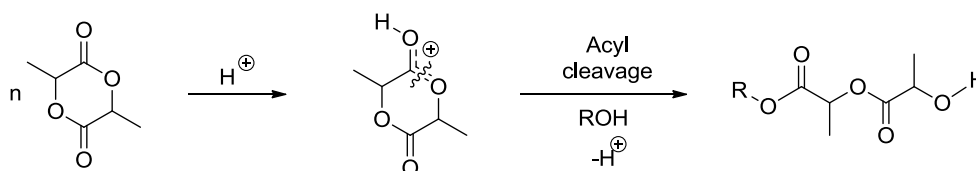
It was then demonstrated that the thiourea and amine moieties may be two separate species, with DBU or (-)-sparteine in conjugation with a thiourea-based co-catalyst proving to be highly successful in the formation of poly(carbonate)s, allowing for the same tight control observed during the application of thioureas as the sole catalytic species yet at a drastically increased rate of reaction (Scheme 1.15).^{23,25,43}



Scheme 1.15 - ROP of cyclic carbonates with thiourea/(-)-sparteine co-catalysts

Alongside the anionic-based routes to poly(ester)s and poly(carbonate)s it is also possible to conduct cationic acid-catalysed ROP of both cyclic esters and carbonates. It has been

proposed that acid-catalysed ROP proceeds through an activated-monomer mechanism in which the cyclic species is activated *via* protonation therefore making it more prone to ring-opening in the presence of a nucleophilic species (Scheme 1.16).⁴⁴

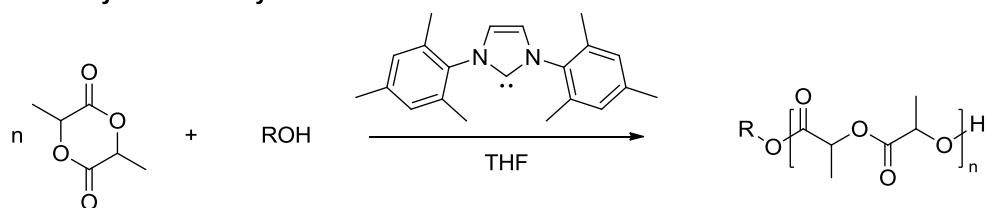
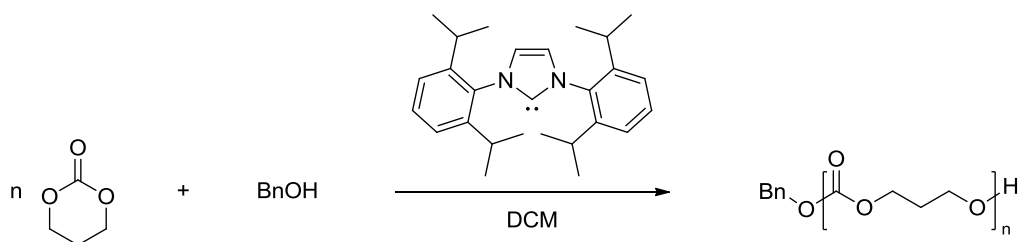


Scheme 1.16 - Cationic ROP of lactide

A range of acidic catalysts have been employed with the most widely employed being trifluoromethanesulfonic acid and methanesulfonic acid.⁴⁵⁻⁴⁸ For example, Bourissou *et al.* has successfully reported the acid-catalysed ROP of lactide using triflic acid.⁴⁴

There have also been reports of acid-catalysed ROP of cyclic carbonates, however, the polymerisation is poorly controlled with broad dispersities compared to poly(ester)s due to competing propagation mechanisms specific to the carbonate functionality.^{49,50}

In 2002, Hedrik and co-workers reported the first example of the use of an *N*-heterocyclic carbene (NHC) in the organocatalysed ROP of a range of cyclic esters including *L*-lactide, ϵ -caprolactone and β -butyrolactone with a variety of alcohol initiators resulting in poly(ester)s with a high degree of control over molecular weight and narrow dispersities (Scheme 1.17).²²

NHC-Catalysed ROP of cyclic esters:**NHC-Catalysed ROP of cyclic carbonates:****Scheme 1.17 - *N*-Heterocyclic carbene-catalysed ROP of cyclic esters and carbonates**

Following this initial report, the area of *N*-heterocyclic carbene-catalysed ROP has seen a great deal of interest with a variety of monomers having been shown to be successfully ring-opened,^{21,35} including trimethylene carbonate, thereby allowing access to poly(carbonate)s (Scheme 1.17).⁴³

There have been two plausible mechanisms proposed for the catalytic activity of NHCs in ROPs; the first being a nucleophilic zwitterionic mechanism initiating with attack of the carbene on the cyclic ester, and the second involving the carbene activating the alcohol towards nucleophilic attack in a chain-end activated mechanism (Figure 1.1).³⁵

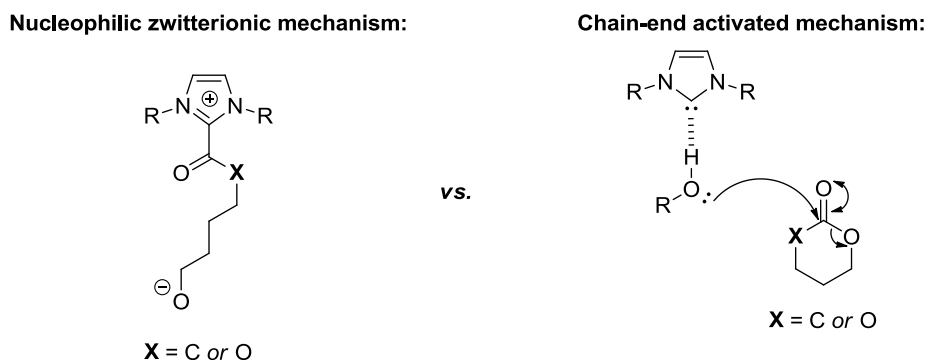


Figure 1.1 - Proposed modes of activation in *N*-heterocyclic carbene-catalysed ROP

Initially, the nucleophilic mechanism was proposed by Hedrik *et al.* with it being favoured over activation of the alcohol based on a pK_a argument that the carbene was unlikely to be protonated by the alcohol.²² This led to the suggestion that the alcohol could be activated towards nucleophilic attack *via* hydrogen-bonding with the carbene.^{51,52} However, mechanistic investigations were conducted in which attempts were made to form zwitterions with NHCs and lactide in the absence of alcohol initiators, with the observation of cyclic poly(ester)s being formed, which in itself provides strong evidence for the nucleophilic mechanism.⁵³

Finally, a wide range of cyclic esters and cyclic carbonates have also been demonstrated to undergo ROP with enzymatic catalysis,^{54,55} with a good review of the area being reported by Gross and co-workers.⁵⁶ Enzymatic catalysis has the added benefit of potentially allowing easy access to poly(ester)s and poly(carbonate)s from macrocyclic lactones and esters, with them often being better substrates than smaller lactones.⁴¹

Overall, there has been a large amount of reports of metal-free organocatalysed ring-opening polymerisations with the area still receiving increasing interest, allowing a range of conditions to be attempted and tailored for different monomers, with the added advantage of avoiding the cost of removing metal impurities from the resulting poly(ester)s and poly(carbonate)s making them potentially suitable for a range of more sensitive applications.

1.4 Functionalisation

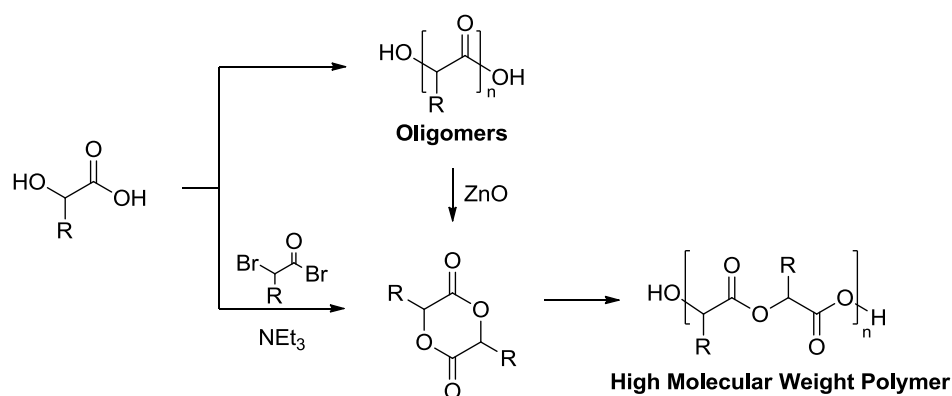
To help improve the suitability for specific applications, the poly(ester)s and poly(carbonate)s properties, including solubility and bulk mechanical properties must be modified. There are a number of methods for achieving such modification of properties, the simplest, and therefore the most common of these involves copolymerisation of the ester or carbonate monomer with a second monomer species. The introduction of functionality can be achieved through copolymerisation of a non-functionalised monomer with a small quantity of functional comonomer and can allow for a dramatic change in properties, perhaps most significantly allowing for cross-linking. However, whilst the use of such copolymerisations can allow the tuning of many properties in both poly(ester)s and poly(carbonate)s,^{33,57,58} the scope of this technique is limited by the selection of suitable comonomers and whilst this method is a valid technique for obtaining functionalised polymers on the inclusion of a functional monomer, this method was not utilised during the studies presented in this thesis and therefore will not be discussed further.

A second method, allowing for both a greater range of possible modifications as well as more specific control over properties and reactivity is the incorporation of functional groups along the polymer backbone. These may be obtained through two significantly different general methods, the first is the post-polymerisation functionalisation, this involves the addition of functional species to a pre-made polymer chain *via* reaction with (usually pendant) reactive groups such as alkenes or carboxylic acids. Such modification can provide access to a wide range of functionalised polymers starting with the same polymeric species and reactions with a range of functional species. However, this method may have issues achieving complete functionalisation as it relies on all of the reactive groups being readily accessible for reaction. This may prove to be problematic if there is significant coiling of the polymer chain.

An alternative method of functionalisation is achieved pre-polymerisation through the synthesis of functionalised monomers, therefore as the polymerisation proceeds, every repeat unit is already functionalised and, as such, complete incorporation of the desired functional species is achieved. However, using this method, functional groups are limited to those which will not react, or otherwise interfere with, the polymerisation species or conditions. This means that particularly reactive species must be protected in order to be used, however doing so reintroduces the problem of incomplete conversion due to the inaccessibility of some protected species.

1.4.1 Poly(ester)s

The seminal work investigating the utilisation of functional monomers to produce functionalised poly(ester)s was conducted by Baker and co-workers, who have demonstrated the synthesis and subsequent ROP of a selection of substituted 1,4-dioxane-2,5-diones from α -hydroxyacids *via* two different methods (Scheme 1.18).^{59,60}



Scheme 1.18 - Route to disubstituted cyclic diesters utilised by Baker et al.

The first of these methods involved the initial production of low molecular weight oligomers by refluxing the α -hydroxyacid in toluene in the presence of *p*-toluenesulfonic acid. The

isolated oligomers were then cracked in the presence of zinc oxide to yield the substituted 1,4-dioxane-2,5-diones. The second synthetic method involved the initial reaction of the α -hydroxyacid with a structurally-related α -bromoacyl bromide, liberating hydrogen bromide. This was followed by treatment with triethylamine in refluxing acetone to induce cyclisation and thus yield the substituted monomer species. Utilising these two methods, Baker and co-workers have reported the successful synthesis of several disubstituted cyclic diesters **I-IV** (Figure 1.2). All of these monomers have been successfully polymerised *via* ROP in melt conditions using tin octanoate.

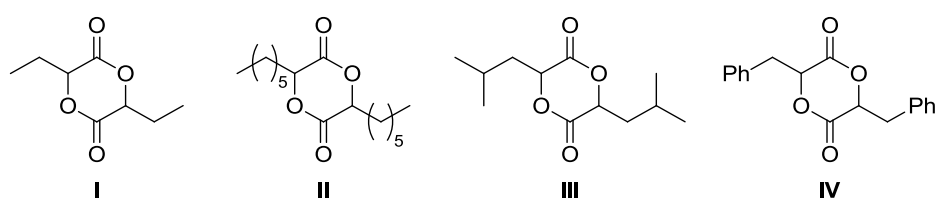


Figure 1.2 - Disubstituted cyclic diesters reported by Baker *et al.*

Following on from this research, in 2006 Weck and co-workers utilised a similar synthetic method to produce asymmetrically substituted 1,4-dioxane-2,5-diones from *L*-amino acids.⁶¹ Using this methodology, asymmetrically substituted monomers have been synthesised from lysine, serine and glutamic acid with benzyl-protected alcohol, amine and acid groups respectively (Figure 1.3).

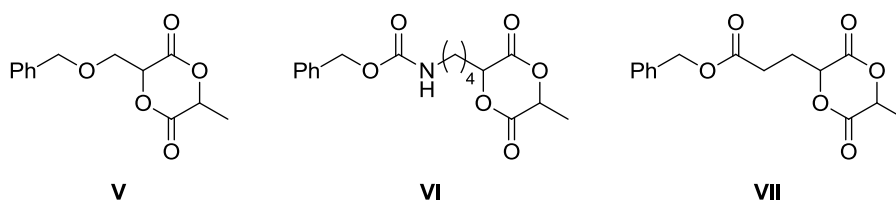
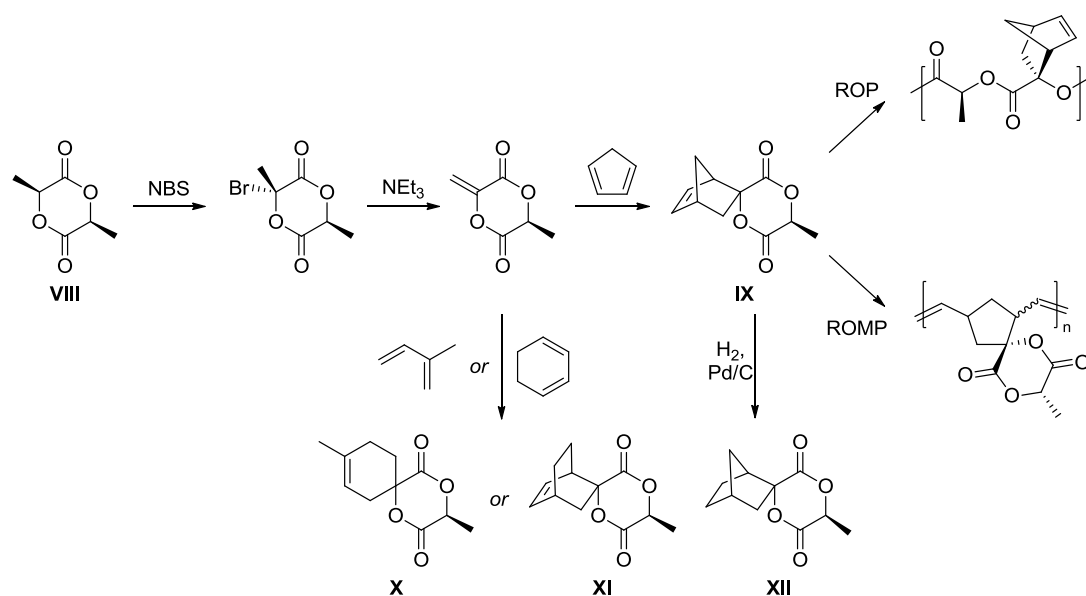


Figure 1.3 - Asymmetrically substituted 1,4-dioxane-2,5-diones reported by Weck *et al.*

These monomers have been subsequently polymerised *via* ROP before the benzyl groups were removed under hydrogenation conditions, yielding poly(ester)s with pendant alcohol, amine and carboxylic acid groups.

The presence of chiral centres in these cyclic diesters also lends itself to the possibility of synthesising enantiopure monomers which themselves can undergo ROP. One such example is the synthesis of the enantiomerically pure bifunctional monomer **IX** from *L*-lactide **VIII**, reported by Hillmyer and Jing, which includes functionality allowing it to undergo both ROP and ring-opening metathesis polymerisation (ROMP) (Scheme 1.19).⁶²



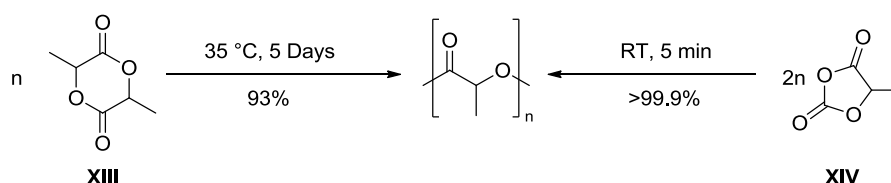
Scheme 1.19 - Enantiomerically pure bifunctional monomers by Hillmyer and Jing

The route also provided the opportunity to introduce different synthetic handles throughout its synthesis to obtain a range of chiral functionalised monomers such as **X**, **XI** and **XII**.⁵⁸ These novel monomers were then all successfully subjected to ROP with TBD yielding functional poly(lactide)s.

With increasing functionalisation of cyclic diesters the effects of steric hindrance can lead to increasingly longer reaction times. In order to overcome this, *O*-carboxyanhydrides have been utilised as an activated equivalent of cyclic esters.

***O*-Carboxyanhydrides**

In the past few years, Bourissou and co-workers have expanded on the early work of Kricheldorf and Jonte,⁶³ having reported the successful synthesis and ROP of *O*-carboxyanhydrides derived from both lactic and glutamic acids.^{64,65} *O*-carboxyanhydrides provide an activated equivalent to glycolides for the synthesis of poly(ester)s by ROP. Such polymerisations proceed extremely rapidly compared to lactide polymerisations under similar conditions, the OCA prepared from *L*-lactic acid (*L*-lacOCA, **XIV**) underwent ROP using *neo*-pentanol as initiator with 4-dimethylaminopyridine (DMAP) as catalyst. Using a monomer/catalyst/initiator ratio of 20/1/1, complete conversion was achieved after only five minutes at room temperature, to give a final polymer with a number-average molecular weight (M_n) of 2100 g.mol⁻¹ and a dispersity (D_M) of 1.20. In contrast, the ROP of lactide **XIII** using the same catalyst/initiator system with a ratio of 10/1/1 (thereby producing a polymer with a DP of 10) reached only 93% conversion after heating at 35 °C for five days (Scheme 1.20).

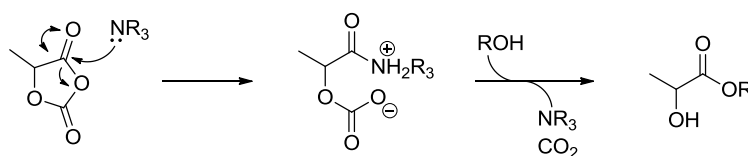


Scheme 1.20 - Comparative ROP of lactide **XIII and *L*-lacOCA **XIV** using *neo*-pentanol and DMAP**

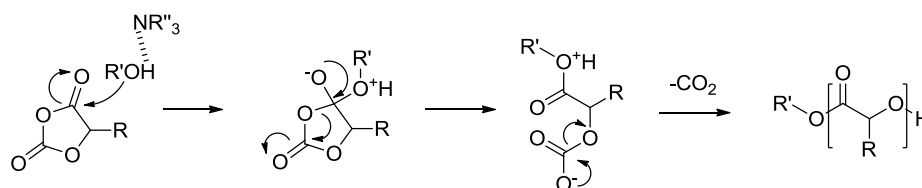
This high monomer activity arises from several factors, the first of which is the high reactivity of the anhydride group present within the OCA ring structure, making it more susceptible to nucleophilic attack than the esters present in lactides. A second source of increased activity is the relief of the slightly increased strain in the five-membered OCA ring ($\Delta H = -19.5 \text{ kcal.mol}^{-1}$), such strain in the lactide ring is notably lower ($\Delta H = -15.7 \text{ kcal.mol}^{-1}$).³² By far, the most significant source of activation however, is the entropic gain from ring-opening the OCA structure, due to the liberation of carbon dioxide from the intermediate carbonic acid.⁶⁶

There has been some investigation into the exact mechanism of OCA ring-opening and discussion over the role of the amine catalyst.⁶⁷ The initially proposed mechanism utilised the amine as a nucleophile, opening the ring before being replaced with the alcoholic species present in the reaction mixture (Scheme 1.21).

Proposed Nucleophilic Amine-Catalysed ROP of OCAs:



General Base-Catalysed ROP of OCAs:

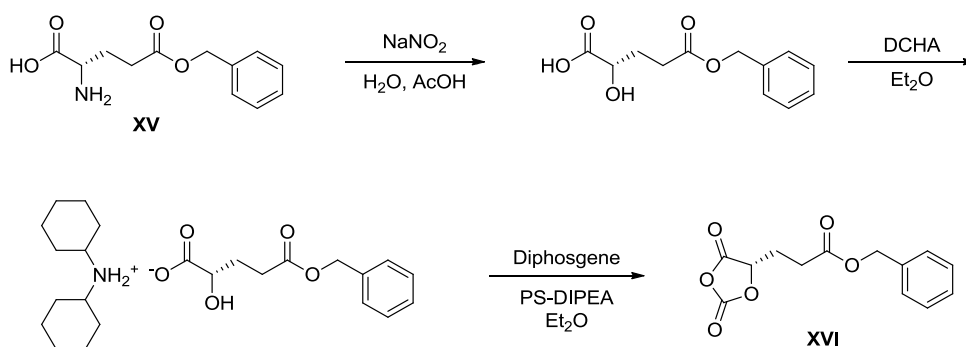


Scheme 1.21 - Proposed Mechanisms for ROP of OCAs

Computational studies however, have suggested a general base-catalysed mechanism would be more likely. In such a mechanism, the amine activates the alcoholic initiator *via*

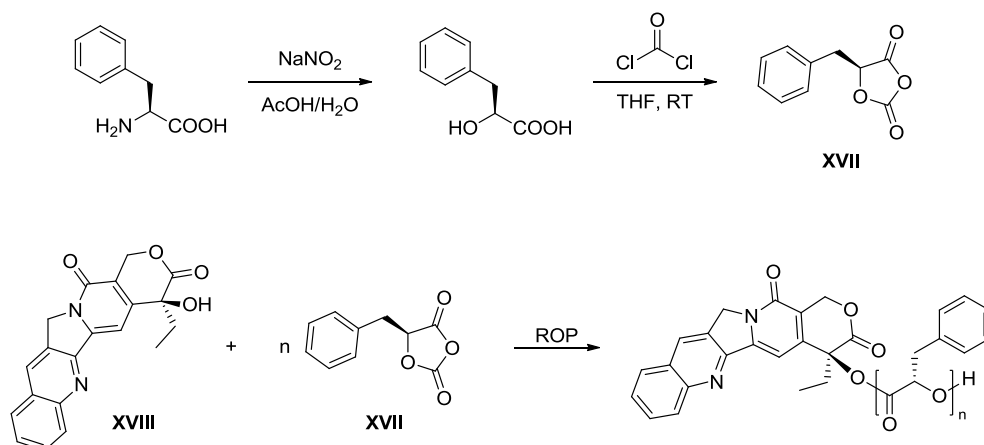
hydrogen bonding, thereby making it more nucleophilic in nature, enough to be able to readily attack the ring system (Scheme 1.21).

Bourissou and co-workers have also demonstrated the synthesis of a benzyl ester-functionalised OCA **XVI** derived from γ -benzyl *L*-glutamic acid **XV** using the route outlined in Scheme 1.22. Once polymerised *via* DMAP-catalysed ROP, the pendant benzylic esters may be subsequently converted to carboxylic acid groups *via* hydrogenation conditions.⁶⁵



Scheme 1.22 - Bourissou and co-workers' synthesis of BnzGluOCA **XVI**

More recently, Cheng *et al.* have reported the synthesis of a novel chiral OCA **XVII** which was subsequently submitted to ring-opening polymerisation. Interestingly, hydroxyl-containing drugs, such as **XVIII**, were utilised as the initiators in an interesting novel strategy towards polymer-drug conjugates for nanoparticulate drug discovery (Scheme 1.23).⁶⁸



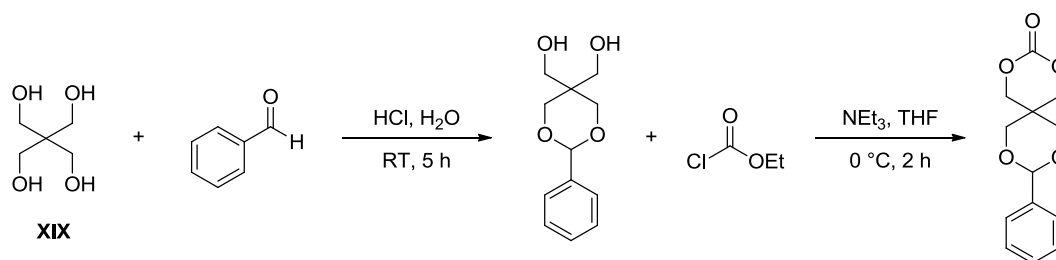
Scheme 1.23 - ROP of novel OCA XVII with hydroxyl-containing frug XVIII

1.4.2 Poly(carbonate)s

As the viability of ROP as a technique for producing highly controlled poly(carbonate)s was realised, there has been an increasing interest in the development of cyclic carbonates incorporating functional groups. Initial research efforts focussed on the individualistic design and synthesis of each novel monomer, requiring the synthetic route to be redesigned for every new functional group required.

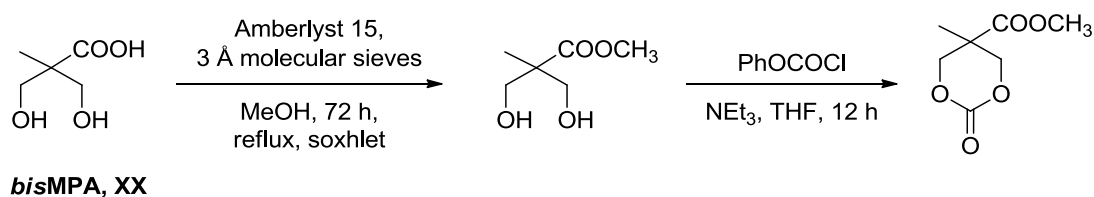
A number of routes have been utilised in the synthesis of functional cyclic carbonates from a range of starting materials including pentaerythritol,⁶⁹ glycerol,^{70,71} trimethyloalkanes,^{72,73} amino acids, sugars and *bis*-MPA, with the latter being the most commonly reported.⁷⁴

The use of pentaerythritol **XIX** as a precursor to cyclic carbonates has been reported, enabling incorporation of two pendant hydroxyl groups in each repeat unit of the resulting poly(carbonate) after deprotection (Scheme 1.24).⁶⁹

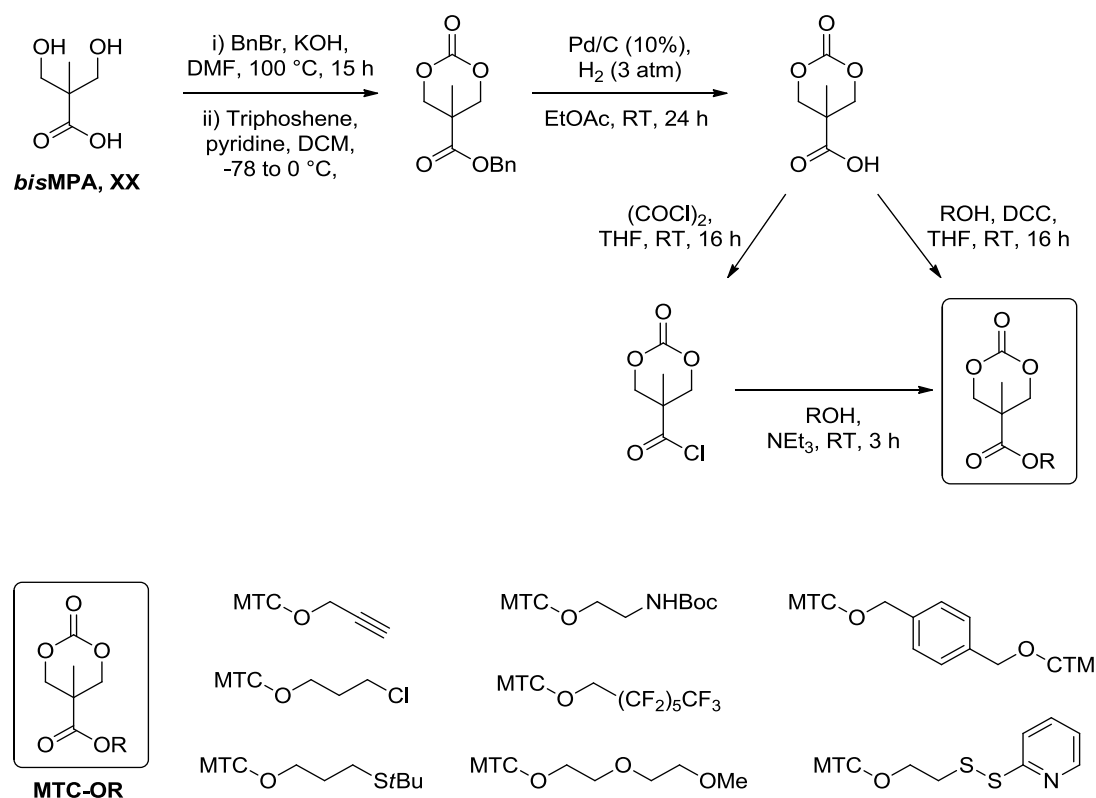


Scheme 1.24 - Cyclic carbonates formed from pentaerythritol XIX

Originally reported by Frechet and co-workers for the efficient synthesis of biodegradable dendrimers,^{75,76} the use of 2,2-bis-(hydroxymethyl)propionic acid (*bis*-MPA, **XX**) has since been expanded to form cyclic carbonates, which successfully underwent ROP with the first report in 1996 (Scheme 1.25).⁷⁷

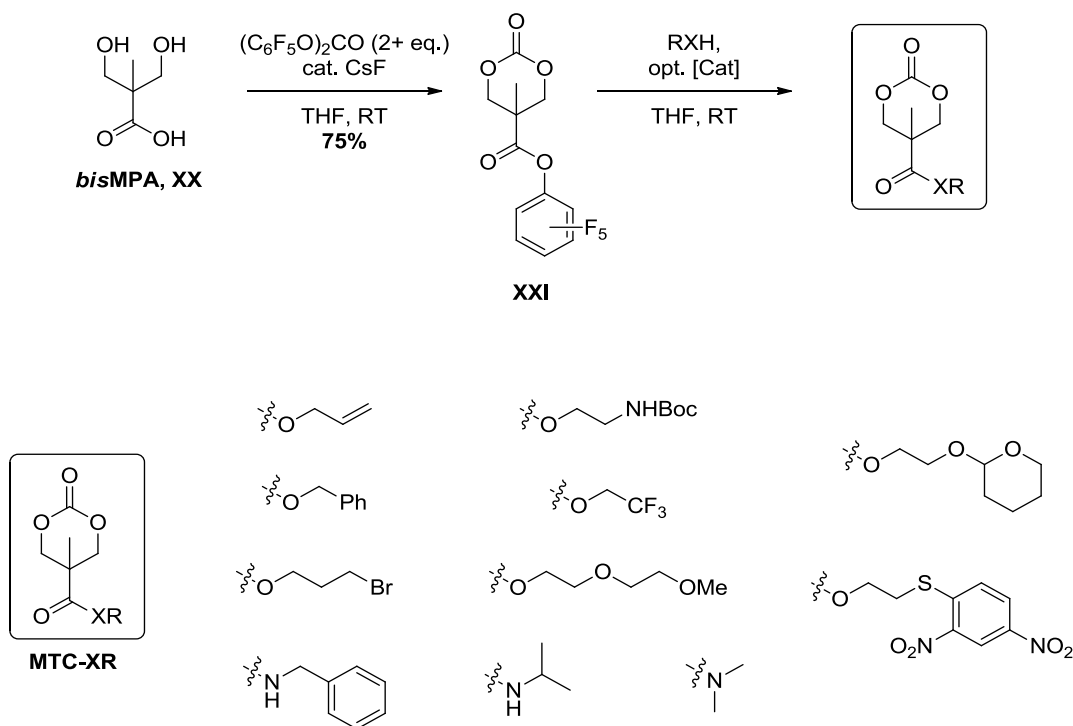
Scheme 1.25 - First known report of cyclic carbonates formed from *bis*MPA

However, it was not until a report by Hedrick and co-workers in 2008 that a major leap forward in the accessibility of functionalised cyclic carbonates occurred, with the development of a common route to cyclic carbonates derived from *bis*MPA **XX**. Enabling access to a wide range of pendant functional groups, made possible by incorporating a pendant acid group which could be used as a handle for the addition of further functionality onto these monomers (Scheme 1.26).⁷⁸



Scheme 1.26 Synthesis of cyclic carbonates via a common intermediate as reported by Hedrick *et al.*

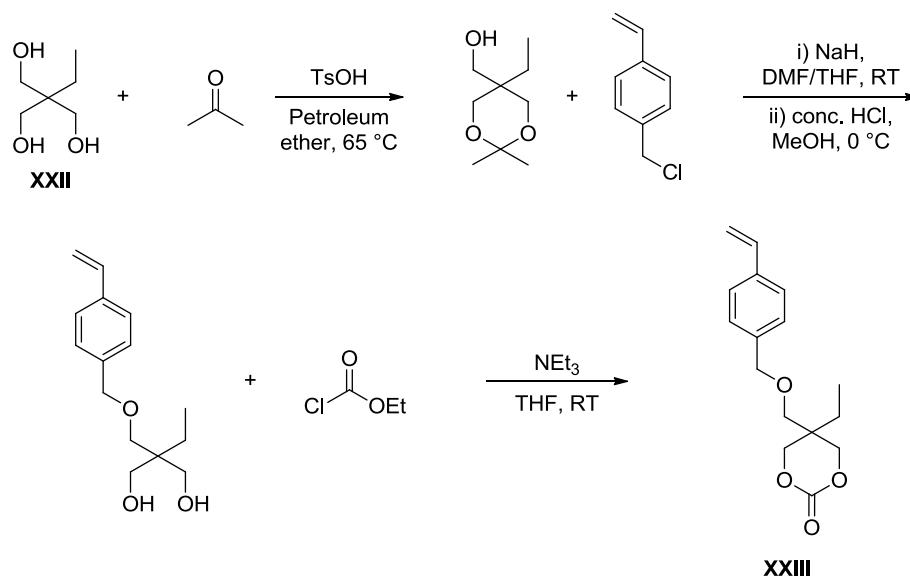
The same group later developed this further by designing an alternative synthesis which proceeded *via* a novel cyclic carbonate intermediate with an active pentafluorophenyl ester **XXI**, avoiding the need for the use of toxic reagents such as phosgene derivatives.⁷⁹ This provided a simple and efficient synthesis of functionalised cyclic carbonates from a common intermediate (Scheme 1.27).



Scheme 1.27 - Synthesis of cyclic carbonates via an activated pentafluorophenyl ester **XXI** reported by Hedrick *et al.*

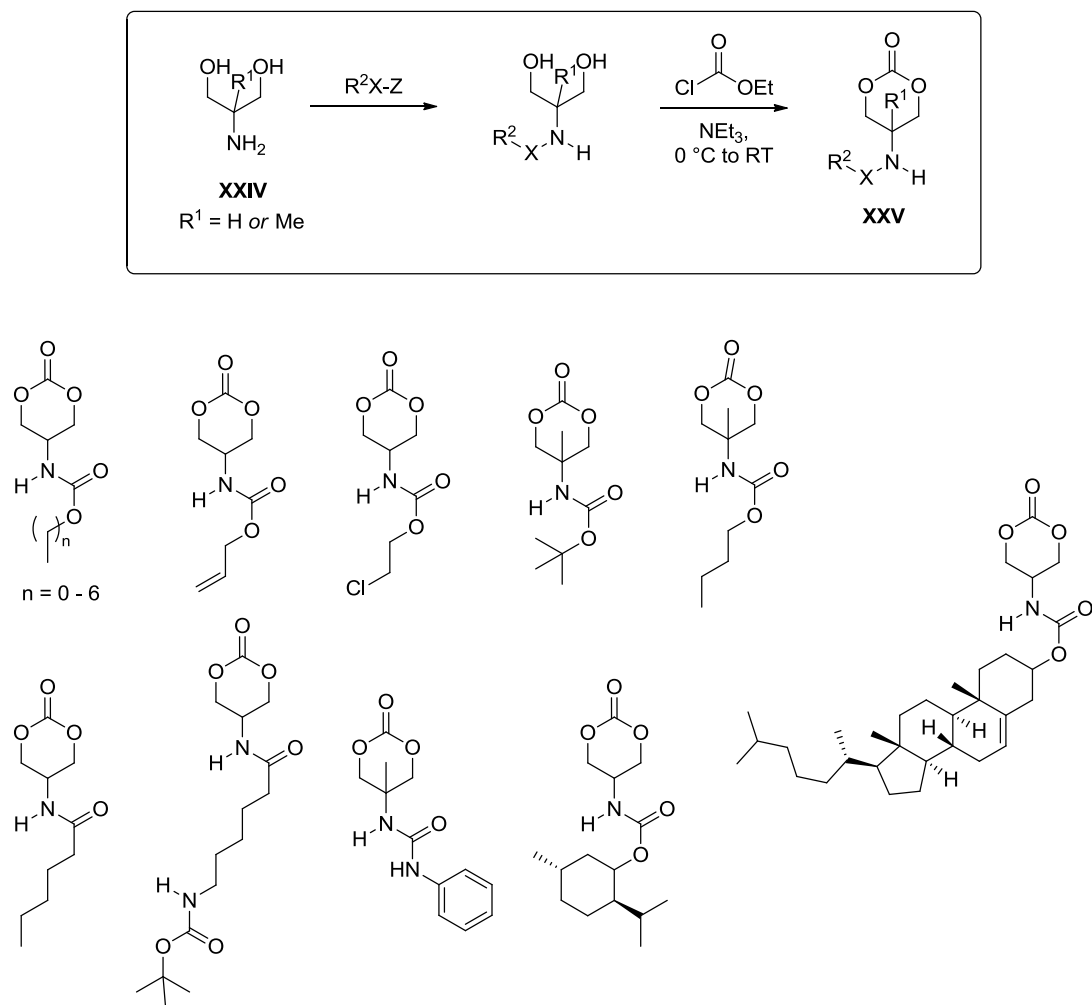
So far, the development of this method of monomer synthesis has focussed on the formation of esters *via* the addition of functional alcohols,^{78,79} there has been relatively little attention paid to the addition of other heteroatomic species, such as amines or thiols. The few reported functionalisations involving amines to form the corresponding amide have only involved the use of achiral amines.^{79,80}

An alternative approach to the use of *bisMPA* **XX** as a precursor in the formation of cyclic carbonates is the use of glycerol and its derivatives. For example, styrenic functionality may be introduced using trimethylolpropane **XXII** as the precursor (Scheme 1.28).⁷³



Scheme 1.28 - Synthesis of a styrene-functionalised cyclic carbonate XXIII from trimethylolpropane XXII

The synthesis of new cyclic carbonates is still receiving great interest and constantly being developed due to the use of functional biodegradable polymers in biomedical and environmentally friendly products. For example, in 2013 Hedrick, Yang and co-workers have reported a new synthesis of aliphatic cyclic carbonates **XXV** starting from 2-amino-1,3-propane diols **XXIV** (Scheme 1.29).^{81f} By chemoselectively reacting the amino group with a range of electrophiles, a range of diols could be formed which, after subsequent cyclisation, afford a novel set of cyclic carbonates, which have been shown to undergo organocatalysed ROP.



Scheme 1.29 - Synthesis of novel cyclic carbonates XXV from amino-1,3-propane diols XXIV reported by Hedrick, Yang and co-workers

1.5 Conclusions

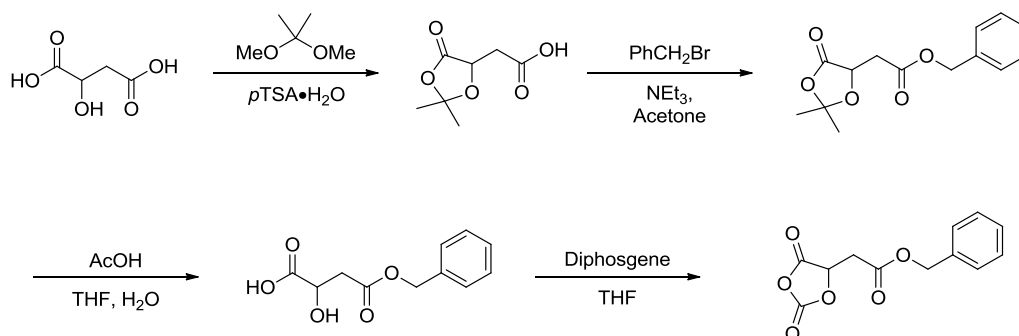
Overall, there has been increasing interest in recent years in the synthesis of novel cyclic esters and carbonates with a variety of incorporated functionality. Many of these have subsequently been shown to successfully undergo organocatalysed ring-opening polymerisations affording the respective poly(ester)s and poly(carbonate)s with a high degree of control over molecular weight, dispersity, and end-group fidelity whilst retaining the desired functionality. These functional poly(ester)s and poly(carbonate)s offer a significant amount of potential, particularly due to their biodegradable and biocompatible natures, for the synthesis and applications of new materials suitable for use in highly demanding applications such as tissue engineering, drug delivery and microelectronics.

Chapter 2

Synthesis and Ring-Opening Polymerisation of Functional *O*-
Carboxyanhydride Monomers Derived from *L*-Malic Acid

2.1 Introduction

Following the report by Bourrisou and co-workers of the synthesis and ROP of a benzyl-functionalised *O*-carboxyanhydride derived from *L*-glutamic acid, work within our own group has led to the synthesis of an analogous benzyl ester-functionalised OCA derived from malic acid *via* the route outlined in Scheme 2.30. This monomer has been successfully polymerised *via* organocatalysed ROP. The pendant benzylic esters on the resulting homopolymer were subsequently deprotected under hydrogenation conditions, yielding a poly(ester) with hydrophilic characteristics.



Scheme 2.30 - Synthesis of BnMalOCA

Further work has investigated the polymerisation of BnMalOCA, initiating from Me(PEO)_{5k}OH to give an amphiphilic block copolymer of the type PEO_{5k}-*b*-PBMA.⁸² Such block copolymers were then shown to readily self-assemble using both solvent switch and direct dissolution methodologies, forming micelles with good stability in aqueous solutions, making them promising candidates for drug delivery applications. Their ability to encapsulate hydrophobic drug molecules was demonstrated through the use of fluorescence microscopy to study the encapsulation of pyrene.

If such micelles were to then undergo deprotection of the pendant benzylic esters, the resulting hydrophilic acid groups should destabilise the assembled structure sufficiently to rupture the micelles and liberate any encapsulated molecules. Unfortunately, due to the harsh nature of the hydrogenation procedure and the unsuitable nature of such a deprotection mechanism for *in vivo* drug release, the method of deprotection would need to be developed further. Therefore, the initial aim of this project was the development of monomers which would allow for the incorporation of suitable functional groups capable of responding to an applied external stimulus (*e.g.* light, heat or pH changes).

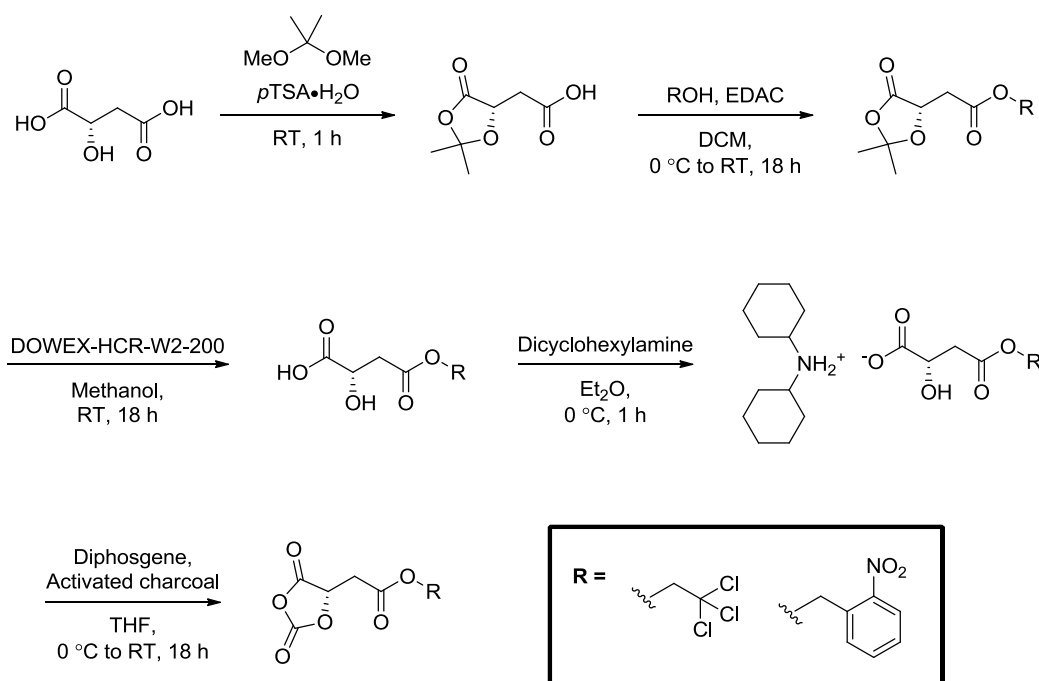
2.2 Results and Discussion

2.2.1 Synthesis of Functionalised O-Carboxyanhydrides from L-Malic Acid

A number of novel functionalised O-carboxyanhydrides have been synthesised from *L*-malic acid following the route outlined in Scheme 2.31. The initial acetonide-protection of the α -hydroxyacid was achieved using the acid-catalysed addition of 2,2-dimethoxypropane; yields were reasonable, averaging 70%. The acetonide-protected malic acid species provided a common scaffold upon which a wide variety of functionalities could be attached *via* ester formation. Functional esters were initially synthesised *via* a Steglich esterification,⁸³ using *N,N'*-dicyclohexylcarbodiimide (DCC), whilst this gave good overall yields (70-75%), the resulting *N,N'*-dicyclohexylurea (DCU) by-product severely complicates and prolongs the purification.

The synthesis of the functionalised esters was simplified by exchange of the coupling reagent, DCC for *N*-(3-dimethylaminopropyl)-*N'*-ethylcarbodiimide hydrochloride (EDAC) due to the considerably easier removal of EDAC and its by-products compared to DCC and the resulting DCU. Two different functionalised alcohols were coupled to the acetonide-

protected species, giving the corresponding esters, incorporating 2,2,2-trichloroethyl and 2-nitrobenzylic functionalities in respectable yields (approx. 55-65%).



Scheme 2.31 - Synthesis of O-Carboxyanhydrides from L-Malic Acid

Once the functional esters had been formed, the acetonide protecting group could be removed. This was initially achieved by stirring in a 1:1:1 mixture of water, tetrahydrofuran (THF) and acetic acid. However, whilst successful, the removal of residual acetic acid proved to be an arduous task. A far more efficient method was realised using acidic DOWEX resin in methanol, although the resulting product contained only a low level of impurities, it proved to be considerably simpler to continue to the next step rather than attempt the isolation of the functionalised α -hydroxyacids.

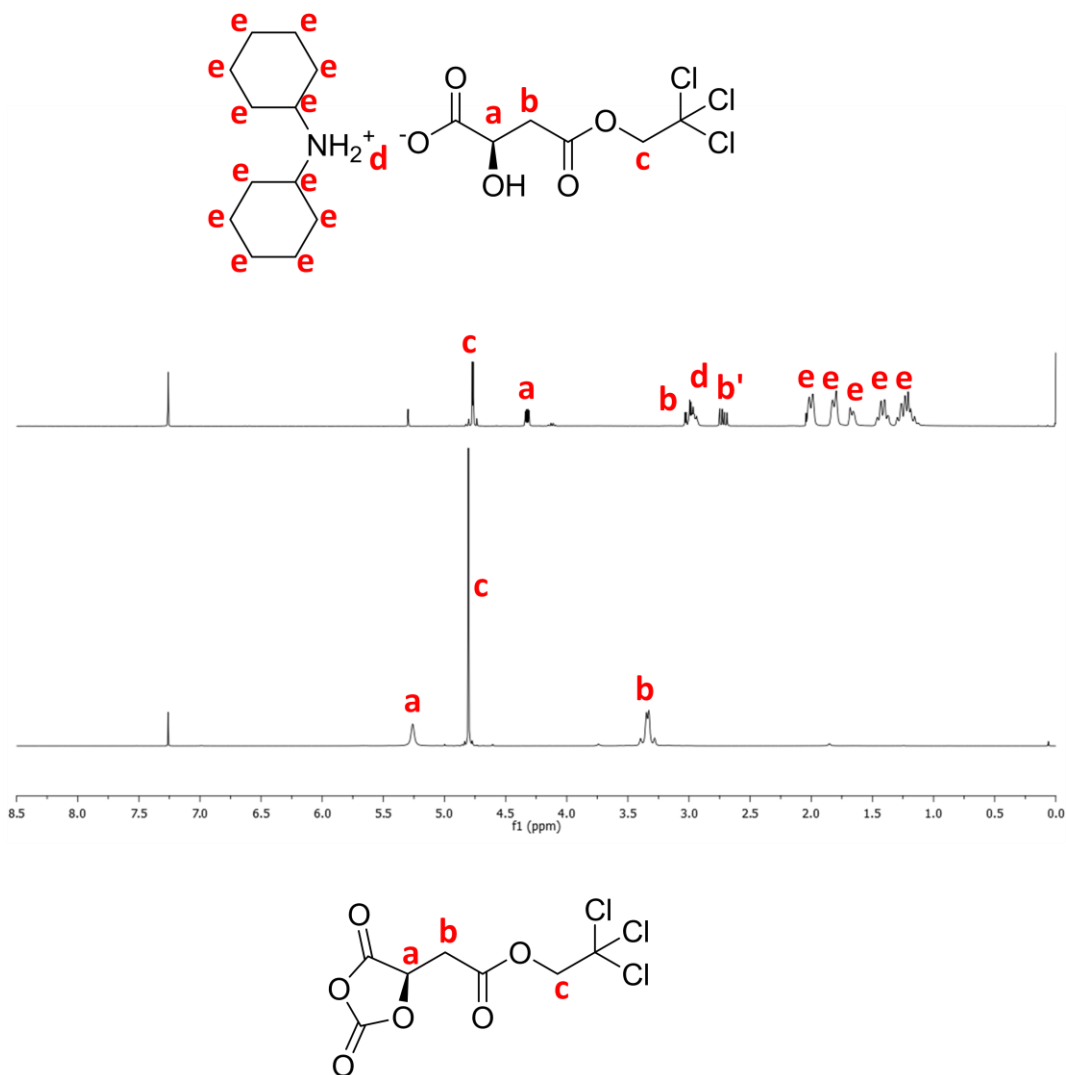


Figure 2.4 - Comparison of ^1H NMR spectra of TCEMal diol and TCEMalOCA

The formation of the respective N,N -dicyclohexylamine salts serves multiple purposes, with two major advantages. The first is the simple and fast purification that is achieved (on the assumption that any diacid has been removed previously) and the second is the greatly improved shelf-stability that the salt possesses in comparison to the free α -hydroxyacid, allowing significant batches of the direct monomer precursor to be synthesised and stored for later use. Finally, the easily isolated, pure salts could be cyclised to form the respective O -carboxyanhydrides (OCAs), using diphosgene in THF in the presence of activated

charcoal (aiding the degradation of diphosgene to phosgene).⁸⁴ The resulting crude OCAs could be purified via recrystallisation from dry solvents and under a nitrogen atmosphere.

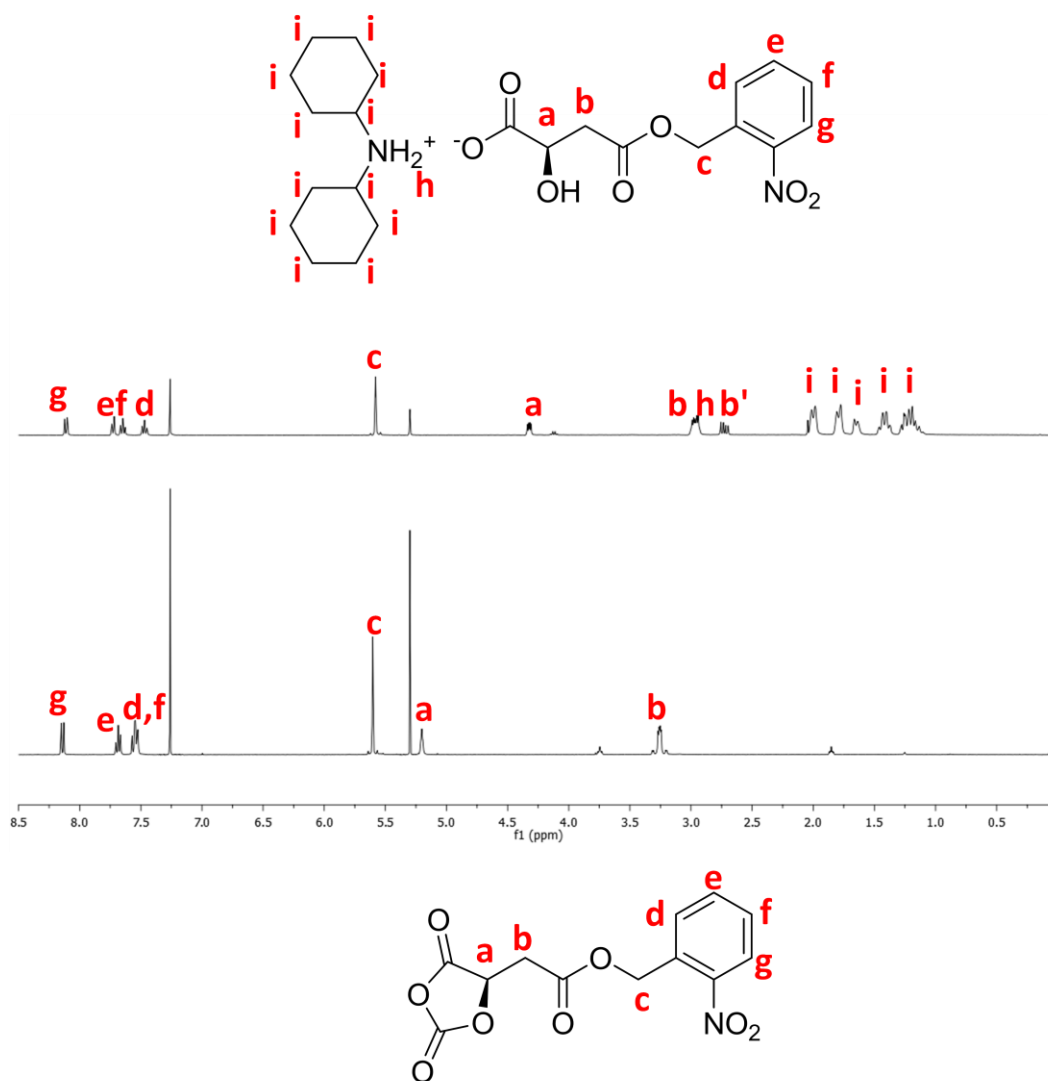


Figure 2.5 - Comparison of ¹H NMR spectra of NBMal diol and NBMalOCA

2.2.2 Ring-opening polymerisation of (S)-2,2,2-trichloroethyl 2-(2,5-dioxo-1,3-dioxolan-4-yl)acetate

The organocatalysed ring-opening polymerisation of TCEMalOCA was investigated using a series of substituted pyridines as catalysts and initiated using 4-methoxybenzyl alcohol. All polymerisations were conducted at a monomer concentration of 0.25M in dried deuterated dichloromethane under a dry, inert nitrogen atmosphere. Reaction progress was most easily monitored using ^1H NMR spectroscopy, with the relative concentration of monomer to initiator ($[\text{M}]/[\text{I}]$) determined by the ratio of integrals of the peaks corresponding to the methine proton in the monomer (5.42 ppm) and the methoxy group of 4-methoxybenzyl alcohol (3.68 ppm). Monomer conversion was calculated by comparison of the integrals of the peaks corresponding to the methine proton of the monomer (5.42 ppm) and the methine proton of the polymer (5.63 ppm).

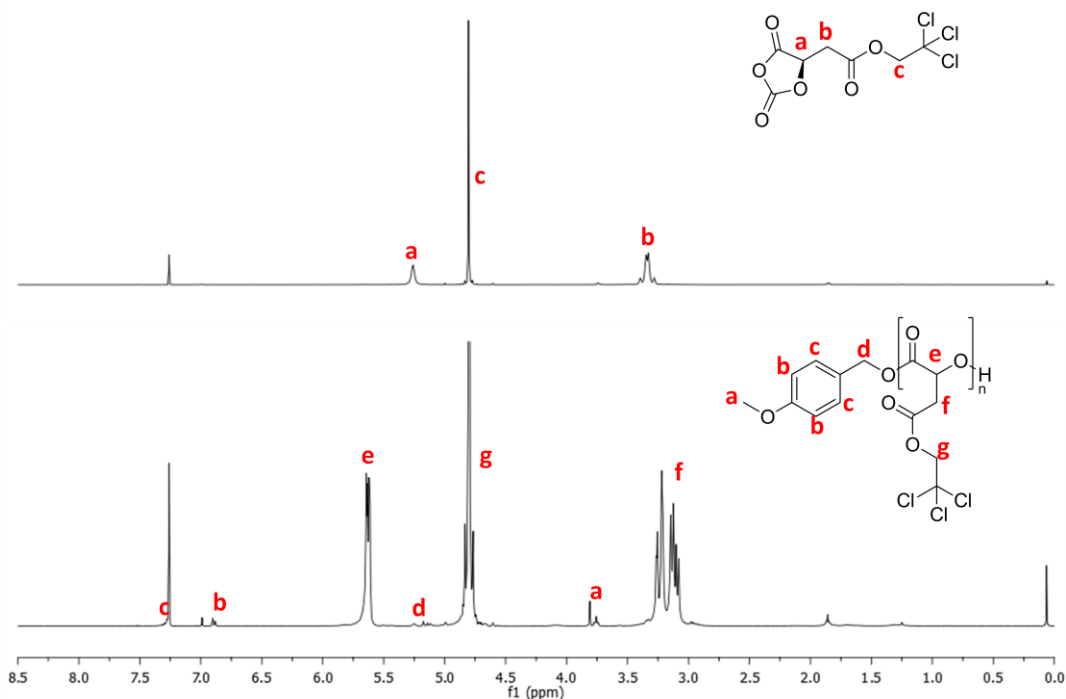
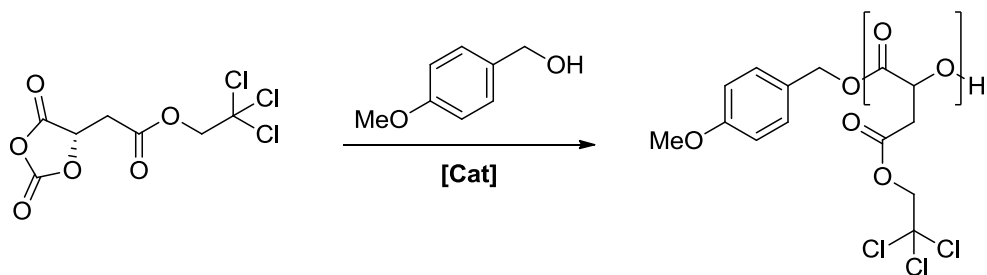
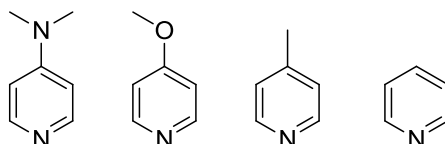


Figure 2.6 - Comparison of ^1H NMR spectra of TCEMalOCA and P(TCEMA)



Catalysts:



Scheme 2.32 - Ring-opening polymerisation of TCEMalOCA with substituted pyridine catalysts

Table 2.1 - Catalyst screening for the polymerisation of TCEMalOCA ($[M]_0/[I]_0 = 20$)

Entry	Catalyst (Loading (eq.)) ^a	Monomer Conversion (%) ^b	Time (h)	M_n (g.mol ⁻¹) ^b	M_n (g.mol ⁻¹) ^c	D_M ^c
1	DMAP (1)	89	0.5	4660	2030	1.40
2	MeOPyr (1)	93	3	5530	2520	1.32
3	MePyr (1)	92	4	5472	980	1.45
4	Pyridine (1)	94	5	5588	4980 ^d 1250 ^d	1.09 ^d 1.13 ^d

^a Catalysts equivalents relative to initial alcohol concentration. ^b Calculated by ¹H NMR analysis. ^c Determined by GPC analysis, calibrated against poly(styrene) standards. ^d GPC trace showed bimodal distribution.

The first step in the investigation of the ring-opening polymerisation of TCEMalOCA involved the screening of a series of substituted pyridines as catalysts, all were tested at a catalyst loading of 1 equivalent with respect to the 4-methoxybenzyl alcohol. The initial reaction involved the polymerisation of TCEMalOCA using 4-(dimethylamino)pyridine (DMAP) (Table 2.1, Entry 1). Although this catalyst has previously shown great promise in

the control of the ROP of lacOCA,⁸⁵ and indeed rapidly reached completion with TCEMalOCA, at 89% monomer conversion after only 30 minutes, the GPC analysis of the resulting polymer shows a far broader distribution than would be expected from a controlled polymerisation ($\bar{D} = 1.40$, Figure 2.7).

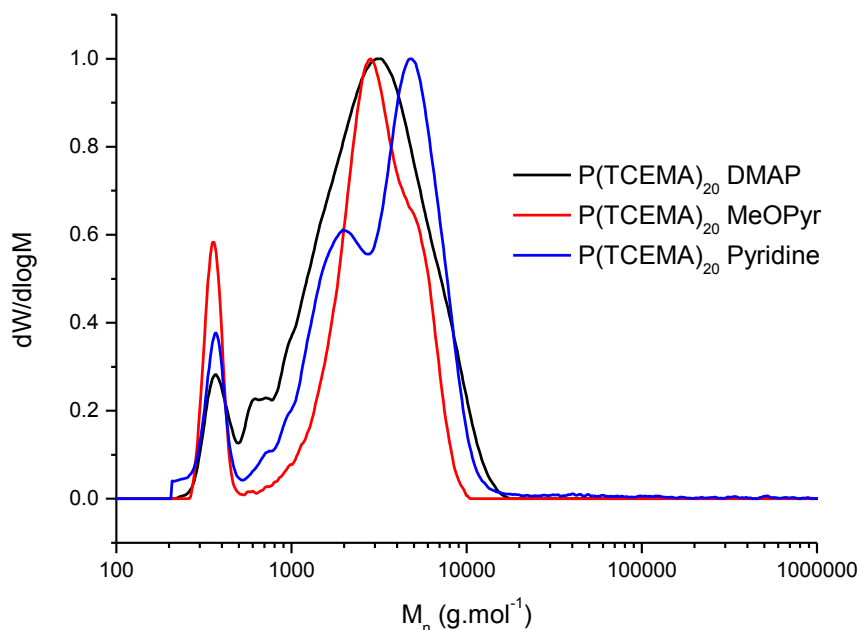


Figure 2.7 - GPC traces of P(TCEMA) obtained using 1 equivalent of 4-(dimethylamino)pyridine, 4-methoxy pyridine and pyridine

The molecular weight observed by GPC for the poly(2,2,2-trichloroethylmalic acid), P(TCEMA) obtained using DMAP is significantly lower than would be expected when compared to the molecular weight calculated from the ^1H NMR spectrum ($M_n = 2030 \text{ g}\cdot\text{mol}^{-1}$ by GPC vs. $M_n = 4660 \text{ g}\cdot\text{mol}^{-1}$ by ^1H NMR).

The analysis of the resulting polymeric material by matrix-assisted laser desorption/ionisation time-of-flight mass spectrometry (MALDI ToF MS) sheds some light on the unexpectedly broad distribution, showing distributions for multiple species (Figure 2.8). It should be noted that the peaks observed in the MALDI-ToF mass spectra for

P(TCEMA) are considerably broadened compared to those observed for other polymers due to the presence of three chlorine atoms per repeat unit. With each chlorine possessing two stable isotopes ^{35}Cl and ^{37}Cl (75.78 and 24.22% respective abundance), each repeat unit possesses a mass range of 6 Da. This mass range as a result of isotopic variation is greatly magnified when analysing the corresponding polymer, with even a low degree of polymerisation, the mass range becomes significant, for example, with only a DP of 10, the polymer possesses a variation of 60 Da, giving rise to the unusually broad peaks.

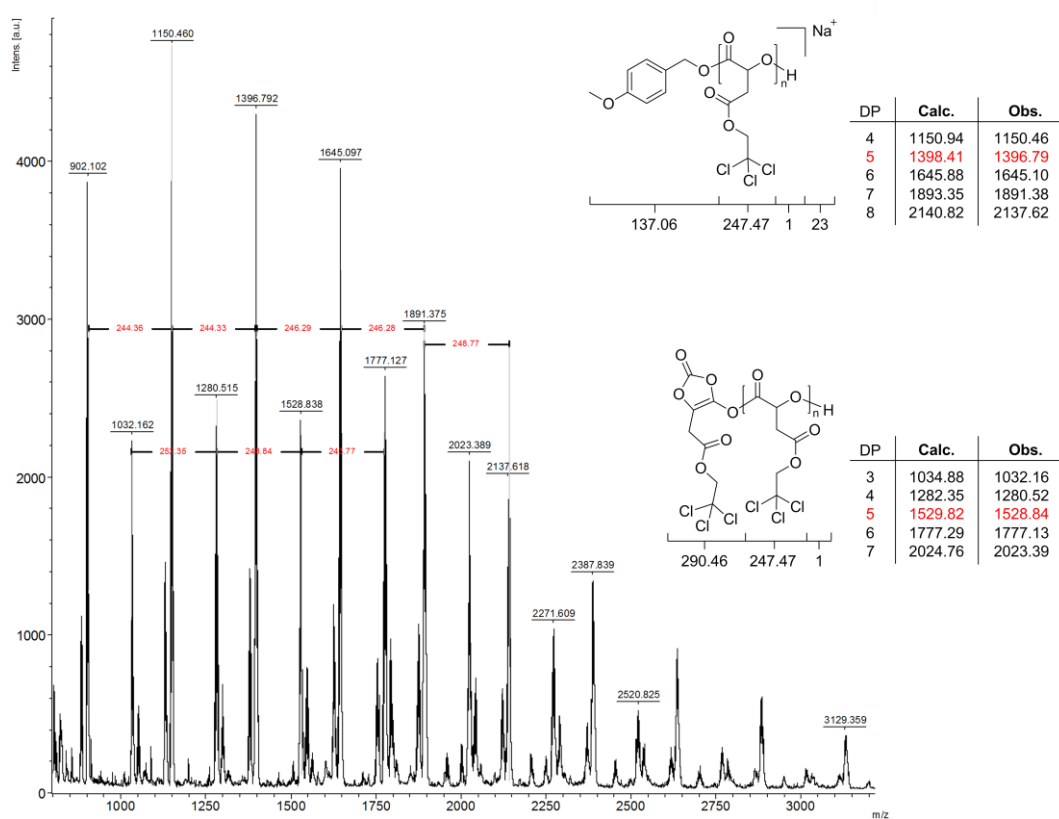
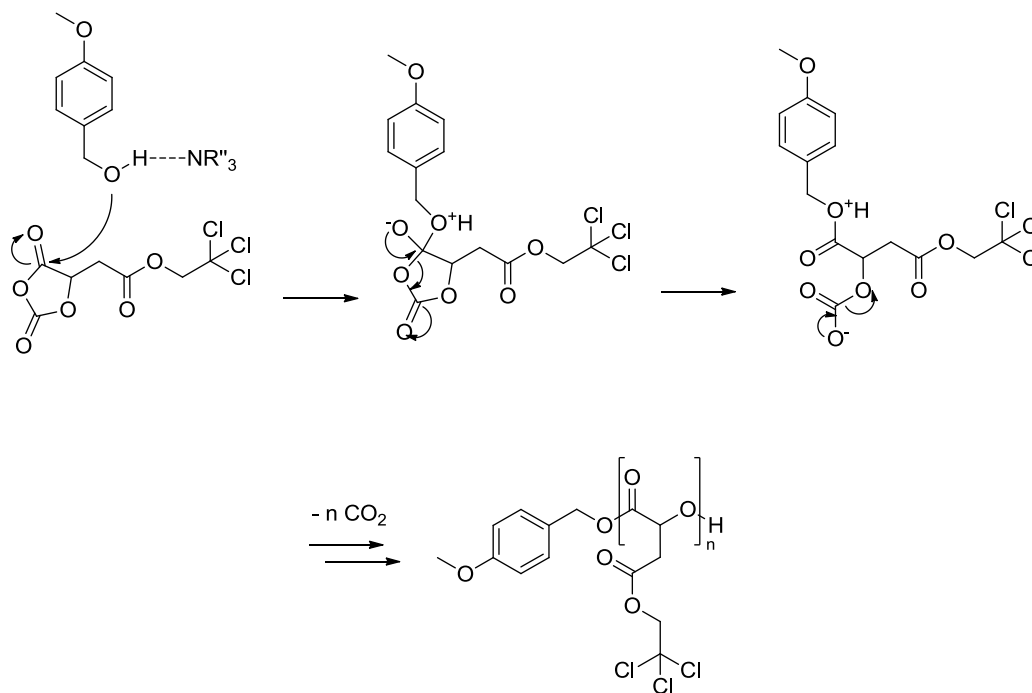


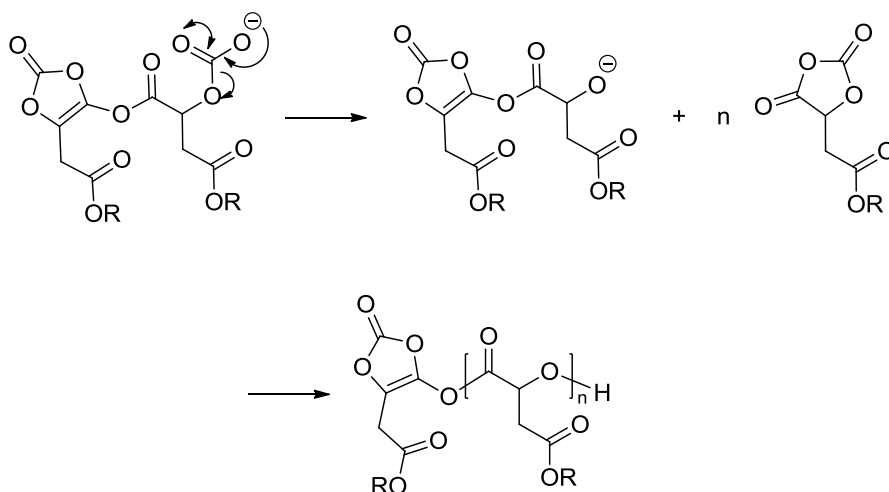
Figure 2.8 - MALDI ToF mass spectrum of P(TCEMA) obtained using 1 equivalent of 4-(dimethylamino)pyridine

The higher intensity distribution observed in the MALDI ToF mass spectrum relates to the P(TCEMA) species obtained through the expected ring-opening mechanism initiating from 4-methoxybenzyl alcohol with the subsequent loss of carbon dioxide from each monomer addition to leave a polymer with a hydroxyl chain-end (Scheme 2.33).⁸⁶



Scheme 2.33 - Desired base-catalysed ring-opening polymerisation mechanism of TCEMalOCA

The secondary mass distribution was attributed to the autoinitiated species of P(TCEMA) resulting from the deprotonation of TCEMalOCA by DMAP (Scheme 2.34). This deprotonation of the acidic methine proton adjacent to the anhydride, results in the formation of an enolate, enabling temporary stabilisation of the anion. This delocalised charge proceeds to ring-open a second monomer ring, leading to propagating of the resulting poly(ester) chain. The original ring is preserved as a chain end after undergoing deprotonation as the anhydride functionality is transformed to give an ester-functionalised five-membered cyclic carbonate.



Scheme 2.34 - Activated monomer mechanism of autoinitiated ring-opening polymerisation of O-carboxyanhydrides

In order to eliminate the side-product as a result of the deprotonation, the pK_a of the catalyst species needed to be reduced. The next trialled catalyst was 4-methoxypyridine (Table 2.1, Entry 2), although this reaction proved to be considerably slower than that using DMAP, taking 3 hours to reach 93% monomer conversion, the GPC analysis of the resulting polymer showed a narrowed distribution ($\mathcal{D} = 1.32$, Figure 2.7). Although the chromatogram showed a slight high molecular weight shoulder, the molecular weight observed by GPC proved to be slightly higher than that obtained using DMAP, ($M_n = 2520 \text{ g}\cdot\text{mol}^{-1}$), however this still failed to meet the expected molecular weight calculated from analysis of the ^1H NMR spectra.

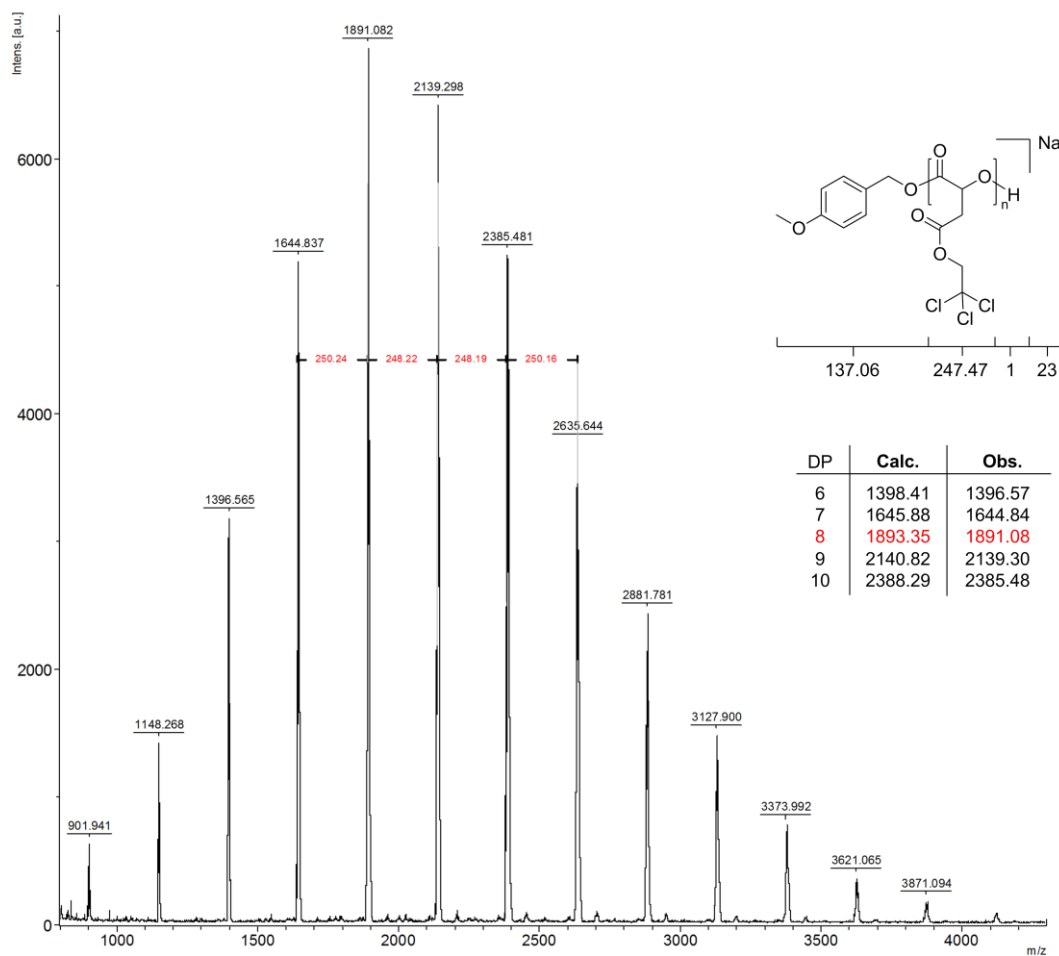


Figure 2.9 - MALDI ToF mass spectrum of P(TCEMA) obtained using 1 equivalent of 4-methoxybenzyl alcohol

Pleasingly, the mass spectra obtained from MALDI ToF MS analysis of the resultant polymer showed the desired result, a single distribution relating to the initiation from 4-methoxybenzyl alcohol to give P(TCEMA).

With the notable improvement in the obtained species, along with the narrowing of the polymer distribution, it was decided to attempt polymerisation with a yet less basic catalyst. To this end, a polymerisation using 4-methylpyridine was attempted, again the reaction proved to be slower, due to a lower affinity for hydrogen bond association with the initiating alcohol. The reaction reached 92% conversion after 4 hours (Table 2.1, Entry 3), however analysis of the final material *via* GPC showed only low weight oligomeric material ($M_n =$

980 g.mol⁻¹ $\bar{D} = 1.45$). Interestingly, the MALDI ToF MS analysis of this material showed a single distribution with considerably higher weights than those suggested by GPC analysis, this distribution again could be attributed to the expected methoxybenzyl-initiated species, with a peak at maximum intensity relating to a polymer with eight repeat units (Figure 2.9).

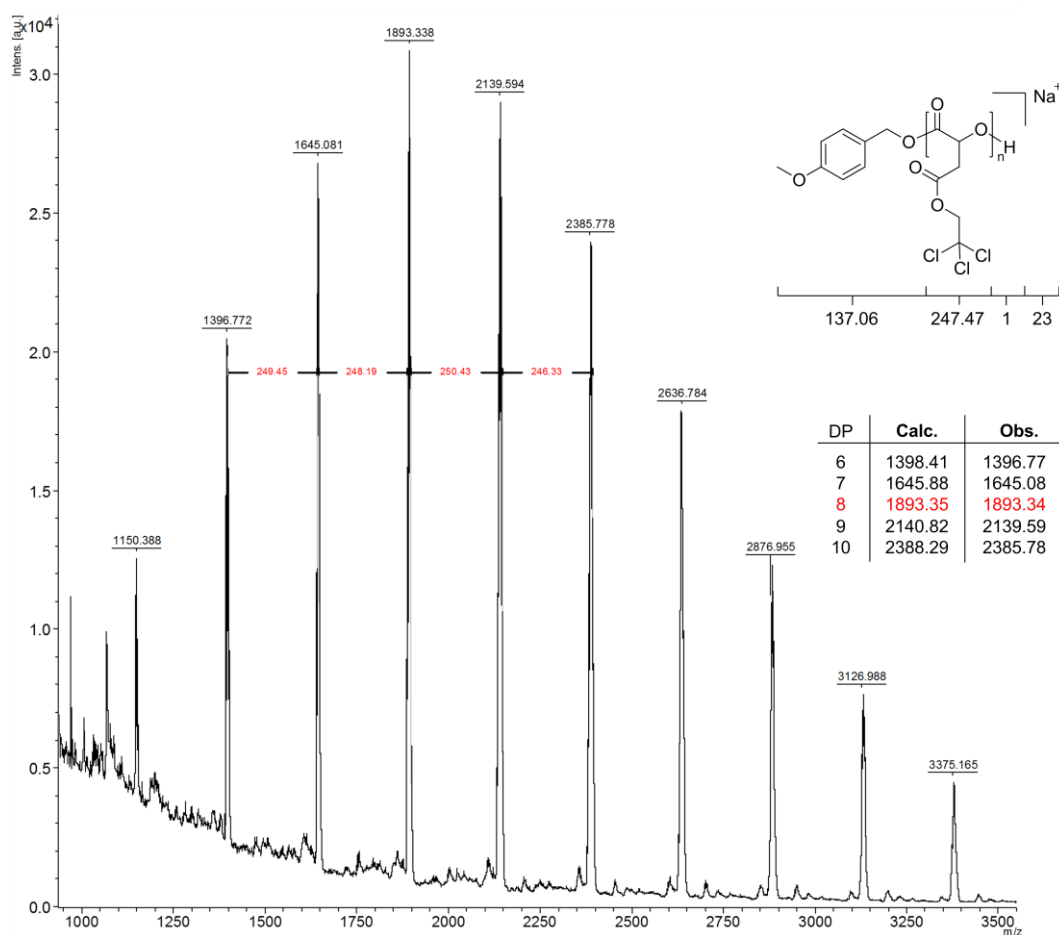


Figure 2.10 - MALDI-ToF mass spectra of P(TCEMA) obtained using 1 equivalent of 4-methylpyridine

Finally, a further reduction in the basicity of the polymerisation catalyst was attempted, with the reaction using pyridine to achieve 94% after 5 hours. Unfortunately the GPC analysis of this polymer showed a material possessing a bimodal distribution (Figure 2.7). Again the corresponding MALDI spectrum showed only a single distribution, still relating to the P(TCEMA) species initiated from 4-methoxybenzyl alcohol (Figure 2.11).

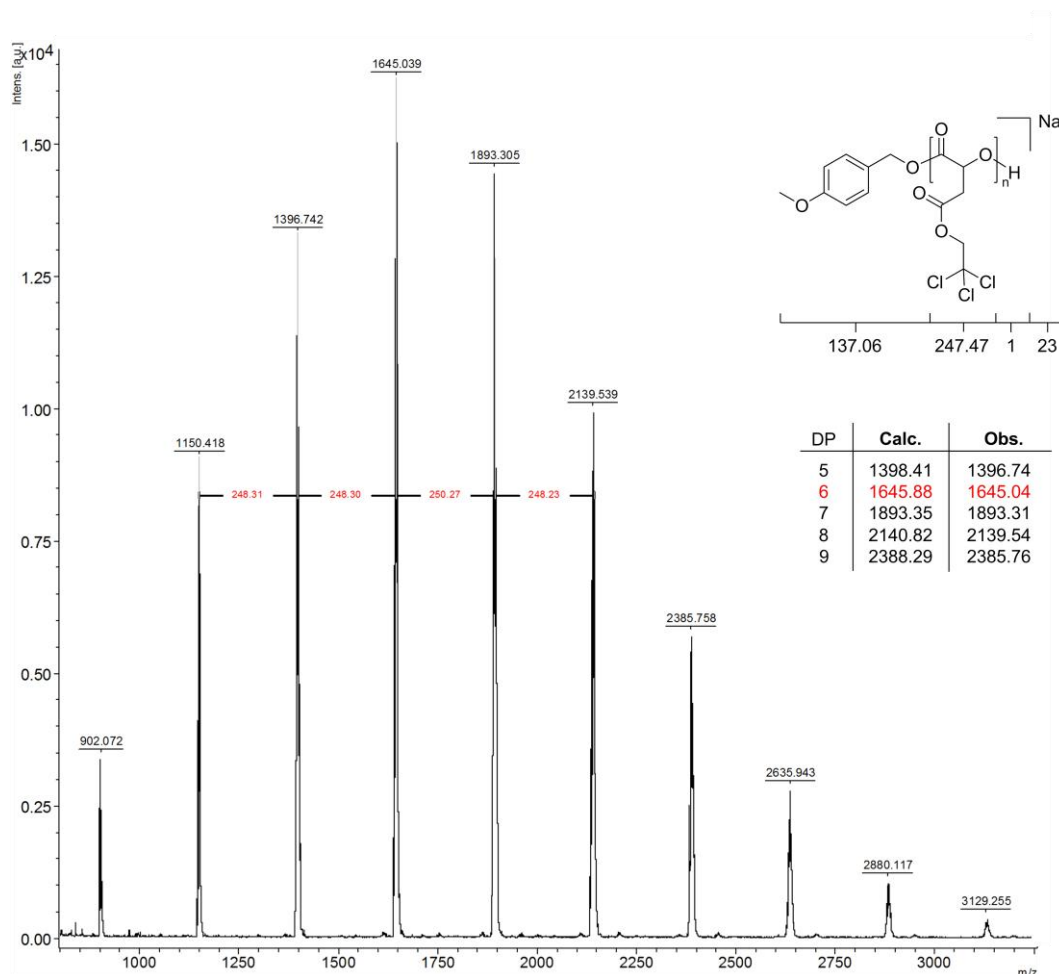


Figure 2.11 - MALDI ToF mass spectrum of P(TCEMA) obtained using 1 equivalent of pyridine

With no notable improvement in the species observed by MALDI ToF mass spectrometry from reduction of the catalyst pK_a below that of 4-methoxypyridine, coupled with the GPC chromatogram showing the narrowest distribution as well as the highest observed molecular weight, it was decided that for further investigation of the ring-opening polymerisation of TCEMalOCA, 4-methoxypyridine would be used as the catalyst of choice.

Table 2.2 - Catalyst equivalent screening for the polymerisation of TCEMalOCA ($[M]_0/[I]_0 = 20$)

Entry	Catalyst (Loading (eq.)) ^a	Monomer Conversion (%) ^b	Time (h)	M_n (g.mol ⁻¹) ^b	M_n (g.mol ⁻¹) ^c	D_M ^c
1	MeOPyr (0.5)	91	7	5414	1380	1.42
2	MeOPyr (1)	93	3	5530	2520	1.32
3	MeOPyr (3)	91	2	5414	2100	1.23
4	MeOPyr (5)	92	1.5	5472	1860	1.40

^a Catalysts equivalents relative to initial alcohol concentration. ^b Calculated by ¹H NMR analysis. ^c Determined by GPC analysis, calibrate against poly(styrene) standards. ^d GPC trace showed bimodal distribution.

Having shown 4-methoxypyridine to have the best apparent control of any of the pyridine catalysts trialled, variation of the equivalents used in the polymerisation was subsequently investigated (Table 2.2).

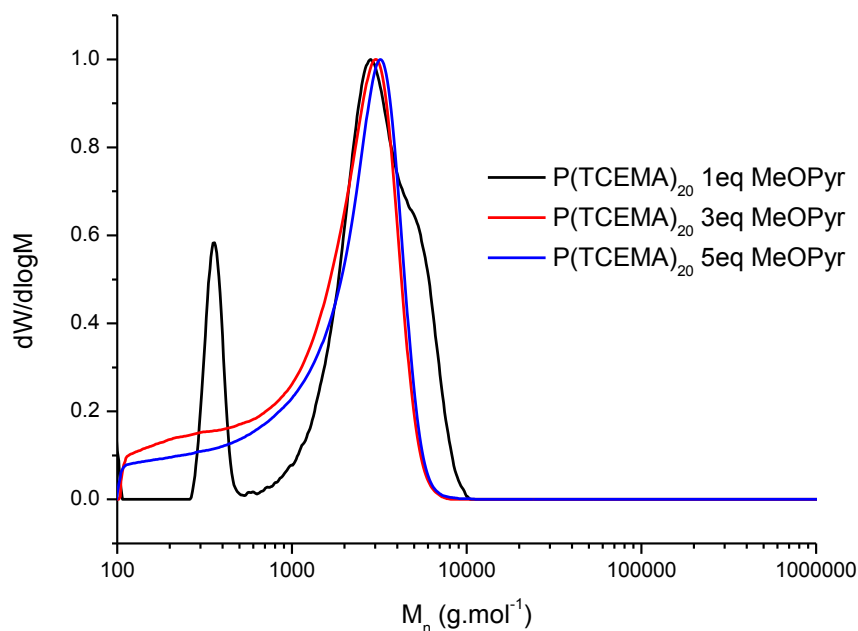


Figure 2.12 - GPC traces of P(TCEMA) obtained using 1,3 and 5 equivalents of 4-methoxypyridine

Shifting the catalyst loading in the opposite direction, the use of 3 equivalents of 4-methoxypyridine led to reaction completion being reached in 2 hours at 91% conversion (Table 2.2, Entry 3). Whilst the GPC analysis showed a unimodal trace with no sign of a high molecular weight shoulder, the observed molecular weight was lower ($M_n = 2090$ g.mol⁻¹, $D = 1.23$) and the chromatogram showed significant tailing at lower weights.

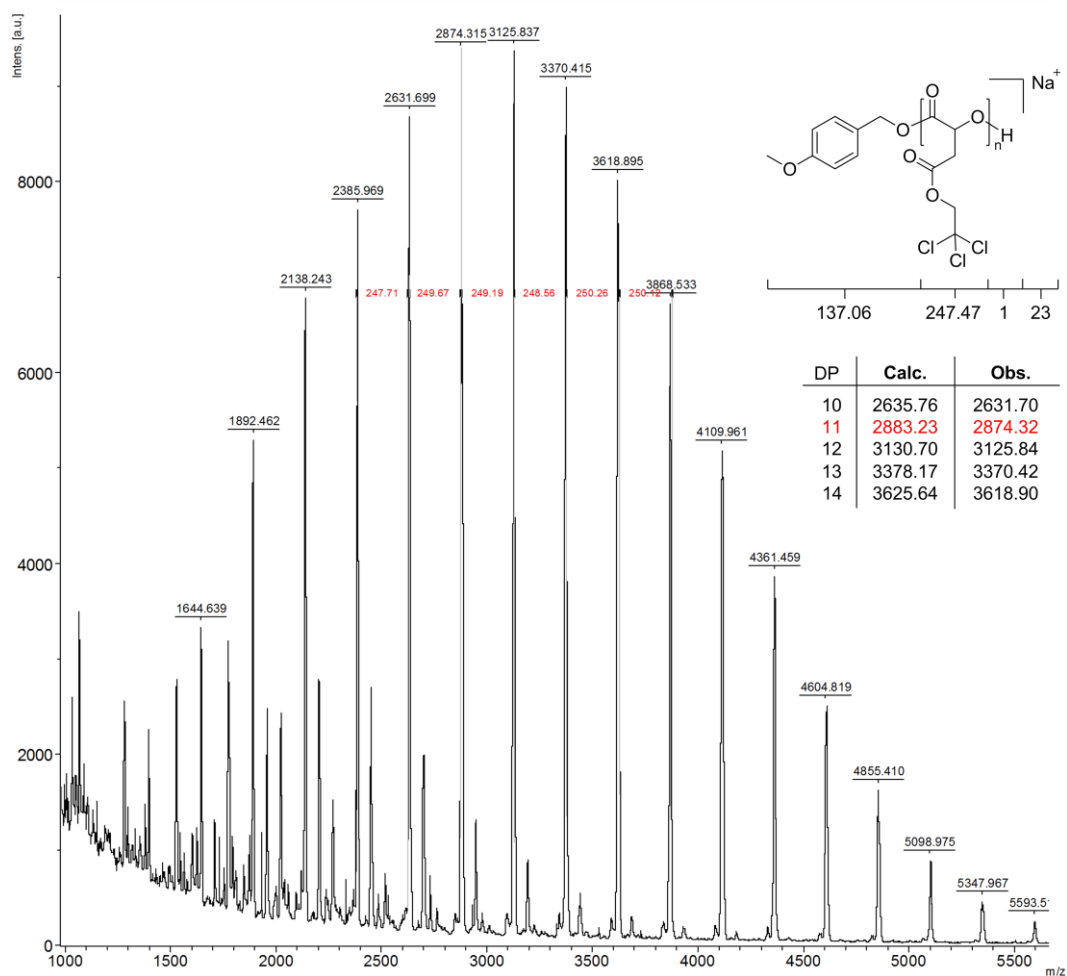
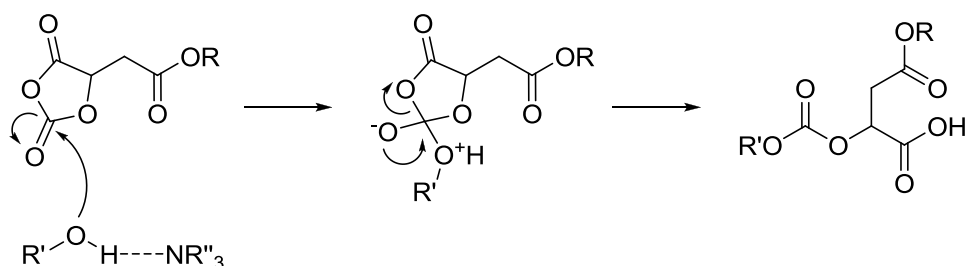


Figure 2.14 - MALDI ToF mass spectrum of P(TCEMA) obtained using 3 equivalents of 4-methoxypyridine

However, despite the apparent improvements to polymer control observed in the GPC chromatogram, analysis of the MALDI ToF mass spectrum showed a secondary distribution alongside the desired polymer species (Figure 2.14). This secondary distribution is

significantly shifted towards lower molecular weights and is attributed to a polymer species in which the alternative carbonyl is subject to nucleophilic attack (Scheme 2.35).



Scheme 2.35 - Ring-opening of O-carboxyanhydrides at the alternative carbonyl leads to carboxylate terminated polymer species

Under this alternative mechanism for the ring-opening of OCAs, the intermediate species created prevents the loss of carbon dioxide, leading to the formation of a carbonate linkage and carboxylic acid end group. The formation of this carboxylate chain end is responsible for the early termination of the polymer chain due to the significantly reduced nucleophilicity compared to the alternative hydroxyl chain end.

Further increase in the catalyst loading, using 5 equivalents of 4-methoxypyridine showed the expected reduction in reaction time, taking 1.5 hours to reach 92% conversion (Table 2.2, Entry 4). The resulting GPC chromatogram shows both a slight reduction in observed molecular weight, and a slight broadening ($M_n = 1860$, $D = 1.40$), although these are not significant changes in comparison to the results obtained using 3 equivalents.

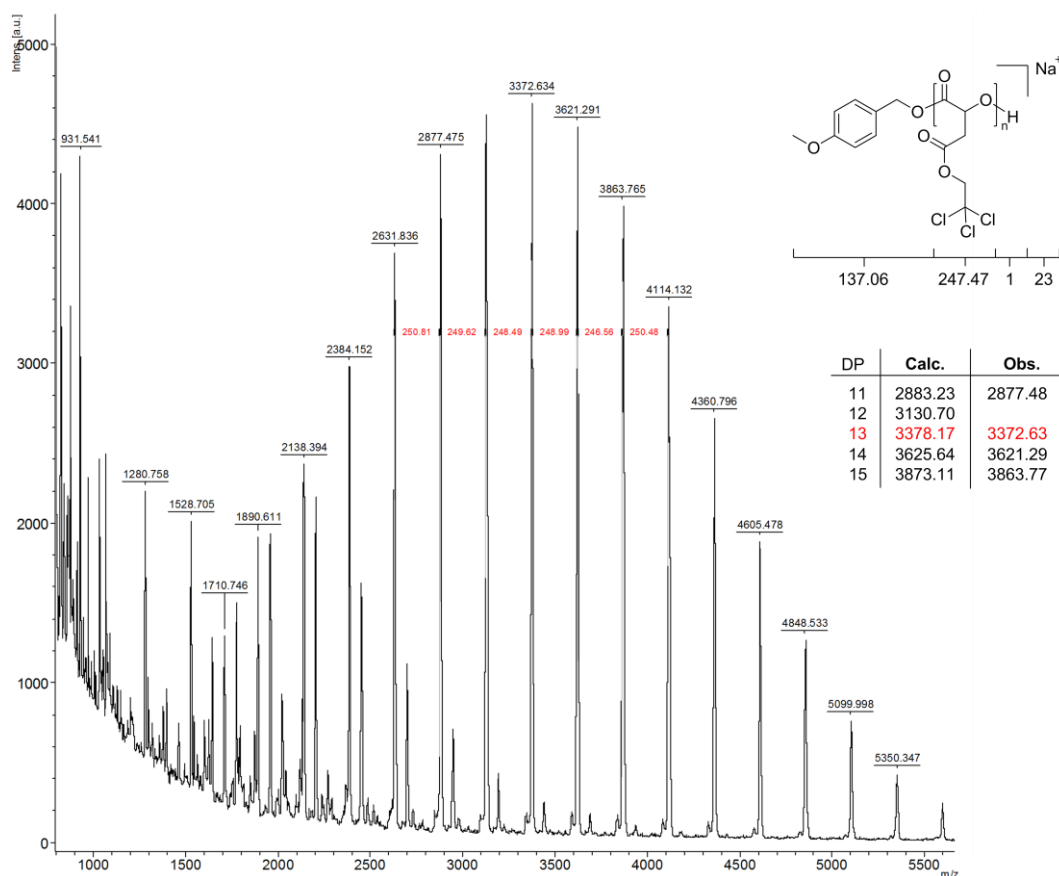


Figure 2.15 - MALDI ToF mass spectrum of P(TCEMA) obtained using 5 equivalents of 4-methoxy pyridine

The results obtained when the polymer was analysed by MALDI ToF MS were equally comparable to those from the previous reaction. The spectrum showed a high molecular weight distribution relating to the desired 4-methoxybenzyl-initiated polymer (Figure 2.15) with a secondary distribution attributed to the mis-insertion of a monomer to yield carboxylate-terminated polymer chains.

With the apparent introduction of different by-products with an increase in the catalyst loading as well as a loss of control from the alternative reduction, it was deemed that a single equivalent of 4-methoxy pyridine remained the optimal catalytic system.

Table 2.3 - Attempted variation of molecular weight for the polymerisation of TCEMalOCA

Entry	Catalyst (Loading (eq.)) ^a	[M] ₀ /[I] ₀ ^b	Monomer Conversion (%) ^b	Time (h)	M _n (g.mol ⁻¹) ^b	M _n (g.mol ⁻¹) ^c	<i>D</i> _M ^c
1	MeOPyr (1)	20	95	3.5	4810	1880	1.17
2	MeOPyr (1)	50	86	6	10712	1720	1.48
3	MeOPyr (1)	75	94	12	17475	2020	1.64
4	MeOPyr (1)	100	92	22	22761	2140	1.60

^a Catalysts equivalents relative to initial alcohol concentration. ^b Calculated by ¹H NMR analysis. ^c Determined by GPC analysis, calibrated against poly(styrene) standards.

Based on the results obtained from the previous screening of catalytic systems, a single equivalent of 4-methoxypyridine relative to alcohol was employed for a further four reactions to investigate the increase of molecular weight with increased starting monomer to initiator ratio. These four reactions were targeted at DPs of 20, 50, 75 and 100.

The reaction times for equilibrium monomer conversion to be reached proved consistent with expectations, requiring 3.5, 6, 12 and 22 hours to reach 95, 86, 94 and 92 % conversion respectively. However, analysis of the resulting polymeric materials showed a lack of any significant variation in the observed molecular weight, or indeed any trend towards increase with increasing target weight.

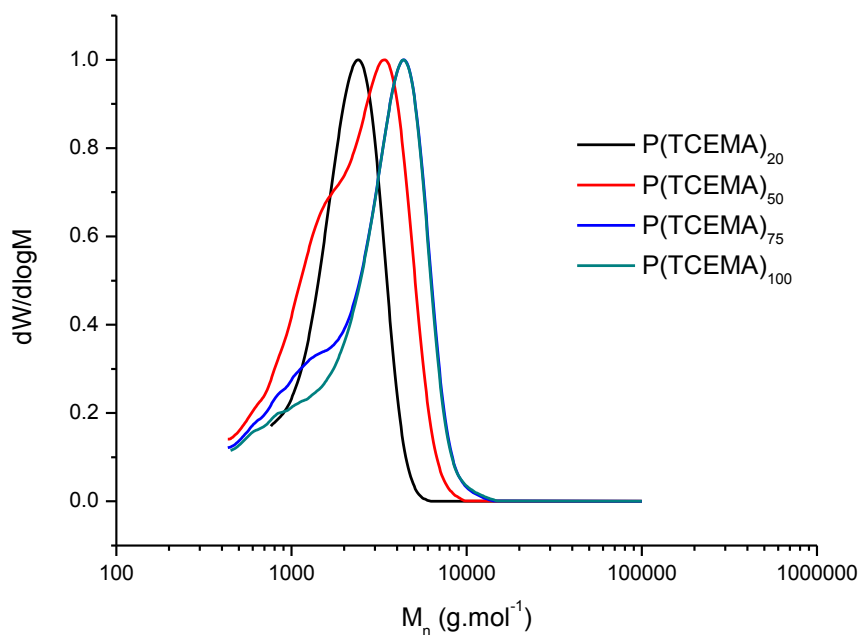


Figure 2.16 - GPC traces of P(TCEMA) obtained using 1 equivalent of 4-methoxypyridine with targeted degrees of polymerisation of 20, 50, 75 and 100

However it was noted that whilst the number-average molecular weights showed no increase, the peak weights observed did show a slight increase, ($M_p = 2500, 3300, 4200$ and 4200 g.mol^{-1}), yet compared to the expected weights as calculated by analysis of the ^1H NMR spectra this increase may be considered insignificant. It is interesting to note that the GPC chromatograms for polymers targeted at DPs of 75 and 100 appear to overlap almost precisely (with the exception of the low-weight shoulders, which appear to decrease with increasing target). This may suggest the presence of some limiting mechanism so far unknown.

2.2.3 Ring-opening polymerisation of (R)-2-nitrobenzyl 2-(2,5-dioxo-1,3-dioxolan-4-yl)acetate

The organocatalysed ring-opening polymerisation of NBMalOCA was investigated using a series of substituted pyridines as catalysts and initiated using 4-methoxybenzyl alcohol. All polymerisations were conducted at a monomer concentration of 0.25 M in dried deuterated chloroform under a dry, inert nitrogen atmosphere. Reaction progress was most easily monitored using ^1H NMR spectroscopy, with the relative concentration of monomer to initiator ($[\text{M}]/[\text{I}]$) determined by the ratio of integrals of the peaks corresponding to the methine proton in the monomer (5.42 ppm) and the methoxy group of 4-methoxybenzyl alcohol (3.68 ppm). Monomer conversion was calculated by comparison of the integrals of the peaks corresponding to the methine proton of the monomer (5.24 ppm) and the methine proton of the polymer (5.63 ppm).

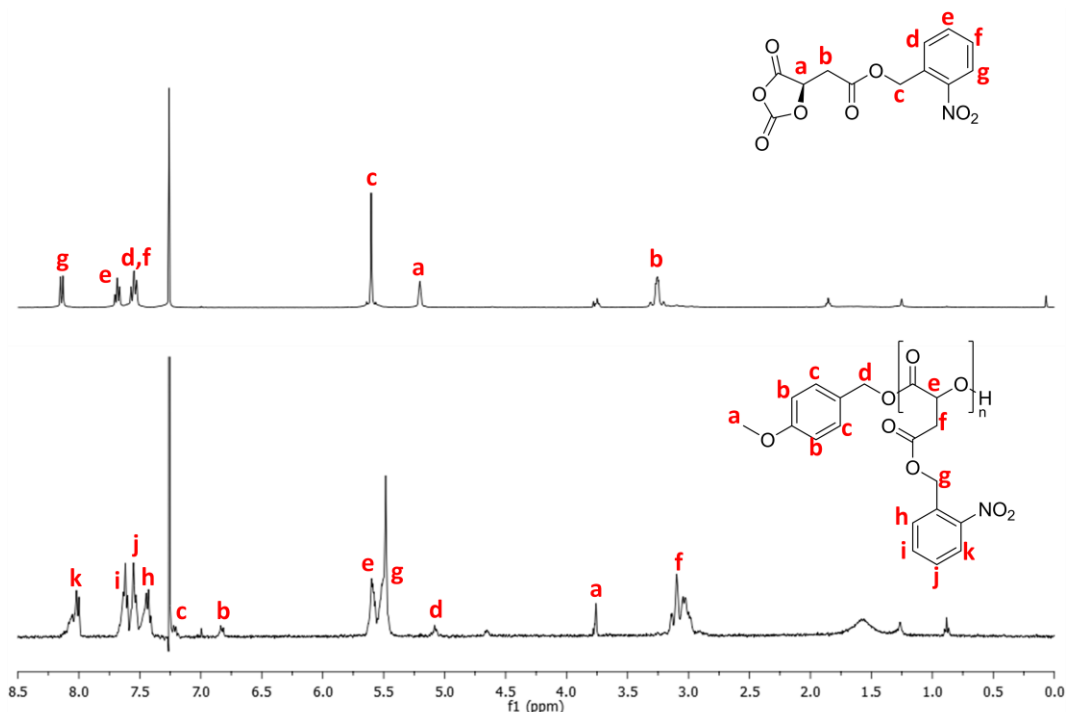
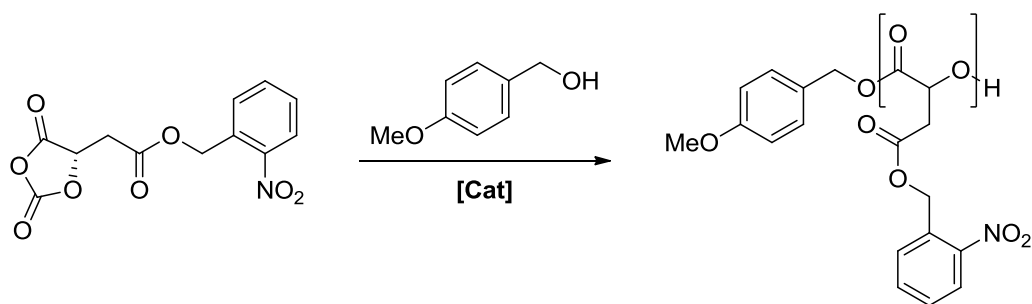
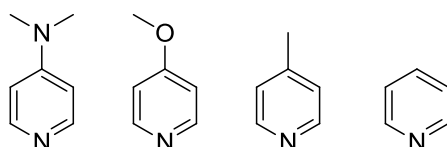


Figure 2.17 - Comparison of ^1H NMR spectra of NBMalOCA and P(NBMA)



Catalysts:



Scheme 2.36 - Ring-opening polymerisation of NBMalOCA from 4-methoxybenzyl alcohol with substituted pyridine catalysts

As with the ring-opening polymerisation of TCEMalOCA, the polymerisation of NBMalOCA was initially investigated using a single equivalent of 4-(dimethylamino)pyridine, 4-methoxypyridine, 4-methylpyridine and pyridine.

Table 2.4 - Catalyst screening for the polymerisation of NBMalOCA ($[M]_0/[I]_0 = 20$)

Entry	Catalyst (Loading (eq.)) ^a	Monomer Conversion (%) ^b	Time (h)	M_n (g.mol ⁻¹) ^b	M_n (g.mol ⁻¹) ^c	D_M^c
1	DMAP (1)	93	1	4810	2040	1.40
2	MeOPyr (1)	78	8	4056	2370	1.38
3	MePyr (1)	93	13	4810	1710	1.46
4	Pyridine (1)	88	22	4559	4720	1.12

^a Catalysts equivalents relative to initial alcohol concentration. ^b Calculated by ¹H NMR analysis. ^c Determined by GPC analysis, calibrated against poly(styrene) standards.

The initial reaction with 1 equivalent of DMAP proceeded more slowly than the corresponding polymerisation of TCEMalOCA, reaching 93% monomer conversion after 1 hour (Table 2.4, Entry 1). As with the previous monomer, the molecular weight observed by GPC analysis proved to be considerably lower than that calculated from analysis of the ^1H NMR spectra ($M_n = 2040$ vs. $4810 \text{ g}\cdot\text{mol}^{-1}$ respectively) with an equally broad dispersity ($\mathcal{D} = 1.40$).

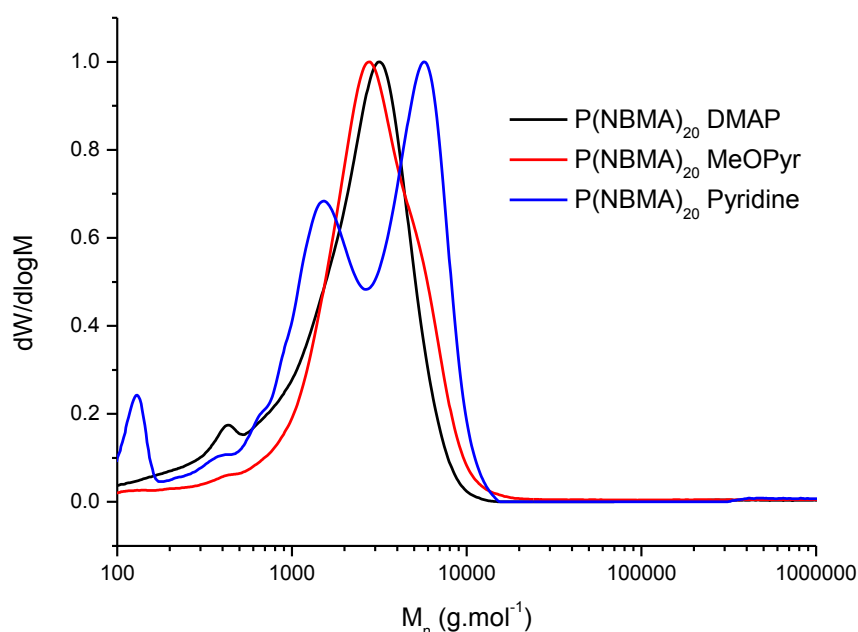


Figure 2.18 - GPC traces of P(NBMA) obtained using 1 equivalent of 4-(dimethylamino)pyridine, 4-methoxypyridine, 4-methylpyridine and pyridine

Analysis of the polymer by MALDI ToF MS showed a main distribution relating to the desired poly(2-nitrobenzylmalic acid), P(NBMA) initiated from 4-methoxybenzyl alcohol. Again, as with the trichloroethyl-functional monomer, a secondary distribution was observed corresponding to the autoinitiated species (Scheme 2.34).

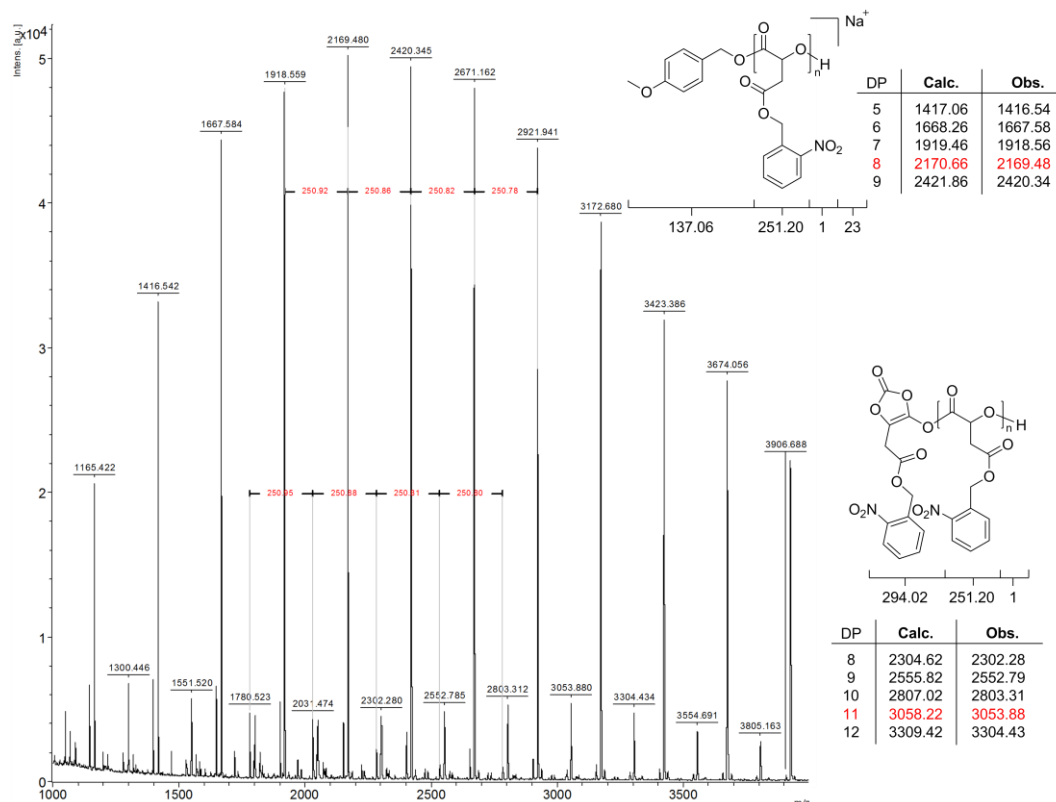


Figure 2.19 - MALDI ToF mass spectrum of P(NBMA) obtained using 1 equivalent of 4-(dimethylamino)pyridine

The use of 4-methoxypyridine as polymerisation catalyst drastically reduced the polymerisation rate, with the reaction reaching only 78% monomer conversion within 8 hours (Table 2.4, Entry 2). Once precipitated, the polymer showed a comparable dispersity ($\mathcal{D} = 1.38$) yet had a raised molecular weight ($M_n = 2370 \text{ g}\cdot\text{mol}^{-1}$) as observed by GPC, this higher value for the molecular weight may be considered a significant improvement when allowing for the comparatively low conversion.

Interestingly, unlike the corresponding reaction for the polymerisation of TCEMalOCA, the MALDI ToF spectrum still showed a significant quantity of autoinitiated P(NBMA) (Figure 2.20).

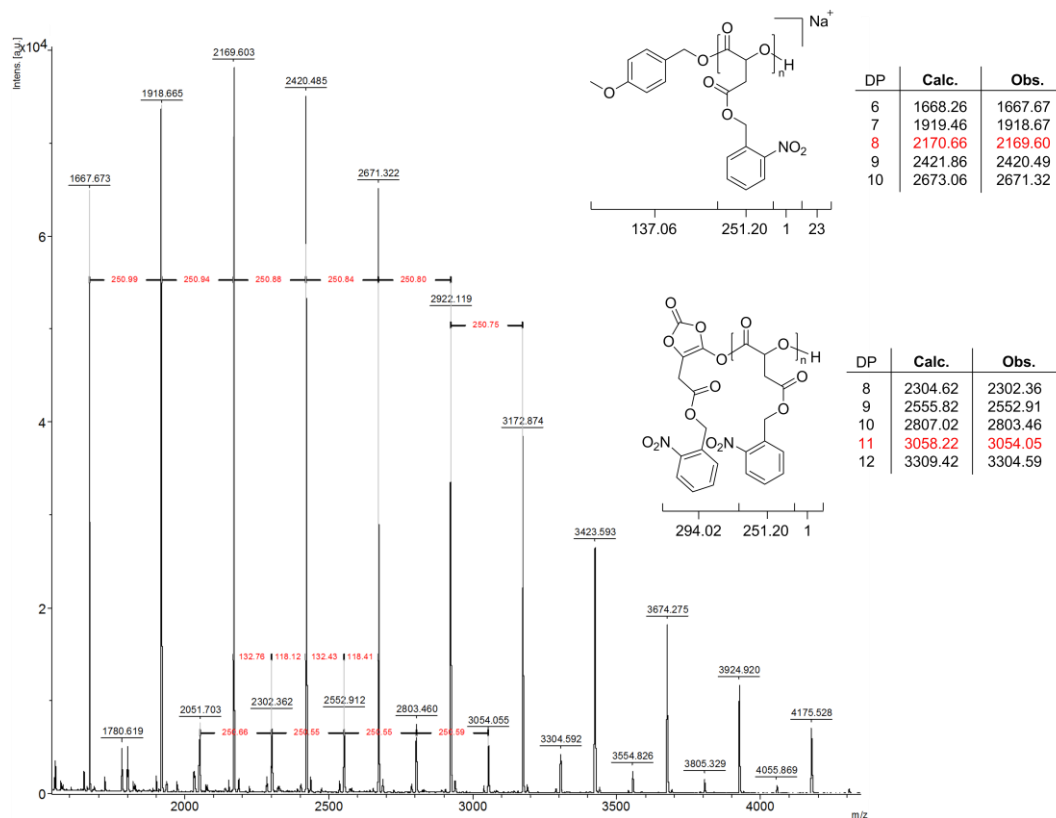


Figure 2.20 - MALDI ToF mass spectrum of P(NBMA) obtained using 1 equivalent of 4-methoxybenzylpyridine

Subsequent polymerisation of NBMA/OCA using a single equivalent of 4-methylpyridine reached equilibrium after 13 hours at 93% conversion, however the results obtained from GPC analysis showed an anomalously low molecular weight with a slightly broadened dispersity ($M_n = 1710 \text{ g.mol}^{-1}$, $D = 1.46$). Further analysis of the resultant polymeric material by MALDI ToF MS again showed a major distribution relating to the methoxybenzyl-initiated P(NBMA), the spectrum also contained a secondary distribution relating to the autoinitiated species.

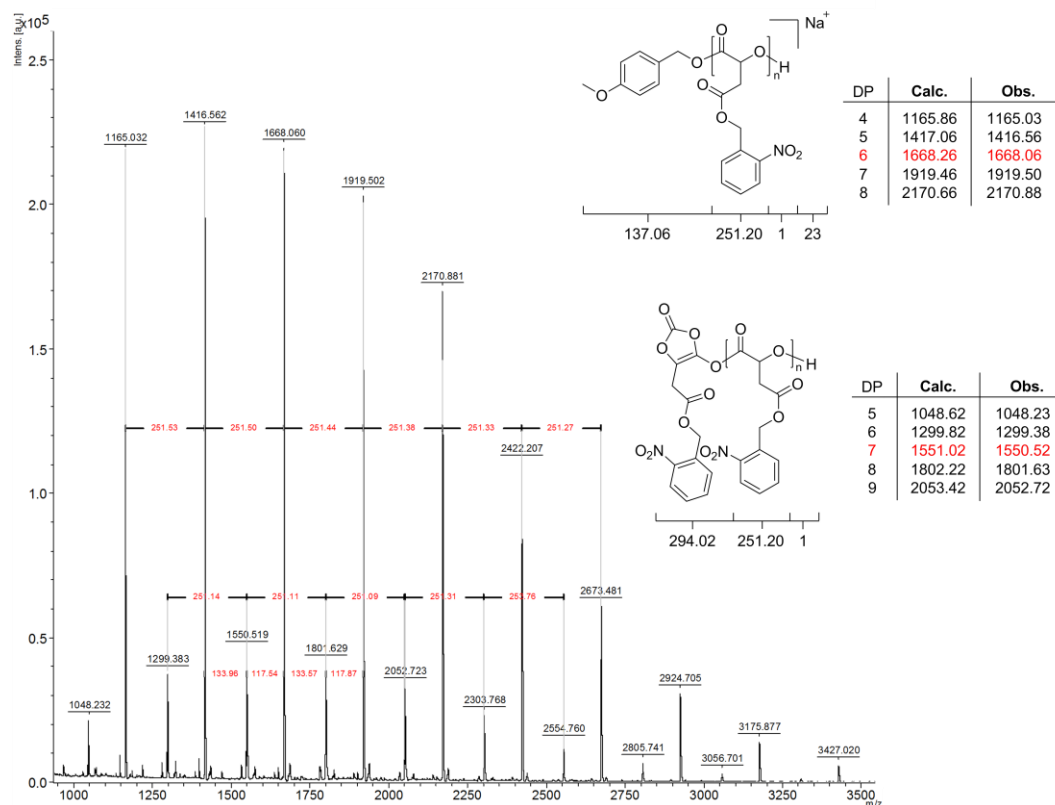


Figure 2.21 - MALDI ToF mass spectrum of P(NBMA) obtained using 1 equivalent of 4-methylpyridine

In a final attempt to enable the elimination of the autoinitiated polymeric side product, the catalyst pK_a was again reduced significantly by switching to the use of 1 equivalent of pyridine (Table 2.4, Entry 4). The reaction proceeded very slowly, finally reaching equilibrium at 88% monomer conversion after 22 hours. However the GPC analysis showed a well-separated bimodal distribution, with the higher molecular weight distribution showing a molecular weight in reasonable agreement with that calculated from the ^1H NMR spectrum ($M_n = 4720$ vs. 4559 $\text{g}\cdot\text{mol}^{-1}$) and a roughly calculated narrow dispersity ($D = 1.12$).

Even with the reduction in pK_a that comes with using pyridine, the MALDI ToF mass spectrum showed a small distribution corresponding to the autoinitiation of NBMA/OCA. Interestingly, the main distribution, relating to the methoxybenzyl-initiated P(NBMA),

showed none of the high molecular weight material implied by the GPC chromatogram, instead the distribution had the lowest peak of any catalyst screened.

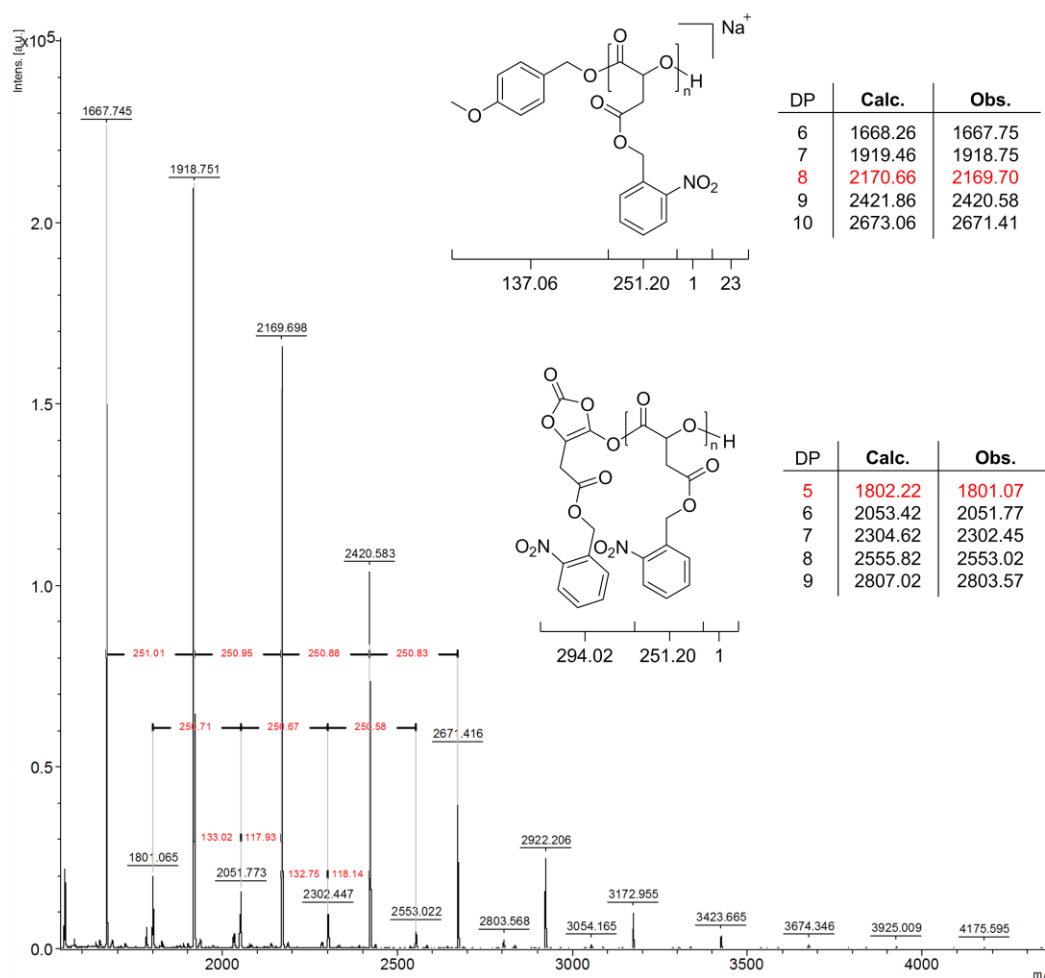


Figure 22 - MALDI ToF mass spectrum of P(NBMA) obtained using 1 equivalent of pyridine

Unlike the corresponding catalyst screen for the polymerisation of TCEMalOCA, reduction of the catalyst pK_a showed no significant effect on the elimination of the autoinitiated polymeric species from the reaction. As previously determined for TCEMalOCA, 4-methoxypyridine was determined to be the preferred catalyst for the ring-opening polymerisation of NBMAOCA.

Table 2.5 - Catalyst equivalent screening for the polymerisation of NBMAOCA ($[M]_0/[I]_0 = 20$)

Entry	Catalyst (Loading (eq.)) ^a	Monomer Conversion (%) ^b	Time (h)	M_n ($\text{g}\cdot\text{mol}^{-1}$) ^b	M_n ($\text{g}\cdot\text{mol}^{-1}$) ^c	\mathcal{D}_M ^c
1	MeOPyr (0.5)	75	23	3906	1410	1.51
2	MeOPyr (1)	78	8	4056	2370	1.38
3	MeOPyr (3)	84	5	4358	1150	1.76
4	MeOPyr (5)	81	3	4207	1260	1.79

^a Catalysts equivalents relative to initial alcohol concentration. ^b Calculated by ¹H NMR analysis. ^c Determined by GPC analysis, calibrated against poly(styrene) standards.

The screening of catalyst equivalent variation was initially conducted with a reduction of catalyst loading, using 0.5 equivalents (Table 2.5, Entry 1). Compared to the use of a single equivalent, the reaction proceeded unexpectedly slow, taking 23 hours to reach only 75% monomer conversion.

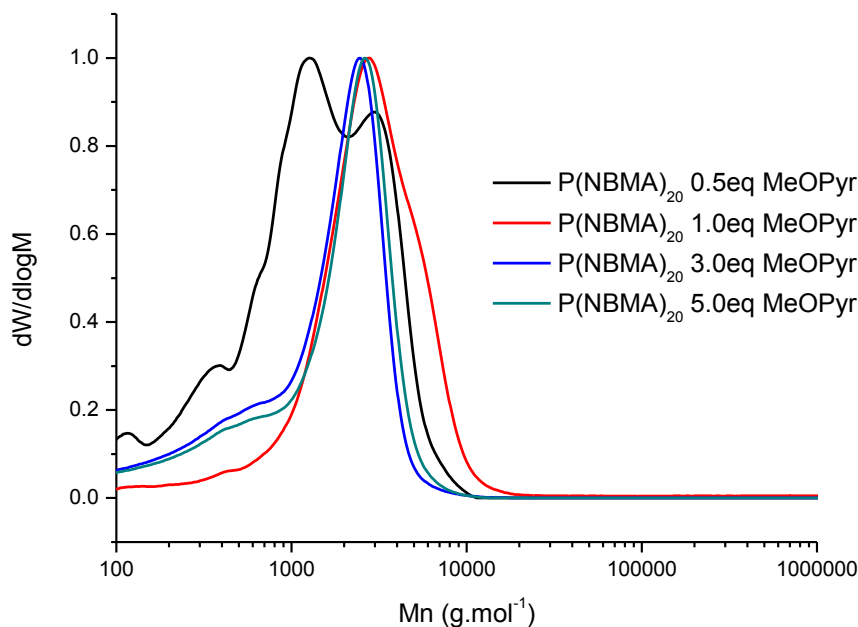


Figure 2.23 - GPC traces of P(NBMA) obtained using 0.5, 1, 3 and 5 equivalents of 4-methoxy pyridine

Having been quenched and precipitated at 75% conversion, the GPC analysis showed a significantly bimodal distribution, with a molecular weight far lower than that expected from analysis of the ^1H NMR spectra or compared to the weights observed for the use of a single equivalent of 4-methoxyppyridine ($M_n = 1410 \text{ g}\cdot\text{mol}^{-1}$, $\bar{D} = 1.51$). The MALDI ToF MS analysis showed a major distribution relating to the desired methoxybenzyl-initiated polymeric species, it also showed a series of minor distributions, one of which relates to the autoinitiation of NBMAOCA.

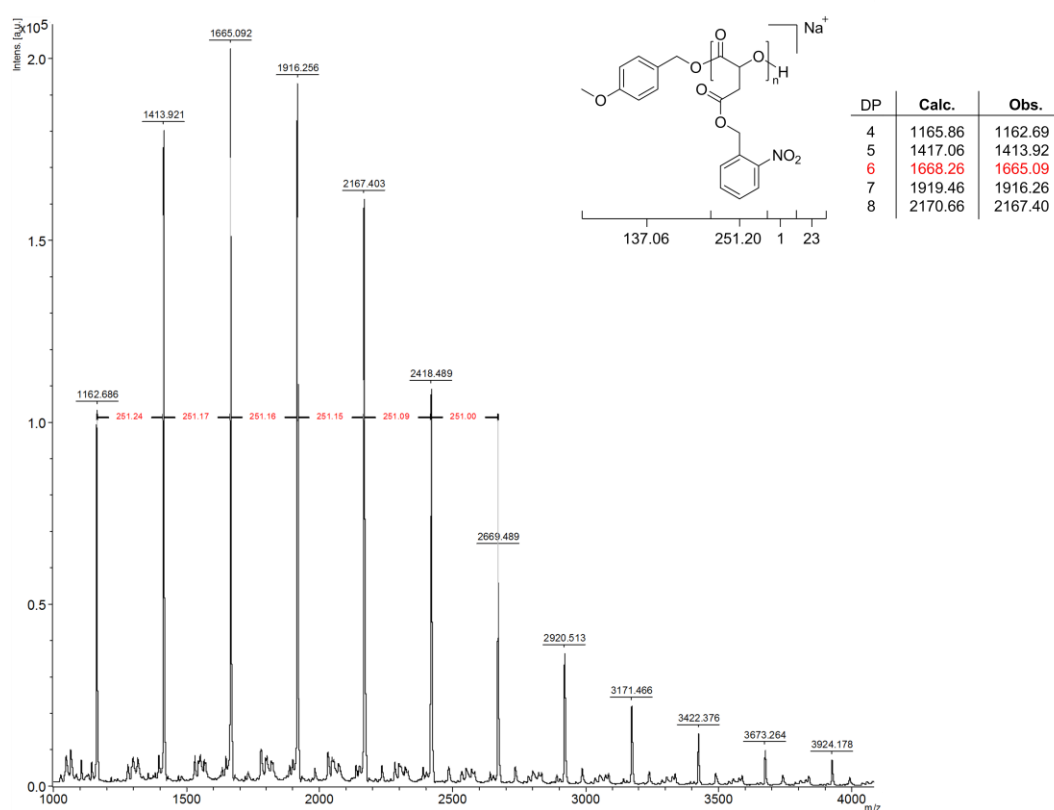


Figure 2.24 - MALDI ToF mass spectrum of P(NBMA) obtained using 0.5 equivalents of 4-methoxyppyridine

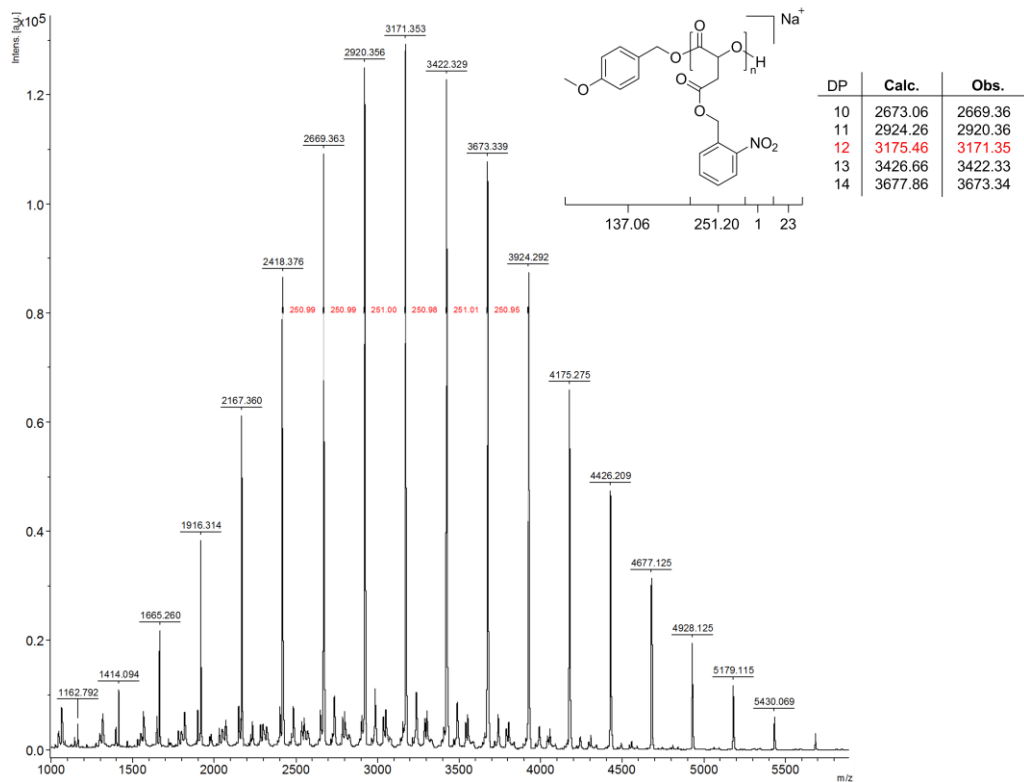


Figure 2.25 - MALDI ToF mass spectrum of P(NBMA) obtained using 3 equivalents of 4-methoxy pyridine

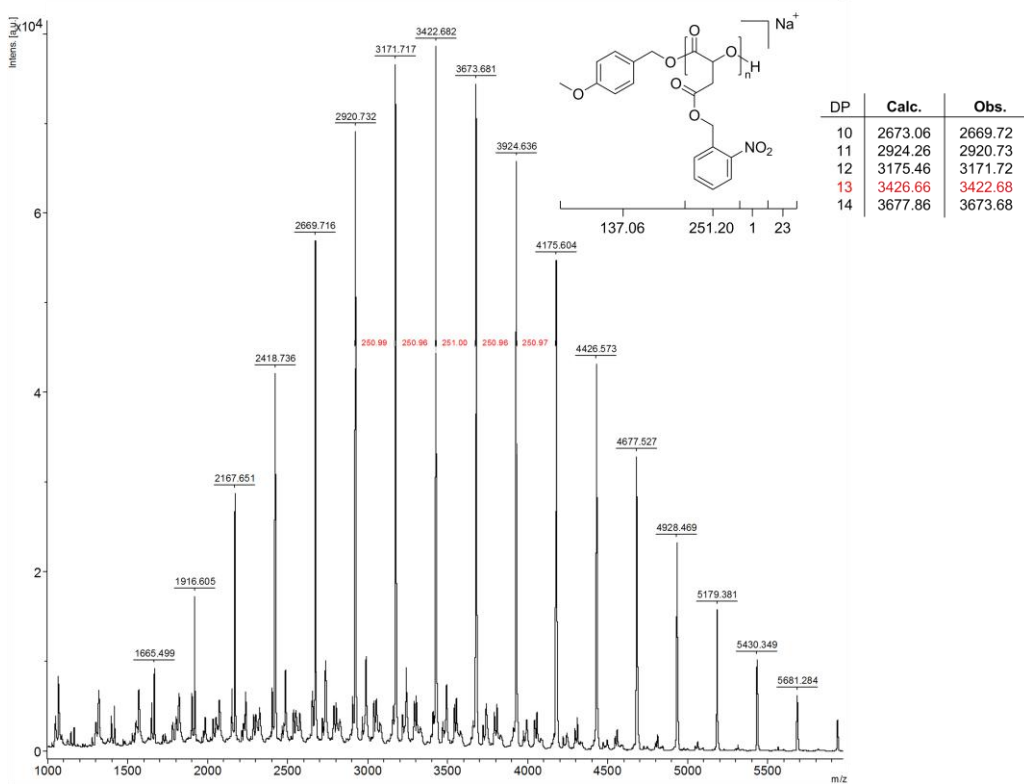


Figure 2.26 - MALDI ToF mass spectrum of P(NBMA) obtained using 5 equivalents of 4-methoxy pyridine

The reactions using both 3 and 5 equivalents of 4-methoxypyridine reached 84 and 81% conversion after 5 and 3 hours respectively. The GPC analyses of both polymers were very closely matched, both showed a significant low weight tail and reported low observed molecular weights (M_n) of 1148 and 1262 $\text{g}\cdot\text{mol}^{-1}$ respectively ($\mathcal{D} = 1.76$ and 1.79).

The MALDI ToF mass spectra of both polymers showed several minor distributions alongside the expected methoxybenzyl-initiated species. Of these minor distributions, masses corresponding to both autoinitiated and mis-inserted monomer species could be identified.

With the bimodality of 0.5 equivalents and the development of mis-inserted monomer units with both 3 and 5 equivalents, it was decided that the use of a single equivalent of 4-methoxypyridine was again the best of the screened catalyst systems.

Table 2.6 - Attempted variation of molecular weight for the polymerisation of NBMaIOCA

Entry	Catalyst (Loading (eq.)) ^a	$[M]_0/[I]_0$ ^b	Monomer Conversion (%) ^b	Time (h)	M_n ($\text{g}\cdot\text{mol}^{-1}$) ^b	M_n ($\text{g}\cdot\text{mol}^{-1}$) ^c	\mathcal{D}_M ^c
1	MeOPyr (1)	20	81	9	4056	1730	1.42
2	MeOPyr (1)	50	84	17	10688	2800	1.95
3	MeOPyr (1)	75	82	26	15587	2510	1.75

^a Catalysts equivalents relative to initial alcohol concentration. ^b Calculated by ¹H NMR analysis. ^c Determined by GPC analysis, calibrated against poly(styrene) standards.

In an attempt to vary the molecular weight with respect to the monomer to initiator ratio, reactions using a single equivalent of 4-methoxypyridine were conducted starting monomer to initiator ratios of 20, 50 and 75. These reactions reached equilibrium conversion (81, 84 and 82%) within 9, 17 and 26 hours respectively. However there again appears to be little trend in the molecular weights obtained with variation of the monomer to initiator ratio, with

GPC analyses showing M_n values of 1730, 2790 and 2510 $\text{g}\cdot\text{mol}^{-1}$, all three polymers showed severe low weight shouldering, becoming bimodal for the reactions targeted at DP 50 and 75 (Figure 2.27).

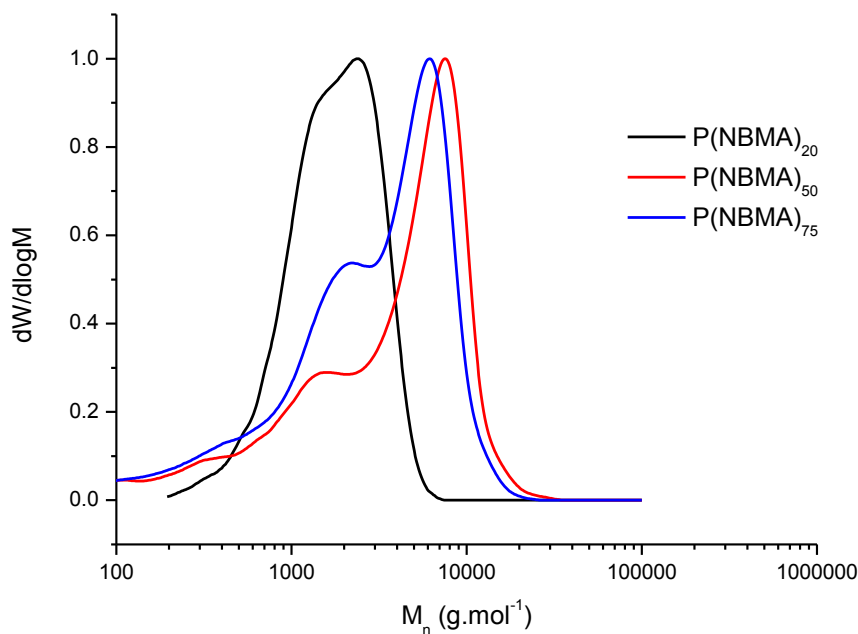


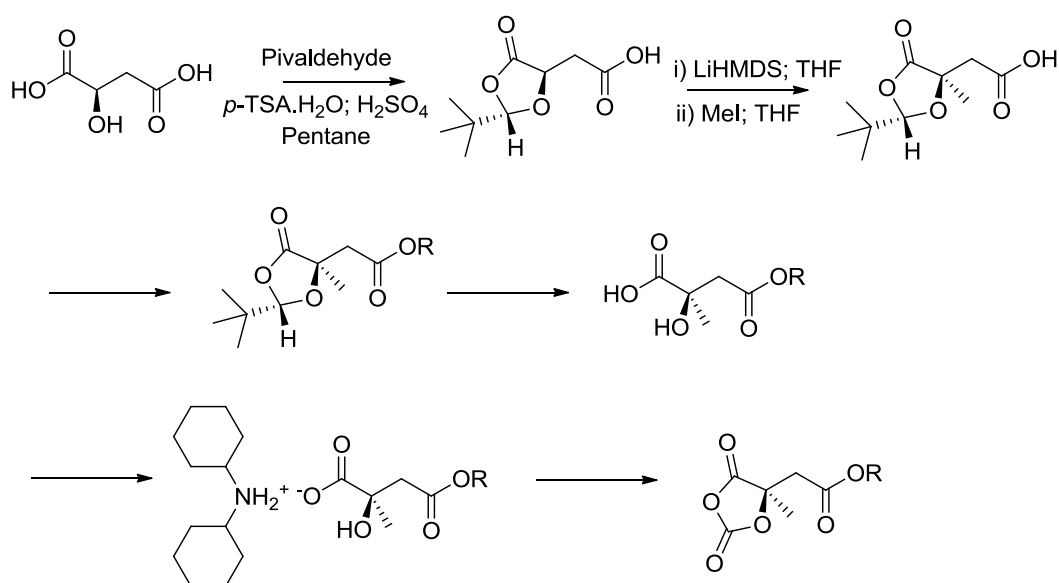
Figure 2.27 - GPC traces of P(NBMA) obtained targeting degrees of polymerisation of 20, 50 and 75

As with the trichloroethyl-functionalised MalOCA, there seems to be little control over the molecular weight obtained based on variation of reaction conditions, pointing to a potential issue with the monomer reactivities. A loss of control for both monomers is potentially attributed to the number of side-reactions possible.

2.4 Conclusions and Future Work

The synthesis of two novel *O*-carboxyanhydride monomers has been achieved via a common synthetic route, allowing for the inclusion of a potentially wide range of functionalities. The ring-opening polymerisation of both monomers was attempted and screened using a selection of substituted pyridine catalysts. However, all reactions produced material with lower molecular weights and broader dispersities than desirable. The lack of fine control over the polymerisations of both monomers was attributed to numerous side reactions as a result of the monomer core structure.

It should be possible to eliminate the autoinitiation of the *O*-carboxyanhydrides by simply eliminating the acidic methine proton adjacent to the ring. This could easily be achieved by the chiral methylation of malic acid as reported by Seebach *et al.*⁸⁷



Scheme 2.37 - Proposed chiral methylation of *l*-malic acid to eliminate autoinitiation of functionalised MalOCAs

Chapter 3

Synthesis and ring-opening polymerisation of functional chiral cyclic
carbonates derived from *L*-leucine

3.1 Introduction

Although cyclic carbonates are an abundant and commonly-used route in the synthesis of poly(carbonate)s, the synthesis of chiral poly(carbonate)s is surprisingly under-reported for the amount of interest that the resulting materials garner from the biomedical community. The inclusion of stereocentres in poly(carbonate)s has typically been achieved *via* synthesis from chiral starting materials such as sugars (Figure 3.28).^{33,88} As well as allowing for the introduction of a large number of chiral centres to the monomer the addition of sugar moieties gives rise to a dramatic increase in the biocompatibility of the corresponding poly(carbonate)s.

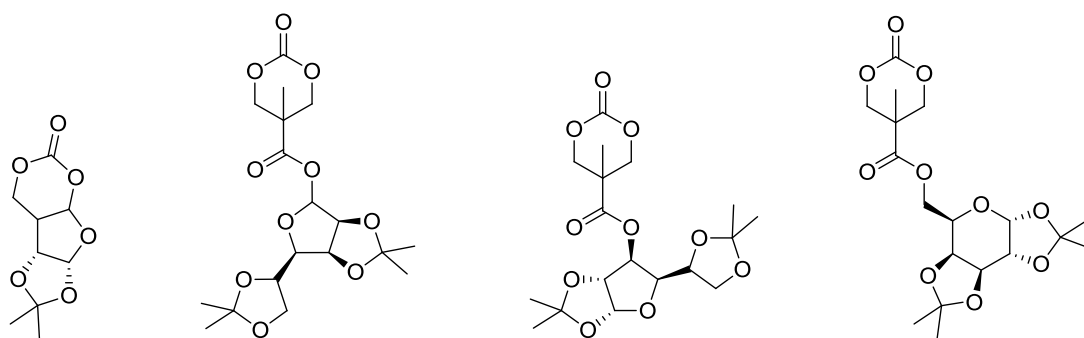
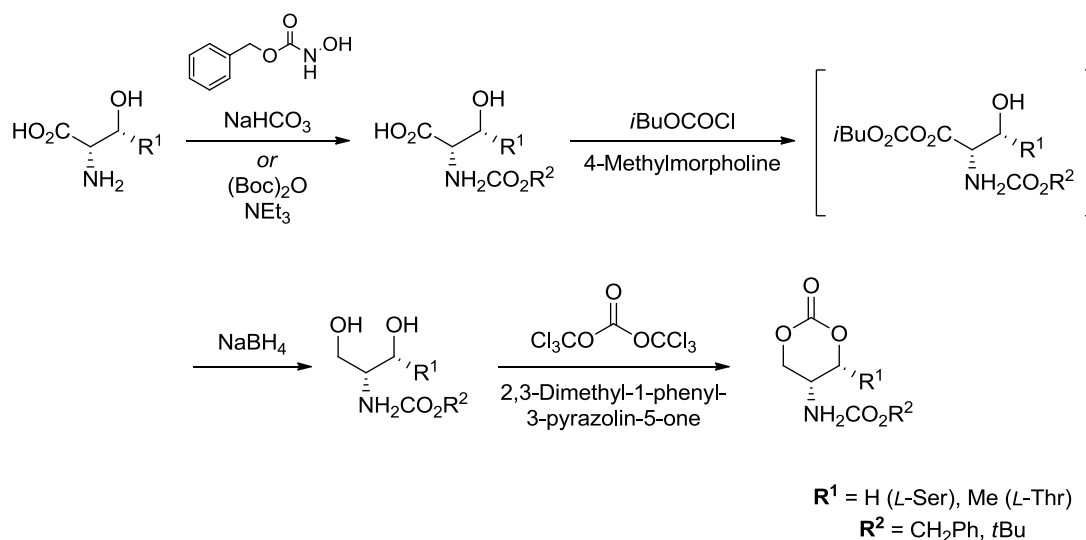


Figure 3.28 - Cyclic carbonates functionalised with pendant sugar moieties

Whilst Endo and co-workers have reported the synthesis of cyclic carbonates derived from the amino acids *L*-serine and *L*-threonine (Scheme 3.38), the possibilities for functionalisation are mostly limited to the protection of the amino functionality.⁸⁹



Scheme 3.38 - Synthesis of cyclic carbonates derived from *L*-serine and *L*-threonine as reported by Endo and co-workers

The addition of functionality to an amino acid through the formation of the corresponding ester would allow for access to a wider range of useful monomers. The inherently chiral amino ester could subsequently be tethered to a cyclic carbonate framework through formation of an amide linkage. Hedrick and co-workers have previously reported the use of 2,2-bis(hydroxymethyl)propionic acid (*bis*MPA) as a useful framework for the synthesis of cyclic carbonates bearing a wide range of functionalities.^{78,79}

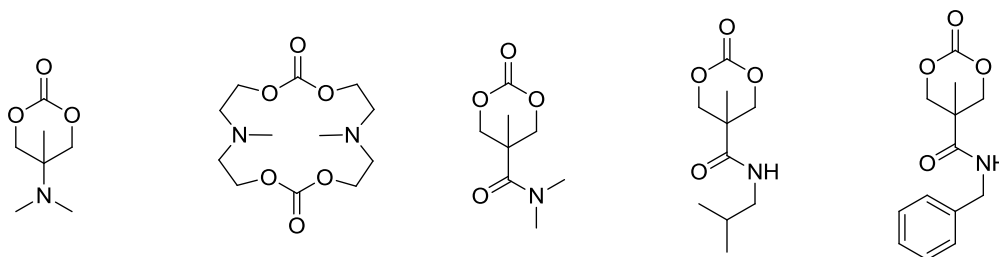


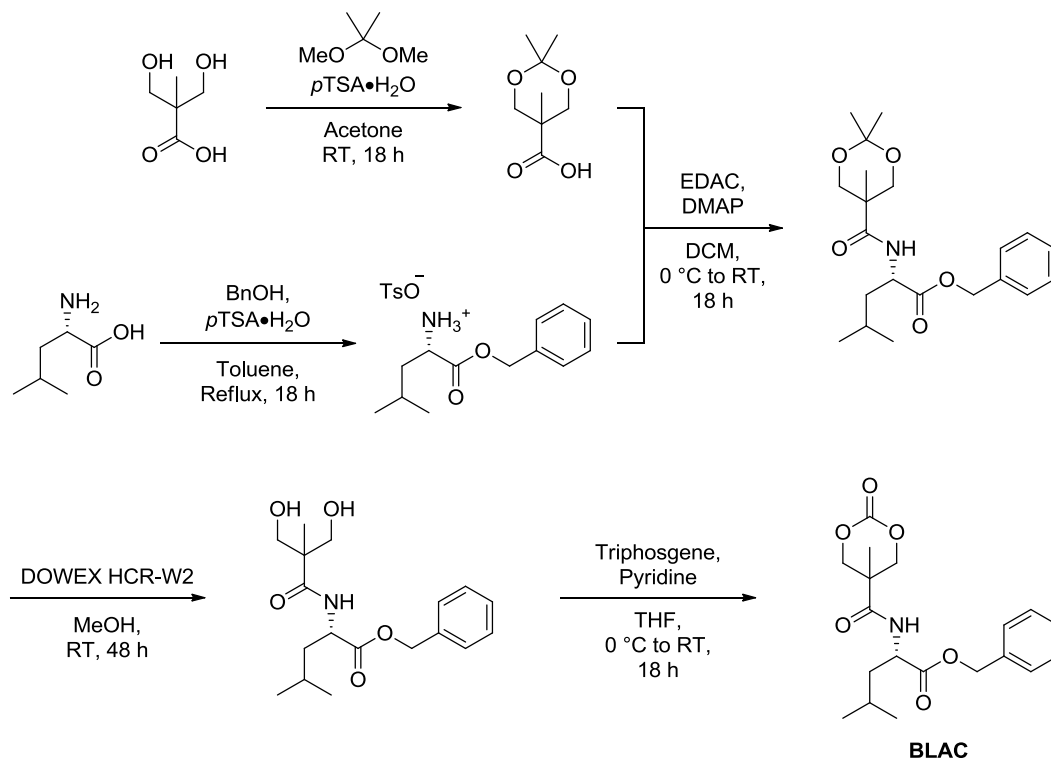
Figure 3.29 - Selection of reported amino- and amido-functionalised cyclic carbonates

Whilst the majority of nitrogen-containing cyclic carbonates possess carbamate or urea functionalities,⁸⁹⁻⁹¹ a few amine-containing monomers have been reported (Figure 3.29).^{92,93} However, of those cyclic carbonates that incorporate amide functionalities, the only reports of polymerisation relate to those bearing tertiary amides. For secondary amides, only the monomer synthesis is reported.^{78,79}

3.2 Results and Discussion

3.2.1 Synthesis of (S)-Benzyl 4-methyl-2-(5-methyl-2-oxo-1,3-dioxane-5-carboxamido)pentanoate

The synthesis of a cyclic carbonate species containing pendant amino ester functionality was achieved using the synthetic scheme shown in Scheme 3.39. This initially involved the synthesis of *O*-benzyl-*L*-leucine tosylate, *via* esterification of *L*-leucine with benzyl alcohol and *p*-toluenesulfonic acid monohydrate under reflux in toluene whilst fitted with Dean-Stark apparatus to allow removal of the water produced over the course of the reaction. In parallel with the synthesis of the benzyl ester, the acetonide-protection of 2,2-*bis*(methylhydroxy)propionic acid (*bis*MPA) was conducted using 2,2-dimethoxypropane and *p*-toluenesulfonic acid monohydrate, this framework has been used to great effect to allow access to functionalised cyclic carbonates since its initial use by Hedrick and co-workers.^{78,79}

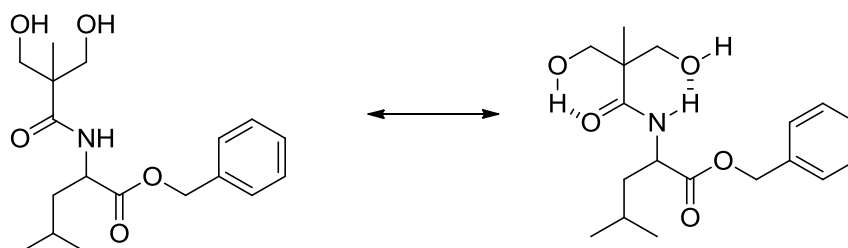


Scheme 3.39 – Synthesis of *O*-benzyl-*L*-leucine carbonate (BLAC)

Once the synthesis of the acetonide-protected *bis*MPA and *O*-benzyl-*L*-leucine tosylate was complete, they could be coupled *via* a modified Steglich coupling, using *N*-(3-dimethylaminopropyl)-*N'*-ethylcarbodiimide hydrochloride (EDAC) to give the amido species. Deprotection of the acetonide was achieved by reaction with DOWEX HCR-W2 acidic resin in methanol, liberating the desired diol in very good yield. Finally, the cyclisation to the final amido-carbonate (BLAC) was achieved by reaction of the diol with triphosgene in the presence of pyridine in tetrahydrofuran.

It should be noted that several solvents were trialled for this cyclisation, including DCM, dioxane and tetrahydrofuran, however, the desired cyclisation product was only observed when the reaction was conducted in tetrahydrofuran. Such selectivity can be explained by the ability of tetrahydrofuran to disrupt hydrogen bonding in dissolved species. In other non-disruptive solvents, it seems plausible that the amido-diol forms a stable six-membered

species by hydrogen bonding between the amide proton and one of the hydroxyl oxygens (Scheme 3.40), preventing the diol from achieving the configuration required to allow for cyclisation to the corresponding carbonate.



Scheme 3.40 - "Free" diol species and hydrogen-bond stabilised bicyclic diol species

Pleasingly, the cyclisation in THF was achieved in good yield with the monomer being purified *via* column chromatography on silica gel to yield pure BLAC (Figure 3.30).

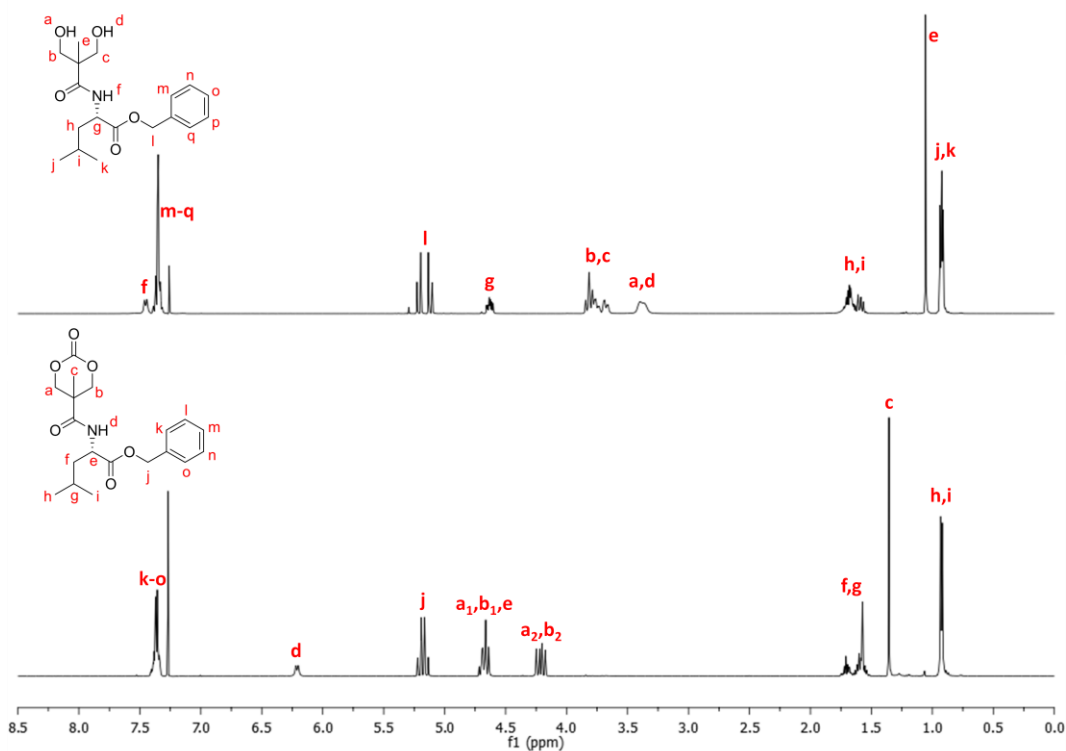
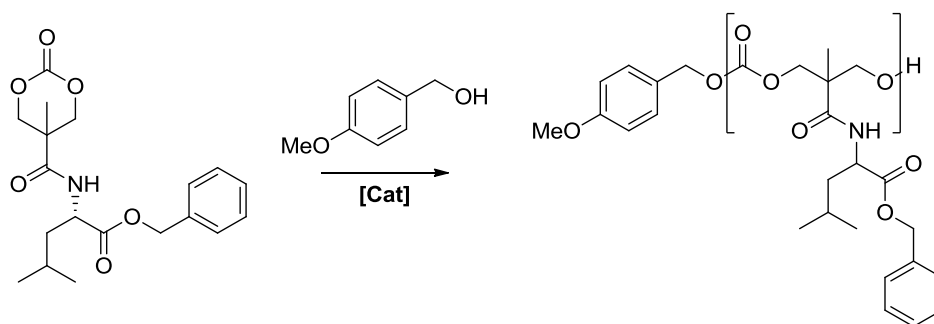


Figure 3.30 - Comparison of ^1H NMR spectra for amido diol and amido carbonate (BLAC)

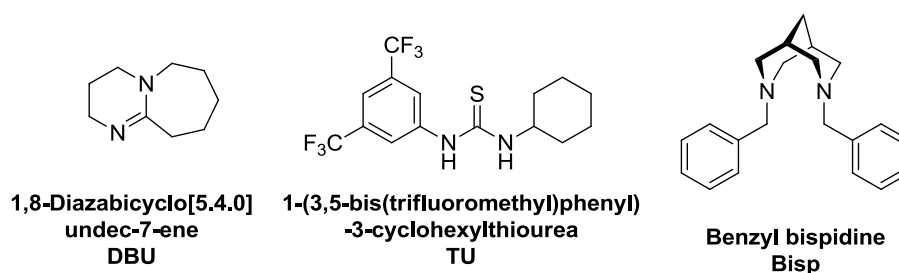
The isolated carbonate was subsequently dried by dissolving in anhydrous dichloromethane and storing over 3 Å molecular sieves for 24 hours, this was repeated three times before removal of the solvent. The drying process led to traces of an unknown degradation product which could be easily removed *via* recrystallisation from anhydrous diethyl ether before the final carbonate was transferred to a glovebox and stored under a nitrogen atmosphere for use in the subsequent ring-opening polymerisation studies.

3.2.2 Ring-Opening Polymerisation of *O*-benzyl-*L*-leucine amido carbonate, BLAC

The organocatalysed ring-opening polymerisation of BLAC was investigated using a number of organocatalytic systems and initiating from 4-methoxybenzyl alcohol. All polymerisations were conducted at a monomer concentration of 0.25 M in anhydrous deuterated chloroform under a dry, inert nitrogen atmosphere. Reaction progress was most easily monitored using ¹H NMR spectroscopy, with the relative concentration of monomer to initiator ([M]/[I]) determined by the ratio of integrals of the peaks corresponding to the methylene protons on the monomer ring (4.66 & 4.20 ppm) and the methoxy group of 4-methoxybenzyl alcohol (3.81 ppm). Monomer conversion was calculated by comparison of the integrals of the peaks corresponding to the methylene protons on the monomer ring (4.66 & 4.20 ppm) and the methylene protons of the polymer backbone (4.35 ppm).



Catalysts:



Scheme 3.41 - Attempted polymerisation of BLAC with a selection of organocatalysts

Table 3.7 - Catalyst screening for the attempted polymerisation of BLAC

Entry	Catalyst (Loading (mol%)) ^a	$[M]_0/[I]_0$ ^b	Monomer Conversion (%) ^b	Time (h)	M_n (g.mol ⁻¹) ^b	M_n (g.mol ⁻¹) ^c	D_M ^c
1	DBU (10)	16	61	40	3692	820	1.11
2	DBU/TU (10/5)	16	64	26	3867	820	1.01
3	Bisp/TU (10/10)	18	47	240	3218	- ^d	- ^d

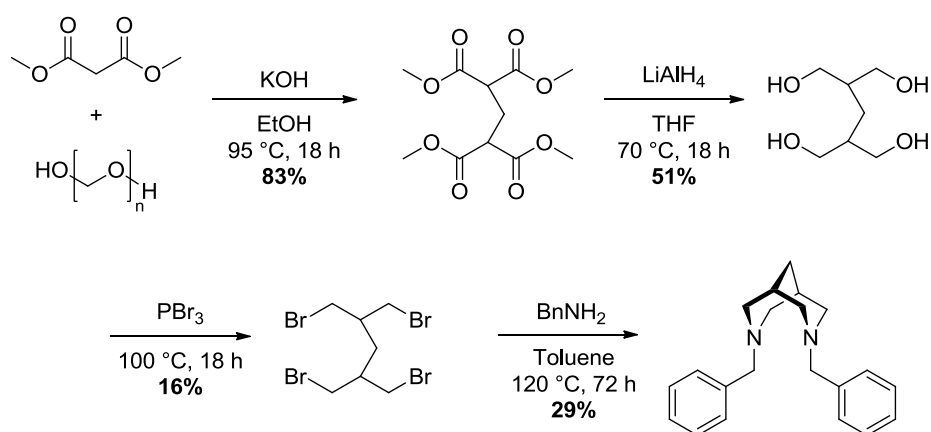
^a Catalyst loadings calculated in relation to monomer concentration; ^b Determined by ¹H NMR spectral analysis; ^c Determined by GPC analysis in chloroform, calibrated against poly(styrene) standards; ^d Insufficient material recovered.

The first attempted polymerisation was conducted using 10 mol% DBU (Table 3.7, Entry 1) and reached an apparent monomer conversion of 61% within 40 hours, as determined by analysis of the crude ¹H NMR spectrum. Based on the starting ratio of monomer to initiator

and the apparent conversion, a theoretical molecular weight of $3692 \text{ g}\cdot\text{mol}^{-1}$ was calculated from analysis of the ^1H NMR spectra used to monitor the reaction.. However analysis by gel permeation chromatography showed only a narrow oligomeric distribution with an observed molecular weight of $820 \text{ g}\cdot\text{mol}^{-1}$ and dispersity of 1.11.

For the subsequent polymerisation attempt, a thiourea co-catalyst was introduced at 5 mol% alongside the 10 mol% DBU loading (Entry 2). Although the reaction reached equilibrium conversion in a shorter time, 64% in 26 hours, GPC analysis again showed no significant molecular weight species. The observed molecular weight of $820 \text{ g}\cdot\text{mol}^{-1}$ showed no discernible difference from that observed without the co-catalyst.

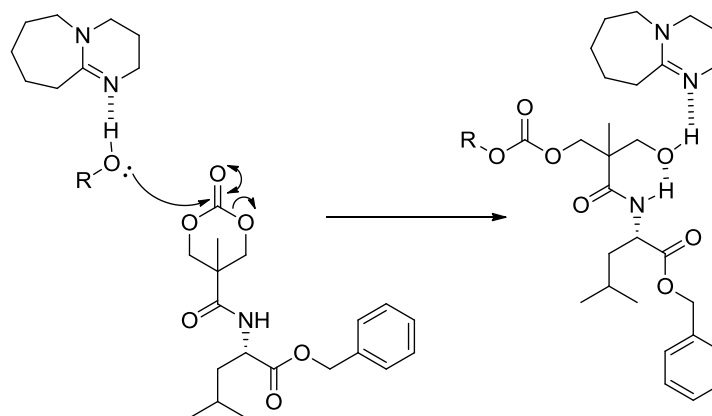
(-)-Sparteine along with a thiourea co-catalyst, has proven to be a useful system for the polymerisation of more sensitive monomers. Unfortunately (-)-sparteine is no longer commercially available and in light of this shortage, work within our group has recently shown that benzyl bispidine may function as an efficient replacement.⁹⁴ Therefore, benzyl bispidine was synthesised in four synthetic steps from dimethylmalonate and paraformaldehyde as shown in Scheme 3.42.



Scheme 3.42 - Synthesis of benzyl bispidine

In a final attempt to produce polymeric species of a significant weight, and to investigate whether the basic nature of DBU had any bearing on the previously failed attempts, benzyl bispidine was utilised at a loading of 10 mol% with a further 10 mol% of thiourea as co-catalyst (Table 3.7, Entry 3). This reaction proved to be considerably slower than either of those previously attempted, reaching an apparent conversion of only 47% after 10 days. Although the calculated molecular weight for the reaction should have been 3218 g.mol^{-1} , almost no material was recovered from the quenched reaction, proving insufficient for analysis by GPC.

The failure to produce polymeric material under any of the trialled organocatalytic systems, although disappointing, is an interesting result, with the cyclisation step from the monomer synthesis providing a hint towards a potential answer. During the cyclisation step it was noted that a solvent disruptive of hydrogen bonding was required for the reaction to proceed (Scheme 3.39). It is plausible that a similar interaction is at work during polymerisation of the carbonate monomer, after initial ring-opening by a hydroxyl species; the resulting hydroxyl group that should otherwise act as the propagating chain end is drawn into the same hydrogen-bonded six-membered ring as suggested for the diol (Scheme 3.43). By adopting such a configuration, the hydroxyl oxygen is associated with the amide group and prevented from readily proceeding with further nucleophilic attack, and thus any propagation of the polymer chain as a result of its reduced nucleophilicity.

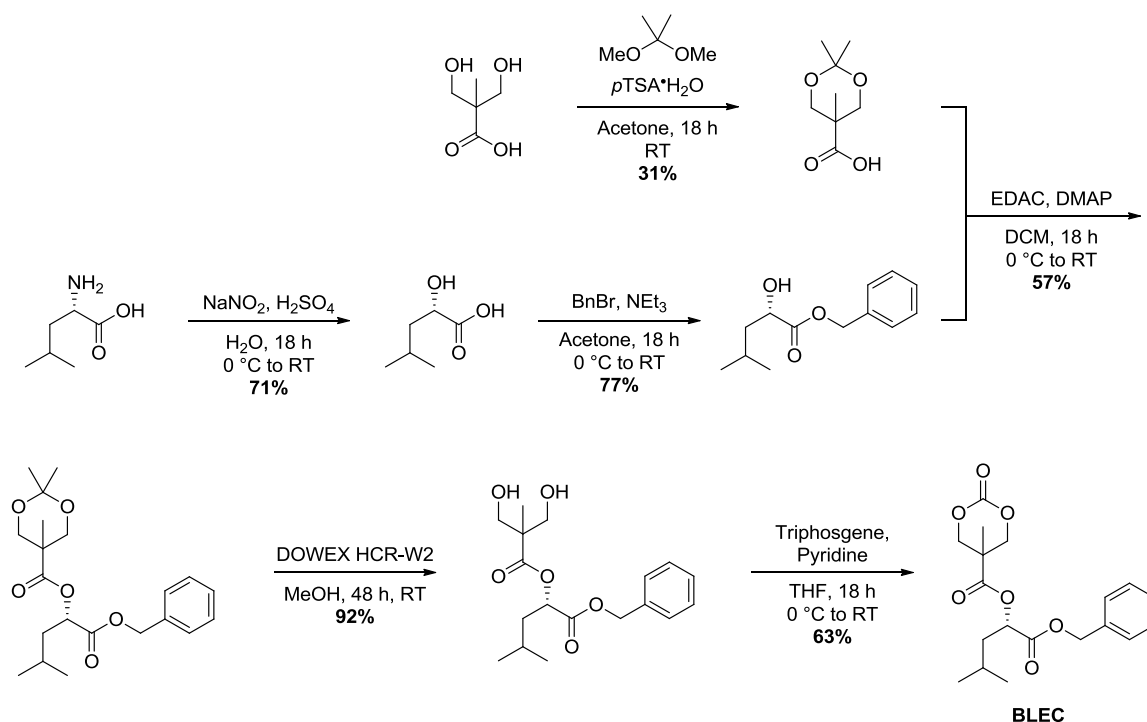


Scheme 3.43 - Hydrogen bonding between the amide proton and hydroxyl lone-pair, preventing further propagation of the polymer chain

Although disruption of the problematic hydrogen bonding could be achieved by exchanging the reaction solvent for THF or another equally disruptive solvent, this would also impede the polymerisation as the propagation mechanism itself relies heavily on hydrogen bonding to activate either the chain end or the monomer (depending on the catalytic system). Therefore an easy alternative is the removal of the problematic amide proton, to give a monomer species which could be easily polymerised under more usual ring-opening polymerisation conditions.

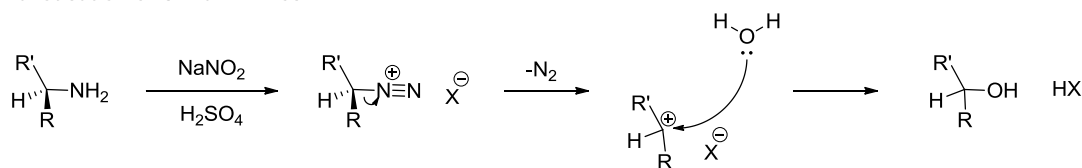
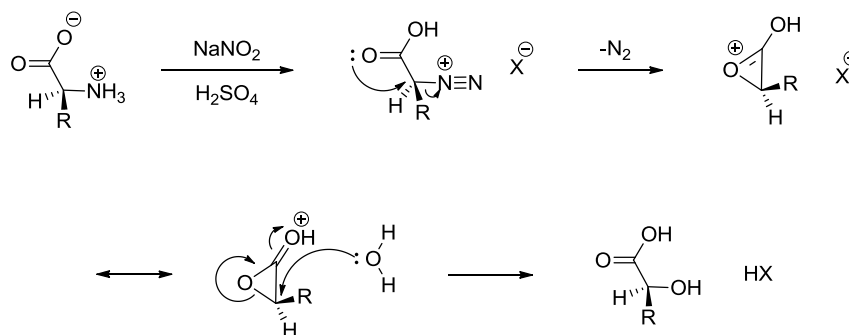
3.2.3 Synthesis of *O*-benzyl-*L*-leucinic ester carbonate, BLEC

With the hypothesis that the presence of an amide proton in BLAC is responsible for the lack of chain propagation, and therefore the attainment of any polymeric material, the simplest solution is the elimination of the secondary amide moiety. Perhaps the simplest method for achieving this elimination is the exchange for an analogous ester group.



Scheme 3.44 - Synthesis of *O*-benzyl-*L*-leucinic ester carbonate, BLEC

The synthesis of the ester-containing BLAC analogue, *O*-benzyl-*L*-leucinic ester carbonate (BLEC) was obtained using a synthetic methodology identical to that utilised for the synthesis of BLAC (Scheme 3.39), yet with the additional step of converting *L*-leucine to *L*-leucinic acid via diazotisation using an excess of sodium nitrite in aqueous sulfuric acid.⁹⁵ Whilst diazotisation of a chiral amine to an alcohol usually results in racemisation, conducting the reaction on an α -amino acid instead leads to retention of the stereochemistry.

Diazotisation of Chiral Amines:**Diazotisation of Chiral α -Amino acids:**Scheme 3.45 - Diazotisation of amines and α -amino acids

The retention of the stereocentre is achieved due to the interaction of the adjacent acid functionality with the resulting diazonium salt; the carbonylic oxygen acts as a nucleophile to displace the diazonium species and liberate nitrogen whilst forming a highly strained protonated lactone. With amino acid R -functionality introducing steric hinderance on one face of the molecule, the subsequent nucleophilic attack by water proceeds by attack from the less-hindered face, thereby leading to retention of the original stereochemistry.⁹⁶

The resulting *L*-leucinic acid, obtained in an appreciably high yield (71%), was readily converted to the corresponding benzyl ester using benzyl bromide under basic conditions, this too was obtained in good yield (77%) before undergoing a modified Steglich coupling reaction with acetonide-protected *bis*MPA. The resulting ester-coupled species was deprotected using DOWEX sulfonic acid resin to yield the corresponding diol. The final cyclisation step was conducted under the same reaction conditions employed for the synthesis of BLAC and the crude product purified by column chromatography on silica gel to yield pure BLEC (Figure 3.31).

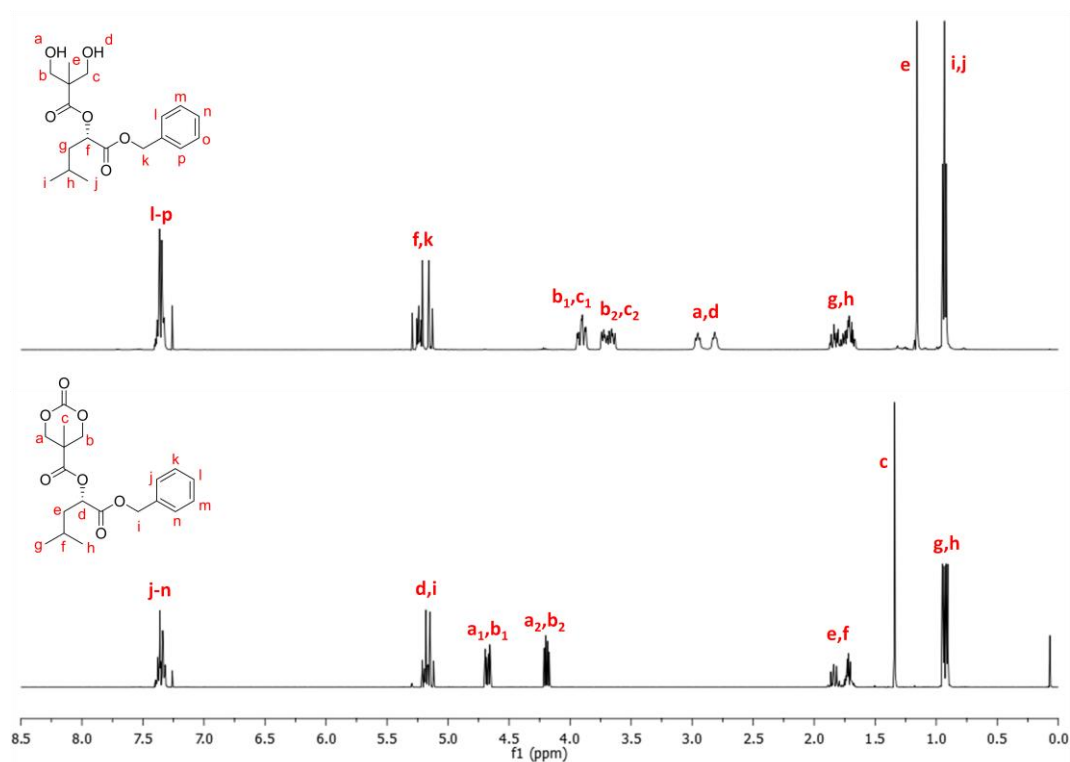
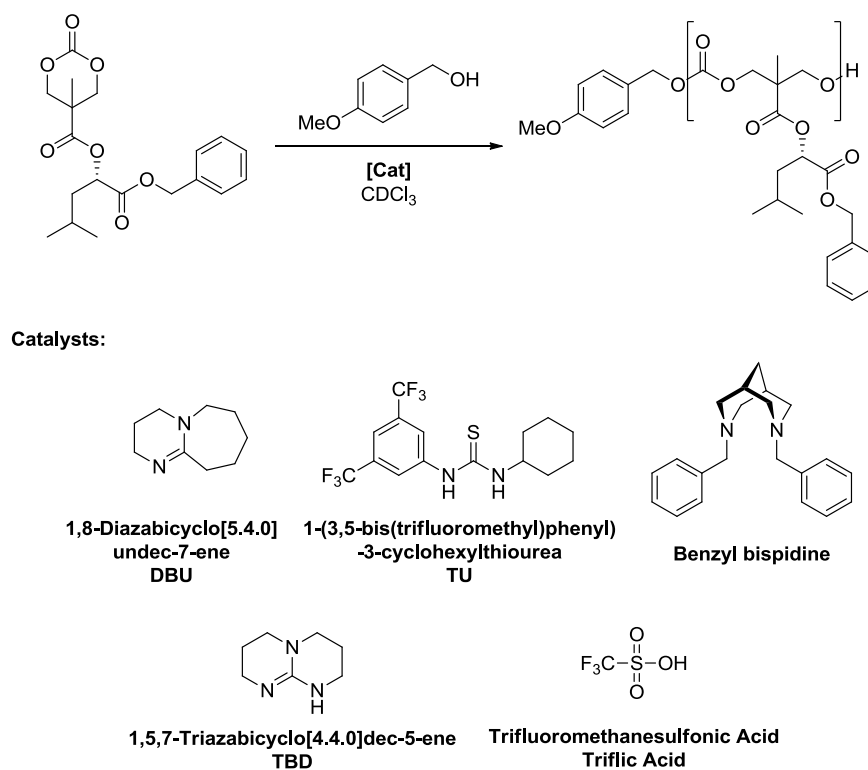


Figure 3.31 - Comparison of ¹H NMR spectra for diol and carbonate (BLEC).

The isolated carbonate was subsequently dried by dissolving in anhydrous dichloromethane and storing over 3 Å molecular sieves for 24 hours, this was repeated three times before removal of the solvent. The drying process led to traces of an unknown degradation product which could easily be removed *via* recrystallisation from anhydrous diethyl ether before the final carbonate was transferred to a glovebox and stored under a nitrogen atmosphere for use in the subsequent ring-opening polymerisation studies.

3.2.4 Ring-Opening Polymerisation of *O*-benzyl-*L*-leucinic ester carbonate, BLEC - Catalyst screening

The organocatalysed ring-opening polymerisation of BLEC was investigated using a series of organocatalysts and initiating from 4-methoxybenzyl alcohol. All polymerisations were conducted at a monomer concentration of 0.25 M (unless otherwise specified) in dried deuterated chloroform under a dry, inert nitrogen atmosphere. Reaction progress was most easily monitored using ^1H NMR spectroscopy, with the relative concentration of monomer to initiator ($[\text{M}]/[\text{I}]$) determined by the ratio of integrals of the peaks corresponding to the methylene protons on the monomer ring (4.66 & 4.20 ppm) and the methoxy group of 4-methoxybenzyl alcohol (3.81 ppm). Monomer conversion was calculated by comparison of the integrals of the peaks corresponding to the methylene protons on the monomer ring (4.66 & 4.20 ppm) and the methylene protons of the polymer backbone (4.29 ppm).



Scheme 3.46 - General ring-opening polymerisation of BLEC and catalysts employed in the condition screening

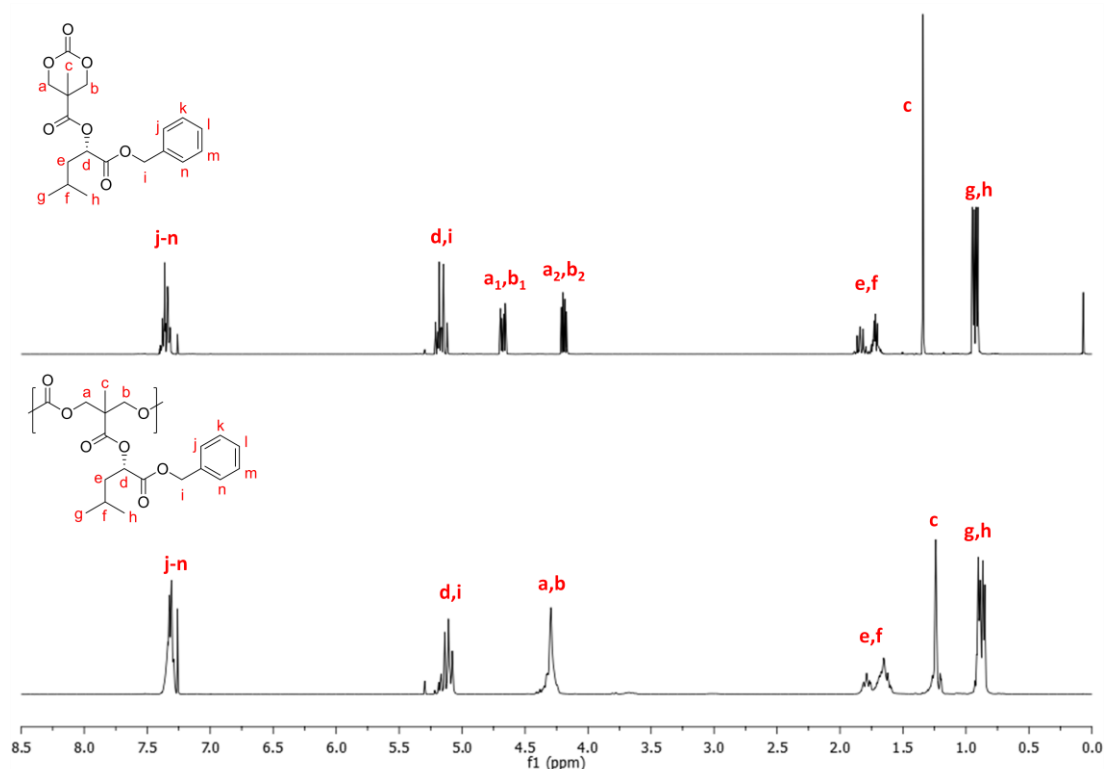
Figure 3.32 - Comparison of ¹H NMR spectra for BLEC and p(BLEC)

Table 3.8 - Catalyst screening for polymerisation of BLEC

Entry	Catalyst (Loading (mol%)) ^a	[M] ₀ /[I] ₀ ^b	Monomer Conversion (%) ^b	Time (h)	<i>M</i> _n (g.mol ⁻¹) ^b	<i>M</i> _n (g.mol ⁻¹) ^c	<i>D</i> _M ^c
1	DBU (10)	24	67	22	5855	4910	1.11
2	DBU (10) ^d	-	-	4 ^e	-	6270	1.11
3	DBU (5)	20	61	37	4442	3900	1.09
4	DBU/TU (10/10)	23	80	20	6838	5530	1.23
5	Bisp/TU (10/10)	18	43	1080	2956	-	-
6	Triflic Acid (10) ^e	19	68	46	4842	2770	1.53

^a Catalyst loadings calculated in relation to monomer concentration; ^b Determined by ¹H NMR spectral analysis; ^c Determined by GPC analysis in chloroform, calibrated against poly(styrene) standards; ^d Reaction conducted at [M]₀ = 2.0 M; ^e Conducted in D₂-methylene chloride

The first polymerisation conducted utilised DBU as catalyst a loading of 10 mol%, relative to the monomer with the polymerisation reaching 67% conversion after only 3 hours (Table 3.2, Entry 1). Analysis of the final polymer by gel-permeation chromatography showed a single distribution with an observed molecular weight (M_n) of 4910 g.mol⁻¹, slightly lower than would be expected from the theoretical weight calculated by analysis of the ¹H NMR spectra ($M_n = 5855$ g.mol⁻¹). The observed dispersity was also found to be narrow ($D_M = 1.11$, Figure 3.33).

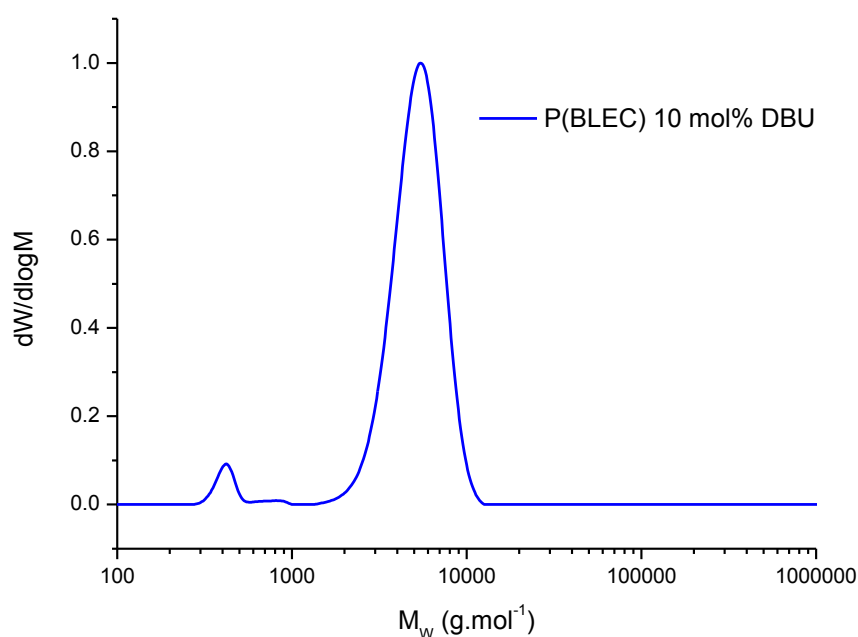
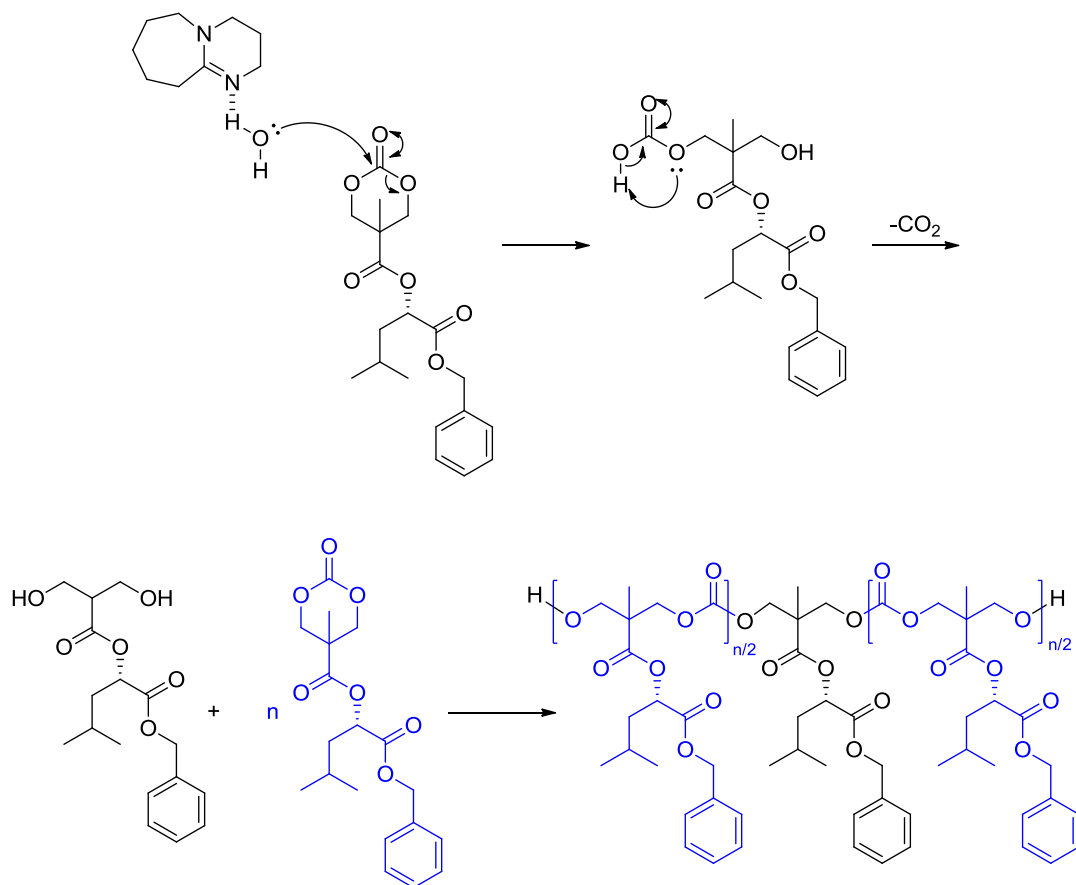


Figure 3.33 - GPC traces for P(BLEC) obtained using 10 mol% DBU

The obtained polymer was analysed by MALDI-ToF mass spectrometry with the resulting spectra showing a single distribution, however the observed masses did not relate to the expected polymeric species initiated from 4-methoxybenzyl alcohol (Figure 3.34). Instead, the masses related closely to a species initiated from water (Scheme 3.47).



Scheme 3.47 - Initiation of BLEC from water with the loss of carbon dioxide leading to formal initiation from the corresponding diol

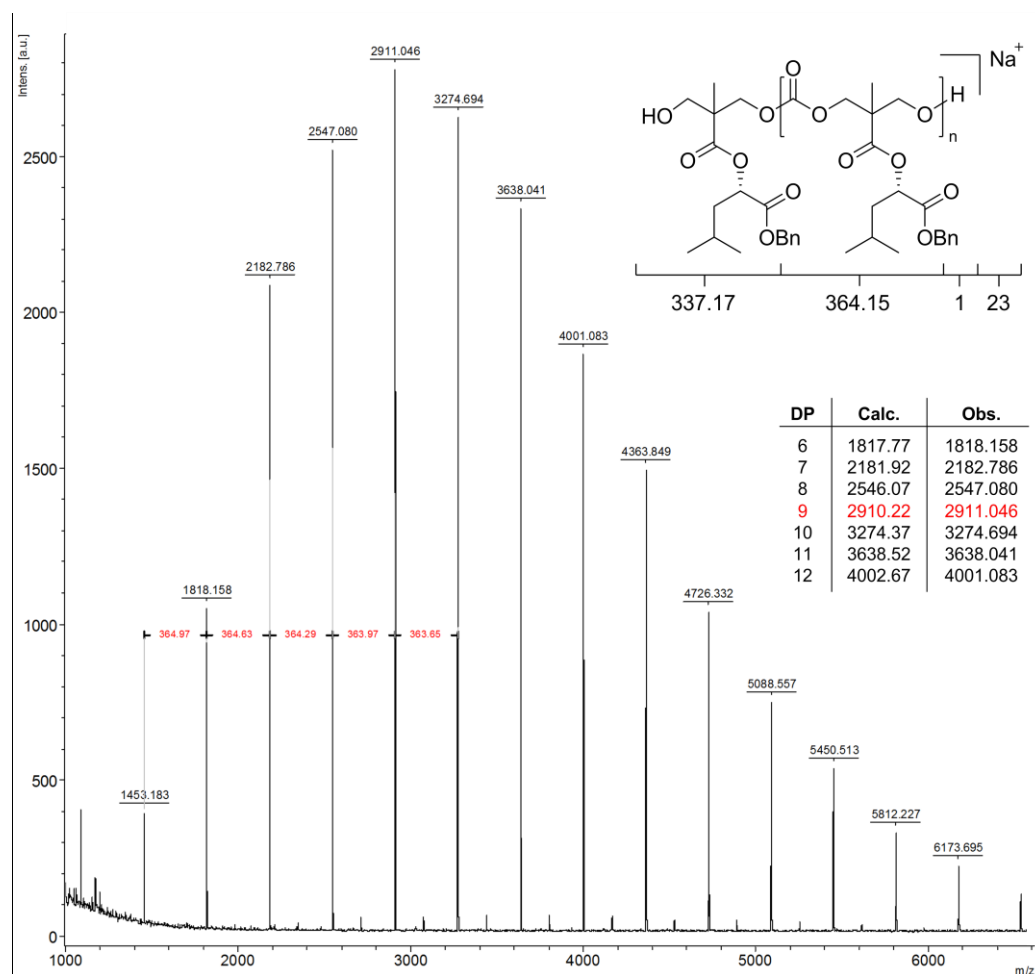


Figure 3.34 - MALDI-ToF mass spectrum of P(BLEC) obtained using 10 mol% DBU at 0.25 M

With the monomer, catalyst and alcohol having been subjected to strenuous drying processes before commencing polymerisation, the observation of such a species as the apparent sole polymerisation product initially proved difficult to resolve against our expectations. However it was noted that whilst the ^1H NMR spectra of the isolated polymer following the treatment with acidic amberlyst resin showed no remaining initiator signals (Figure 3.35), which would support such water-initiation, there is strong evidence from the analysis of ^1H NMR spectra obtained during the course of the reaction that the 4-methoxybenzyl alcohol does indeed act as an initiator (Figure 3.36).

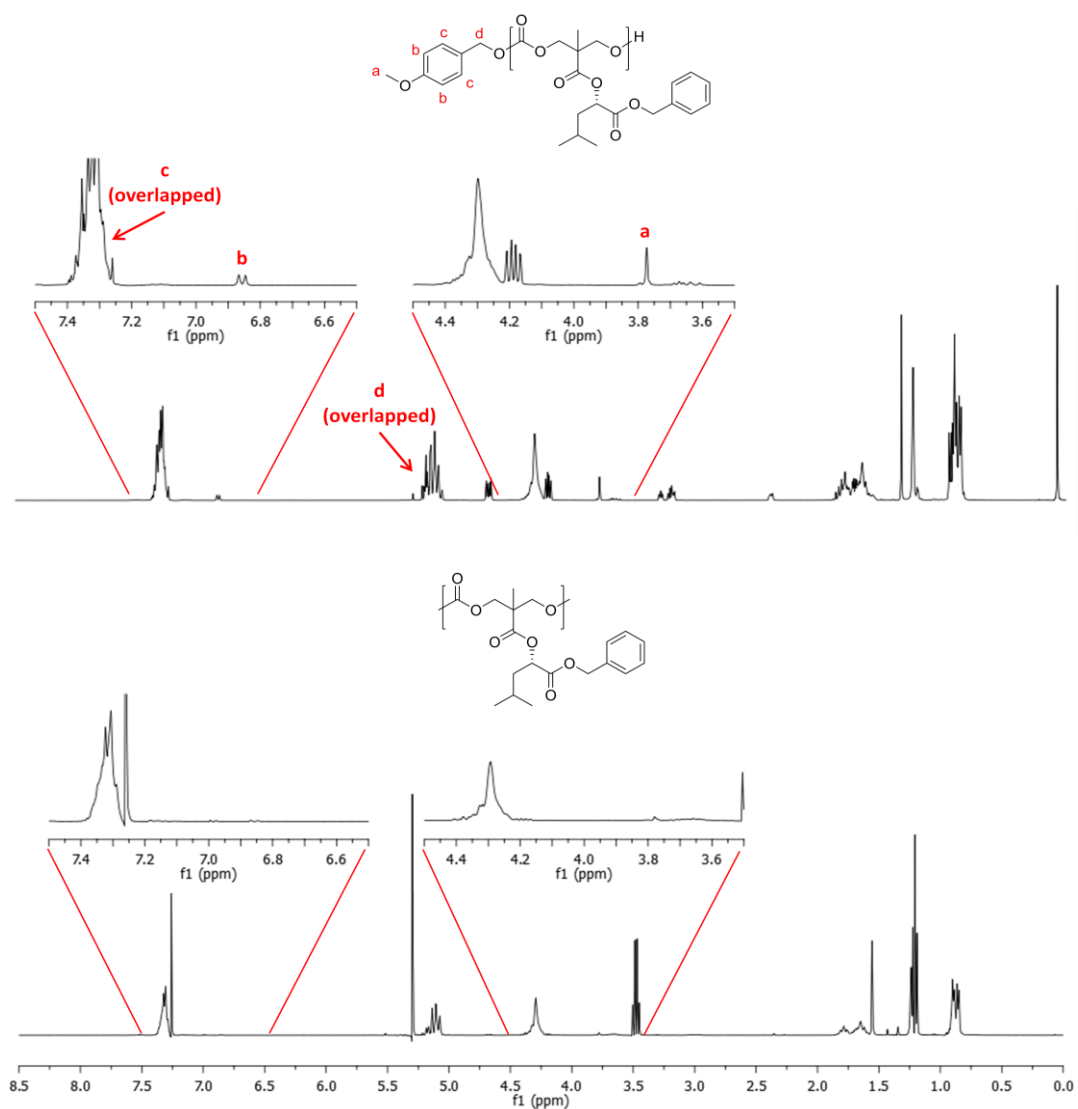


Figure 3.35 - Comparison of ^1H NMR spectra showing 4-methoxybenzyl alcohol present in the crude reaction mixture (top) and absent following acidic workup to yield pure polymer (bottom)

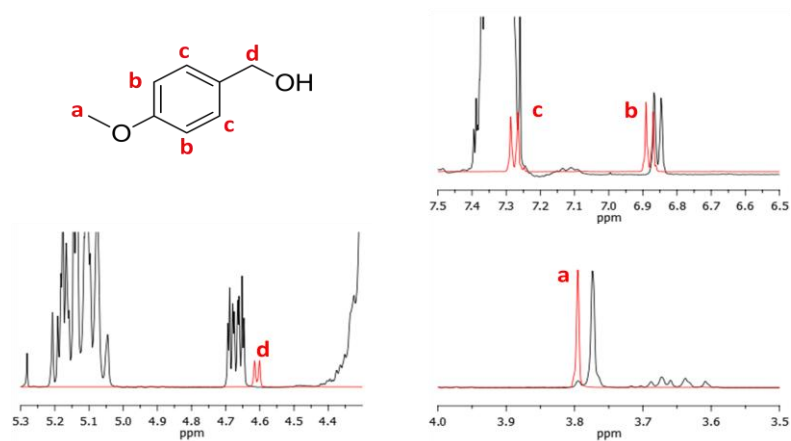
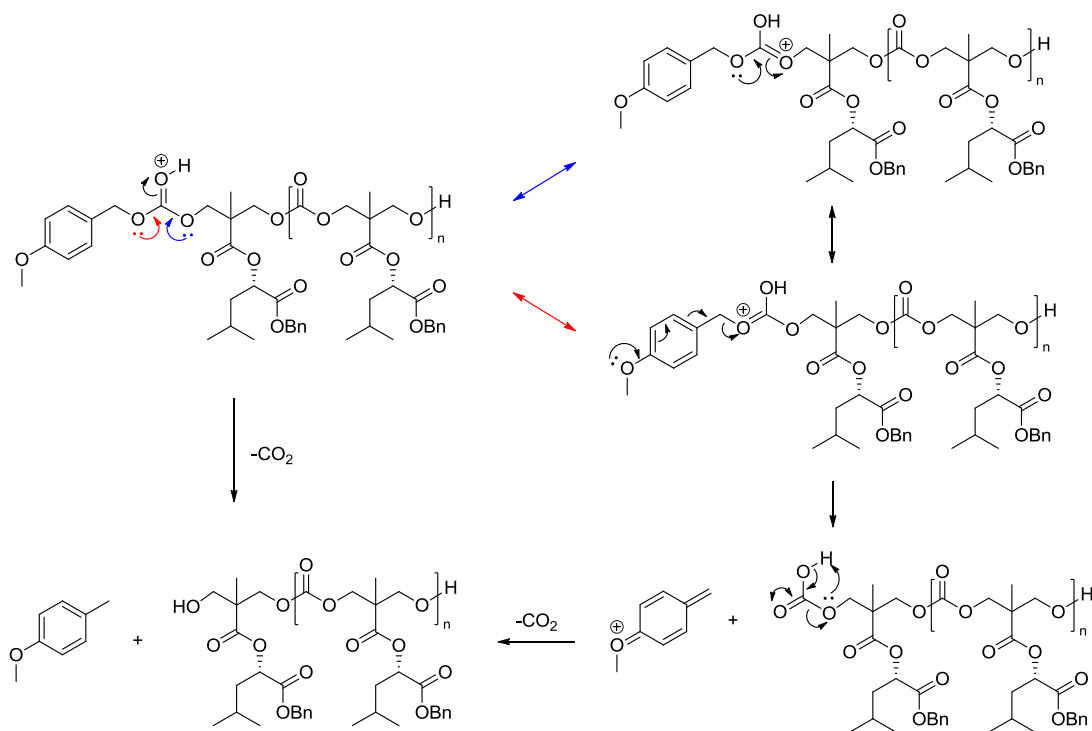


Figure 3.36 - Comparison of ^1H NMR spectra of crude BLEC polymerisation (black) and 4-methoxybenzyl alcohol (red)

There are significant differences in chemical shift between the pure, "uninitiated" 4-methoxybenzyl alcohol and the corresponding signals in the ongoing polymerisation. Although one of the aromatic signals (7.29 ppm) is lost under the aromatic signals from both the monomer and polymer, the second set of aromatic signals at 6.89 ppm for the pure alcohol shows a slight shift upfield to 6.86 ppm. The benzylic methylene signal, present at 4.61 ppm for the free alcohol is not observed, if the alcohol is initiated from, the benzylic signal should shift to a position overwhelmed by the monomer and polymer benzylic signals.

Perhaps most significantly in this comparison is the shift observed in the methoxy signal, this is observed at 3.81 ppm for the uninitiated species, whilst there is a slight signal observed in the spectrum of the crude polymer at this position, the major methoxy signal present has a chemical shift of 3.77 ppm. The observation of a shifted methoxy signal, alongside a trace of residual uninitiated species, coupled with the absence of an observed benzylic signal strongly supports the conclusion that the 4-methoxybenzyl alcohol does indeed act as initiator for the polymerisation of BLEC.

The proposed explanation for the loss of the 4-methoxybenzyl alcohol during the purification process involves the protonation of the carbonylic oxygen with the resulting charged species being stabilised *via* delocalisation across the two adjacent oxygen atoms (Scheme 3.48). One of the resonance states places a positive charge on the benzylic oxygen, such an arrangement allows for one of the lone pairs on the methoxy-oxygen to donate into the phenyl ring and subsequently cleave the benzylic C-O bond, yielding a carbonic acid which rapidly degrades with the loss of carbon dioxide to form a terminal hydroxyl group. The resulting methoxybenzylic species undergoes re-aromatisation to yield 4-methoxytoluene.



Scheme 3.48 - Proposed mechanism for the cleavage of 4-methoxybenzylic end-group to give 4-methoxytoluene and hydroxyl-terminated telechelic P(BLEC)

This suggested post-polymerisation cleavage of the initiator is further supported by the narrow dispersity of the resulting polymer as observed by GPC (Figure 3.33) and the uniform nature of the distribution. Initiation from water would likely lead to both a broader dispersity, as well as a non-uniform distribution, possessing either a high weight tail or shoulder due to the competing initiation mechanisms.

With the identity and origin of the obtained polymeric species resolved, the polymerisation condition screening was continued. Initially the monomer concentration was increased eight-fold from 0.25 M to 2.0 M (Table 3.8, Entry 2). Due to issues of scale, this reaction was not monitored via ¹H NMR spectroscopy and was instead allowed to run at room temperature for 4 hours before being quenched by stirring with acidic amberlyst resin. GPC analysis of the resulting polymer showed a distribution with a dispersity comparable to that obtained from a lower initial monomer concentration ($D_M = 1.11$) yet with a much higher

observed molecular weight at $6270 \text{ g}\cdot\text{mol}^{-1}$ (Figure 3.37). This increased weight relates nicely with the expected increase due to the greater monomer concentration leading to a higher equilibrium conversion.

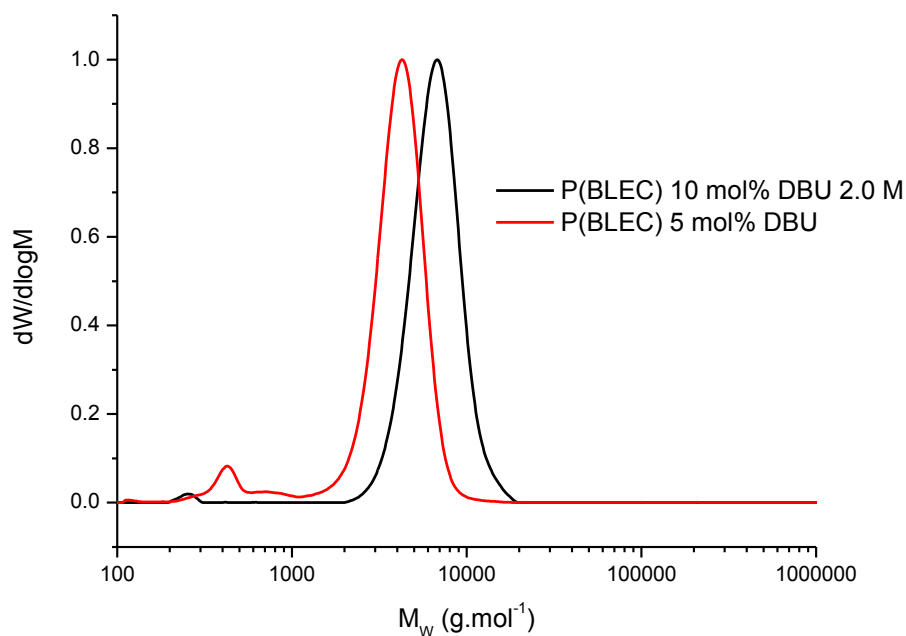


Figure 3.37 - GPC traces of P(BLEC) obtained using 10 mol% DBU at 2.0 M and 5 mol% DBU at 0.25 M

MALDI-ToF MS analysis again showed a clean single distribution relating to the polymer having undergone end-group cleavage, although this was again notably increased in molecular weight compared to the spectrum obtained for the reaction conducted at 0.25 M and showed a peak mass corresponding to a polymer with 12 repeat units.

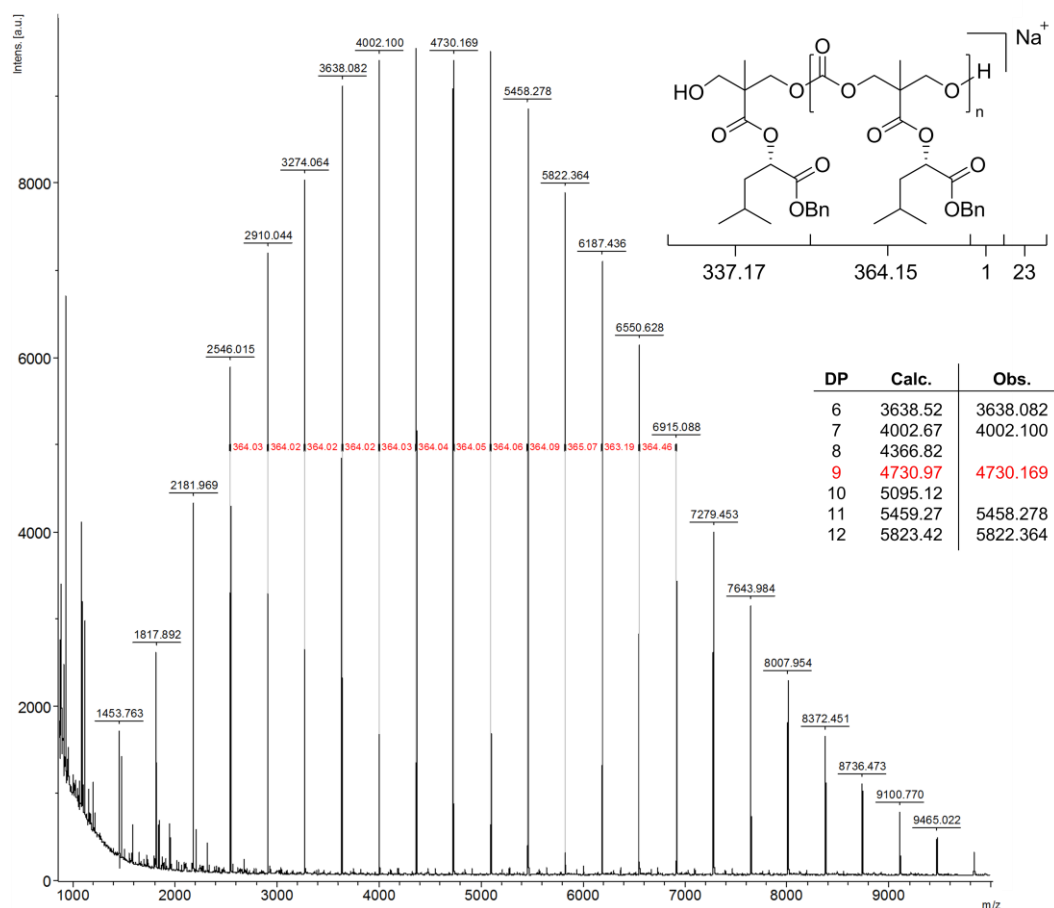


Figure 3.38 - MALDI-ToF mass spectrum of P(BLEC) obtained using 10 mol% DBU at 2.0 M

With no notable variation in either observed species or dispersity in the resulting polymers obtained from reactions conducted at 0.25 M and 2.0 M, it was decided that to allow monitoring of the reactions by ^1H NMR spectroscopy and within the limitations of the available material, all further polymerisation studies would be conducted at the lower of the two concentrations.

The reduction of the catalyst loading to 5 mol% of DBU was attempted (Table 3.8, Entry 3), with the polymerisation reaching a conversion of 61% after 37 hours as determined by ^1H NMR spectral analysis, giving the obtained polymer a calculated molecular weight of 4440 $\text{g}\cdot\text{mol}^{-1}$. Analysis of the polymer by GPC showed an observed mass lower than that

calculated from the ^1H NMR spectrum, with a molecular weight of $3898 \text{ g}\cdot\text{mol}^{-1}$ and a very narrow dispersity of 1.09 (Figure 3.37).

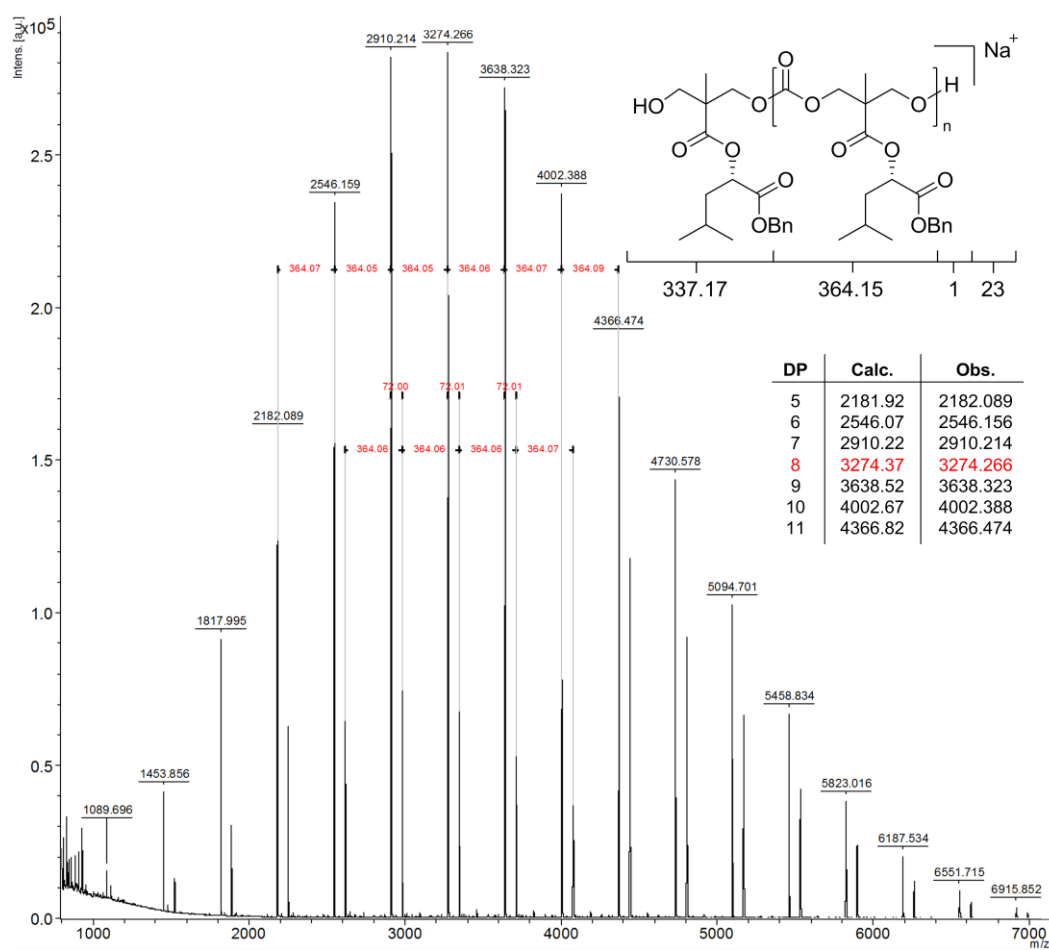


Figure 3.39 - MALDI-ToF mass spectrum of P(BLEC) obtained from using 5 mol% of DBU

Whilst the analysis of the obtained material by both ^1H NMR spectroscopy and GPC showed a polymer with no significant variation from those obtained using higher levels of catalyst loading, analysis of the MALDI-ToF mass spectrum showed two distributions (Figure 3.39); whilst the major distribution corresponds to the masses of the telechelic species produced following end-group cleavage (having a peak DP of 8), the identity of the minor distribution remains elusive.

Next, the effect of the introduction of a thiourea co-catalyst was trialled with a loading of 10 mol% for both DBU and thiourea (Table 3.8, Entry 4). As was expected, the reaction proceeded faster than observed in the absence of a co-catalyst, reaching a higher equilibrium conversion of 80% within only 20 hours. Analysis of the ^1H NMR spectra gave a calculated molecular weight of $6838 \text{ g}\cdot\text{mol}^{-1}$. Subsequent analysis of the isolated polymer by GPC showed an observed molecular weight considerably lower than that calculated, being reported at $5530 \text{ g}\cdot\text{mol}^{-1}$ (Figure 3.40). The distribution also possesses a dispersity which, whilst still narrow ($\mathcal{D}_M = 1.23$), proved considerably broader than anything observed for the polymerisations in the absence of the thiourea co-catalyst.

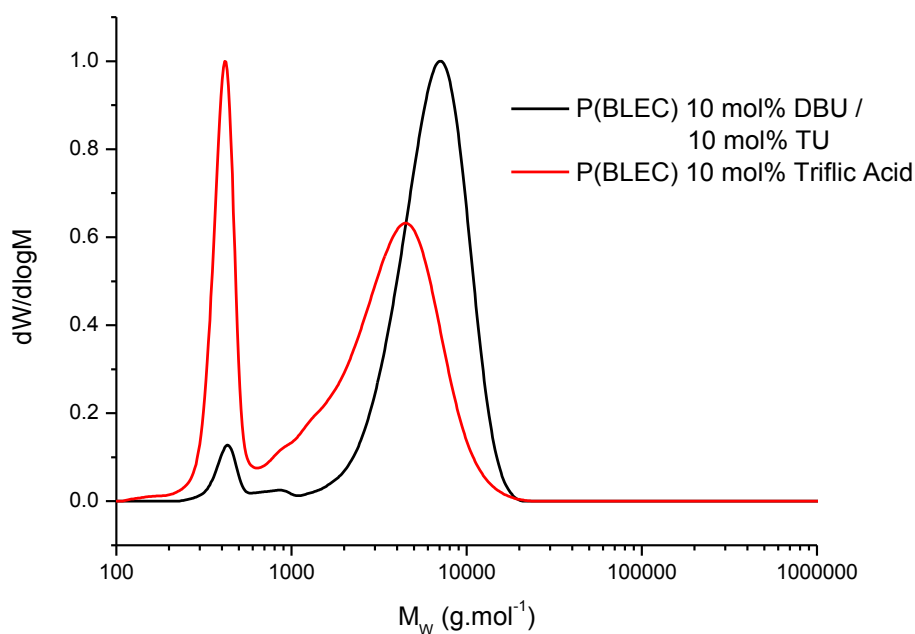


Figure 3.40 - GPC traces of P(BLEC) obtained using 10 mol% DBU with 10 mol% thiourea and 10 mol% triflic acid

Subsequent analysis of the polymer by MALDI-ToF mass spectrometry revealed a major distribution relating to the end-cleaved polymeric species (Figure 3.41), with an observed peak DP of 5. However it was noted that this distribution existed alongside a couple of

(relatively minor) secondary distributions, presumably responsible for the slight broadening observed in the GPC analysis.

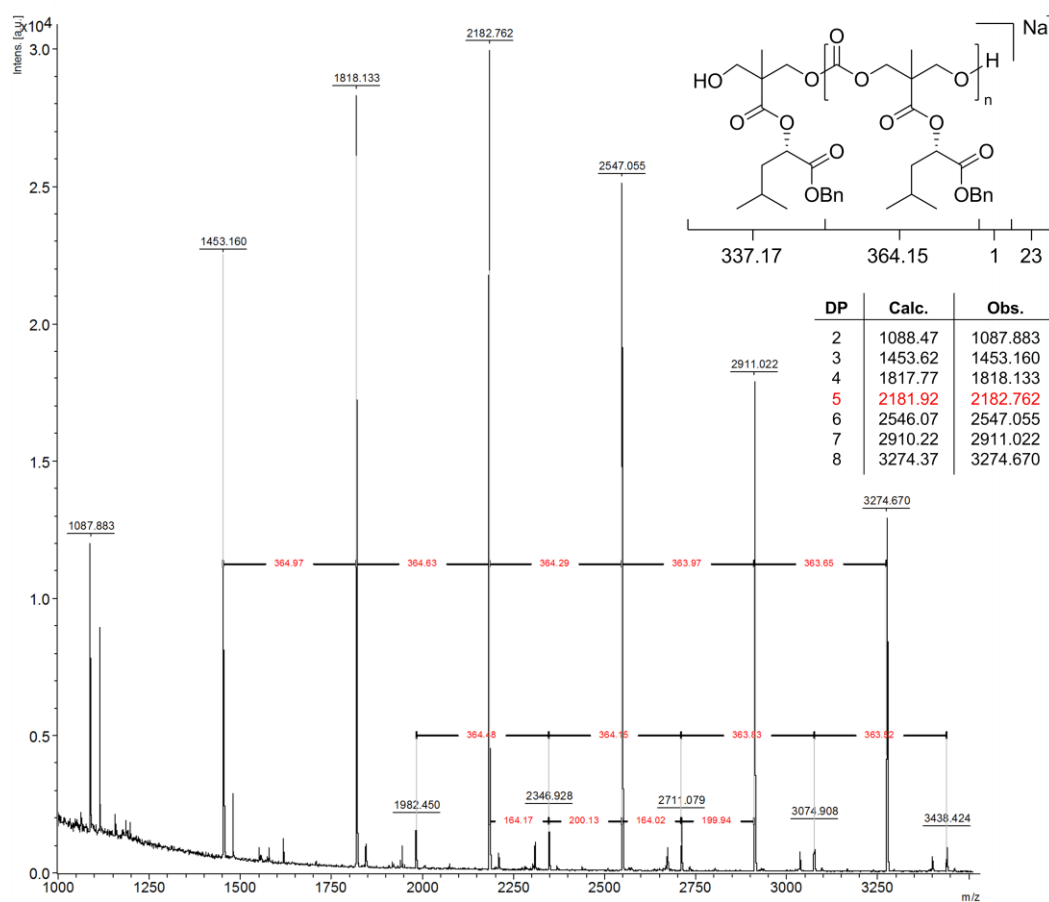


Figure 3.41 - MALDI ToF mass spectrum of P(BLEC) obtained using 10 mol% DBU with 10 mol% thiourea co-catalyst

A second dual-catalytic system was then investigated, using the (-)-sparteine analogue benzyl bispidine in conjunction with the thiourea co-catalyst, both were used at a loading of 10 mol% with regard to the monomer concentration (Table 3.8, Entry 5). However, the reaction proved to be extremely slow, reaching only 43% conversion after 45 days, at which point the reaction was quenched to allow for analysis of the (albeit low weight) polymeric material. Unfortunately, a negligible quantity of material was recovered, thwarting any attempts to analyse the reaction products.

The final catalyst employed as a candidate for the polymerisation of BLEC was trifluoromethane sulfonic acid (Table 3.8, Entry 6) with a catalyst loading of 10 mol%. The reaction achieved 68% monomer conversion after 46 hours as determined by ^1H NMR spectral analysis, for a calculated molecular weight of $4840 \text{ g}\cdot\text{mol}^{-1}$. However, the molecular weight observed by analysis of the GPC chromatogram proved to be significantly lower, at $2770 \text{ g}\cdot\text{mol}^{-1}$, with an extremely broad dispersity ($D_M = 1.53$) and low-weight tailing (Figure 3.40).

The analysis of the isolated polymer by MALDI-ToF MS shows a major distribution apparently corresponding to the end-cleaved polymeric species (Figure 3.42). However, due to the nature of the mechanism for the cationic ring-opening of cyclic carbonates, it is possible to have competing mechanisms for the chain propagation.

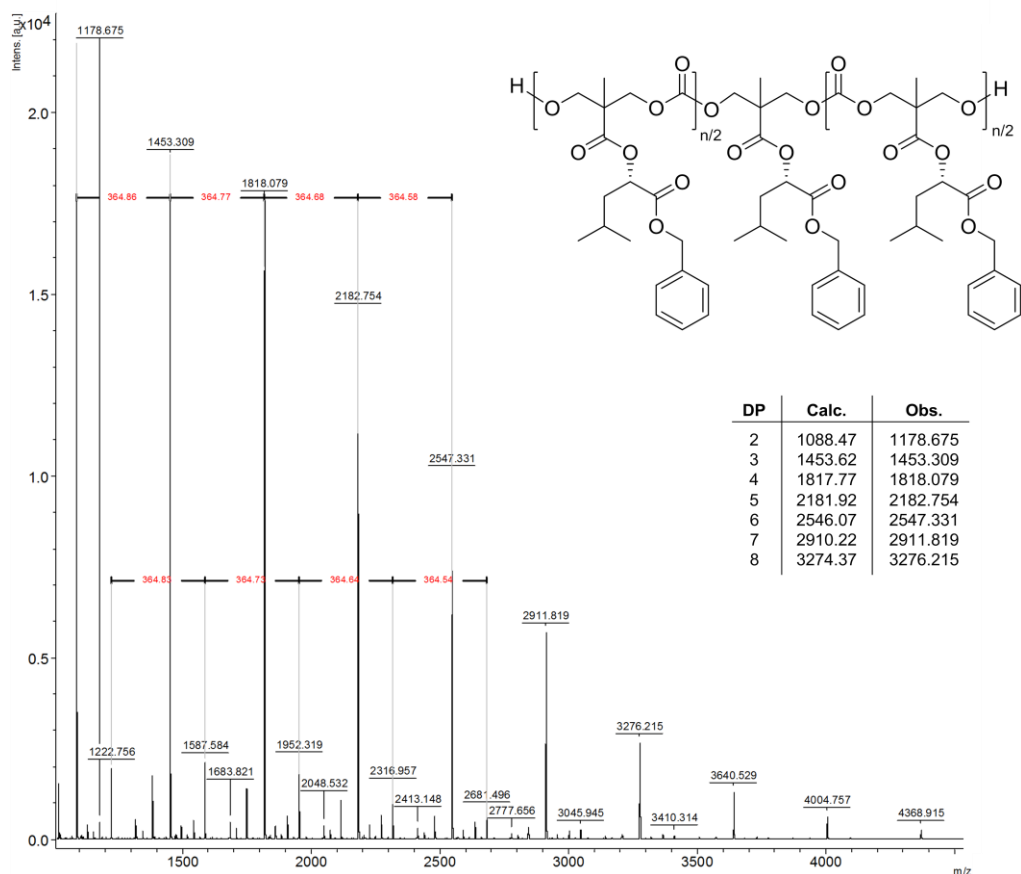
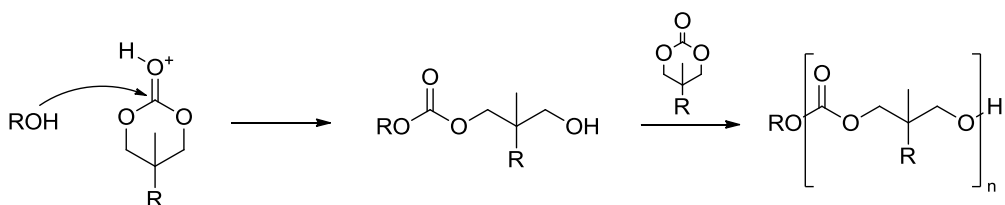


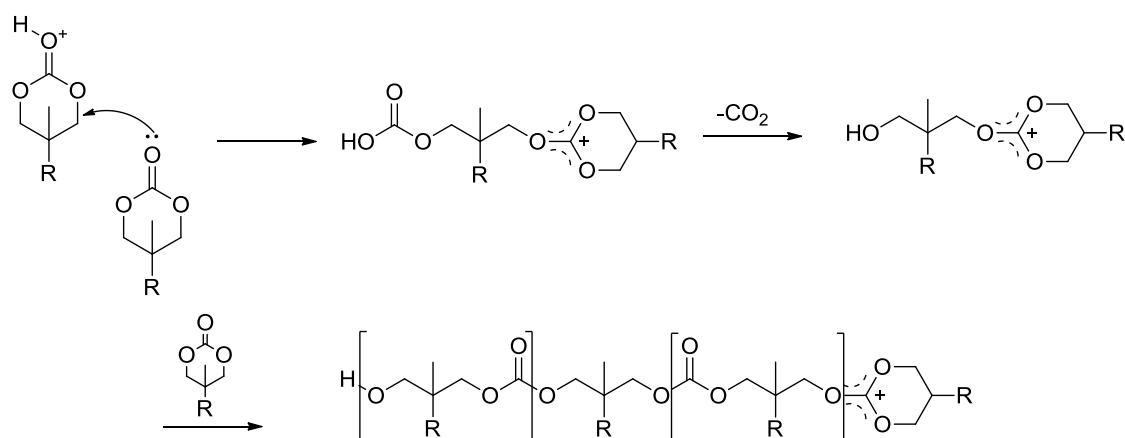
Figure 3.42 - MALDI-ToF mass spectrum of P(BLEC) obtained using 10 mol% trifluoromethane sulfonic acid

The intended cationic polymerisation mechanism involves the activation of the carbonate *via* protonation of the carbonyl, rendering it more susceptible to nucleophilic attack by the alcoholic initiator and subsequent opening of the cyclic carbonate (Scheme 3.49).



Scheme 3.49 - Intended activated monomer mechanism for the cationic ring-opening polymerisation of cyclic carbonates

However a second competing mechanism exists in the form of an activated chain-end mechanism.^{97,98} This mechanism proceeds *via* initiation from an activated monomer with the initial nucleophilic attack on the α -carbon by a carbonyl oxygen on a second unactivated monomer (Scheme 3.50). This leads to the ring-opening of the activated monomer with the formation of a carbonic acid group and retention of the attacking monomer as an activated chain-end species. The carbonic acid is unstable and will quickly decompose to release carbon dioxide and leave a hydroxyl chain-end. From this asymmetric species, propagation may proceed by either an activated monomer or an activated chain-end mechanism (*via* the hydroxyl and activated ring chain-ends respectively).



Scheme 3.50 - Synthesis of telechelic poly(carbonate) *via* joint activated chain-end and activated monomer mechanisms

It is the presence of these competing mechanisms, particularly the auto-initiation of the cyclic carbonate, that leads to the extremely broad dispersity of the resulting polymer, as well as the low-weight tailing and considerably lower molecular weight compared to the expectation.

With the originally trialled catalyst loading of 10 mol% DBU offering the best control of any investigated system (Table 3.2, Entry 1), it was decided to proceed with further investigations using this system as the chosen catalyst.

3.2.5 Ring-Opening Polymerisation of BLEC - Investigation of polymerisation control

Having selected 10 mol% DBU as the catalyst system which offered the best results from the initial catalyst screening investigation, our focus turned to the investigation of polymerisation control. Initial reactions were conducted with varying monomer to initiator ratios, giving target degrees of polymerisation of 50, 100 and 250 (Table 3.9).

Table 3.9 - Polymerisation of BLEC initiated from 4-methoxybenzyl alcohol using 10mol% DBU

Entry	$[M]_0/[I]_0^a$	Monomer Conversion (%) ^a	Time (h)	M_n (g.mol ⁻¹) ^a	M_n (g.mol ⁻¹) ^b	D_M^b
1	24	67	22	5855	4910	1.11
2	53	69	44	13455	8160	1.13
3	98	72	46	25832	15900	1.19
4	243	57	48	50576	23700 ^c 49500 ^c	1.09 ^c 1.03 ^c

^a Calculated by analysis of ¹H NMR spectra; ^b Determined by GPC analysis in CHCl₃, calibrated against poly(styrene) standards; ^c GPC trace showed bimodal distribution.

The correlation between the starting monomer to initiator ratio and the molecular weight as observed by gel-permeation chromatography shows a linear relationship (Figure 3.43), although the intercept is non-zero (4460 g.mol⁻¹, —), which would usually imply an elevated rate of propagation compared to that of initiation. However, whilst the chromatograms for

P(BLEC)₂₄ and P(BLEC)₅₃ showed well-defined, narrow and unimodal traces (Figure 3.44), the trace for P(BLEC)₉₈ possessed a high-weight shoulder whilst that for P(BLEC)₂₄₃ showed obvious bimodality. As a result of the bimodal distribution observed by GPC analysis, exclusion of the results for P(BLEC)₂₄₃ showed a tighter correlation with a drastically lowered intercept (884 g.mol⁻¹, —), potentially implying the lack of any significant difference between the rates of initiation and propagation.

Significantly, the occurrence of bimodality in the analysis of higher molecular weight samples lends further support for the earlier proposed end-group cleavage mechanism (Scheme 3.48) as an alternative to water-initiation as a source of the species observed in the MALDI-ToF MS analyses.

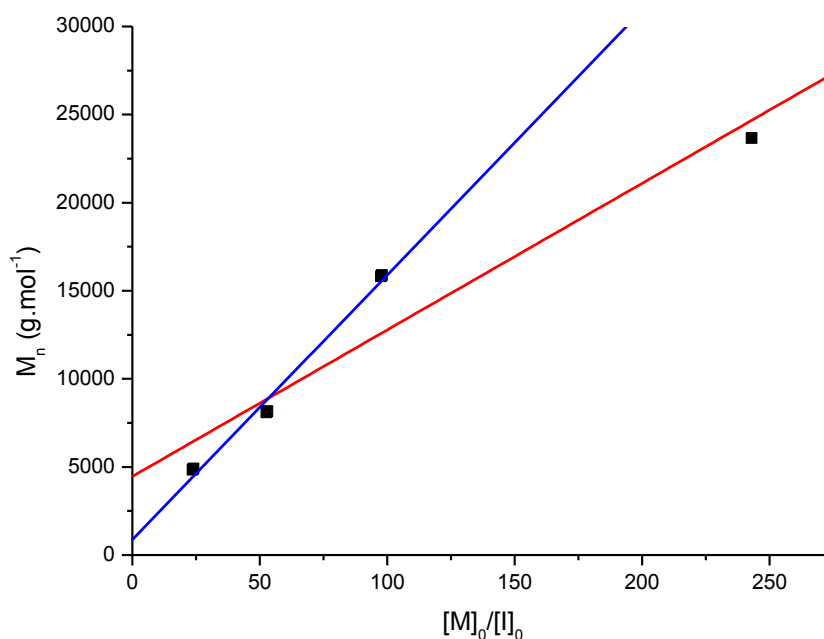


Figure 3.43 - $[M]_0/[I]_0$ vs. M_n for P(BLEC) initiated from 4-methoxybenzyl alcohol with trendlines inclusive (—) and exclusive (—) of P(BLEC)₂₄₃

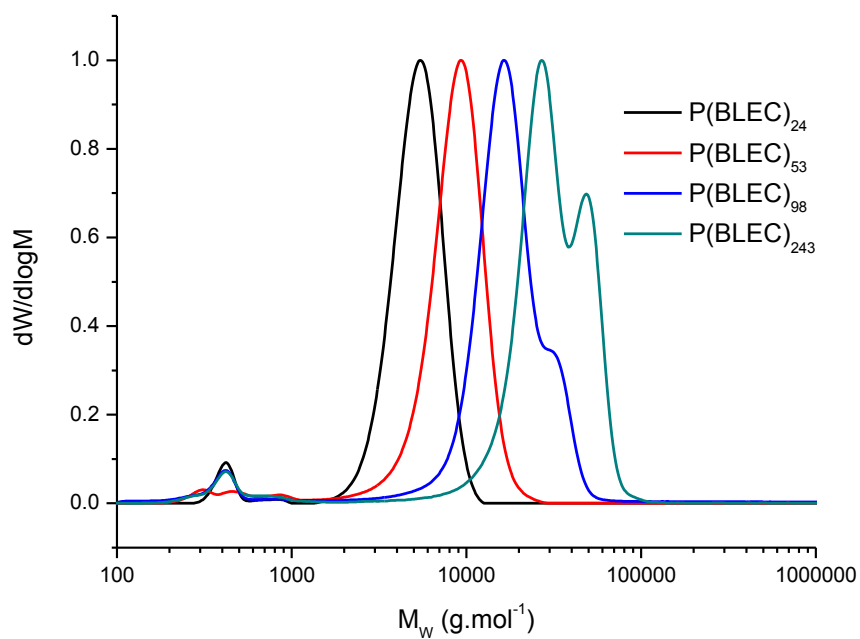


Figure 3.44 - GPC traces of P(BLEC) obtained using 10 mol% DBU with targeted degrees of polymerisation of 24, 53, 98 and 243

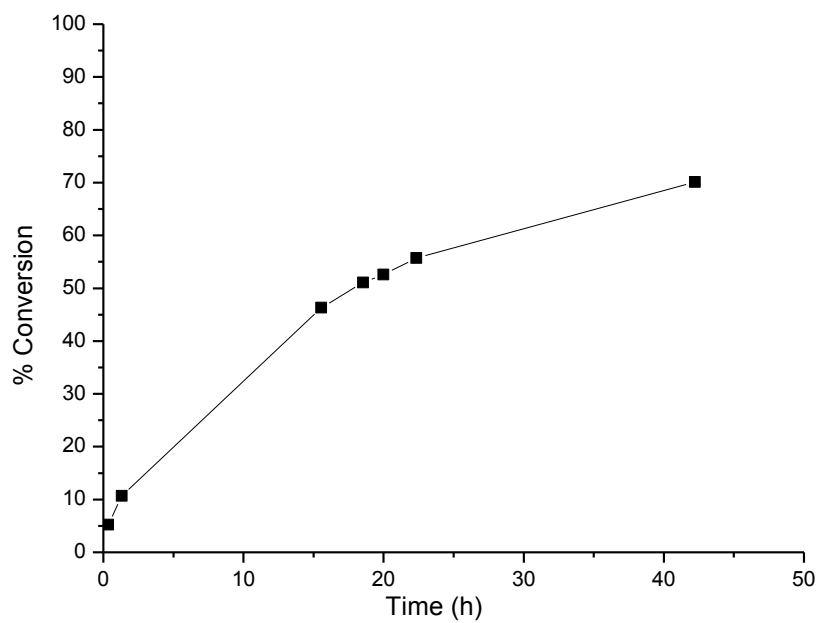


Figure 3.45 - Plot of monomer conversion vs. time for $P(\text{BLEC})_{50}$

In order to determine the living nature of the polymerisation of BLEC using 10 mol% of DBU, a series of identical reactions were conducted with a targeted degree of polymerisation of 50. These reactions were monitored via ^1H NMR spectroscopy and individually quenched at various degrees of monomer conversion (Table 3.10).

After quenching, the resulting polymers were subjected to GPC analysis, both the observed molecular weights and dispersities were plotted against the monomer conversion (Figure 3.46). The molecular weights showed a linear correlation with the reaction progression whilst the dispersities remained narrow ($D_M \leq 1.15$) throughout.

Table 3.10 - Polymerisation of BLEC targeting DP50 and analysed at certain conversions

Entry	Monomer Conversion (%) ^a	Time (h)	M_n (g.mol ⁻¹) ^a	M_n (g.mol ⁻¹) ^b	D_M ^b
1	11.89	5	2165	3770	1.09
2	40.12	8	7305	5780	1.15
3	51.45	12	9368	6220	1.08
4	50.74	15	9238	6360	1.10
5	81.26	46	14795	7960	1.13

^a Calculated from ^1H NMR spectra. ^b Determined by GPC analysis in CHCl_3 , calibrated against poly(styrene) standards.

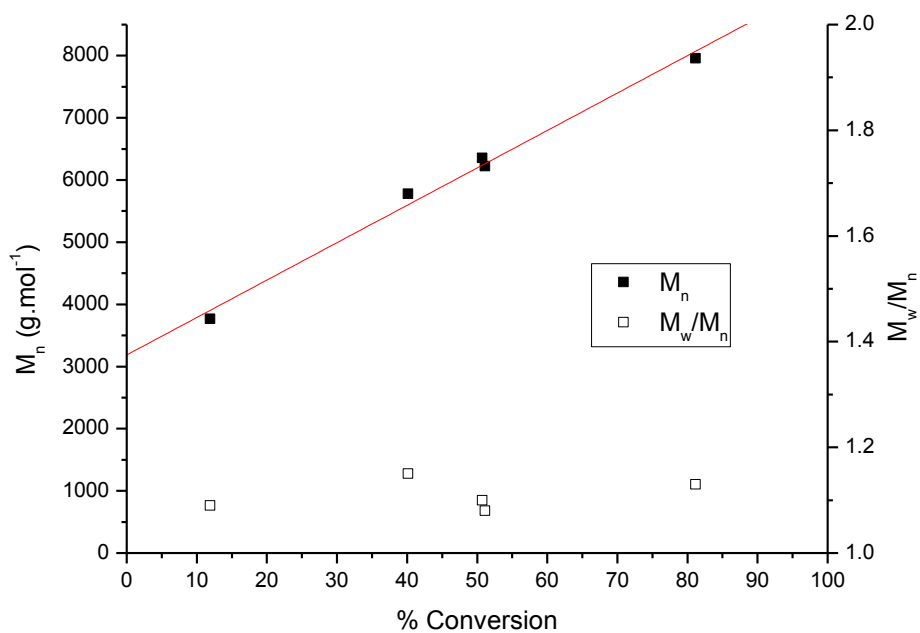
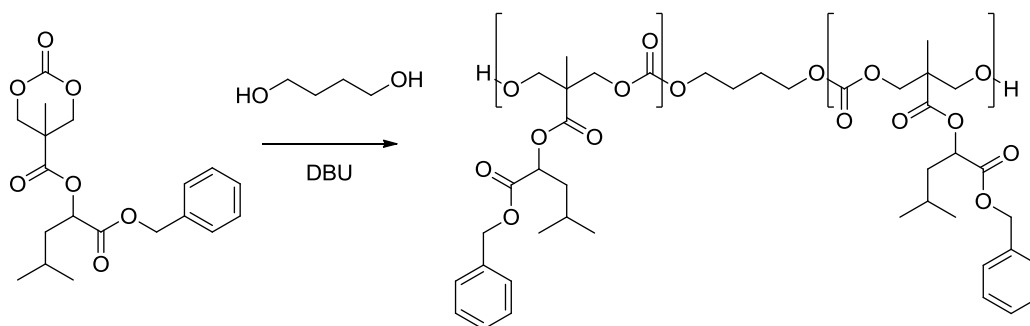


Figure 3.46 - Plot of Molecular weight (M_n) and dispersity (M_w/M_n , D_M) vs. monomer conversion

With the living nature of the polymerisation of BLEC shown, it was considered important that the identity of the high molecular weight secondary distribution observed for polymerisations targeting the synthesis of P(BLEC)₉₈ and P(BLEC)₂₄₃ (Figure 3.44) was confirmed as being initiated from water.

Support for water initiation as the second distribution would offer further support for the controlled synthesis of a telechelic poly(carbonate) *via* elimination of the methoxy-benzyl initiator. If the water initiation is responsible for the observed impurity, it should be possible to resolve the bimodality into a unimodal distribution by attempted initiation from a diol species.



Scheme 3.51 - Synthesis of P(BLEC) initiating from 1,4-butanediol

The initial polymerisation reactions attempted towards the resolution of the high molecular weight bimodality were initiated from 1,4-butanediol (1,4-BD) with monomer to initiator ratios of 98 and 223 (Scheme 3.51).

Table 3.11 - Higher molecular weight P(BLEC) initiated from 1,4-butanediol

Entry	$[M]_0/[I]_0^a$	Monomer Conversion (%) ^a	Time (h)	M_n (g.mol ⁻¹) ^a	M_n (g.mol ⁻¹) ^b	D_M^b
1	98	81	23	29044	7320	1.19
2	223	74	32	60230	12100	1.45

^a Calculated from analysis of ¹H NMR spectra. ^b Determined by GPC analysis in CHCl₃, calibrated against poly(styrene) standards.

Although both reactions proceeded considerably quicker than those initiated from 4-methoxybenzyl alcohol, reaching 81% and 74% monomer conversion within 23 and 32 hours, respectively, this may be attributed to the propagation from both ends of the chain effectively halving the required number of unit additions per propagating chain-end in order to access a material with the same degree of polymerisation.

However, analysis of the resulting polymers by GPC showed disappointing results, with the polymer targeting DP 98 showing a molecular weight considerably lower than expected at 7320 g.mol⁻¹ (Figure 3.47). However, whilst the dispersity still remains acceptable at $D =$

1.19, the chromatogram shows a significant low-weight tail compared to the idealised symmetrical distribution.

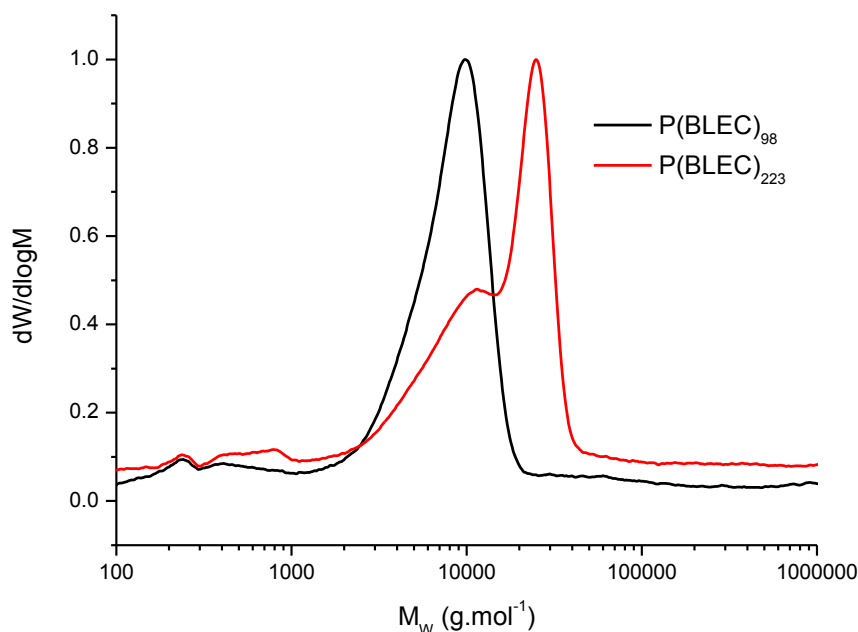
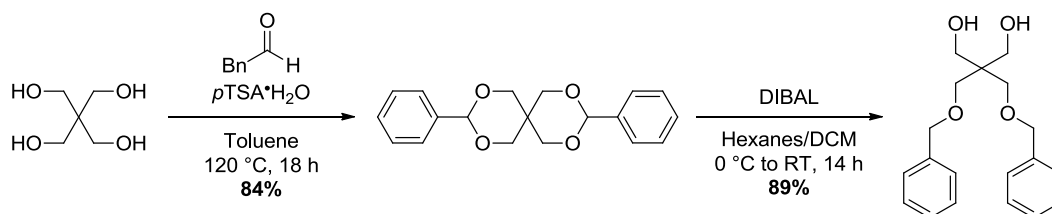


Figure 3.47 - P(BLEC) initiated from 1,4-butanediol with target degrees of polymerisation of 98 and 223

In the case of the polymerisation with a target DP of 223, the observed molecular weight remains very low compared to expectations, with an M_n of only 12100 g.mol⁻¹ compared to the calculated molecular weight of 60230 g.mol⁻¹ based on the conversion observed by ¹H NMR spectroscopy. The obtained chromatogram still remains obviously bimodal, yet interestingly the higher weight of the two distributions is the most intense, a switch from the previously-observed bimodal distribution in which the lower weight distribution dominated.

Both the low weight tailing and the preference for the higher weight species in the bimodal distribution could be explained if the 1,4-BD were in fact a poor initiating species in comparison with the trace water, it is not unknown for alkyl alcohols to be poor initiating species. To overcome this we required the use of a diol possessing less of a pure alkyl

character. Unfortunately, the obvious benzylic diols proved to be insoluble in chlorinated solvents, rendering them useless. The answer lay in the synthesis of *bis*((benzyloxy)methyl)propane-1,3-diol (*bis*BMPD) from pentaerythritol (Scheme 3.52).



Scheme 3.52 - Synthesis of *bis*BMPD from pentaerythritol

This synthesis involved the initial tetra-protection of pentaerythritol as the corresponding dibenzylacetal using benzaldehyde and *p*-toluenesulfonic acid monohydrate in refluxing toluene overnight. The isolated dibenzylacetal was subsequently reduced using diisobutylaluminium hydride (DIBAL) to yield the dibenzylic ether diol, (*bis*BMPD).

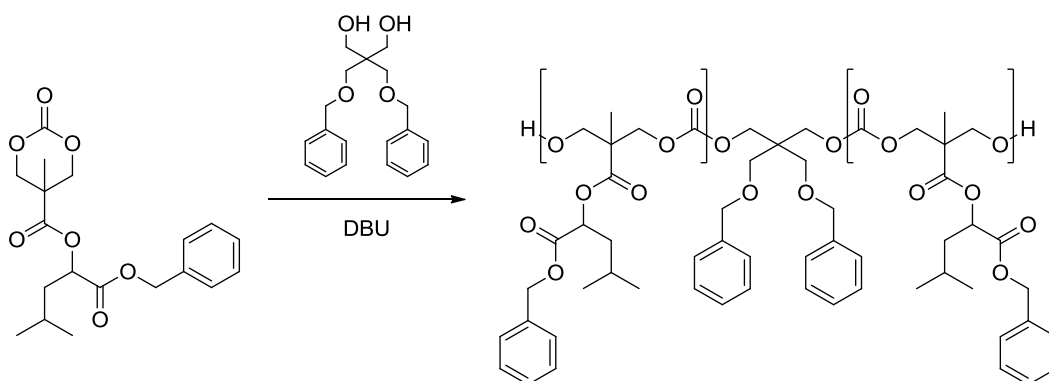
As with the those using 1,4-BD, the two reactions conducted with *bis*BMPD were targeted at high molecular weights, with initial monomer to initiator ratios of 97 and 216 (Table 3.12).

Table 3.12 - Higher molecular weight P(BLEC) initiated from *bis*BMPD

Entry	$[M]_0/[I]_0^a$	Monomer Conversion (%) ^a	Time (h)	M_n (g.mol ⁻¹) ^a	M_n (g.mol ⁻¹) ^b	\mathcal{D}_M^b
1	97	78	26	27551	12800	1.11
2	216	70	28	55059	20100	1.14

^a Calculated by ¹H NMR spectral analysis. ^b Determined by GPC analysis in CHCl₃, calibrated against poly(styrene) standards

As was observed with reactions initiated from 1,4-BD, the reaction times were considerably shorter than for those initiated from a monofunctional alcohol reaching monomer conversions of 78 and 70% in 26 and 28 hours, respectively.



Scheme 3.53 - Synthesis of P(BLEC) initiated from bisBMPD using 10 mol% DBU

Analysis of the resulting polymers by GPC gave observed molecular weights of 12800 and 20100 $\text{g}\cdot\text{mol}^{-1}$, these are still far lower than the corresponding weights calculated from analysis of the ^1H NMR spectra (27551 and 55059 $\text{g}\cdot\text{mol}^{-1}$).

Significantly however, the dispersities of both resultant polymers remained pleasingly narrow ($D_M = 1.11$ and 1.14), with the corresponding chromatograms showing only unimodal, symmetrical distributions (Figure 3.48).

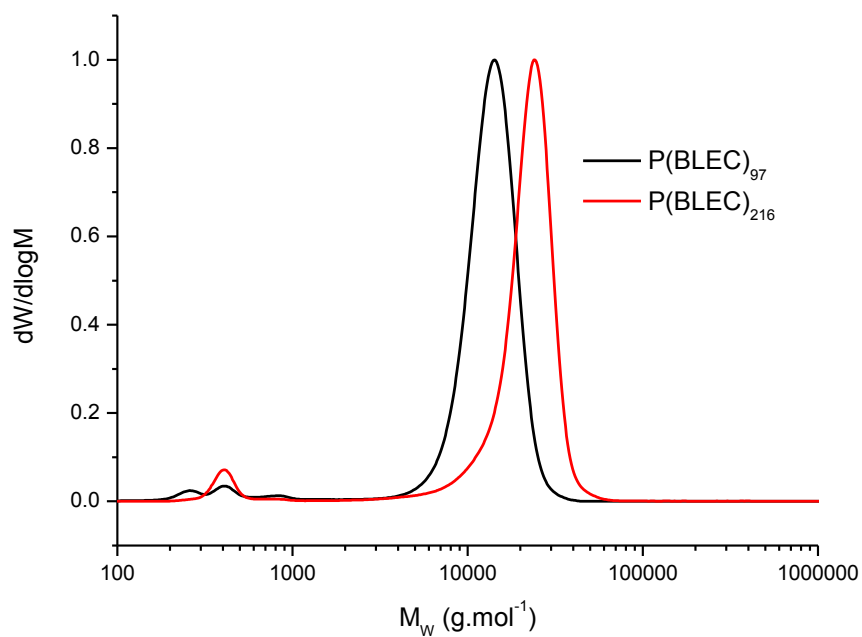


Figure 3.48 - GPC traces of P(BLEC) initiated from *bis*BMPD with targeted degrees of polymerisation of 97 and 216

The absence of any bimodality or shouldering in either of these distributions lends further evidence to the argument that the previously observed species in the MALDI-ToF mass spectra arise not from initiation from water, but rather by the post-polymerisation cleavage of the 4-methoxybenzyl end-group.

3.3 Conclusions and Future Work

In conclusion, the synthesis of two novel chiral monomers has been successfully achieved by incorporation of two amino acid derivatives onto a cyclic carbonate framework, *O*-benzyl-*L*-leucine amido carbonate (BLAC) and *O*-benzyl-*L*-leucinic ester carbonate (BLEC).

The ring-opening polymerisation of BLAC with basic organocatalytic systems was attempted, yet failed to yield polymeric material. However a likely mechanism for the disruption of such polymerisation reactions is proposed based on previous observations during the monomer synthesis. The proposed mechanism restricts the polymerisation of a six-membered cyclic carbonate bearing a secondary amine on the ring at the 5-position based on preferential intramolecular hydrogen bonding over the intermolecular hydrogen bonding required for chain propagation.

It is possible that the use of an acidic catalyst could allow access to polymeric material from the ring-opening of BLAC due to the lack of reliance on intermolecular hydrogen bonding, such a reaction could conceivably be conducted in a disruptive solvent, such as tetrahydrofuran, to further remove the problem of intramolecular hydrogen bonding.

The ring-opening polymerisation of BLEC using a range of organocatalysts was then investigated with a mechanism proposed for the post-polymerisation cleavage of the 4-methoxybenzyl initiating species to yield a hydroxyl-functionalised telechelic poly(carbonate). The possibility of the observed telechelic species originating due to initiation from water is discussed and shown to be highly unlikely due to the demonstrated control of molecular weight with monomer conversion and initial monomer to initiator ratio. Further evidence is provided by the observation of bimodality at very high target molecular

weights, with the higher weight distribution demonstrated to be derived from a diol initiation source (i.e. water).

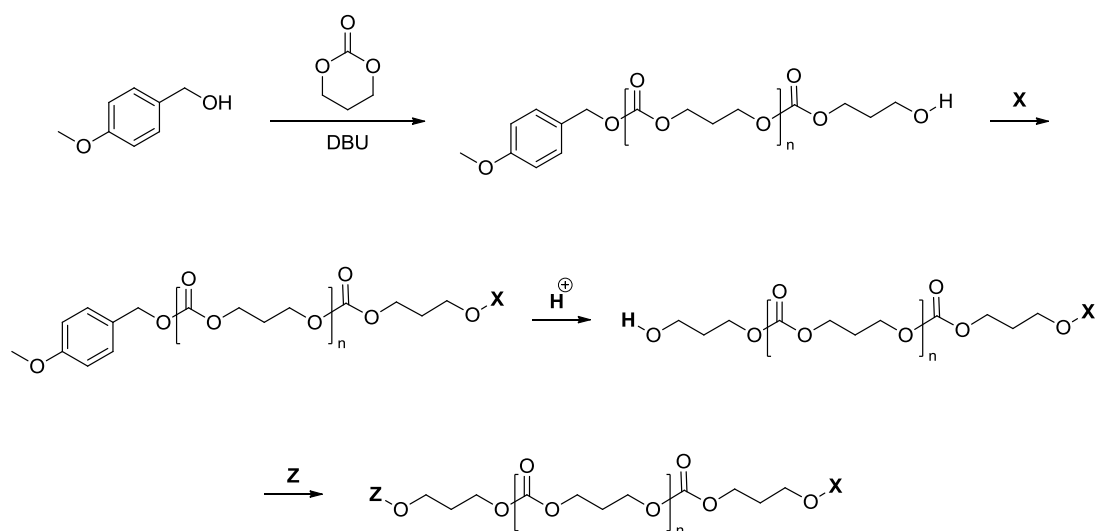


Figure 3.49 - Proposed methodology for accessing bifunctional poly(carbonate)s bearing differing α - and ω - chain ends

Such a controlled method to the synthesis of hydroxyl-functionalised telechelic polymers could prove to have many applications in the formation of ABA triblock structures. If the reaction purification can be modified to preserve the 4-methoxybenzyl end group, it would be possible to gain access to bifunctional poly(carbonate)s bearing different functionalities on either of the α - or ω - chain ends (Figure 3.49).

Chapter 4

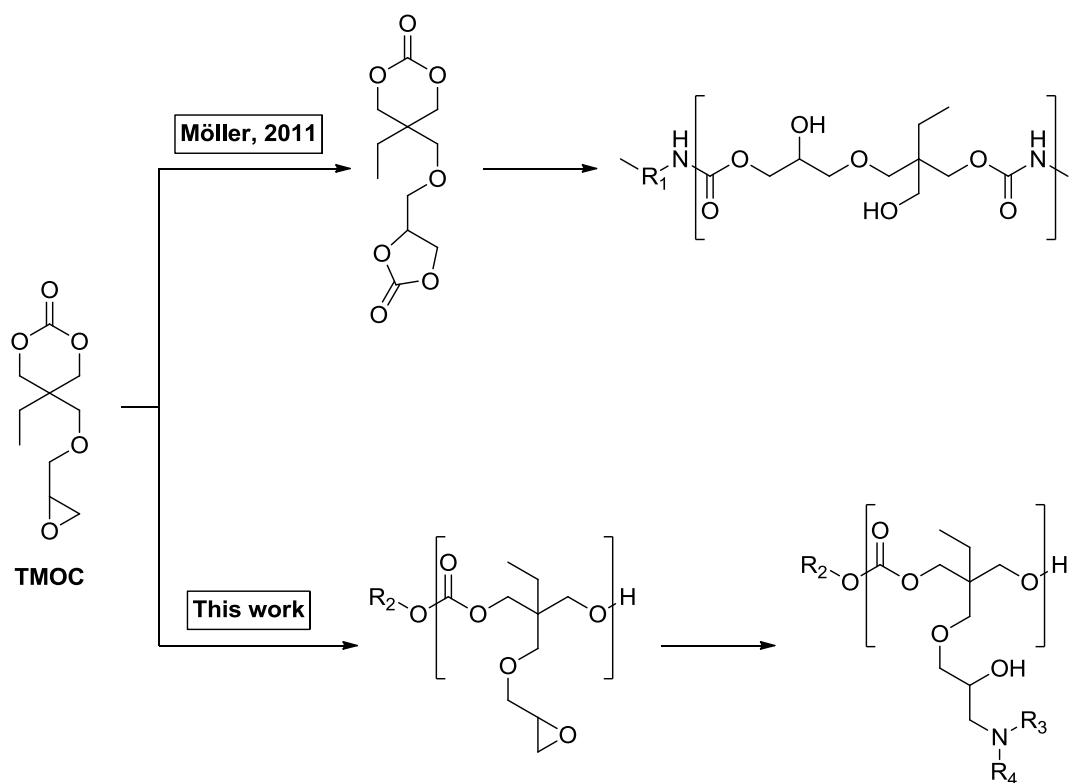
The Synthesis, Ring-Opening Polymerisation and Post-Polymerisation

Functionalisation of an Epoxide-Functional Cyclic Carbonate

4.1 Introduction

Due to the extensive synthesis required to access the carbonates presented in Chapter 3 and the inherent difficulties in scaling such a synthesis to provide appreciable quantities of monomer, a new monomer was sought which would allow for the desired access to functionalised chiral poly(carbonate)s with a minimum number of synthetic steps required.

In 2011, Möller and co-workers reported the synthesis of a bi-functional monomer containing both six- and five-membered cyclic carbonates.⁹⁹ The reported synthesis of this bi-functional monomer is achieved in three steps from commercially-available starting material, with the final step of the monomer synthesis involving the ring-expansion of an epoxide-functionalised cyclic carbonate (TMOC). Möller then proceeds to utilise this di-carbonate in the formation of a range of poly(urethane)s (Scheme 4.1).



Scheme 4.54 - Möller and co-workers use of TMOC in the synthesis of poly(urethanes) and the proposed use of TMOC in this work to access amino-functional poly(carbonates)

It was envisaged that the epoxide-functionalised carbonate TMOOC may be polymerised with the resulting poly(carbonate) offering the potential for the easy incorporation of a wide variety of functionalities by reaction of the pendant epoxide groups with a range of amines. The use of amino acids or their derivatives would enable the inclusion of chiral centres, allowing for easy access to desired chiral, functionalised poly(carbonate)s.

Such pendant functionality has been used for non-degradable polymers such as poly(glycidyl methacrylate) (PGMA) and poly(glycidyl acrylate) (PGA),¹⁰⁰ and shown to be useful for a range of post-polymerisation functionalisation, finding particular application in surface modification. The epoxide group itself has also been utilised for the formation of poly(ether)s via anionic ring-opening, as well as for the formation of poly(carbonate)s in the presence of carbon dioxide.¹⁰¹⁻¹⁰³

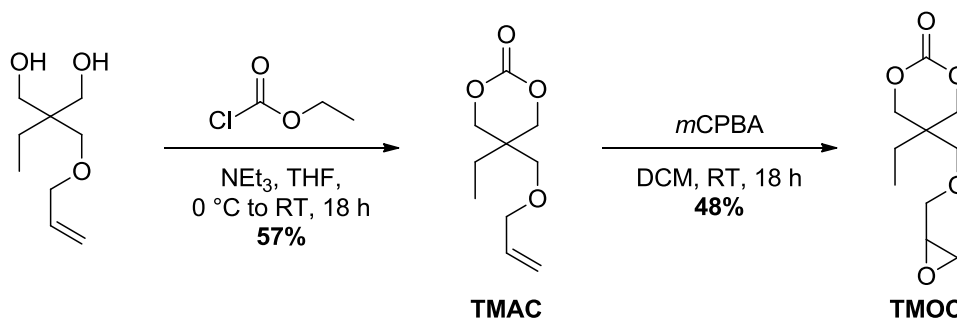
The incorporation of epoxide functionality into a degradable polymer species could prove highly desirable, allowing access to the same range of post-polymerisation modification options demonstrated for PGMA and PGA materials, whilst possessing the benefits of biocompatibility and biodegradability making the resulting product suitable for a far wider range of applications. Indeed, some attempts at the incorporation of epoxide functionality have been reported, however most involve post-polymerisation modification, either through addition of an epoxide-containing species or the epoxidation of a pendant or terminal alkene.^{104,105} Interestingly, there are reports of the use of glycidol as an initiator in the enzymatic ring-opening polymerisation of ϵ -caprolactone, yielding an end-functional homopolymer.¹⁰⁶

Whilst ring-opening polymerisation of both epoxides and cyclic carbonates has been widely reported, to the best of our knowledge the proposed selective ring-opening polymerisation of a cyclic carbonate in the presence of a pendant epoxide (with retention of the epoxide functionality for post-polymerisation functionalisation) would be the first report of such selectivity.

4.2 Results and Discussion

4.2.1 Synthesis of 5-Ethyl-5-((oxiran-2-ylmethoxy)methyl)-1,3-dioxan-2-one, TMOC

The synthesis of TMOC was conducted according to the procedure reported by Möller, starting from commercially-available trimethylolpropane allyl ether and achieved in just two steps (Scheme 4.55).⁹⁹ The diol first undergoes ring-closure using ethyl chloroformate in the presence of triethylamine in tetrahydrofuran, with the crude product being purified by vacuum distillation to afford the allyl-functionalised cyclic carbonate (TMAC). TMAC was subsequently epoxidised using *m*-chloroperoxybenzoic acid (*m*CPBA) in dichloromethane and purified by column chromatography to yield the final pure carbonate TMOC in an overall 27% yield.



Scheme 4.55 - Synthesis of TMOC

A comparison of the ¹H NMR spectra for the allyl diol, TMAC and TMOC is shown in Figure 4.50. The methylene protons adjacent to both hydroxyl groups in the allyl diol are observed to shift downfield from 3.62 and 3.59 ppm to 4.32 and 4.12 ppm upon cyclisation to the carbonate TMAC. The subsequent epoxidation to TMOC shows the full retention of the carbonate functionality (methylene signals at 4.32 and 4.13 ppm), whilst also demonstrating the complete loss of the allyl methine and methylene signals at 5.84 and 5.22

ppm respectively and appearance of the corresponding epoxide protons with signals at 3.11, 2.79 and 2.57 ppm.

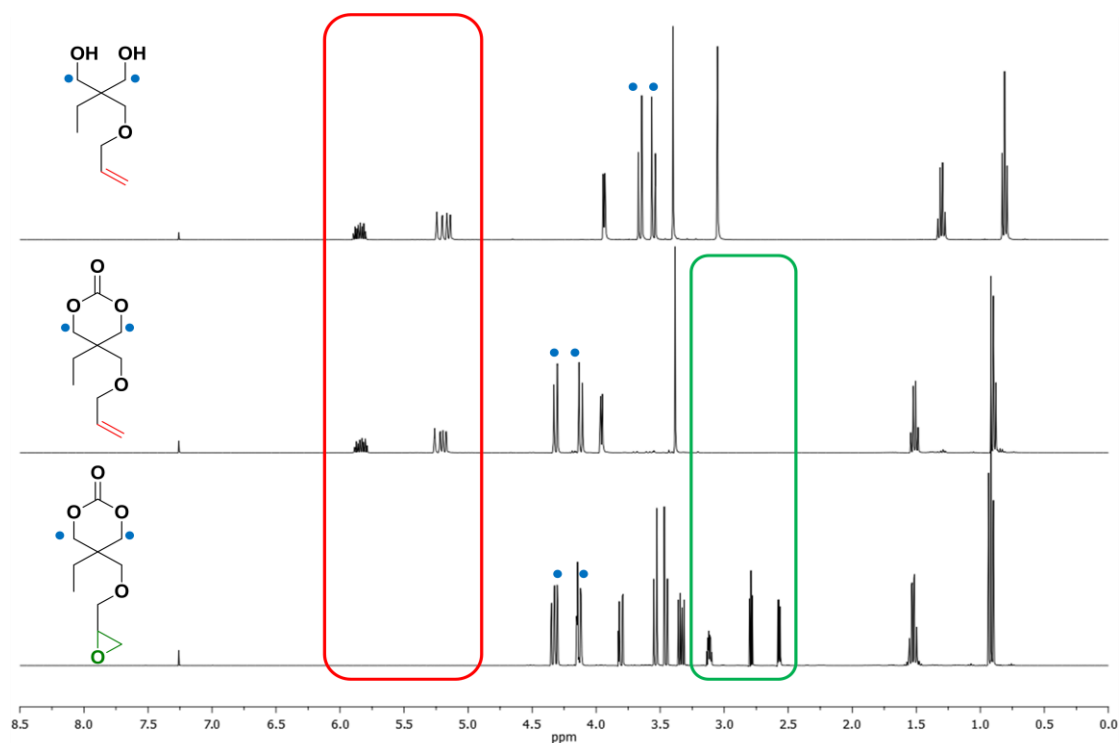


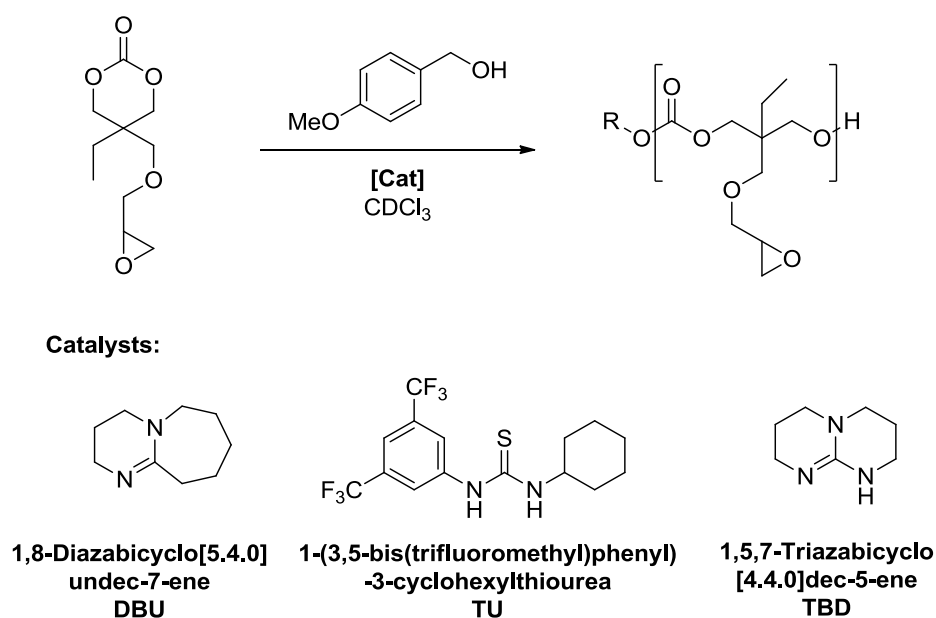
Figure 4.50 - Comparison of ¹H NMR spectra for allyl-functionalised diol, carbonate (TMAC,) and epoxide-functionalised carbonate (TMOC)

Although purification of the epoxide-functional carbonate proceeded smoothly, the subsequent drying required for attempted ring-opening polymerisation (ROP) proved to be more problematic. Initial attempts at drying the monomer in dichloromethane (DCM) over calcium hydride led to complete degradation of the monomer with no identifiable species observed in the ¹H NMR spectrum, whilst attempted drying over 3 Å molecular sieves led to the retention of the cyclic carbonate but loss of the epoxide functionality. Next, stirring the monomer with phosphorous pentoxide at room temperature, followed by attempted distillation under reduced pressure and at elevated temperatures was attempted, but unfortunately yielded only an insoluble mass. Subsequent analysis of the monomer after stirring over phosphorous pentoxide at room temperature, without proceeding to distil, again

showed the complete loss of the epoxide signals from the ^1H NMR spectrum, presumably as a result of the acid-sensitivity of the epoxide functionality.

The monomer was finally successfully dried under a static vacuum and stored over phosphorous pentoxide, with the drying agent being changed at least once a day over the course of two weeks. Two points are worth noting with regard to this drying process, firstly, the extensive drying time is required as the use of phosphorous pentoxide to dry a liquid monomer is unfortunately highly inefficient. Secondly the monomer must be dried under a static vacuum as subjecting it to an active vacuum causes the phosphoric acid produced from the drying process to be drawn over the monomer sample, leading to degradation of the epoxide functionality. The dried monomer was then transferred to a glovebox and stored under a nitrogen atmosphere for use in the subsequent ring-opening polymerisation studies.

4.2.2 Ring-opening polymerisation of TMOE - Catalyst screening



Scheme 4.56 - Catalysts employed in the screening of ring-opening polymerisation conditions for TMOE

The organocatalysed ring-opening polymerisation of the epoxide-functionalised carbonate was first investigated using a series of organocatalysts with initiation from 4-methoxybenzyl alcohol (Scheme 4.56). All polymerisations were conducted in dried deuterated chloroform under a dry, inert nitrogen atmosphere. Reaction progress was most easily monitored using ^1H NMR spectroscopy, with the relative concentration of monomer to initiator ($[\text{M}]/[\text{I}]$) determined by measuring the ratio of integrals of the peaks corresponding to the methylene protons on the monomer ring, at 4.32 and 4.13 ppm, and the methoxy group of 4-methoxybenzyl alcohol at 3.81 ppm. Monomer conversion was calculated by comparison of the integrals of the peaks corresponding to the methylene protons on the monomer ring, at both 5.84 and 5.22 ppm, and the methylene protons of the polymer backbone at 4.10 ppm (Figure 4.51).

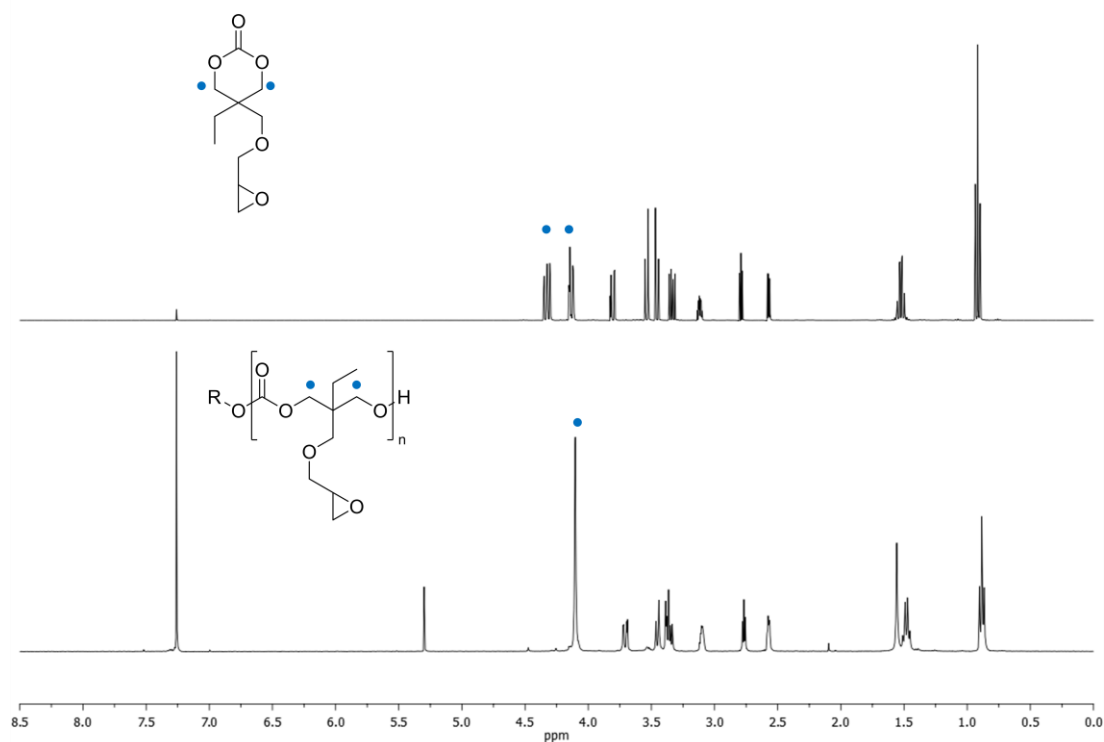


Figure 4.51 - Comparison of ^1H NMR spectra for TMOC and P(TMOC)

Table 4.13 - Catalyst screening for polymerisation of TMOC ($[M]_0/[I]_0 = 20$)

Entry	Catalyst (Loading (mol%)) ^a	$[M]_0$ (mol.dm ⁻³)	Time (h)	Monomer Conv. (%) ^b	DP ^b	M_n (g.mol ⁻¹) ^b	M_n (g.mol ⁻¹) ^c	\mathcal{D}_M ^c
1	DBU (10)	0.5	49	54	10	2300	2560	1.28
2	DBU (10)	1.0	27	75	10	2300	2770	1.28
3	DBU (5)	1.0	49	73	16	3600	3130	1.14
4	DBU / TU (10 / 5)	1.0	12	71	14	3160	2860	1.13
5	DBU / TU (5 / 5)	1.0	22	73	17	3810	2860	1.22
6	TBD (5)	1.0	< 20 min	74	16	3600	4380	1.43
7	TBD (5)	0.5	< 20 min	53	14	3160	3210	1.37
8	TBD (1)	1.0	< 20 min	72	19	4242	4060	1.18

^a Catalyst loading relative to initial monomer concentration; ^b Determined by ¹H NMR spectral analysis; ^c Determined by GPC analysis in CHCl₃, calibrated against poly(styrene) standards.

The homopolymerisation of TMOC was initially attempted using 10 mol% DBU (with respect to starting monomer), at an initial monomer concentration of 0.5 M, with the reaction reaching 54% conversion after 49 hours (Table 4.13, Entry 1). Analysis of the ¹H NMR spectrum of the isolated polymer shows an apparent degree of polymerisation (DP) of 10 and calculated molecular weight of 2300 g.mol⁻¹, with analysis of the isolated polymer by gel permeation chromatography (GPC) showing an observed molecular weight (M_n) of 2560 g.mol⁻¹ and a dispersity (\mathcal{D}_M) of 1.28. Whilst there was decent agreement between both the calculated and observed molecular weights, the GPC trace showed a significant low weight shoulder. The dispersity observed in the GPC analysis was within the realm of a living polymerisation, it remained broader than would perhaps be desirable (Figure 4.52).

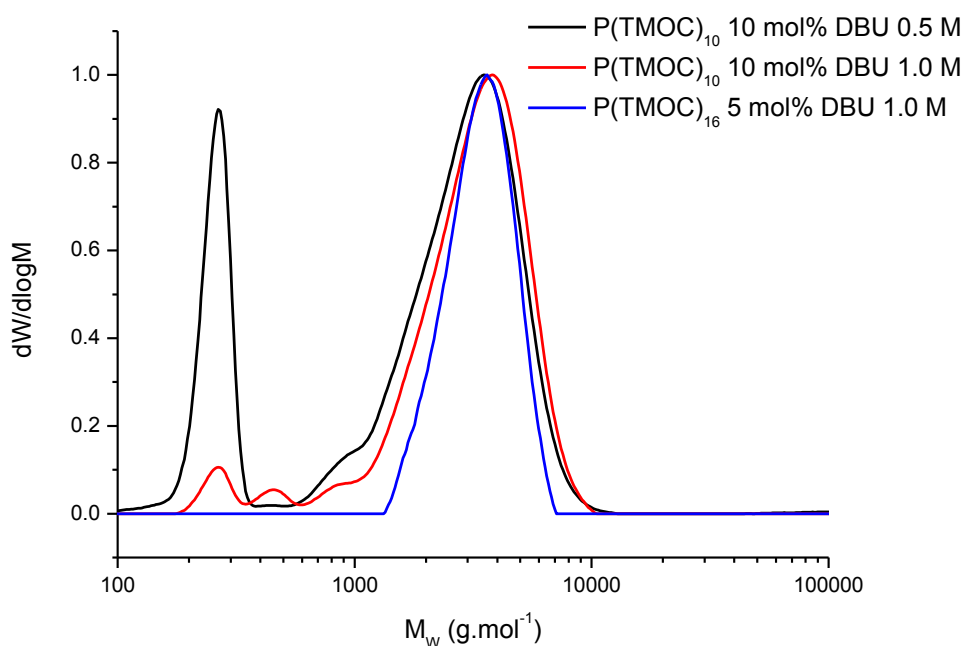


Figure 4.52 - GPC traces of P(TMOC) obtained using 10 mol% DBU at 0.5 M & 1.0 M and 5 mol% DBU at 1.0 M

MALDI-ToF MS analysis of the obtained polymer shows two distributions (Figure 4.53); the major observed distribution corresponding to the calculated molecular weight for the poly(carbonate) initiated from 4-methoxybenzyl alcohol and bearing a single sodium charge, the peak weight of which corresponds to a DP of 9, in close agreement with that calculated by analysis of the ^1H NMR spectrum.

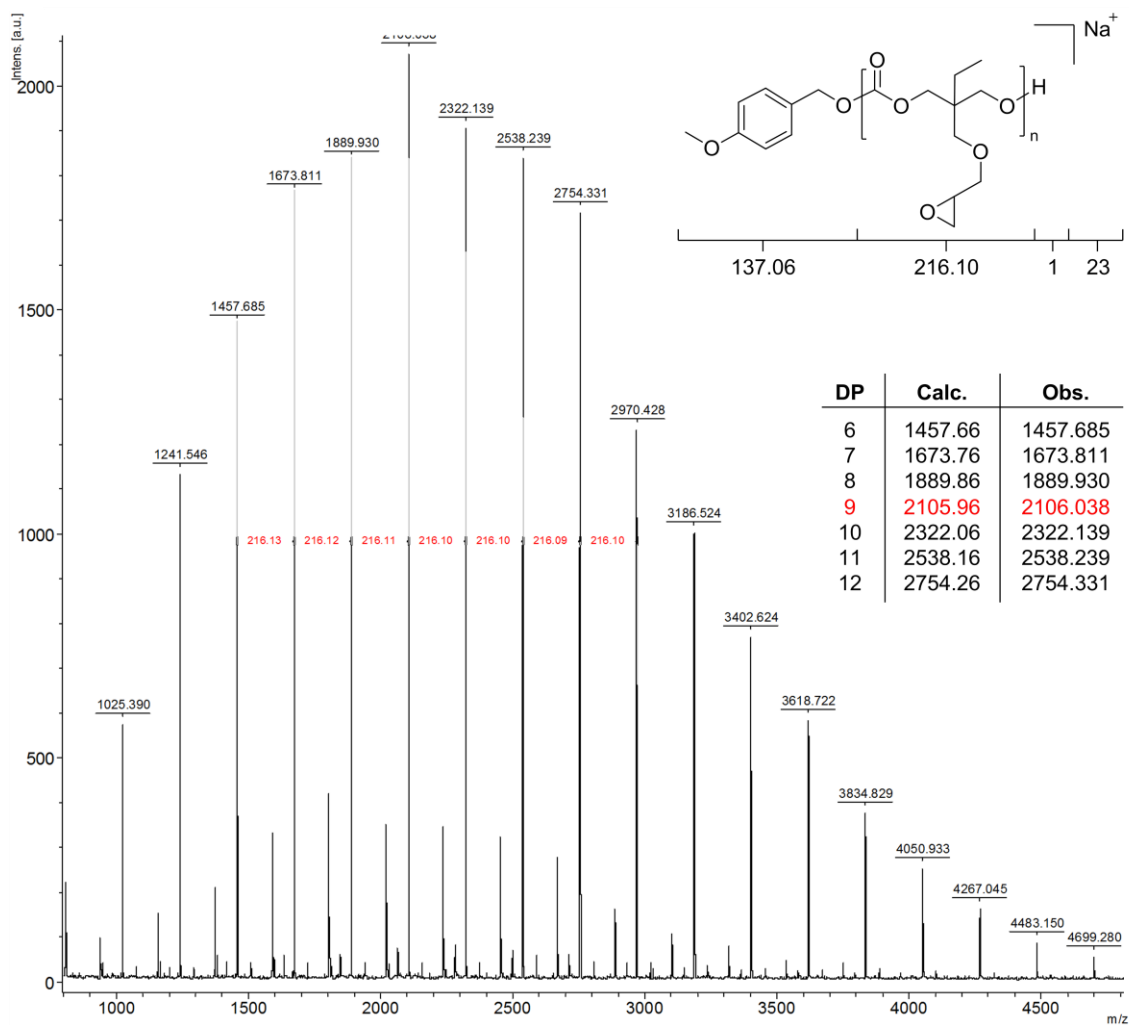


Figure 4.53 - MALDI-ToF MS spectrum of P(TMOC)₁₀ obtained using 10 mol% DBU at 0.5 M

The second, minor distribution observed in the MALDI spectrum (Figure 4.54) unfortunately eluded identification, having eliminated the possibility of water-initiation and ring-opening of the pendant epoxide groups.

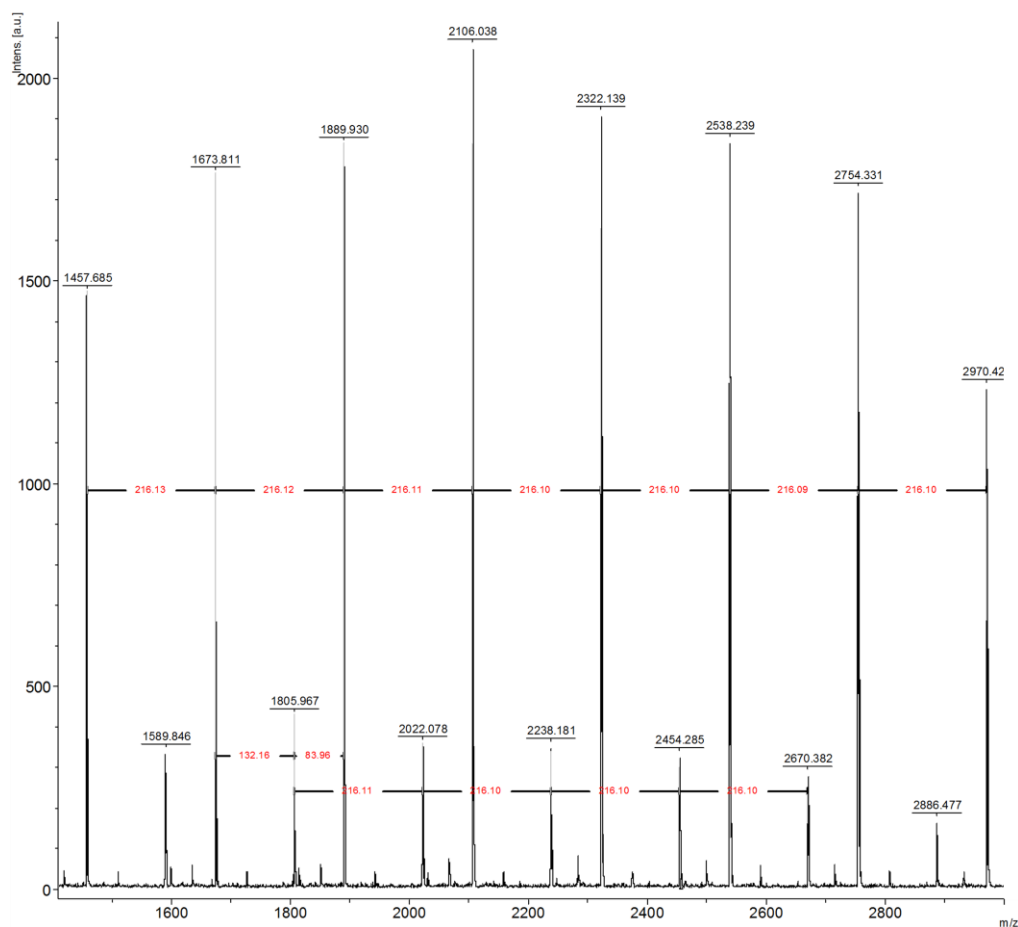


Figure 4.54 - Expansion of MALDI-ToF MS spectrum of P(TMOC)₁₀ obtained using 10 mol% DBU at 0.5 M

The polymerisation was next repeated under the same conditions, yet with an increase in the initial monomer concentration, at 1.0 M (Table 4.13, Entry 2). This led to the expected increase in polymerisation rate, with the reaction achieving 75% conversion after only 27 hours at room temperature. The increase in conversion achieved at reaction equilibrium corresponds with the expected thermodynamics of ring-opening polymerisation, specifically that an increase in initial monomer concentration leads to the monomer-polymer equilibrium shifting to favour the formation of polymeric species. Again, ¹H NMR analysis showed a DP of 10 with a corresponding calculated molecular weight of 2300 g.mol⁻¹, lower than would otherwise be expected given the increased monomer conversion.

The GPC analysis of the resulting polymer (Figure 4.52) showed a slight increase in the observed molecular weight, with an M_n of 2770 and an identical dispersity ($D_M = 1.28$) when compared to the polymer obtained from the reaction conducted at 0.5 M (Table 4.13, Entry 1). The resulting MALDI-ToF spectrum (Figure 4.55) again shows a major distribution relating to the poly(carbonate) initiated from 4-methoxybenzyl alcohol and bearing a single sodium charge, with a peak degree of polymerisation of 7. Two minor distributions were also observed, the smaller of the two corresponding to the polymeric species initiated from water and the final distribution remaining unidentified as in the previous reaction.

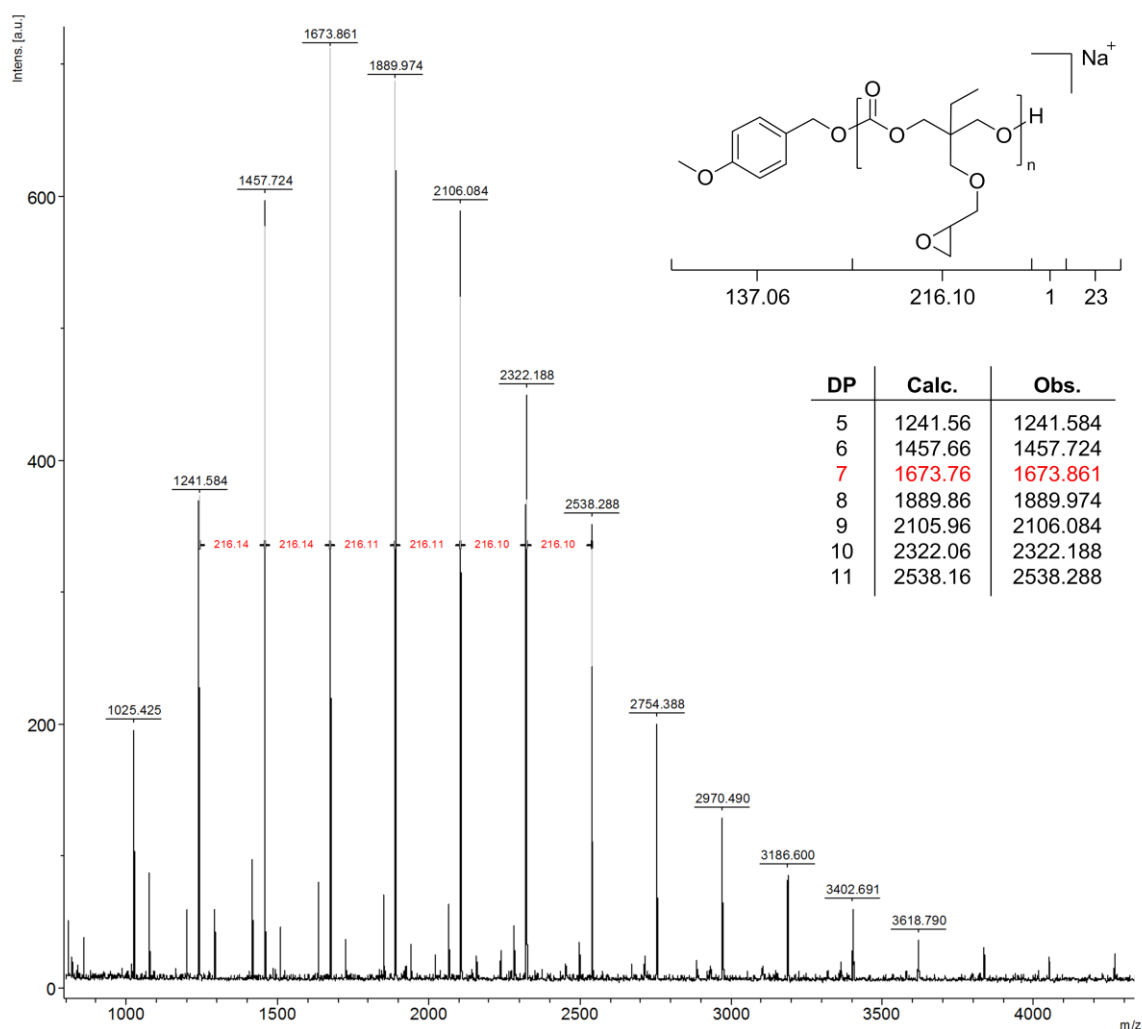


Figure 4.55 - MALDI-ToF MS spectrum of $P(TMOC)_{10}$ obtained using 10 mol% DBU at 1.0 M

Reduction of the catalyst loading from 10 mol% to 5 mol% of DBU, still conducted at an initial monomer concentration of 1.0 M showed the expected decrease in the rate of polymerisation (Table 4.13, Entry 3). The reaction reached 73% conversion after 49 hours, with final ^1H NMR spectral analysis showing a DP of 16 with a calculated molecular weight of $3600 \text{ g}\cdot\text{mol}^{-1}$. The isolated polymer was analysed by GPC and showed both an increased molecular weight ($M_n = 3131 \text{ g}\cdot\text{mol}^{-1}$) and a narrowing of the dispersity, $D_M = 1.14$ (Figure 4.52). The GPC chromatogram also shows no trace of either low weight species or shoulder as was observed in both the previous reactions conducted using 10 mol% of DBU (Table 4.13, Entries 1 & 2). The analysis of the resultant polymer by MALDI-ToF MS shows a single distribution relating to the targeted polymeric species initiated from 4-methoxybenzyl alcohol, with a peak DP of 8. Although the second, unidentified species was still present, it no longer formed a significant distribution, being reduced to a trace in the spectrum (Figure 4.56).

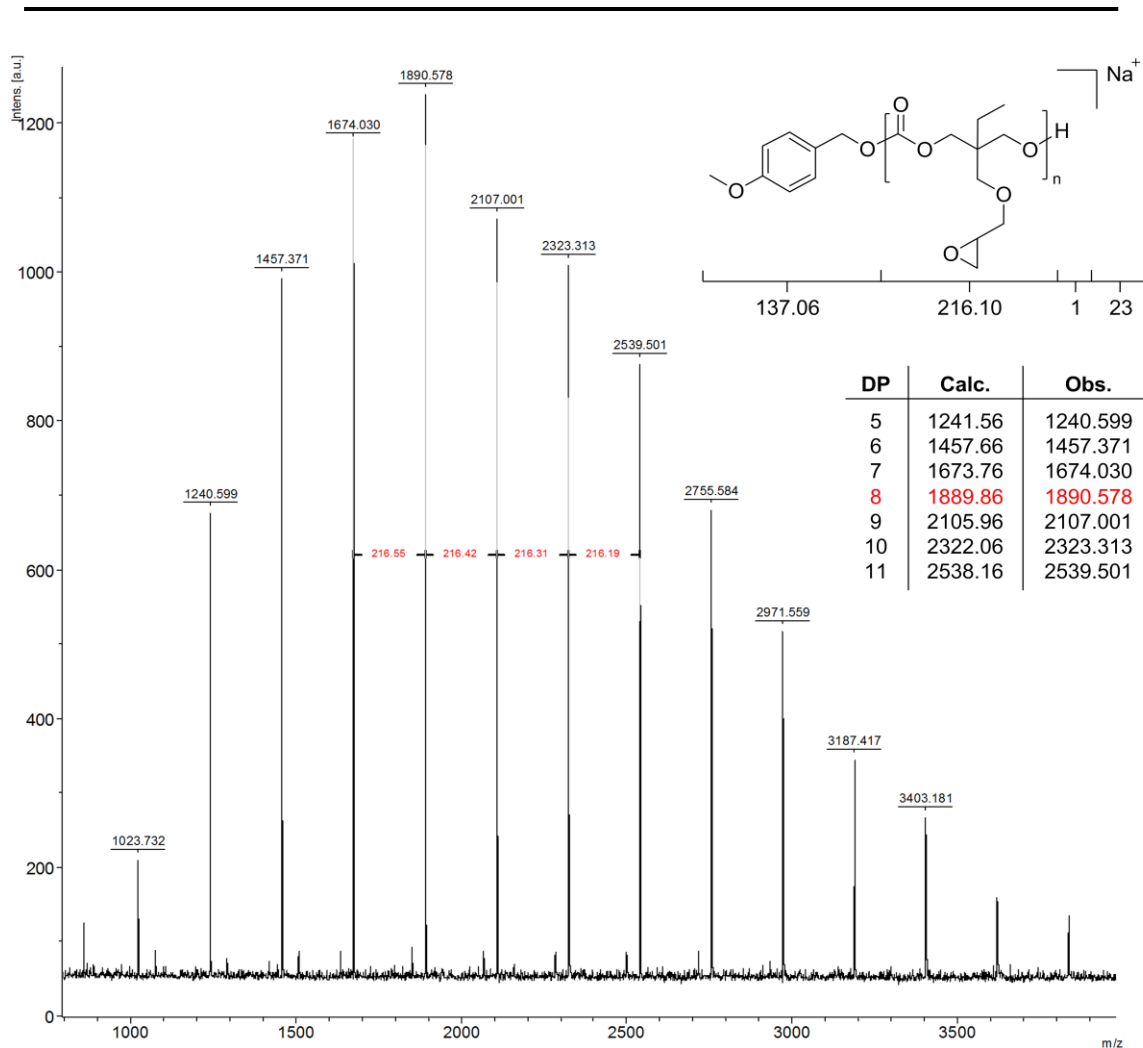


Figure 4.56 - MALDI-ToF MS spectrum of P(TMOC)₁₆ obtained using 5 mol% DBU at 1.0M

Although the reduction of the DBU catalyst loading from 10 to 5 mol% appears to offer better control than that obtained at higher loadings, the reaction time remains longer than would be desirable at 49 hours for a targeted DP 20. In an attempt to reduce the required reaction time and retain control over the resulting polymers, the thiourea co-catalyst TU was introduced to the polymerisation (Table 4.13, Entries 4 & 5).

The catalyst loadings were 10 and 5 mol% for DBU and thiourea respectively at an initial monomer concentration of 1.0 M (Table 4.13, Entry 4). After only 12 hours at room temperature, the reaction had reached 71.7% conversion, with the final ¹H NMR spectrum showing a DP of 14 and giving a calculated molecular weight of 3160 g.mol⁻¹.

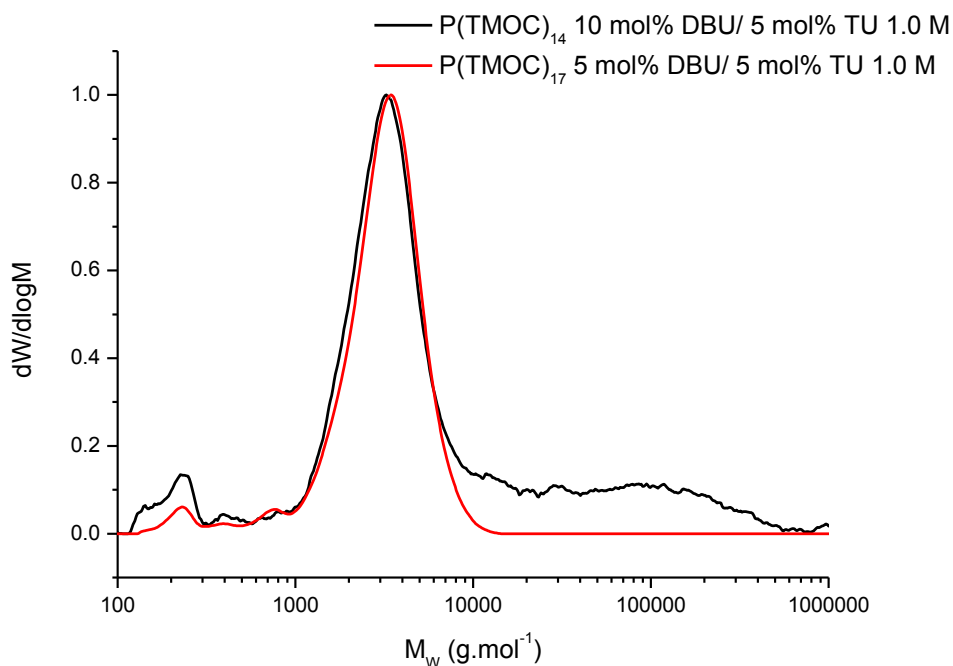


Figure 4.57 - GPC traces of P(TMOC) obtained using 10 mol% DBU / 5 mol% TU and 5 mol% DBU / 5 mol% TU at 1.0 M

The GPC analysis of the obtained polymer (Figure 4.57) shows a distribution with an observed molecular weight (M_n) of 2860 g.mol⁻¹ and a suitably narrow dispersity ($D_M = 1.13$), both comparable to those observed for the polymer obtained from the use of 5 mol% DBU (Table 4.13, Entry 3). It should be noted that very little polymer was isolated from this reaction (28 mg; 26%), impeding the signal-to-noise ratio of both the GPC and MALDI-ToF MS analyses.

The MALDI-ToF spectrum of the resulting polymer again shows the major distribution relating to the 4-methoxybenzyl alcohol-initiated species, with a peak degree of polymerisation of 7. Although, as already noted, the signal-to noise ratio for this analysis was lower than would be desirable, there was no apparent secondary distribution observed (Figure 4.58).

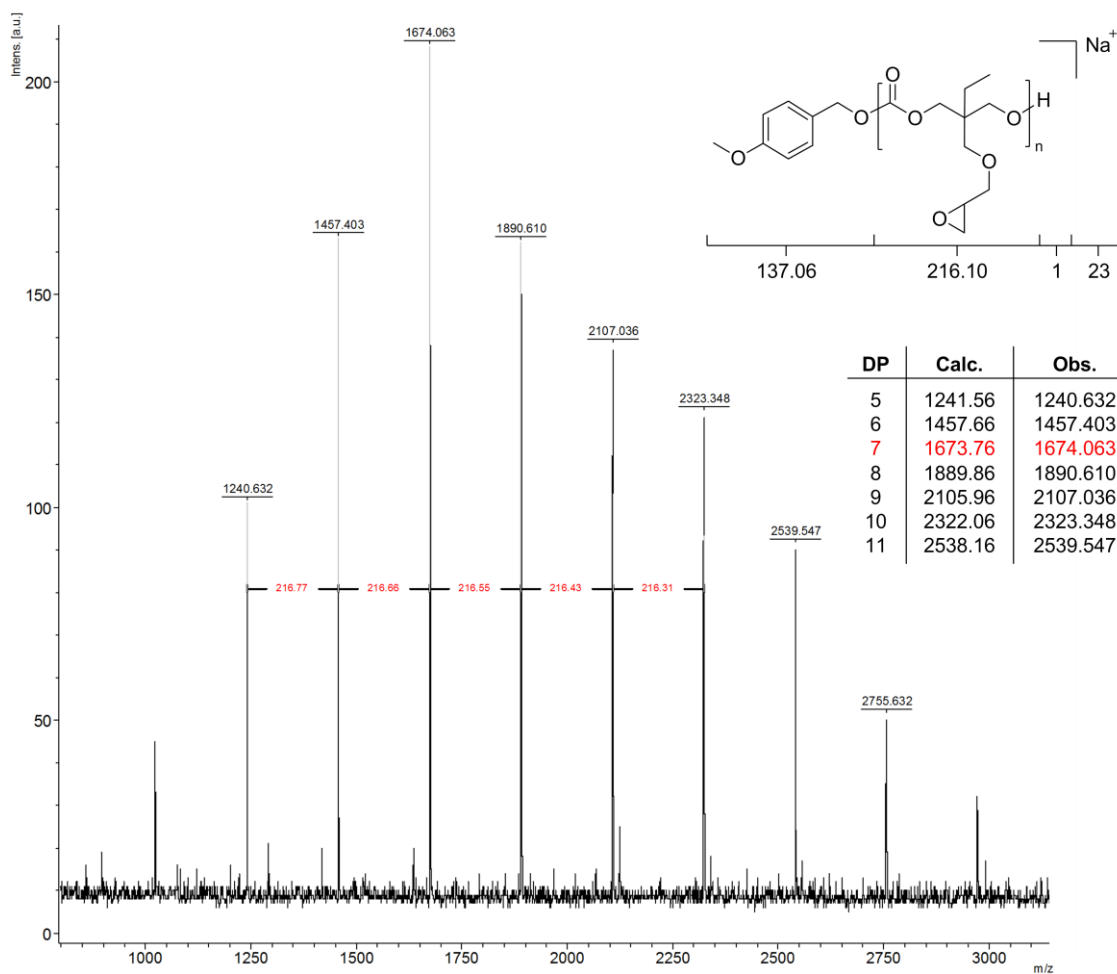


Figure 4.58 - MALDI-ToF MS spectrum of P(TMOC)₁₄ obtained using 10 mol% DBU and 5 mol% thiourea at 1.0 M

The reduction of both the DBU and thiourea co-catalyst loadings to 5 mol% increased the reaction time to 22 hours, with the reaction reaching equilibrium at 73% conversion over this time (Table 4.13, Entry 5). The ¹H NMR spectrum of the isolated polymer showed a DP of 17, relating to a calculated molecular weight of 3810 g.mol⁻¹.

Although the ¹H NMR spectrum suggested a higher molecular weight than that obtained from the previous reaction (using 10 and 5 mol% of DBU and thiourea respectively), the GPC analysis shows a distribution with an M_n of 2860 g.mol⁻¹ and $D_M = 1.22$ (Figure 4.57). Although the distribution is slightly broader, there appears to be no appreciable difference in

the obtained polymer when compared with that recovered from the reaction using a higher loading of DBU (Table 4.13, Entry 4).

Unlike the other monomers described previously in this thesis, TMOc possesses no pendant ester functionalities, meaning that it is possible to screen catalysts which would normally be excluded due to their tendency to cause transesterification as a side-reaction during the course of the polymerisation. A perfect example of such a catalyst is 1,5,7-triazabicyclo[4.4.0]dec-5-ene (TBD, Scheme 4.55).

The first TBD-catalysed polymerisation was conducted using a catalyst-loading of 5 mol% at an initial monomer concentration of 1.0 M (Table 4.1, Entry 6). Whilst a large increase in the rate of polymerisation was expected, the reaction speed proved to be an order of magnitude greater than any of those previously observed, reaching 74% conversion after less than twenty minutes. ^1H NMR spectral analysis showed an apparent DP of 16, giving a calculated molecular weight of $3600 \text{ g}\cdot\text{mol}^{-1}$.

The GPC analysis of the obtained polymer (Figure 4.59) showed a material with a molecular weight higher than any of those previously analysed, with an M_n of $4380 \text{ g}\cdot\text{mol}^{-1}$. However, whilst the molecular weight was vastly improved, the resulting dispersity was also considerably broader than that of previous reactions, $D_M = 1.43$. There are significant low weight signals and a tail on the chromatogram which appear to correlate with the expected masses of oligomers.

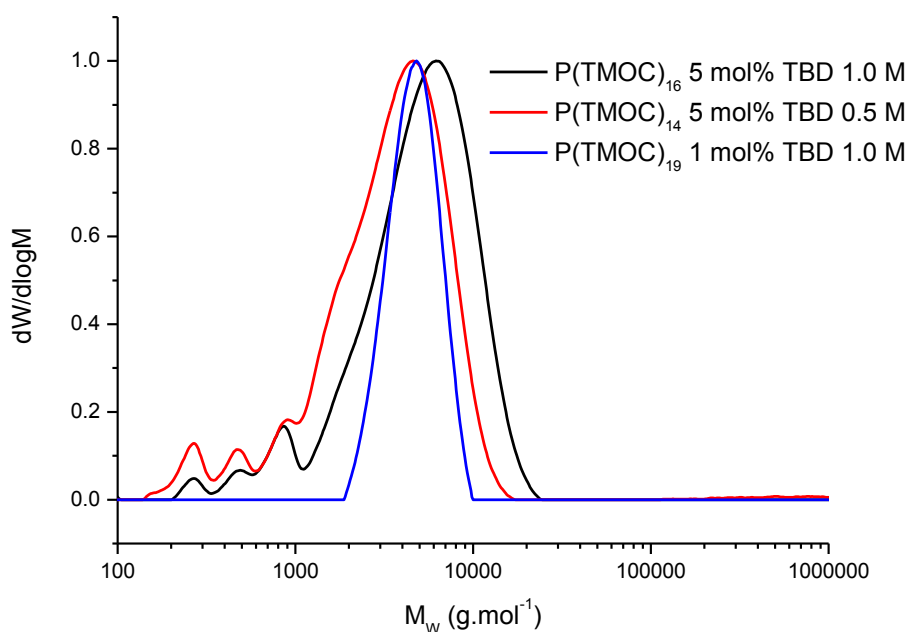


Figure 4.59 - GPC traces of P(TMOC) obtained using 5 mol% TBD at 1.0 & 0.5 M and 1 mol% at 1.0 M

Coupled with the extremely short reaction time, the broad dispersity, and presence of identifiable oligomers it is plausible to conclude that the propagation rate of the polymerisation is significantly greater than that of the initiation step. It was therefore believed that the rate of propagation needs to be significantly reduced, relative to the initiation rate.

In an attempt to investigate whether control over the polymerisation could be improved simply by reduction of the overall rate, the reaction was repeated with 5 mol% TBD at an initial monomer concentration of 0.5 M (Table 4.13, Entry 7). The rate of reaction still proved to be rapid when compared to those involving both DBU and DBU / thiourea catalyst systems (Table 4.13, Entries 1-5), reaching 53% conversion in less than 20 minutes. The ^1H NMR spectrum showed an apparent DP of 14 and a calculated molecular weight of 3160 g.mol^{-1} .

The GPC analysis of the isolated polymer (Figure 4.59) again shows a broad trace with an M_n of $3210 \text{ g}\cdot\text{mol}^{-1}$ and $D_M = 1.37$. Whilst there is still a good correlation between the calculated molecular weight (determined by ^1H NMR spectral analysis) and that observed by GPC analysis, there is no obvious improvement in control when compared to the reaction conducted at 1.0 M monomer concentration.

Finally, the reduction of the TBD catalyst loading to 1 mol% with an initial monomer concentration of 1.0 M also gave no increase in reaction time, with the polymerisation achieving 72% conversion in less than 20 minutes with the final ^1H NMR spectrum showing a degree of polymerisation of 19, leading to a calculated molecular weight of $4242 \text{ g}\cdot\text{mol}^{-1}$ (Table 4.13, Entry 8).

The polymer obtained from this reaction was submitted for analysis by GPC (Figure 4.59), the results of which showed a significant improvement on the results obtained from the reactions conducted using 5 mol%. The molecular weight showed good agreement with the calculated weight obtained from the ^1H NMR spectral analysis, $M_n = 4057 \text{ g}\cdot\text{mol}^{-1}$, whilst the distribution showed a vastly narrowed dispersity compared with the polymers obtained from higher catalyst loadings, $D_M = 1.18$.

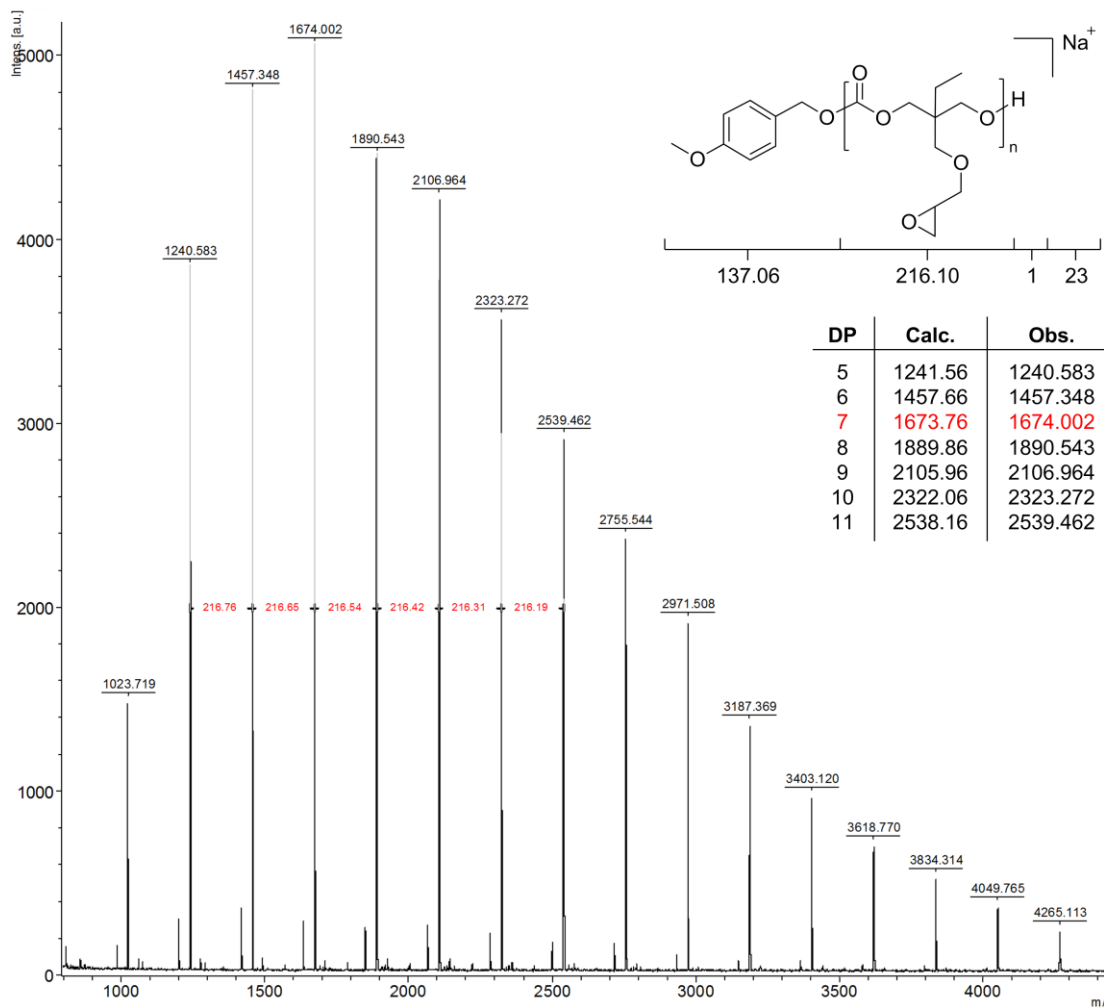


Figure 4.60 - MALDI-ToF MS spectrum of P(TMOC)₁₉ obtained using 1 mol% TBD at 1.0 M

The isolated polymer was subsequently submitted for analysis by MALDI-ToF MS, with the resulting spectrum showing the desired 4-methoxybenzyl alcohol-initiated species at a peak DP of 7. Although this is far lower than implied by both the ¹H NMR and GPC analyses, it is easily conceivable that this discrepancy in masses is due to a low-mass-detection bias in the MALDI-ToF MS system used. There is only a minor secondary distribution observed, yet it is worth noting that the major, desired, polymeric species is detected at higher molecular weights than observed in any previous MALDI-ToF spectrum, suggesting a better agreement with the other analyses conducted than would be implied by the peak DP.

Due to the extremely short reaction time, the good agreement of the observed *versus* calculated molecular weights with a pleasingly narrow dispersity and the higher molecular weights observed with only a minor secondary distribution, it was decided that the use of 1 mol% TBD with an initial monomer concentration of 1.0 M would be selected as the preferred catalyst system for further investigations of the polymerisation of TMOc.

4.2.3 Ring-opening polymerisation of TMOc - Investigation of polymerisation control

With the use of 1 mol% of TBD as the organocatalyst at an initial monomer concentration of 1.0 M selected as the optimal conditions during the catalyst screen (Table 4.1, Entry 8), further investigations were required in order to demonstrate the degree of control obtained over the ring-opening polymerisation of TMOc. Therefore, initial polymerisation tests were conducted targeting various degrees of polymerisation, 53, 72, 95 and 228.

Table 4.14 -Polymerisation of TMOC initiating from 4-methoxybenzyl alcohol using 1 mol% TBD

Entry	$[M]_0/[I]_0^a$	Time (min)	Monomer Conversion (%) ^a	DP ^a	M_n (g.mol ⁻¹) ^a	M_n (g.mol ⁻¹) ^b	\mathcal{D}_M^b
1	20	<20	72	19	4242	4060	1.18
2	53	44	73	104	22602	9110	1.20
3	72	61	72	89	19362	9920	1.18
4	95	72	70	118	25626	10500	1.14
5	228	106	64	459	99282	11900 ^c 28600 ^c	1.05 ^c 1.11 ^c

^a Determined by ¹H NMR spectral analysis. ^b Determined by GPC analysis in CHCl₃, calibrated against poly(styrene) standards. ^c GPC trace showed bimodal distribution.

Initiating from 4-methoxybenzyl alcohol, the exact starting monomer to initiator ratios ($[M]_0/[I]_0$) were 53, 72, 95 and 228 (Table 4.14), with all reaching equilibrium within approximately 1 hour, except for the latter reaction, which reached equilibrium after roughly 2 hours. Initial analysis of the resulting polymers by ¹H NMR spectral analysis showed a large deviation from the expected degrees of polymerisation, giving corresponding DP values of 104, 89, 118 and 459, with calculated molecular weights of 22602, 19362, 25626 and 99282 g.mol⁻¹ respectively.

However, comparison of these calculated M_n values with those observed by GPC analysis shows a different story, with a steady increase in molecular weight observed with an increase in targeted DP (Figure 4.13). Observed M_n values for the reactions with $[M]_0/[I]_0$ of 53, 72 and 95 were 9110, 9920 and 10500 g.mol⁻¹ ($\mathcal{D}_M = 1.12, 1.18$ and 1.14) respectively. Although this does indeed show a trend of increasing observed molecular weight with increased target weight, the increases are well outside of those that would be expected.

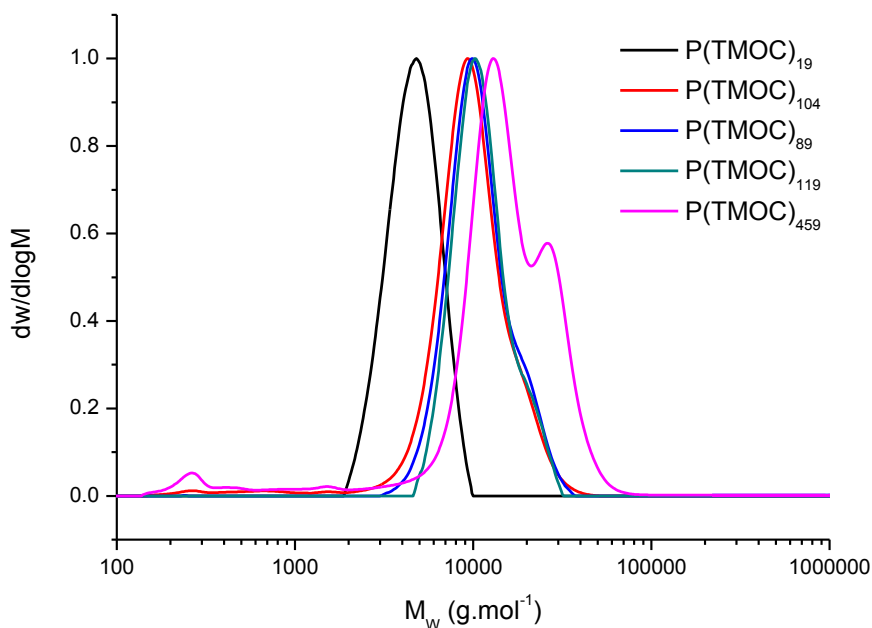
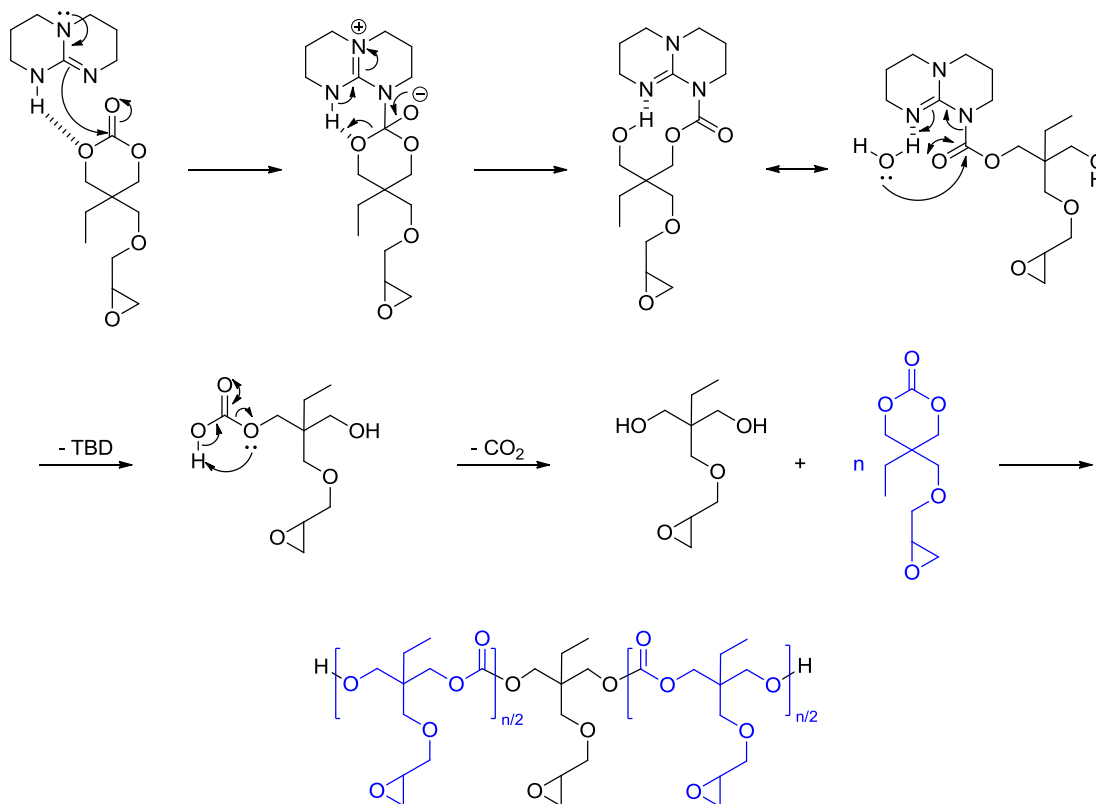


Figure 4.61 - GPC traces of P(TMOC) initiated from 4-methoxybenzyl alcohol with target DPs of 20, 53, 72, 95 and 228

A likely explanation is offered by the analysis of the resulting polymer from the reaction using $[M]_0/[I]_0$ of 228; the GPC chromatogram for this material shows an obvious bimodality (Figure 4.61), with a significant high-weight secondary distribution ($M_n = 11900$ and 28600 g.mol^{-1} with $D_M = 1.05$ and 1.11 when analysed separately). This is consistent with having competing initiation from residual trace water in the monomer and is supported by the slight high weight shoulders observed on the GPC traces of the lower target weight polymers, due to the trace water becoming a more significant source of initiation as the intended initiator concentration is reduced.

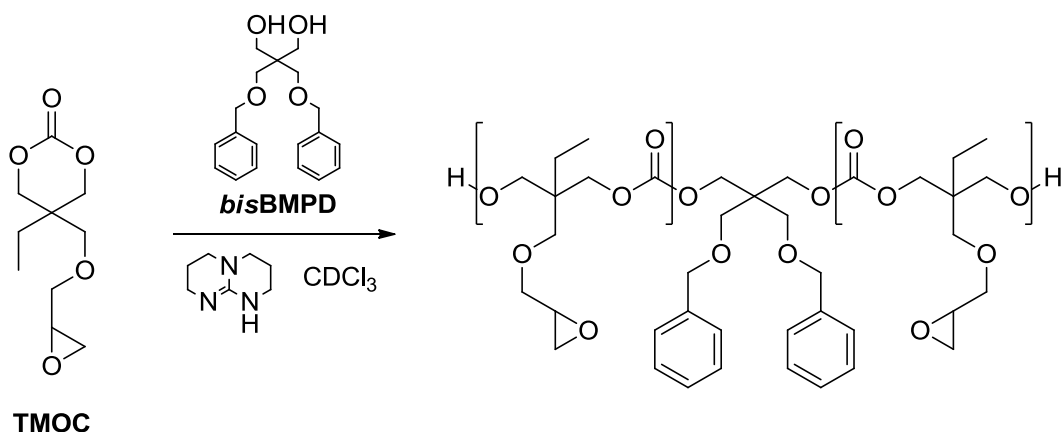
As previously discussed in Chapter 3, initiation from water leads to the formation of a telechelic species bearing a propagating hydroxyl group and a carbonic acid, with the latter subsequently degrading to leave a second hydroxyl group with the release of carbon dioxide (Scheme 4.57). In this manner, the polymer chain may propagate from both ends and assuming equivalent rates of monomer addition compared to mono-functional chains, such

initiation typically leads to a secondary distribution with molecular weights roughly double that of the main mono-functional chains.



Scheme 4.57 - TBD-catalysed initiation of TMOC from residual water to yield telechelic P(TMOC)

Due to the difficulty of removing such traces of water from the monomer, presumably due to it being dried as a liquid film over phosphorous pentoxide, it was deemed preferable to eliminate the bimodality of the competing initiation mechanisms. To this end, the reactions were repeated using 2,2-bis((benzyloxy)methyl)propane-1,3-diol (*bis*BMPD) as the intended initiator, to produce a bifunctional homopolymer (Scheme 4.58).

Scheme 4.58 - Homopolymerisation of TMOC from *bisBMPD* using 1 mol% TBDTable 4.15 - Polymerisation of TMOC initiating from *bisBMPD* using 1 mol% TBD

Entry	$[M]_0/[I]_0^a$	Time (min)	Monomer Conversion (%) ^a	DP ^a	M_n (g.mol ⁻¹) ^a	M_n (g.mol ⁻¹) ^b	D_M^b
1	46	27	71	33	7444	7940	1.15
2	72	30	79	55	12289	12000	1.16
3	106	37	78	60	13314	12900	1.16
4	237	64	75	117	25777	16400	1.23

^a Determined by ¹H NMR spectral analysis; ^b Determined by GPC analysis in CHCl₃, calibrated against poly(styrene) standards.

The reactions initiated from *bisBMPD* had initial monomer to initiator ratios ($[M]_0/[I]_0$) of 46, 72, 106 and 237 as determined by ¹H NMR spectroscopy. The first three reactions reached equilibrium within approximately half an hour (27, 30 and 37 minutes, respectively), with the higher target weight reaction requiring 64 minutes before reaching an equilibrium state (Table 4.15).

All the resulting polymers were analysed by ¹H NMR spectroscopy, revealing a more promising trend in apparent DP than that observed for the polymers initiated from 4-

methoxybenzyl alcohol, with the degree of polymerisation obviously increasing in relation to an increase in $[M]_0/[I]_0$. This ^1H NMR spectral analysis gave DPs of 33, 55, 60 and 117 and calculated molecular weights of 7444, 12289, 13314 and 25777 $\text{g}\cdot\text{mol}^{-1}$ respectively. These calculated weights possess a very tight correlation to those observed by GPC analysis of the same polymers for the first three reactions (Table 4.15, Entries 1-3), with M_n values of 7940, 12000 and 12900 $\text{g}\cdot\text{mol}^{-1}$. The measured dispersities for all three polymers were consistently narrow ($\mathcal{D}_M = 1.15, 1.16$ and 1.16) and showed no sign of a secondary distribution or of any shouldering (Figure 4.62).

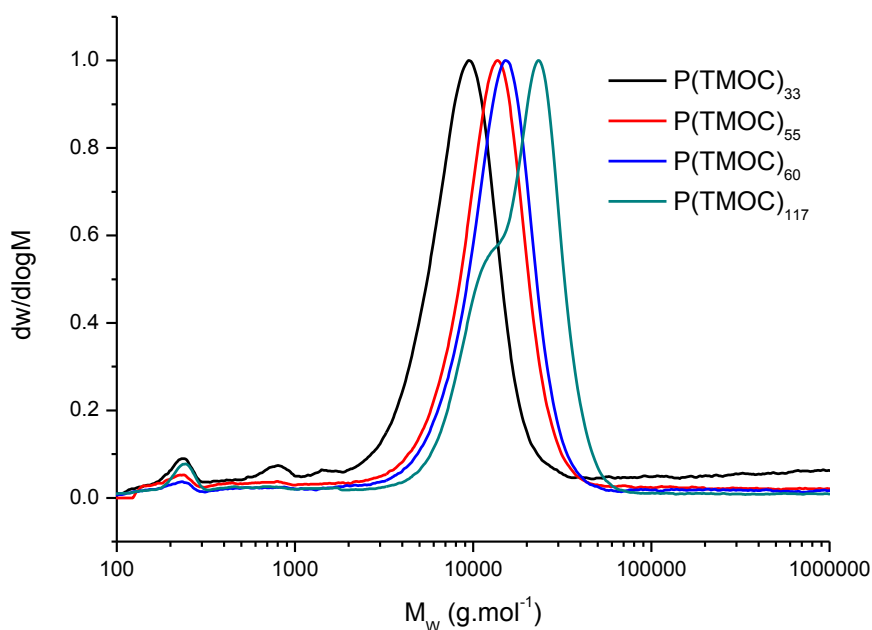


Figure 4.62 - GPC traces of P(TMOC) initiated from bisBMPD with target DPs of 46, 72, 106 and 237

The results of the GPC analysis of the reaction conducted with an $[M]_0/[I]_0$ of 237, however, fail to maintain the tight correlation between the calculated and observed molecular weights seen in the lower-weight polymers. Whilst the chromatogram didn't show a distinct bimodal distribution as seen in the corresponding polymer initiated from 4-methoxybenzyl alcohol, there was still significant shouldering, although on the low-weight side of the distribution.

This shouldering potentially still arises from the competing initiation mechanisms between the residual water and the intended *bis*BMPD. Analysis of the chromatogram gave a molecular weight significantly lower than that calculated from the ^1H NMR spectrum, $M_{n(\text{GPC})} = 16400 \text{ g}\cdot\text{mol}^{-1}$ versus $M_{n(\text{NMR})} = 25777 \text{ g}\cdot\text{mol}^{-1}$, although, even with the shouldering present, the dispersity remained respectably narrow ($\mathcal{D}_M = 1.23$).

The relationship between the starting monomer to initiator ratio and the molecular weight observed by GPC analysis shows a linear correlation, implying the control expected from a living polymerisation (Figure 4.63). The non-zero intercept of the trendlines observed with the inclusion of all four polymers ($7962 \text{ g}\cdot\text{mol}^{-1}$, —) and with the exclusion of the non-unimodal distribution obtained for $\text{P}(\text{TMOC})_{117}$ ($4974 \text{ g}\cdot\text{mol}^{-1}$, —) indicates that the propagation rate remains faster than the rate of initiation.

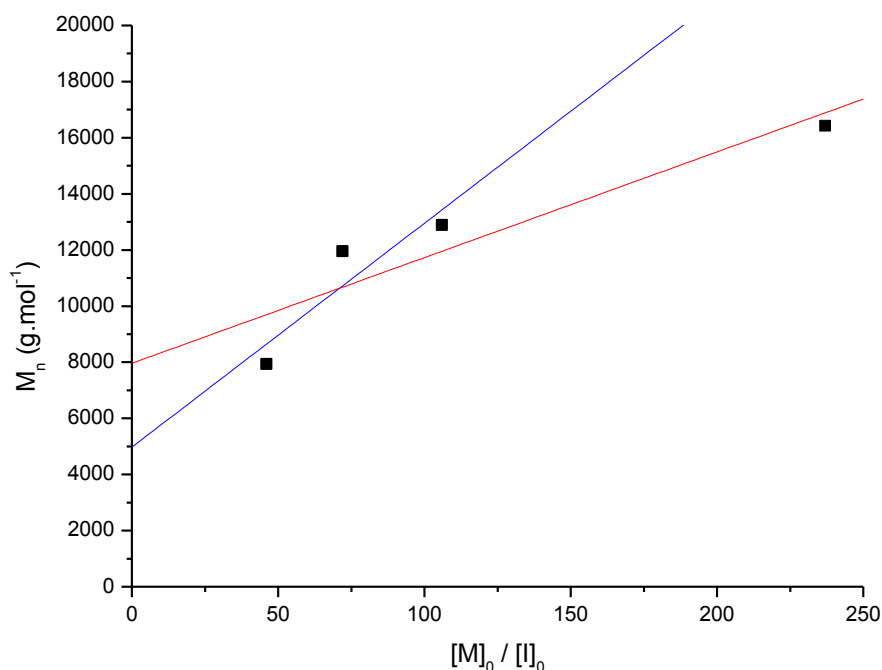


Figure 4.63 - $[M]_0/[I]_0$ vs. $M_{n(\text{GPC})}$ for $\text{P}(\text{TMOC})$ initiated from *bis*BMPD with trendlines inclusive (—) and exclusive (—) of $\text{P}(\text{TMOC})_{117}$

The linear relationship between the targeted degree of polymerisation and the observed molecular weight, along with the narrow dispersities and unimodal distributions observed for polymerisations conducted with a starting monomer to initiator ratio of 100 or less demonstrates that, at least within this domain, it is possible to control the properties of the material obtained from the homopolymerisation of TMOC.

4.2.4 Functionalisation of P(TMOC)

Having established that the homopolymerisation of TMOC may be controlled effectively up to at least a target degree of polymerisation of 100, the polymerisations were scaled up (2.5 g of monomer) to allow the attempted functionalisations to be conducted on common substrates. These two homopolymers were synthesised using starting monomer to initiator ratios of 23 and 91 and the reactions reached equilibrium within 20 and 42 minutes at 75 and 66% total monomer conversion respectively (Table 4.16).

Table 4.16 - Gram-scale synthesis of P(TMOC) initiating from *bis*BMPD using 1 mol% TBD

Entry	$[M]_0/[I]_0^a$	Time (min)	Monomer Conversion (%) ^a	DP ^a	M_n (g.mol ⁻¹) ^a	M_n (g.mol ⁻¹) ^b	D_M^b
1	23	<20	75	20	4636	3630	1.42
2	91	42	66	64	14140	12300	1.13

^a Determined by ¹H NMR spectral analysis; ^b Determined by GPC analysis in CHCl₃, calibrated against poly(styrene) standards.

Analysis of the isolated polymers by ¹H NMR spectroscopy showed apparent degrees of polymerisation of 20 and 64, relating to calculated molecular weights of 4636 and 14140 g.mol⁻¹ respectively. These calculated molecular weights again show a respectable

correlation to the molecular weights observed in the analysis by GPC (3630 and 12300 $\text{g}\cdot\text{mol}^{-1}$ respectively, Figure 4.64) and both polymers also show unimodal distributions with dispersities of $\mathcal{D}_M = 1.42$ and 1.13.

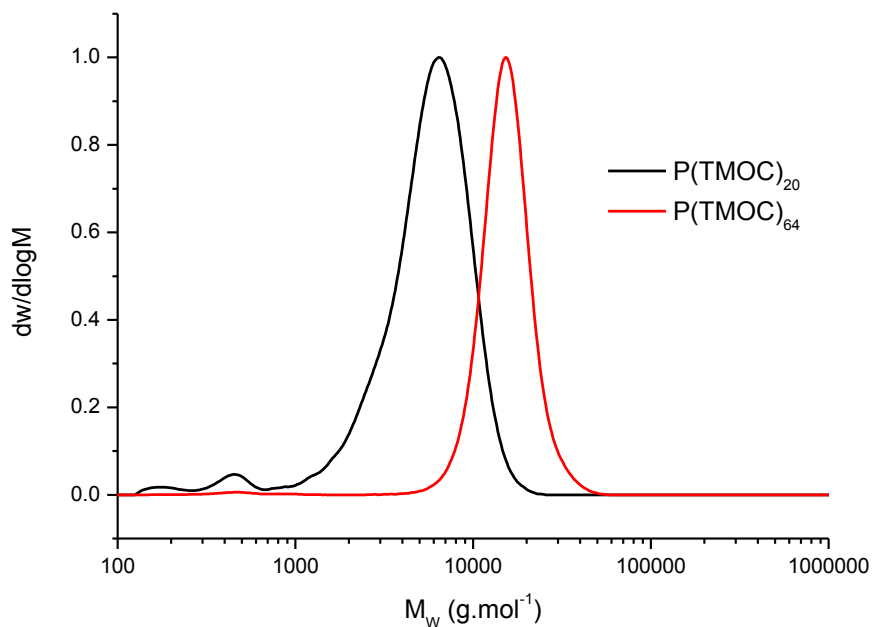


Figure 4.64 - GPC traces of P(TMOC)_{20} and P(TMOC)_{64}

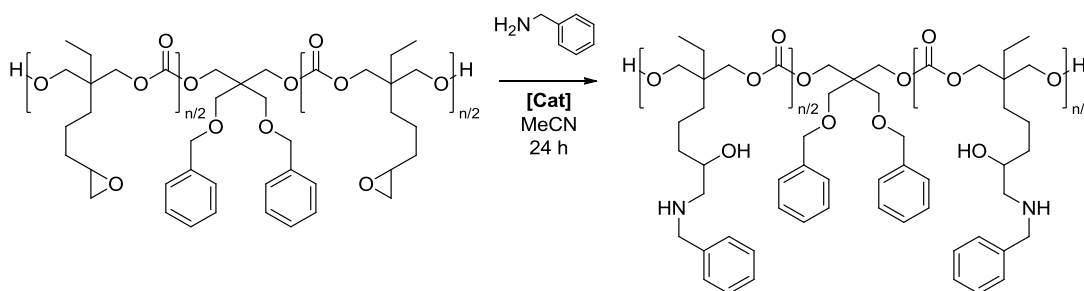
4.2.5 Functionalisation of P(TMOC) - Preliminary condition screening

The addition of amines to epoxides is well-reported in the literature, with a wide variety of conditions and catalysts employed in the reactions. Typically these reactions are conducted in polar solvents, with water, methanol and ethanol being commonly employed. However due to the insolubility of P(TMOC) in all of these solvents, acetonitrile may be employed as a suitable alternative, allowing for a homogenous reaction solution.^{107,108}

Numerous systems have been employed in enabling the addition of amines to epoxides, from simple heating of the reaction, to numerous catalyst species. These range from transition metal and lanthanide species to simpler, commercially available alkali metal species.¹⁰⁹⁻¹¹⁴

Two of these alkali metal species were chosen as potential catalysts for the functionalisation of P(TMOC); lithium bromide and calcium trifluoromethanesulfonate, due to being both cheap and easily accessible.^{115,116} It was also decided to attempt functionalisation at elevated temperatures in the absence of any other catalytic species.

The lower molecular weight polymer, P(TMOC)₂₀, was used as the substrate for the screening of functionalisation conditions with benzylamine used as a model amine (Scheme 4.6). For each of the three activation routes chosen [LiBr, Ca(OTf)₂ and heating], a range of amine equivalents were employed in order to investigate the effect that varying amine concentrations would have on the final functionalised material.



Scheme 4.59 - Test functionalisation of P(TMOC)₂₀ with benzylamine

All test functionalisation reactions were conducted at a polymer concentration of 50 mg.mL⁻¹ in acetonitrile and allowed to run for 24 hours. Benzylamine equivalents are relative to the repeat unit molarity, catalyst loadings are also relative to the concentration of epoxide-bearing repeat units.

Table 4.17 - Catalyst screen for benzylamine addition to P(TMOC)₂₀

Entry	Catalyst	Temp. (°C)	Benzylamine Equivalents	Functionalisation (%) ^a	M_n (g.mol ⁻¹) ^b	D_M ^b
1	LiBr	RT	1	63	- ^c	- ^c
2	LiBr	RT	3	89	9010	1.73
3	LiBr	RT	5	>98	8510	2.07
4	Ca(OTf) ₂	RT	1	>98	6440	2.28
5	Ca(OTf) ₂	RT	3	>98	1180	1.27
6	Ca(OTf) ₂	RT	5	>98	1050	1.14
7	-	85	1	89	- ^c	- ^c
8	-	85	3	>98	8680	1.36
9	-	85	5	>98	6390	1.18

^a Determined by ¹H NMR spectral analysis; ^b Determined by GPC analysis in DMF, calibrated against poly(styrene) standards. ^c Resulting material proved insoluble.

The functionalisations conducted with lithium bromide as the catalyst (Table 4.17, Entries 1 to 3) used 20 mol% LiBr with 1, 3 and 5 equivalents of benzylamine and were all stirred in acetonitrile for 24 hours at room temperature before analysis of the crude reaction mixture by ¹H NMR spectroscopy. The resulting ¹H NMR spectra (Figure 4.65) showed varying degrees of functionalisation, based on the ratios of remaining epoxide signal at 3.08 ppm compared to the ethyl signal at 0.87 ppm (accounting for ethyl chains in both functionalised and un-functionalised repeat units). Increasing amine concentration showed increasing levels of functionalisation, with the polymers exposed to 1, 3 and 5 equivalents of benzylamine showing 63, 89 and greater than 98% functionalisation, respectively.

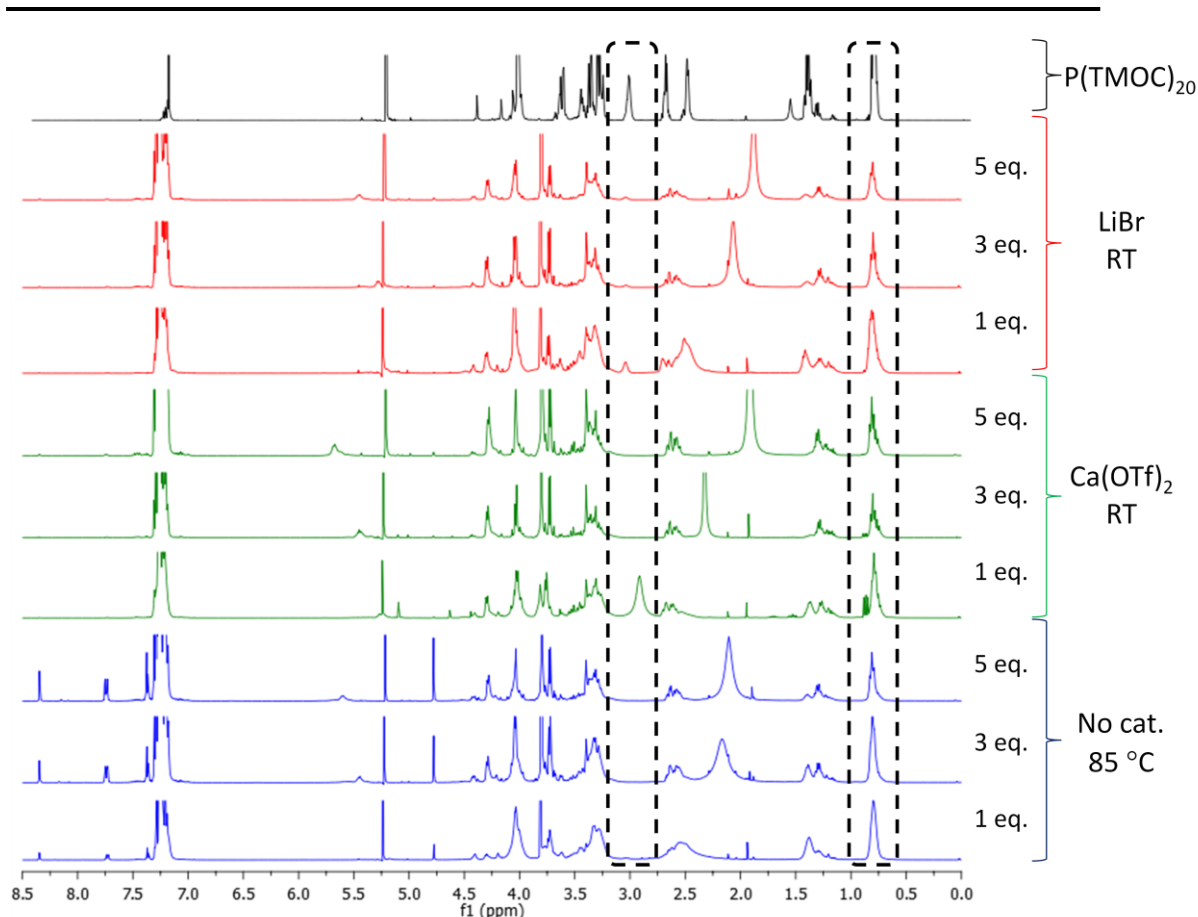


Figure 4.65 - ^1H NMR spectra of crude functionalisation test mixtures. Highlighted signals show residual epoxide and ethyl chain, with the ratio used to calculate conversion

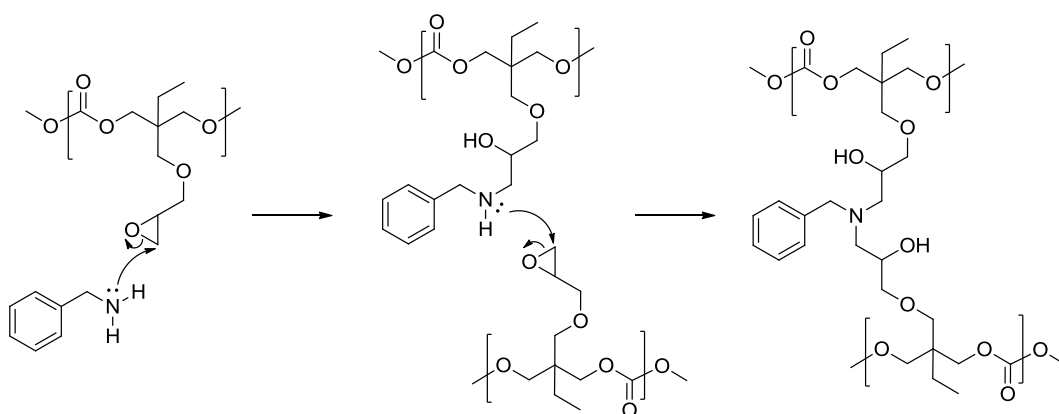
However, upon attempted analysis of the crude polymer by GPC, no material was observed in chloroform, and significantly, the filter used to prepare the samples repeatedly blocked. As chloroform proved to be a poor solvent for the recovered material, leading to apparent aggregation, GPC analysis was conducted in *N,N'*-dimethylformamide (DMF), this proved to be a better solvent for the material obtained from the functionalisation reactions. Both substrate polymers, P(TMOC)_{20} and P(TMOC)_{64} were reanalysed using the DMF system, this showed significantly higher molecular weights than those observed using chloroform with a slight narrowing of the dispersities (Table 4.18).

Table 4.18 - Reanalysis of P(TMOC)₁₀ and P(TMOC)₆₄

Entry	Homopolymer	M_n (CHCl ₃) (g.mol ⁻¹) ^{a,b}	D_M (CHCl ₃) ^b	M_n (DMF) (g.mol ⁻¹) ^{a,c}	D_M (DMF) ^c
1	P(TMOC) ₂₀	3630	1.42	4830	1.29
2	P(TMOC) ₆₄	12300	1.13	14500	1.11

^aCalibrated against poly(styrene) standards. ^bDetermined by GPC analysis in CHCl₃, calibrated against poly(styrene) standards. ^c Determined by GPC analysis in DMF, calibrated against poly(styrene) standards.

Having changed the GPC solvent, it still proved impossible to redissolve the polymer obtained from the reaction using a single equivalent of benzylamine (Table 4.17, Entry 1), suggesting that the polymer had undergone a significant degree of crosslinking through the reaction of the formed secondary amine with a second pendant epoxide (Scheme 4.60).



Scheme 4.60 - Crosslinking of P(TMOC) through epoxide ring-opening by benzyl- primary and secondary amines

Analysis of the reactions using 3 and 5 equivalent of benzylamine (Table 4.17, Entries 2 and 3) by GPC showed two distributions, both overlapping with the higher weight distribution showing a considerably broadened dispersity and elevated molecular weights compared to the starting homopolymer, with values of $M_n = 9010$ g.mol⁻¹, $D_M = 1.73$ and $M_n = 8510$ g.mol⁻¹, $D_M = 2.07$ respectively (Figure 4.66). In the analysis of the reactions using both 3

and 5 equivalents of benzylamine, there is a significant, very narrow, distribution observed at roughly $1000 \text{ g}\cdot\text{mol}^{-1}$. Unfortunately the isolation and subsequent characterisation of this species proved particularly difficult and its identity currently eludes us. It is possible that this species represents the product of some degradation process, as a result of the presence of both the catalyst and benzylamine.

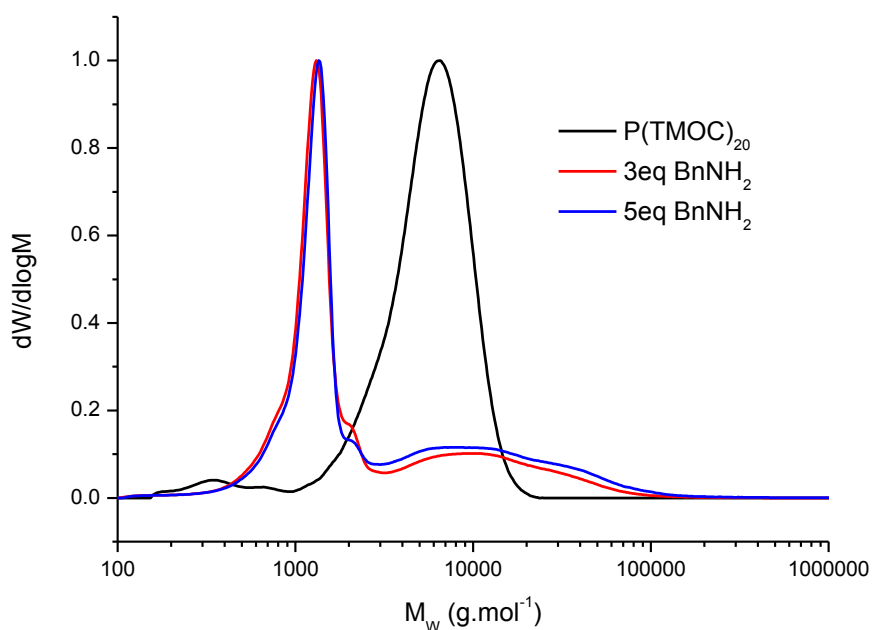


Figure 4.66 - GPC traces of functionalisation tests on $\text{P}(\text{TMOC})_{20}$ using 3 & 5 equivalents of benzylamine with 20 mol% LiBr in acetonitrile at room temperature

The increased molecular weight observed by GPC is consistent with the addition of benzylamine to the original homopolymer, however there are two plausible explanations for the drastic broadening observed. The first may be due to interactions between the pendant hydroxyl and amino groups on the functionalised polymer with the GPC column, leading to streaking of the final polymer. The second possible explanation involves chain-chain coupling as previously suggested for the insolubility of the material obtained from the reaction with one equivalent of benzylamine (Scheme 4.7). With an increase in the amine

concentration, the amount of secondary amines reacting with epoxide species should be significantly reduced, thereby leaving a material with a considerably lower degree of crosslinking and allowing for dissolution and subsequent analysis.

The test functionalisations conducted using calcium triflate as the aminolysis catalyst utilised 50 mol% catalyst loading and were stirred for 24 hours at room temperature with 1, 3 and 5 equivalents of benzylamine (Table 4.17, Entries 4 to 6). ^1H NMR spectral analysis of the crude reaction mixtures all showed no remaining epoxide, giving a functionalisation of >98% for all three reactions (Figure 4.65).

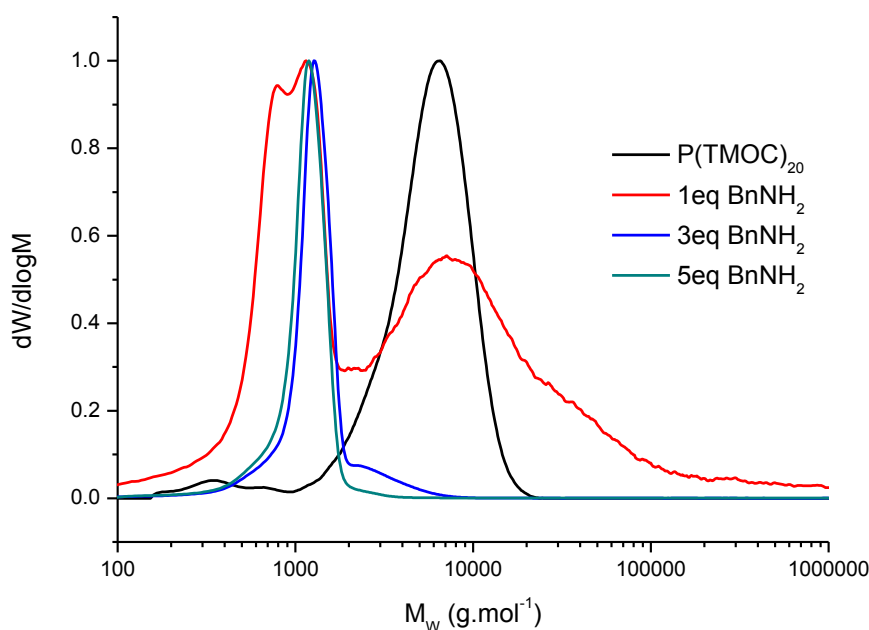


Figure 4.67 - GPC traces of functionalisation tests on $\text{P}(\text{TMOC})_{20}$ using 1, 3 & 5 equivalents of benzylamine with 50 mol% $\text{Ca}(\text{OTf})_2$ in acetonitrile at room temperature

GPC analysis of the material obtained from the use of a single equivalent of benzylamine again showed a greatly broadened distribution with a slightly elevated molecular weight, $M_n = 6440$ and $D_M = 2.28$. However, analysis of the reactions using 3 and 5 equivalents of benzylamine showed no high weight material, instead the only observable distribution was at a drastically lower weight ($M_n = 1180$, $D_M = 1.27$ and $M_n = 1050$, $D_M = 1.14$ respectively), a

distribution that corresponds well with the impurities observed in the reactions using lithium bromide as catalyst.

The final set of functionalisation tests were conducted with no catalytic species present and instead the reaction was carried out in refluxing acetonitrile at 85 °C, again over a 24 hour period, with 1, 3 and 5 equivalents of benzylamine (Table 4.17, Entries 7 to 9). The resulting crude reaction mixtures were analysed by ^1H NMR spectroscopy, whilst the apparent levels of conversion were high, 89% for a single equivalent of benzylamine and >98% for the reactions conducted using 3 and 5 equivalents, all three spectra show three extra signals previously not observed in the other catalytic systems (LiBr and $\text{Ca}(\text{OTf})_2$) at 8.35, 7.74 and 7.37 ppm (Figure 4.68).

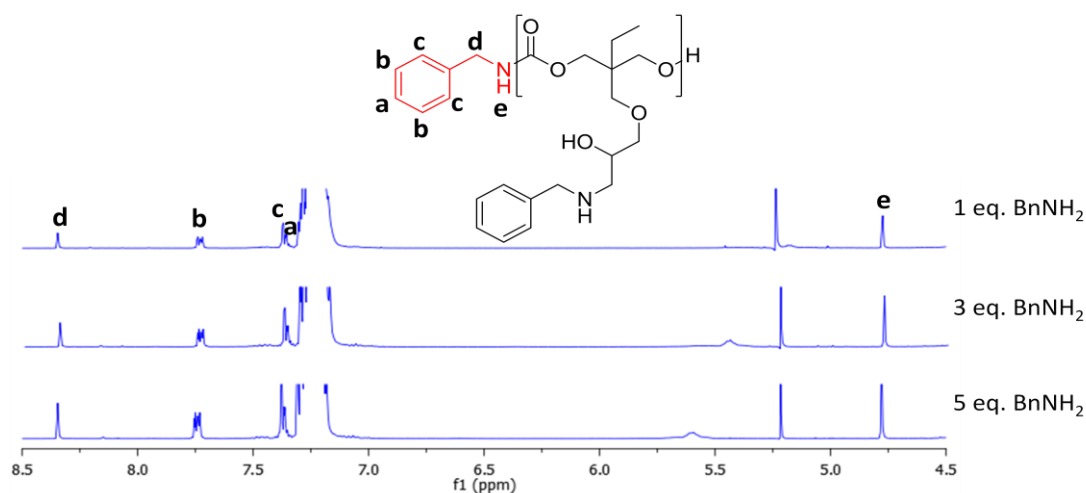
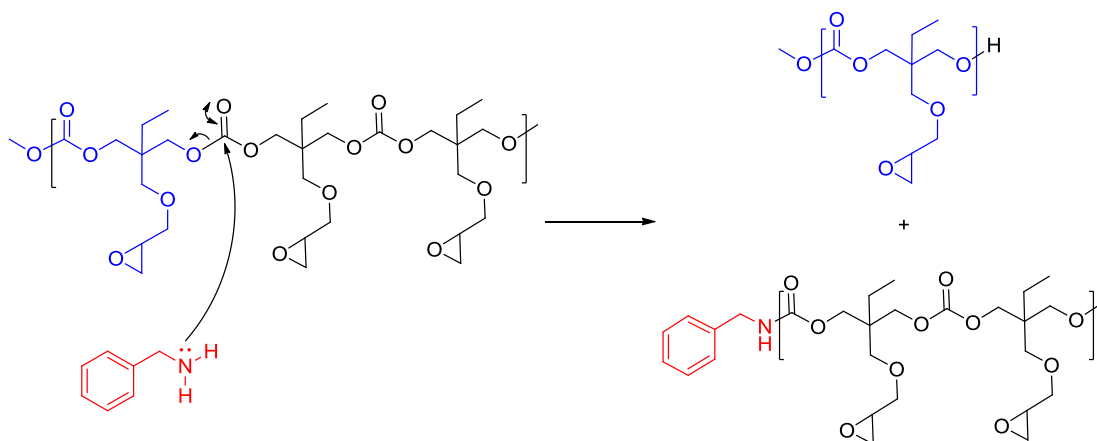


Figure 4.68 - Expansion of ^1H NMR spectra for thermal addition of benzylamine to $\text{P}(\text{TMOC})_{20}$

One plausible explanation consistent with the appearance of these extra signals is the aminolysis of the carbonate linkages with benzylamine which has been reported to proceed readily without any required catalyst at raised temperatures on model small molecules.¹¹⁷ The fact that the intensity of these signals increases with increasing amine concentration is supportive of the formation of the carbamate species in competition with the ring-opening of the epoxide (Scheme 4.61).



Scheme 4.61 - Aminolysis of P(TMOC) by benzylamine

GPC analysis of the reactions conducted with 3 and 5 equivalents of benzylamine again both showed slightly raised molecular weights compared to the starting homopolymer (Figure 4.21). However interestingly the polymer obtained from the use of 5 equivalents of benzylamine resulted in a significantly lower molecular weight ($M_n = 6390$, $D_M = 1.18$) compared to that observed for the material obtained from the use of 3 equivalents of benzylamine ($M_n = 8680$, $D_M = 1.36$). This drop in observed molecular weight with increased benzylamine concentration could potentially be explained by the increased aminolysis of the carbonate backbone.

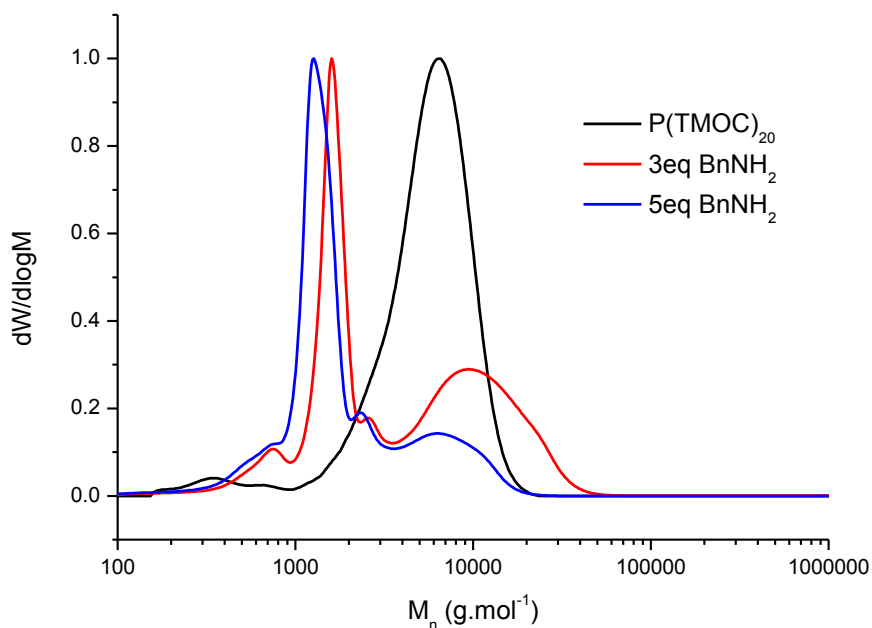
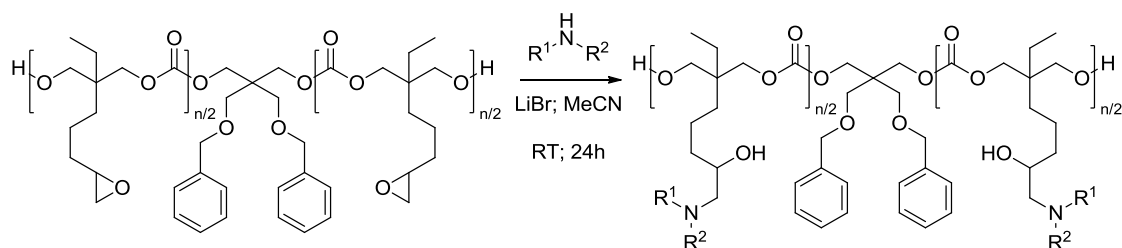


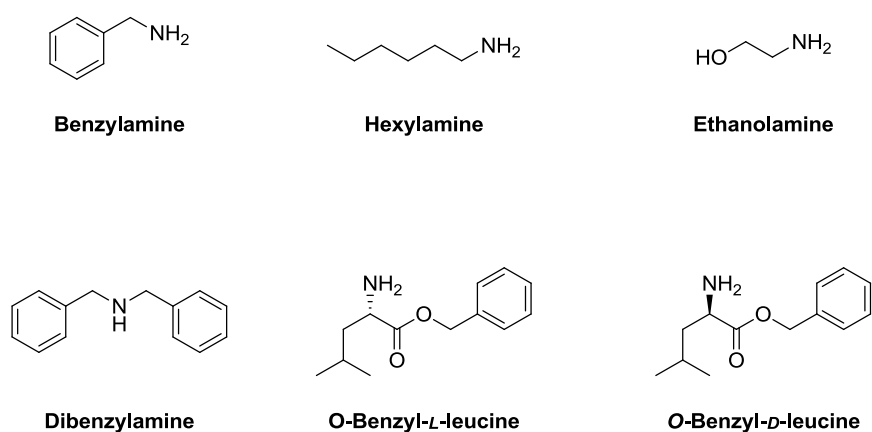
Figure 4.69 - GPC traces of functionalisation tests on P(TMOC)₂₀ using 3 & 5 equivalents of benzylamine in acetonitrile at 85 °C

Based on this preliminary screening of conditions for the addition of benzylamine to the pendant epoxides of P(TMOC), it was decided to utilise lithium bromide as catalyst with five equivalents of amine in further studies to investigate the addition of a range of amines. The high amine equivalent was employed to minimise crosslinking, whilst the catalyst was chosen by the elimination of the calcium triflate systems due to lack of high weight material and thermal addition due to the possibility of further undesirable side reactions.

4.2.6 Functionalisation of P(TMOC) - Amine variation

Scheme 4.62 - Amine screening for addition to P(TMOC)₂₀ and P(TMOC)₆₄

After the preliminary screening of the addition of benzylamine, both precursor homopolymers, P(TMOC)₂₀ and P(TMOC)₆₄ were subjected to the selected functionalisation conditions with a selection of other amines in order to investigate the effect of varying functionalities. The amines employed in these functionalisation tests are shown in Figure 4.70; as well as using benzylamine and hexylamine, ethanolamine was selected to allow the introduction of different reactive functionality and dibenzylamine was used to investigate the effect of using a secondary amine compared to a primary. Finally, in order to attempt the introduction of a chiral amine, both the *L*- and *D*-enantiomers of the amino ester, derived from the salt employed in Chapter 3, were selected for the amine screen.

Figure 4.70 - Amines used in functionalisation tests of P(TMOC)₂₀ and P(TMOC)₆₄

P(TMOC)₂₀ was stirred with the amines shown in Figure 4.70 in the presence of 20 mol% lithium bromide for 24 hours at room temperature, analysis of the resulting ¹H NMR spectra showed high conversion for the three simple primary amines, at 93% for benzylamine and >98% for both hexylamine and ethanolamine (Table 4.19, Entries 1-3).

Table 4.19 - Functionalisation of P(TMOC)₂₀ with various amines

Entry	Amine	Functionalisation (%) ^a	<i>M_n</i> (g.mol ⁻¹) ^b	<i>D_M</i> ^b
1	Benzylamine	93	1450	1.20
2	Hexylamine	>98	1470	1.06
3	Ethanolamine	>98	1380	1.13
4	Dibenzylamine	81	5300	1.18
5	<i>O</i> -Bn- <i>L</i> -Leu	-	5990	1.34
6	<i>O</i> -Bn- <i>D</i> -Leu	-	6190	1.35

^a Determined by ¹H NMR spectral analysis; ^b Determined by GPC analysis in DMF, calibrated against poly(styrene) standards.

However, none of these reactions showed any high weight material when analysed by GPC with respective molecular weights of 1450, 1470 and 1380 g.mol⁻¹ observed with corresponding dispersities of 1.20, 1.06 and 1.13 (Figure 4.71).

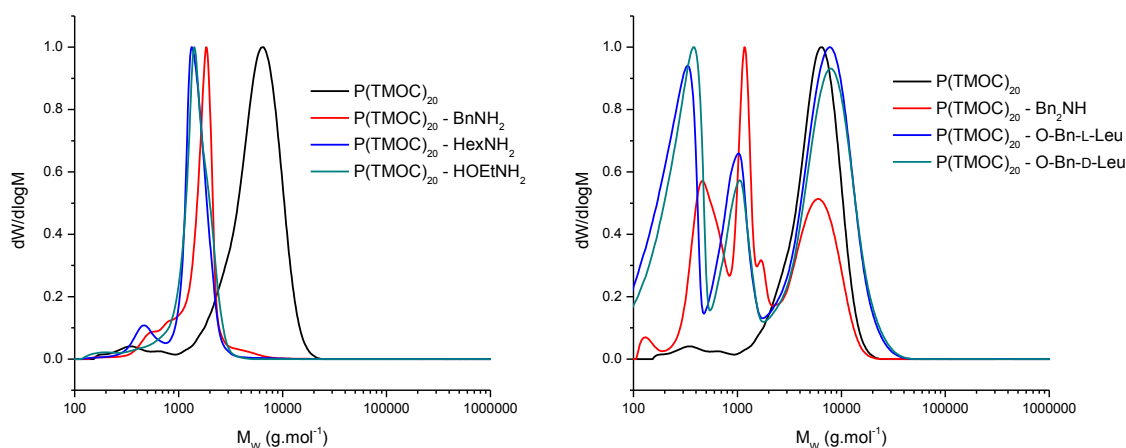


Figure 4.71 - GPC traces for the attempted functionalisations of $P(TMOC)_{20}$

The results of the attempted functionalisations using dibenzylamine and both *O*-benzyl leucines (Table 4.19, Entries 4-7) are significantly different. The reaction with dibenzylamine still shows fairly high conversion, at 81% as determined by 1H NMR spectral analysis, however the resulting GPC chromatogram shows a number of distributions, the highest molecular weight of which showed no significant variation from the starting homopolymer with a molecular weight of 5300 g.mol^{-1} and a dispersity of 1.18. Interestingly, there were several lower molecular weight distributions observed, in contrast to the single species observed for all previous functionalisation attempts.

The attempted functionalisations using both the *L*- and *D*- enantiomers of *O*-benzyl leucine showed no apparent conversion by analysis of the 1H NMR spectra, this was supported by the corresponding GPC analyses (Figure 4.71), showing only slight deviation and broadening compared to the original homopolymer, showing molecular weights of 5990 and 6190 g.mol^{-1} for attempted additions of the *L*- and *D*-enantiomers respectively ($\mathcal{D}_M = 1.34$ and 1.35). As with the functionalisation using dibenzylamine, there were multiple lower molecular weight distributions observed, compared to the single species observed in previous functionalisation tests. The difference between these two sets of amines could

offer some insight into the degradation process, appearing to correlate with the pK_a of the utilised amines. Those with higher pK_a values (benzylamine, hexylamine and ethanolamine) give rise to a single lower molecular weight species, whilst those with lower values (dibenzylamine and the *L*- & *D*- enantiomers of *O*-benzyl leucine) produced multiple such species.

Table 4.20 - Functionalisation of $P(\text{TMOC})_{64}$ with various amines

Entry	Amine	Functionalisation (%) ^a	M_n (g.mol ⁻¹) ^b	\mathcal{D}_M ^b
1	Benzylamine	>98	1370	1.30
2	Hexylamine	>98	1400	1.16
3	Ethanolamine	>98	1770	1.04
4	Dibenzylamine	96	9890	1.30
5	<i>O</i> -Bn- <i>L</i> -Leu	-	17300	1.49
6	<i>O</i> -Bn- <i>D</i> -Leu	-	14800	1.42

^a Determined by ¹H NMR spectral analysis; ^b Determined by GPC analysis in DMF, calibrated against poly(styrene) standards.

The same attempted functionalisation reactions were repeated using $P(\text{TMOC})_{64}$ as the substrate homopolymer. As would be expected, similar results to those observed with $P(\text{TMOC})_{20}$ were obtained, the reactions using benzylamine, hexylamine and ethanolamine (Table 4.20, Entries 1-3) all showed >98% conversion, as calculated from their ¹H NMR spectra. GPC analysis of the same reactions again showed only low weight oligomeric material present (Figure 4.72) with observed molecular weights of 1370, 1400 and 1770 g.mol⁻¹ ($\mathcal{D}_M = 1.30, 1.16$ and 1.04 , respectively).

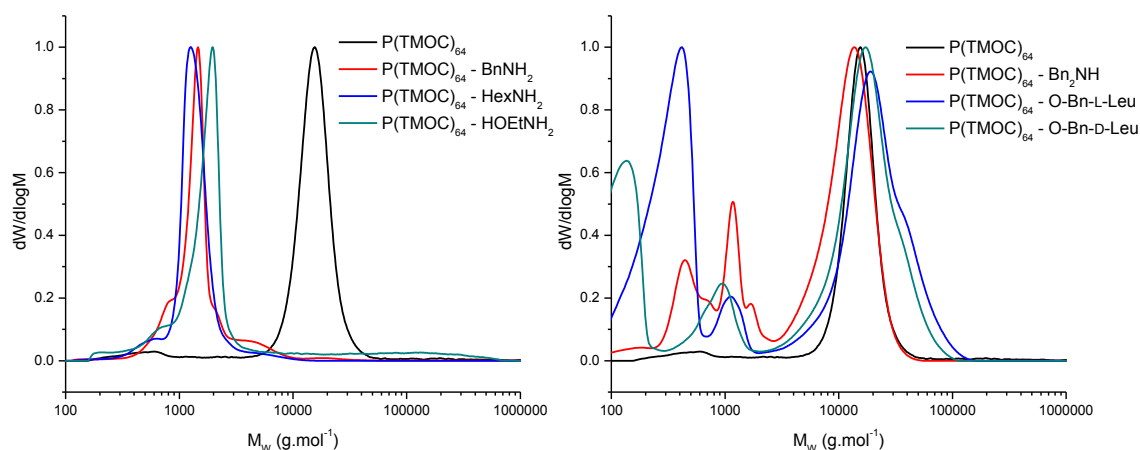
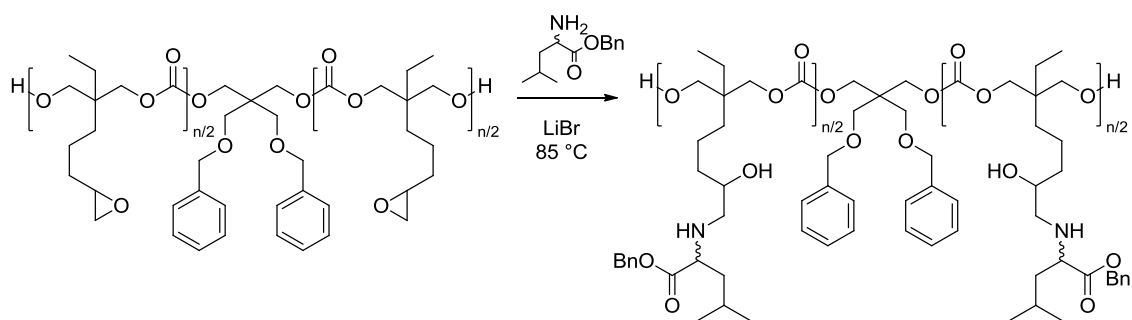


Figure 4.72 - GPC traces for the attempted functionalisations of $P(TMOC)_{64}$

The reaction with dibenzylamine (Table 4.20, Entry 4) showed high conversion, 96%, as determined by 1H NMR spectral analysis, however the results from the GPC analysis show a drop in the observed molecular weight when compared to the starting homopolymer with a slight broadening ($M_n = 9880 \text{ g.mol}^{-1}$, $D_M = 1.30$). It is possible that the lower observed molecular weight is derived from the significantly different solvent interactions with the functionalised polymer compared to the $P(TMOC)$ homopolymer, thereby giving a more tightly folded polymer and a smaller hydrodynamic radius than would be expected. It is perhaps also significant that no high weight tail is observed on the chromatogram, presumably from a lack of chain crosslinking.

The attempted functionalisations using *L*- and *D*-enantiomers of *O*-benzyl leucine (Table 4.20, Entries 5 & 6) again showed no apparent functionalisation when analysed by 1H NMR spectrometry, although the GPC chromatograms differ significantly in their observed molecular weights with the reaction attempted with *O*-benzyl-*D*-leucine showing a molecular weight in close agreement with the original homopolymer ($M_n = 14800 \text{ g.mol}^{-1}$, $D_w = 1.42$). Meanwhile, the reaction with the corresponding *L*-enantiomer shows a raised molecular weight of 17300 g.mol^{-1} ($D_M = 1.49$). Interestingly, both the *L*- and *D*- enantiomers showed a high weight tail and shoulder, potentially indicative of a small degree of functionalisation and subsequent crosslinking.

Scheme 4.63 - Functionalisation of P(TMOC) with *O*-Benzyl Leucine

In an attempt to achieve the desired functionalisation of the P(TMOC) homopolymers with both *O*-benzyl leucine enantiomers, more forcing conditions were employed for the repeat reactions, the same 20 mol% of lithium bromide was used as catalyst, however the reactions were allowed to stir for 24 hours in refluxing acetonitrile (Scheme 4.63).

Table 4.21 - Functionalisation of P(TMOC)₂₀ and P(TMOC)₆₄ with *O*-benzyl leucine at elevated temperature

Entry	DP	Amine	Functionalisation (%) ^a	M_n (g.mol ⁻¹) ^b	\bar{D}_M ^b	$[\alpha]_D^{22}$ ^c
1	20	<i>O</i> -Bn- <i>L</i> -Leu	75	5830	1.27	-0.64 (0.1241 g.mL ⁻¹)
2	20	<i>O</i> -Bn- <i>D</i> -Leu	84	5580	1.31	+0.55 (0.0729 g.mL ⁻¹)
3	64	<i>O</i> -Bn- <i>L</i> -Leu	91	10200	1.51	-0.54 (0.1463 g.mL ⁻¹)
4	64	<i>O</i> -Bn- <i>D</i> -Leu	88	12300	1.38	+0.55 (0.2182 g.mL ⁻¹)

^a Determined by ¹H NMR spectral analysis; ^b Determined by GPC analysis in DMF, calibrated against poly(styrene) standards. ^c Analysed in DMF

The attempted functionalisations using $P(\text{TMOC})_{20}$ as substrate with both the *L*- and *D*-enantiomers showed a drastic improvement with apparent functionalisations of 75 and 84% respectively, based on analysis of the ^1H NMR spectra (Table 4.21, Entries 1 & 2). GPC analysis showed observed molecular weights which were slightly elevated from the original homopolymer yet showed no significant variation in the dispersities ($M_n = 5828$ & 5580 $\text{g}\cdot\text{mol}^{-1}$, $D_M = 1.27$ & 1.31).

A similar improvement was observed for the functionalisation of $P(\text{TMOC})_{64}$ (Table 4.21, Entries 3 & 4) with the reactions achieving slightly higher conversions than achieved for the corresponding $P(\text{TMOC})_{20}$ functionalisations, with the ^1H NMR spectra showing 91 and 88% for the *L*- and *D*- enantiomers respectively. However, in comparison to the functionalisation of the lower weight substrate, the GPC analyses showed a lowered molecular weight for both enantiomers compared to the initial substrate, with molecular weights of 10200 and 12300 $\text{g}\cdot\text{mol}^{-1}$ for the *L*- and *D*- variants respectively, although these showed broadened dispersities (Figure 4.73) there was no significant high weight tail that may be associated with any crosslinking.

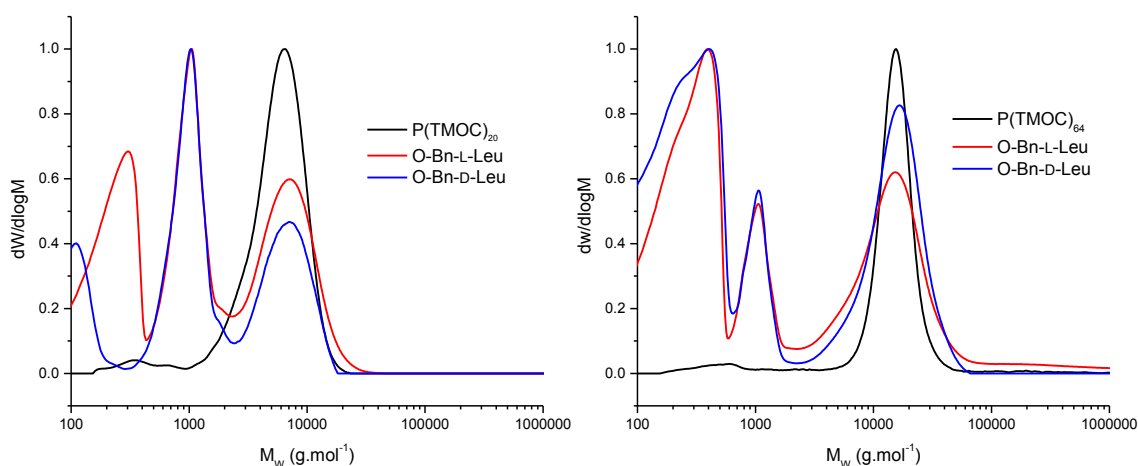


Figure 4.73 - GPC traces for the attempted addition of *O*-benzyl leucines to $P(\text{TMOC})_{20}$ and $P(\text{TMOC})_{64}$

With a respectably high conversion apparently achieved for the addition of both *O*-Bn-*L*-Leu and *O*-Bn-*D*-Leu to P(TMOC)₂₀ and P(TMOC)₆₄, in order to determine the retention of chirality, the removal of the excess amino-ester from the functionalised polymer was required. Due to the inherent similarity in behaviour between the functionalised polymer and the residual amino-ester, this purification proved difficult to achieve. However, the separation was finally realised through repeated washes with a sodium acetate / acetic acid buffer with a pH of 3.46.

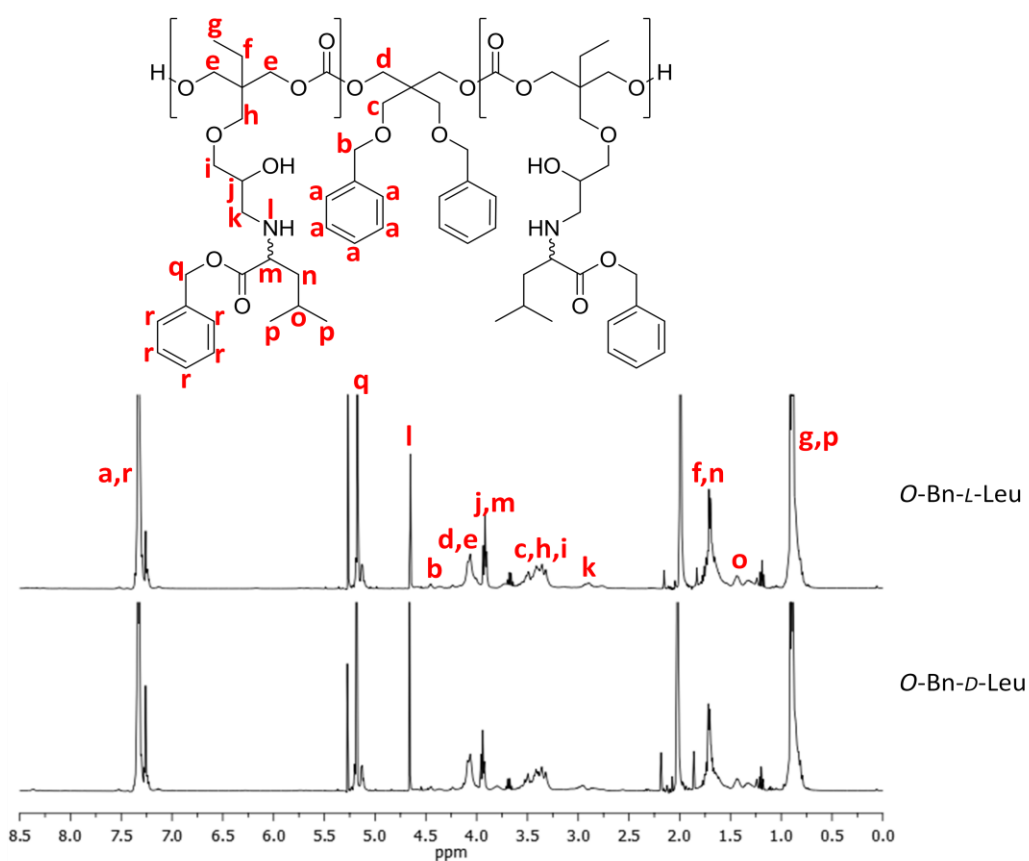


Figure 4.74 - Tentative ¹H NMR spectral assignments of P(TMOC)₆₄ functionalised with *O*-benzyl leucine

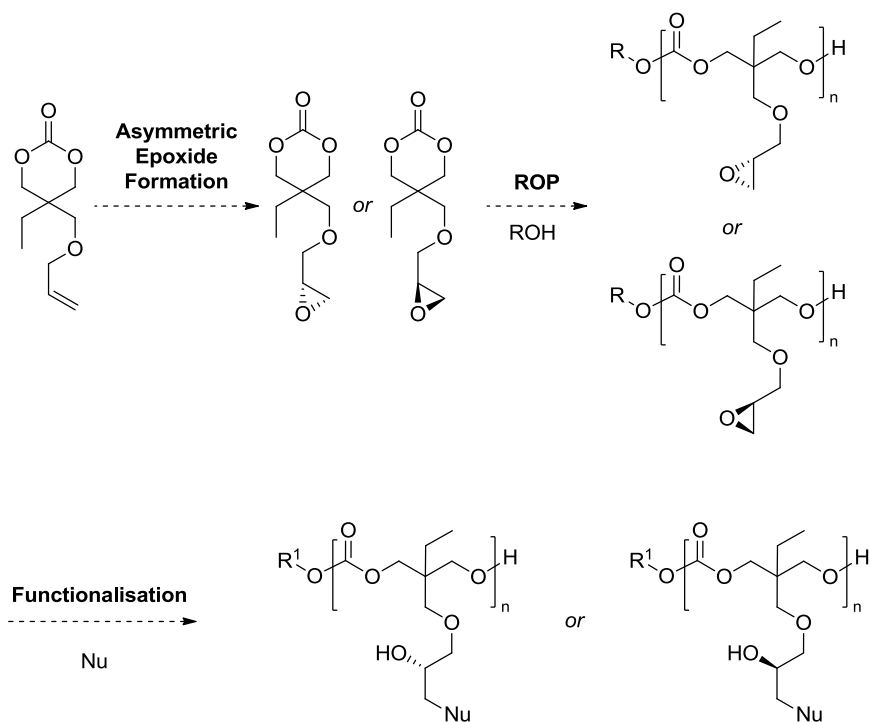
Finally, the isolated polymers (Figure 4.74) were analysed by polarimetry in DMF- all four of the obtained polymers gave low yet definitively non-zero specific rotation values, indicative of the retention of chiral purity in the functionalised polymer.

4.3 Conclusions and Future Work

In conclusion, the synthesis and ring-opening polymerisation of 5-ethyl-5-((oxiran-2-ylmethoxy)methyl)-1,3-dioxan-2-one was successfully achieved and retention of the pendant epoxide functionality shown under all tested polymerisation conditions. The use of low catalyst loading (1 mol%) of 1,5,7-triazabicyclo[4.4.0]dec-5-ene allows for the ROP of TMOC with good control over the achieved molecular weight and narrow dispersities.

Preliminary investigation into the functionalisation of P(TMOC) homopolymers by addition of amines to yield amino alcohols showed high degrees of functionalisation, although analysis of the resulting polymers showed a considerable variation with the pK_a of the amine. Addition of both *L*- and *D*- enantiomers was shown to proceed to high conversion at elevated temperatures and isolation of the functionalised polymer showed retention of the chirality inherent in the aminoesters.

The retention of the epoxide functionality in the P(TMOC) homopolymer is, to the best of the author's knowledge, a first for a degradable polymer. The pendant epoxides offer the opportunity for the addition of a wide range of nucleophiles, allowing access to a number of potentially useful and interesting materials.



Scheme 4.64 - Asymmetric epoxidation allows for expansion of functionalisation methodology whilst retaining chiral nature of the polymer.

As an alternative strategy, the inclusion of chiral centres could be achieved for the functionalisation of the homopolymer with any selected nucleophile with only a slight modification of the synthetic route. It is possible to envision the replacement of the use of *m*-chloroperoxybenzoic acid with an alternative asymmetric epoxidation methodology which would allow for access to stereo-pure P(TMOC).¹¹⁸ After polymerisation, opening of either diastereomer should lead to the formation of a corresponding stereocentre for the resulting hydroxyl group (Scheme 4.64).

Chapter 5

Conclusions and Future Work

5.1 Functionalised *O*-Carboxyanhydrides from *L*-Malic Acid

In Chapter 2, the synthesis of two novel *O*-carboxyanhydride monomer was reported from *L*-malic acid, bearing 2,2,2-trichloroethyl and 2-nitrobenzyl ester functionalities. The ring-opening polymerisation of both OCA monomers was investigated using a series of substituted pyridines. However a number of detrimental side reactions complicates the polymerisation and prevents access to poly(malic acid)s of higher weights.

As outlined in Chapter 2, a number of the side reactions observed in the attempted ring-opening polymerisation of MalOCAs derive from the acidity of the methine proton present on the monomer ring. It should prove possible to replace this proton with an unreactive substituent, such as a methyl group. This could most easily be achieved by using the chiral methylation method reported by Seebach et al. for the methylation of malic acid, utilising a *tert*-butyl acetal as a sterically-directing protecting group (Figure 5.75).⁸⁷

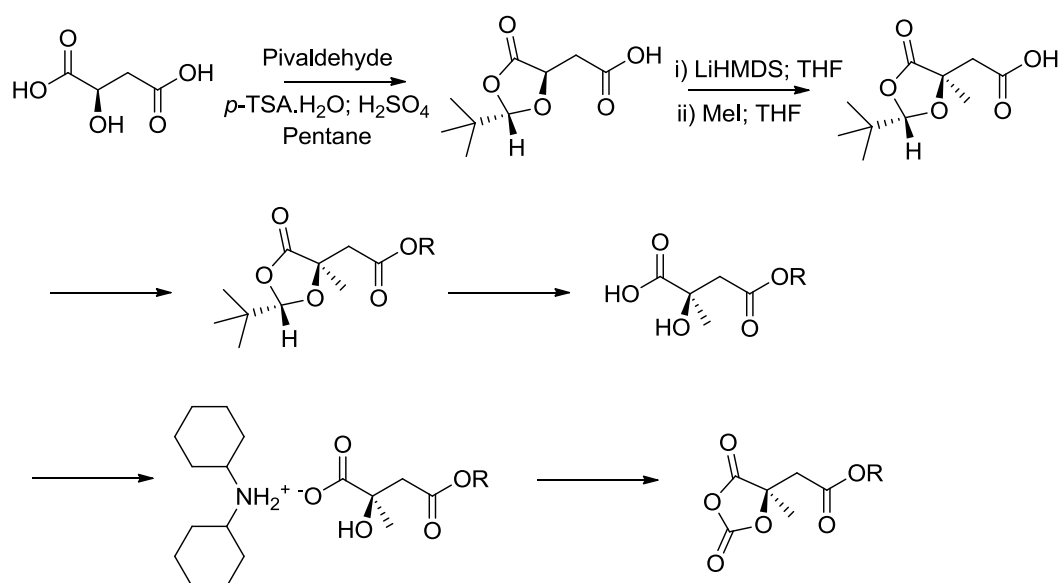


Figure 5.75 - Proposed chiral methylation of *L*-malic acid to eliminate autoinitiation of functionalised MalOCAs

The elimination of side reactions resulting from the presence of this acidic proton should enable better control over the polymerisation of MalOCAs. However, so long as the

propagating chain end may attack either carbonyl on the monomer ring, there remains a method of chain termination within the ongoing polymerisation. Further investigation and development of either the monomer or the polymerisation system will be required in order to overcome this limitation.

5.2 Chiral Functionalised Cyclic Carbonates and Poly(carbonate)s from

***L*-Leucine**

Chapter 3 presented an alternative method for the inclusion of functional groups into chiral, biodegradable and biocompatible polymers through the synthesis of two novel cyclic carbonates. These cyclic carbonates were derived from *bis*(hydroxymethyl)propionic acid bearing chiral, functionalised amino acid derivatives based on *L*-leucine coupled through either amide or ester linkages. The attempted ring opening of the amide-containing cyclic carbonate with a variety of catalyst systems failed to produce any polymeric material and a mechanistic explanation is proposed based on intramolecular hydrogen bonding stabilisation. The exchange of the amide linkage for an ester allows for the controlled synthesis of functionalised poly(carbonate)s bearing a chiral substituent using 1,8-diazabicyclo[5.4.0]undec-7-ene.

When initiated from 4-methoxybenzyl alcohol, the acidic quenching for removal of the DBU results in the cleavage of the benzylic carbonate linkage, resulting in a dihydroxyl telechelic poly(carbonate) which could find numerous uses for the formation of ABA triblocks.

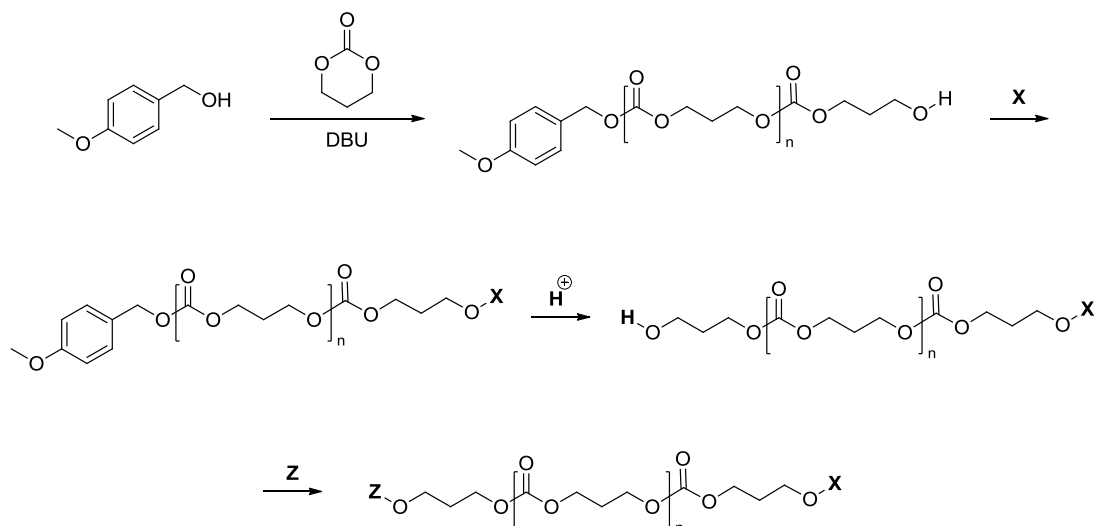


Figure 5.76 - Proposed methodology for accessing bifunctional poly(carbonate)s bearing differing α - and ω - chain ends

Such a controlled method to the synthesis of hydroxyl-functionalised telechelic polymers could prove to have many applications in the formation of ABA triblock structures. If the reaction purification can be modified to preserve the 4-methoxybenzyl end group, it would be possible to gain access to bifunctional poly(carbonate)s bearing different functionalities on either of the α - or ω - chain ends (Figure 5.76).

5.3 Polymerisation of Epoxide-Functionalised Cyclic Carbonate

Chapter 4 presents the synthesis of a cyclic carbonate bearing a pendant epoxide ether functionality. The ring-opening polymerisation of this monomer is investigated using a series of organocatalytic systems, the use of 1,5,7-triazabicyclo[4.4.0]dec-5-ene allowed for the synthesis of well-controlled poly(carbonate)s with full retention of the pendant epoxide functionality, the first known report of such a functionality on a degradable backbone. Preliminary investigations were conducted towards the functionalisation of the homopolymer using a variety of functional amines. The introduction of chirality was achieved by functionalisation with *L*- and *D*-leucine benzyl esters.

The pendant epoxides offer the opportunity for the addition of a wide range of nucleophiles, allowing access to a number of potentially useful and interesting materials by simple variation of the substituent group.

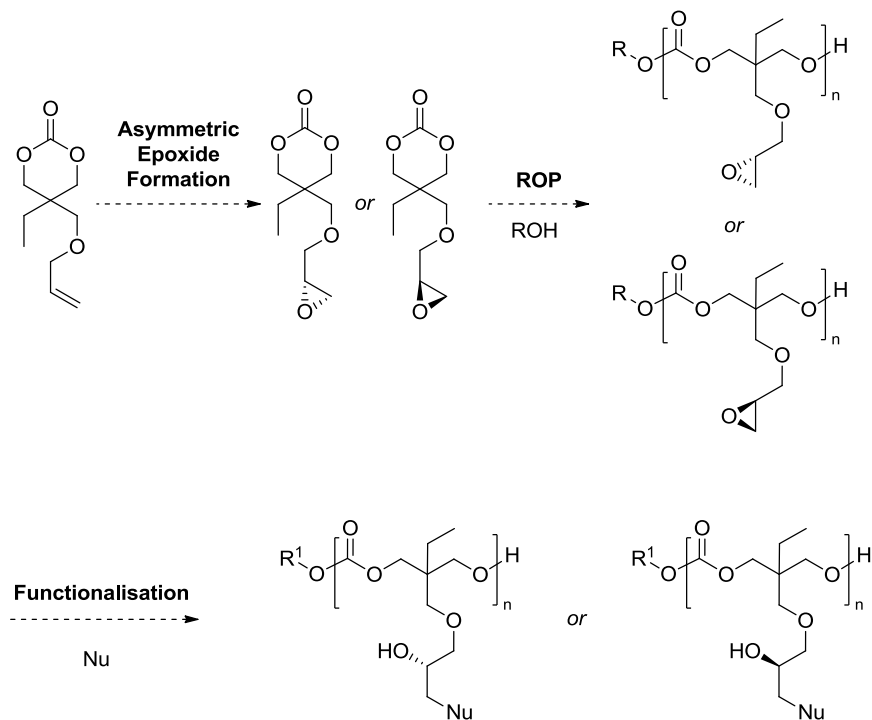


Figure 5.77 Proposed asymmetric epoxidation allows for expansion of functionalisation methodology whilst retaining chiral nature of the polymer.

The trialled functionalisation methodology represents only a cursory investigation into an area which could benefit from a more in-depth study, with multiple variations possible in catalyst system, reaction temperatures and nucleophiles of differing character. To overcome the limitation of requiring a chiral nucleophile when chiral polymers are desired, it should be a fairly simple process to slightly alter the monomer synthesis to utilise one of the many available asymmetric epoxidation methodologies to enable the synthesis of stereo-pure P(TMOC).¹¹⁸ After polymerisation, opening of either diastereomer should lead to the formation of a corresponding stereocentre for the resulting hydroxyl group (Figure 5.77).

Chapter 6

Experimental

6.1 Materials

Solvents were purchased from Fisher Scientific and dry solvents were obtained using an Innovative Technology Inc. Pure Solv MD-4-EN solvent purification system. *N*-(3-diethylaminopropyl)-*N'*-ethyl carbodiimide hydrochloride was purchased from Carbosynth Limited and triphosgene was purchased from TCI Europe N.V. All other chemicals were purchased from Sigma Aldrich or Alfa Aesar and were used directly as supplied. Reagents employed in ring-opening polymerisation reactions were variously dried using 3 Å activated molecular sieves, calcium hydride, sodium or phosphorous pentoxide before storage and further handling in a glovebox under a dry nitrogen atmosphere.

6.2 General Considerations

NMR Spectra: ^1H and ^{13}C Nuclear magnetic resonance (NMR) spectra were recorded on a Bruker DPX-300, DPX-400 or AC-400 spectrometer at 293 K unless stated otherwise, chemical shifts are reported as δ in parts per million (ppm) and referenced to the chemical shift of the residual solvent resonances (CDCl_3 : ^1H : $\delta = 7.26$ ppm, ^{13}C $\delta = 77.16$ ppm; CD_3OD : ^1H : $\delta = 3.31$ ppm, ^{13}C : $\delta = 49.00$ ppm; $\text{D}_6\text{-DMSO}$: ^1H : $\delta = 2.50$ ppm, ^{13}C $\delta = 39.52$ ppm). Data are presented as follows: chemical shift, peak multiplicity (s = singlet, d = doublet, t = triplet, q = quartet, m = multiplet), coupling constants (J / Hz), integration and assignment. Assignments were determined either on the basis of unambiguous chemical shift or coupling patterns, by analysis of 2D NMR (COSY, HMQC, HMBC) or by analogy to fully interpreted spectra for structurally related compounds.

Mass Spectra: Low-resolution mass spectra were recorded on an Esquire 2000 platform with electrospray ionisation. High-resolution mass spectra were recorded on a Bruker UHR-Q-TOF MaXis with electrospray ionisation. High resolution values are calculated to 4 decimal

places from the molecular formula, and all values are within a tolerance of 5 ppm. The parent ion (M^+), ($M+H^+$) or ($M+Na^+$) is quoted.

Infra-red Spectra: FT-IR spectra were recorded on a Perkin Elmer Spectrum 100 FT-IR using a diamond press.

Melting Points: Melting points were recorded in triplicate on a Stanford Research Systems MPA100 Optimelt with a heating rate of $1.0\text{ }^\circ\text{C min}^{-1}$ and are uncorrected.

Optical Rotation: Optical rotation measurements were carried out on an Optical Activity Ltd. AA-10 Automatic Polarimeter.

Elemental Analysis: Elemental analyses were performed in duplicate by Warwick Analytical Services.

GPC: Gel-permeation chromatography (GPC) was used to determine the molecular weights and polydispersities of the synthesised polymers. GPC in chloroform was conducted on a system composed of a Varian 390-LC-Multi detector suite fitted with differential refractive index, light scattering, and ultraviolet detectors equipped with a guard column (Varian Polymer Laboratories PLGel $5\text{ }\mu\text{M}$, $50 \times 7.5\text{ mm}$) and two mixed D columns (Varian Polymer Laboratories PLGel $5\text{ }\mu\text{M}$, $300 \times 7.5\text{ mm}$). The mobile phase was CHCl_3 (HPLC grade) with 2% TEA at a flow rate of 1.0 mL min^{-1} . Samples were calibrated against Varian Polymer Labs Easi-Vials linear poly(styrene) standards ($162 - 240,000\text{ g mol}^{-1}$) using Cirrus v3.2.

GPC in *N,N*-dimethylformamide performed on a Varian 390-LC-Multi detector suite system equipped with a PLGel $3\text{ }\mu\text{m}$ ($50 \times 7.5\text{ mm}$) guard column, two PLGel $5\text{ }\mu\text{m}$ ($300 \times 7.5\text{ mm}$) mixed-C columns, and a PLAST RT autosampler. Detection was conducted using a dual angle light scattering detector (15° and 90°), a viscometer and a DRI detector. The analyses were performed in DMF with $5\text{ mM NH}_4\text{BF}_4$ as the eluent at 323K at a flow rate of 1.0

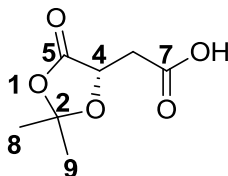
mL·min⁻¹. Poly(methyl methacrylate) (PMMA) (200-1.0 × 10⁶g·mol⁻¹) standards were used for calibration of the DRI and a single narrow molecular weight PMMA standard (73.15K, dn/dc = 0.069, IV = 0.267) was used to calibrate for absolute molecular weight using Cirrus v3.2.

MALDI-ToF Mass Spectra: Polymer mass spectra were acquired by matrix-assisted laser desorption and ionisation time-of-flight (MALDI ToF) mass spectrometry using a Bruker Daltonics Ultraflex II MALDI ToF mass spectrometer, equipped with a nitrogen laser delivering 2 ns laser pulses at 337 nm with positive ion detection performed using an accelerating voltage of 25 kV. Solutions of trans-2-[3-(4-*tert*-butylphenyl)-2-methyl-2-propylidene]malonitrile (DCTB) as matrix (0.3 μL of a 10 g.L⁻¹ acetone solution), sodium trifluoroacetate as cationisation salt (0.3 μL of a 10 g.L⁻¹ acetone solution) and analyte (0.3 μL of a 1 g.L⁻¹ DCM solution) were applied sequentially to the target followed by solvent evaporation to prepare a thin matrix/analyte film. The samples were measured in reflectron ion mode (unless otherwise stated) and calibrated by comparison to 2000 and 5000 g.mol⁻¹ monomethylether poly(ethylene oxide) standards.

Other Techniques: Reactions were monitored by thin layer chromatography (TLC). TLC was conducted on pre-coated aluminium-backed plates (Merck Kieselgel 60 with fluorescent indicator UV₂₅₄). Spots were visualized either by quenching of UV fluorescence (254 nm) or by staining with basic potassium permanganate dip. Flash column chromatography was performed manually according to the method described by Still, Khan and Mitra¹¹⁹ with ZEOprep 60 (25-40 μm) silica gel, applying head pressure by means of compressed air.

6.3 Experimental Details for Chapter 2

6.3.1 (S)-2-(2,2-Dimethyl-5-oxo-1,3-dioxolan-4-yl)acetic acid



To a dried Schlenk flask was added *L*-malic acid (25.32 g, 188.83 mmol, 1.0 eq.) and *p*-toluenesulfonic acid monohydrate (3.59 g, 18.88 mmol, 0.1 eq.). The atmosphere was replaced by nitrogen *via* repeated evacuation/refill cycles before the addition of 2,2-dimethoxypropane (92.77 mL, 755.31 mmol, 4.0 eq.), the flask was sealed and the reaction stirred at room temperature for 1 hour. The vivid yellow reaction solution was quenched by the addition of saturated aqueous sodium hydrogen carbonate (16 mL) and stirring was maintained for five minutes, leading to a colourless solution. The reaction mixture was diluted with dichloromethane (150 mL) and washed with deionised water (2 × 100 mL). The dichloromethane layer was isolated, dried over anhydrous magnesium sulfate and filtered before being concentrated under reduced pressure to yield a white crystalline solid. Crude material was recrystallized from diethyl ether and hexanes at -18 °C overnight, yielding large clear crystals which were isolated *via* filtration and dried under reduced pressure to afford the title compound (11.20 g, 64.20 mmol, 34%). Characterisation data in agreement with those reported in literature.¹²⁰

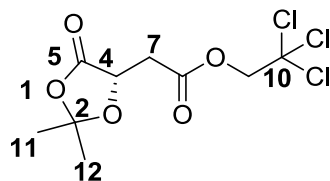
¹H NMR (400 MHz, CDCl₃) δ 4.71 (dd, ³J = 6.5, 3.9 Hz, 1H, *H*⁴), 2.95 (dd, ³J = 56.5, 5.2 Hz, 1H, *H*^{5a}), 2.90 (dd, ³J = 56.5, 5.2 Hz, 1H, *H*^{5b}), 1.62 (s, 3H, *H*⁸), 1.57 (s, 3H, *H*⁹).

¹³C NMR (101 MHz, CDCl₃) δ 175.28 (s, *C*⁷), 171.97 (s, *C*⁵), 111.53 (s, *C*²), 70.52 (s, *C*⁴), 36.15 (s, *C*⁶), 26.89 (s, *C*⁸), 25.96 (s, *C*⁹).

$[\alpha]_D^{22} = +24.75$ (0.079 g.mL⁻¹ in CHCl₃)

Melting Point = 113.0 °C

6.3.2 (S)-2,2,2-Trichloroethyl 2-(2,2-dimethyl-5-oxo-1,3-dioxolan-4-yl)acetate



To a dried Schlenk flask was added (*S*)-2-(2,2-dimethyl-5-oxo-1,3-dioxolan-4-yl)acetic acid (4.62 g, 26.53 mmol, 1.0 eq.) and 4-dimethylaminopyridine (0.49 g, 3.98 mmol, 0.15 eq.). The atmosphere was replaced with nitrogen *via* repeated evacuation/refill cycles before the addition of anhydrous dichloromethane (100 mL) *via* cannula and 2,2,2-trichloroethanol (2.93 mL, 29.18 mmol, 1.1 eq.). The stirring reaction mixture was cooled to 0 °C and maintained during the slow addition of a solution of *N*-(3-diethylaminopropyl)-*N'*-ethyl carbodiimide hydrochloride (5.59 g, 29.18 mmol, 1.1 eq.) in anhydrous dichloromethane (150 mL). Once addition was complete, the flask was sealed and the reaction allowed to warm slowly to room temperature with stirring continued overnight. The reaction was stopped and washed with deionised water (2 × 100 mL). The dichloromethane layer was isolated and dried over anhydrous magnesium sulfate, filtered and concentrated under reduced pressure to yield a pale pink, crystalline solid. The crude product was purified *via* column chromatography (5:1 *n*-Hexane/Ethyl Acetate, $R_f = 0.38$) and the fractions combined and concentrated under reduced pressure to yield a white, crystalline solid (4.73 g, 15.48 mmol, 58%).

$^1\text{H NMR}$ (400 MHz, CDCl_3) δ 4.82 (d, $J = 12.0$ Hz, 2H, H^{10}), 4.70 (d, $J = 12.0$ Hz, H^{10b}), 4.76 – 4.71 (m, 1H, H^4), 3.06 (dd, $J = 23.7, 17.2, 5.2$ Hz, 1H, H^{5a}), 2.94 (dd, $J = 17.2, 5.2$ Hz, H^{5b}), 1.60 (s, 3H, H^{11}), 1.54 (s, 3H, H^{12}).

^{13}C NMR (101 MHz, CDCl_3) δ 171.61 (s, C^5), 167.82 (s, C^7), 111.39 (s, C^2), 94.53 (s, C^{10}), 74.31 (s, C^9), 70.36 (s, C^4), 35.94 (s, C^6), 26.77 (s, C^{11}), 25.86 (s, C^{12}).

IR (ν_{max} / cm^{-1}) 1798, 1741, 1447, 1388, 1287, 1273, 1241, 1219, 1155, 1112, 861, 798, 730, 711, 590.

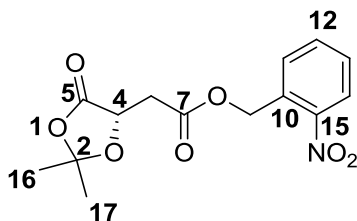
HR-MS: Calculated for $\text{C}_9\text{H}_{12}\text{Cl}_3\text{O}_5$ ($\text{M}+\text{H}^+$) 304.9750, found 304.9744 ($\text{M}+\text{H}^+$) m/z .

Elemental Analysis: Calculated for $\text{C}_9\text{H}_{11}\text{Cl}_3\text{O}_5$ C = 35.38, H = 3.63, Cl = 34.81; Found C = 35.39, H = 3.61, Cl = 34.69.

$[\alpha]_D^{22} = +11.25$ (0.046 $\text{g}\cdot\text{mL}^{-1}$ in CHCl_3)

Melting Point = 71.7 $^\circ\text{C}$

6.3.3 (S)-2-Nitrobenzyl 2-(2,2-dimethyl-5-oxo-1,3-dioxolan-4-yl)acetate



To a dried Schlenk flask was added (S)-2-(2,2-dimethyl-5-oxo-1,3-dioxolan-4-yl)acetic acid (5.52 g, 31.70 mmol, 1.0 eq.), 2-nitrobenzyl alcohol (5.34 g, 34.87 mmol, 1.1 eq.) and 4-dimethylaminopyridine (0.58 g, 4.75 mmol, 0.15 eq.). The atmosphere was replaced with nitrogen *via* repeated evacuation/refill cycles before the addition of anhydrous dichloromethane (100 mL) *via* cannula. The stirring reaction mixture was cooled to 0 $^\circ\text{C}$ and maintained during the slow addition of a solution of *N*-(3-diethylaminopropyl)-*N'*-ethyl carbodiimide hydrochloride (6.68 g, 34.87 mmol, 1.1 eq.) in anhydrous dichloromethane (150 mL). Once addition was complete, the flask was sealed and the reaction allowed to

warm slowly to room temperature with stirring continued overnight. The reaction was stopped and washed with deionised water (3 × 150 mL). The dichloromethane layer was isolated, dried over anhydrous magnesium sulfate, filtered and concentrated under reduced pressure to yield a clear, colourless oil. The crude material was purified *via* column chromatography (2:1 *n*-Hexane/Ethyl Acetate, $R_f = 0.44$), the fractions combined and the solvent removed under reduced pressure to give a non-crystalline white solid (6.27 g, 20.29 mmol, 64%).

^1H NMR (400 MHz, CDCl_3) δ 8.12 (d, $J = 8.2$ Hz, 1H, H^{14}), 7.66 (t, $J = 7.5$ Hz, 1H, H^{12}), 7.60 (d, $J = 7.5$ Hz, 1H, H^{11}), 7.56 – 7.45 (m, 1H, H^{13}), 5.70 – 5.49 (m, 2H, H^9), 4.76 (dd, $J = 6.5, 4.0$ Hz, 1H, H^4), 3.03 (dd, $J = 16.9, 5.3$ Hz, 2H, H^{6a}), 2.93 (dd, $J = 16.9, 5.3$ Hz, 1H, H^{6b}), 1.60 (s, 3H, H^{16}), 1.57 (s, 3H, H^{17}).

^{13}C NMR (101 MHz, CDCl_3) δ 171.97 (s, C^7), 168.72 (s, C^5), 147.56 (s, C^{15}), 133.95 (s, C^{14}), 131.65 (s, C^{10}), 129.17 (s, C^{12}), 129.06 (s, C^{11}), 125.22 (s, C^{13}), 111.42 (s, C^2), 70.67 (s, C^4), 63.72 (s, C^9), 36.28 (s, C^6), 26.85 (s, C^{16}), 25.92 (s, C^{17}).

IR ($\nu_{\text{max}} / \text{cm}^{-1}$) 1787, 1737, 1524, 1387, 1333, 1263, 1167, 1131, 991, 929, 855, 796, 731.

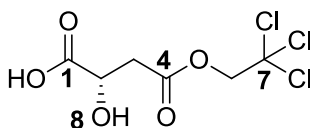
HR-MS: Calculated for $\text{C}_{14}\text{H}_{15}\text{NNaO}_7$ ($\text{M}+\text{Na}^+$) 332.0746, Found 332.0740 ($\text{M}+\text{Na}^+$) m/z .

Elemental Analysis: Calculated for $\text{C}_{14}\text{H}_{15}\text{NO}_7$ C = 54.37, H = 4.89, N = 4.53; Found C = 54.37, H = 4.73, N = 4.55.

$[\alpha]_D^{22} = +4.53$ (0.019 $\text{g}\cdot\text{mL}^{-1}$ in CHCl_3)

Melting Point = 67.4 °C

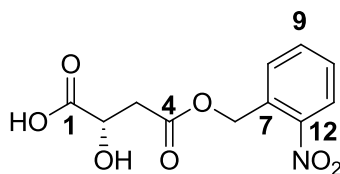
6.3.4 (S)-2-Hydroxy-4-oxo-4-(2,2,2-trichloroethoxy)butanoic acid



To a dried round-bottomed flask was added (*S*)-2,2,2-trichloroethyl 2-(2,2-dimethyl-5-oxo-1,3-dioxolan-4-yl)acetate (4.28g, 14.10 mmol, 1.0 eq.) before being dissolved in methanol (150 mL). To the stirring solution was added pre-washed DOWEX HCR-W2-200 (500 mg) and the resulting mixture sealed and allowed to run overnight at room temperature. The DOWEX resin was removed *via* filtration and the resulting filtrate concentrated under reduced pressure to yield the crude product as a pale pink oil (3.24 g, 12.27 mmol, 87%) which was used immediately without further purification.

$^1\text{H NMR}$ (400 MHz, CDCl_3) δ 4.77 (q, $J = 12.0$ Hz, 2H, H^6), 4.57 (dd, $J = 5.8, 4.7$ Hz, 1H, H^2), 3.25 (s (br), 1H, H^8), 3.04 (dd, $J = 16.6, 4.5$ Hz, 1H, H^{3a}), 2.95 (dd, $J = 16.6, 4.5$ Hz, 1H, H^{3b}).

6.3.5 (S)-2-Hydroxy-4-(2-nitrobenzyloxy)-4-oxobutanoic acid

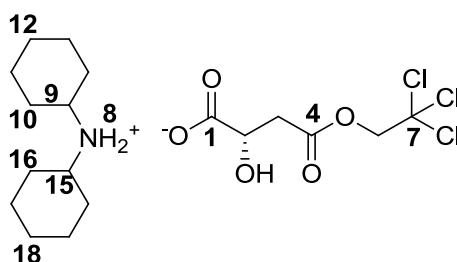


To a dried round-bottomed flask was added (*S*)-2-nitrobenzyl 2-(2,2-dimethyl-5-oxo-1,3-dioxolan-4-yl)acetate (9.92 g, 36.84 mmol, 1.0 eq.) before being dissolved in methanol (150 mL). To this stirring solution was added pre-washed DOWEX HCR-W2-200 (500 mg) and the reaction heated to 50 °C and allowed to stir overnight. The reaction was stopped and The DOWEX resin was removed *via* filtration and the resulting filtrate concentrated under

reduced pressure to yield the crude product as a pale brown oil. The crude product was identified as the title compound (9.53 g, 35.40 mmol, 96%) and was immediately used without further purification.

$^1\text{H NMR}$ (400 MHz, CDCl_3) δ 8.11 (d, $J = 8.1$ Hz, 1H, H^{1l}), 7.75 (d, $J = 7.6$ Hz, 1H, H^{1o}), 7.65 (dd, $J = 18.2, 11.0$ Hz, 1H, H^9), 7.49 (t, $J = 7.4$ Hz, 1H, H^8), 5.57 (q, $J = 11.1$ Hz, 2H, H^6), 4.59 (dd, $J = 6.2, 4.5$ Hz, 1H, H^2), 3.04 (dd, $J = 16.6, 4.5$ Hz, 1H, H^{3a}), 2.95 (dd, $J = 16.6, 6.2$ Hz, 1H, H^{3b}).

6.3.6 Dicyclohexylammonium (*S*)-2-hydroxy-4-oxo-4-(2,2,2-trichloroethoxy) butanoate



To a round-bottomed flask was added (*S*)-2-hydroxy-4-oxo-4-(2,2,2-trichloroethoxy)butanoic acid (7.64 g, 28.94 mmol, 1.0 eq.) before being dissolved in diethyl ether (400 mL) and cooled to 0 °C. Cooling was maintained during the slow addition of *N,N*-dicyclohexylamine (6.90 mL, 34.73 mmol, 1.2 eq) leading to a large quantity of white precipitate. The reaction mixture was allowed to stir for 1 hour before the precipitate was isolated *via* filtration and dried under reduced pressure to yield a fine white powder, identified as the title compound (7.60 g, 17.07 mmol, 59%).

$^1\text{H NMR}$ (400 MHz, CDCl_3) δ 4.75 (d, $J = 14.8$ Hz, 1H, H^{6a}), 4.72 (d, $J = 14.8$ Hz, 1H, H^{6b}), 4.29 (dd, $J = 8.4, 4.0$ Hz, 1H, H^2), 2.97 (dd, $J = 15.7, 4.1$ Hz, 1H, H^{3a}), 2.98 – 2.89 (m, 2H, H^8), 2.68 (dd, $J = 15.6, 8.4$ Hz, 1H, H^{3b}), 1.98 (d, $J = 11.4$ Hz, 4H, *Cyclohexyl*), 1.78 (d, $J =$

12.5 Hz, 4H, *Cyclohexyl*), 1.63 (d, $J = 10.0$ Hz, 2H, $H^{9\&15}$), 1.47 – 1.31 (m, 4H, *Cyclohexyl*), 1.28 – 1.07 (m, 8H, *Cyclohexyl*).

^{13}C NMR (101 MHz, CDCl_3) δ 177.10 (s, C^1), 170.26 (s, C^4), 95.12 (s, C^7), 74.06 (s, C^6), 68.48 (s, C^2), 52.73 (s, $C^{9\&15}$), 40.20 (s, C^3), 29.06 (s, $C^{10,14,16\&20}$), 25.18 (s, $C^{12\&18}$), 24.83 (s, $C^{11,13,17\&19}$).

IR (ν_{max} / cm^{-1}) 3370, 2946, 2859, 1747, 1630, 1555, 1386, 1225, 1156, 1048, 792, 724.

HR-MS: Anion – Calculated for $\text{C}_6\text{H}_6\text{Cl}_3\text{O}_5^-$ (M $^-$) 262.9286, Found 262.9286 (M $^-$) m/z;

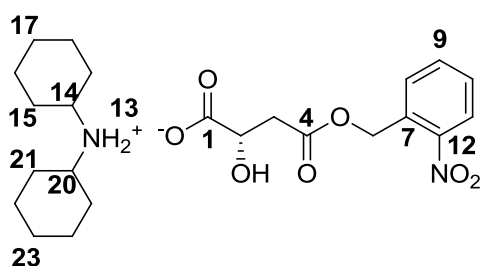
Cation – Calculated for $\text{C}_{12}\text{H}_{24}\text{N}^+$ (M $^+$) 182.1904, Found 182.1903 (M $^+$) m/z.

Elemental Analysis: Calculated for $\text{C}_{18}\text{H}_{30}\text{Cl}_3\text{NO}_5$ C = 48.39, H = 6.77, Cl = 23.80, N = 3.13; Found C = 49.12, H = 6.87, Cl = 22.80, N = 3.24.

$[\alpha]_D^{22} = -9.35$ (0.223 $\text{g}\cdot\text{mL}^{-1}$ in CHCl_3)

Melting Point = 128.2 °C

6.3.7 Dicyclohexylammonium (*S*)-2-hydroxy-4-(2-nitrobenzyloxy)-4-oxobutanoate



To a round-bottomed flask was added (*S*)-2-hydroxy-4-(2-nitrobenzyloxy)-4-oxobutanoic acid (9.53 g, 35.40 mmol, 1.0 eq.) before being dissolved in diethyl ether (500 mL) and cooled to 0 °C. Cooling was maintained during the slow addition of *N,N*-dicyclohexylamine (8.45 mL, 42.48 mmol, 1.2 eq.), leading to a large quantity of white precipitate. The

reaction mixture was allowed to stir for 1 hour before the precipitate was isolated *via* filtration and dried under reduced pressure to yield a fine white powder (10.02 g, 22.24 mmol, 62%).

¹H NMR (400 MHz, CDCl₃) δ 8.10 (d, *J* = 8.2 Hz, 1H, *H*¹¹), 7.72 (d, *J* = 7.7 Hz, 1H, *H*⁹), 7.64 (t, *J* = 7.6 Hz, 1H, *H*⁸), 7.46 (t, *J* = 7.7 Hz, 1H, *H*¹⁰), 5.57 (s, *J* = 16.0 Hz, 2H, *H*⁶), 4.32 (dd, *J* = 8.0, 4.2 Hz, 1H, *H*²), 2.98 (dd, *J* = 15.1, 3.6 Hz, 1H, *H*^{3a}), 2.96 (dd, *J* = 15.3, 4.2 Hz, 2H, *H*¹³), 2.72 (dd, *J* = 15.3, 8.1 Hz, 1H, *H*^{3b}), 1.99 (d, *J* = 12.0 Hz, 4H, *Cyclohexyl*), 1.78 (d, *J* = 13.0 Hz, 4H, *Cyclohexyl*), 1.64 (d, *J* = 11.0 Hz, 2H, *H*^{14&20}), 1.49 – 1.33 (m, 4H, *Cyclohexyl*), 1.30 – 1.10 (m, 8H, *Cyclohexyl*).

¹³C NMR (101 MHz, CDCl₃) δ 177.28 (s, *C*¹), 171.21 (s, *C*⁴), 147.35 (s, *C*¹²), 133.90 (s, *C*¹¹), 132.74 (s, *C*⁷), 128.85 (s, *C*⁹), 128.55 (s, *C*⁸), 125.01 (s, *C*¹⁰), 68.73 (s, *C*²), 62.86 (s, *C*⁶), 52.74 (s, *C*^{14&20}), 40.47 (s, *C*³), 29.00 (s, *C*^{15,19,21&25}), 25.17 (s, *C*^{17&23}), 24.81 (s, *C*^{16,18,22&24}).

IR (ν_{\max} / cm⁻¹) 3459, 2942, 2861, 1736, 1627, 1571, 1519, 1333, 1144, 1090, 730.

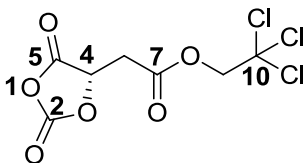
HR-MS: Anion - Calculated for C₁₁H₁₀NO₇⁻ (M⁻) 268.0462, Found 268.0463 (M⁻) *m/z*;

Cation - Calculated for C₁₂H₂₄N⁺ (M⁺) 182.1904, Found 182.1903 (M⁺) *m/z*.

Elemental Analysis: Calculated for C₂₃H₃₄N₂O₇ C = 61.32, H = 7.61, N = 6.22; Found C = 61.17, H = 7.62, N = 6.09.

$[\alpha]_D^{22} = -10.13$ (0.225 g.mL⁻¹ in CHCl₃)

Melting Point = 153.8 °C

6.3.8 (S)-2,2,2-Trichloroethyl 2-(2,5-dioxo-1,3-dioxolan-4-yl)acetate

To a dried Schlenk flask was added dicyclohexylammonium (*S*)-2-hydroxy-4-oxo-4-(2,2,2-trichloroethoxy)butanoate (10.10 g, 22.69 mmol, 1.0 eq.), the flask was sealed and the atmosphere exchanged for nitrogen *via* repeated evacuation and refill cycles. Anhydrous tetrahydrofuran (500 mL) was added *via* cannula and the stirring solution cooled to 0 °C before the careful addition of diphosgene (3.3 mL, 27.23 mmol, 1.2 eq.). Activated charcoal (approx. 2 g) was added and the flask resealed and the reaction mixture allowed to stir at room temperature overnight. The yellow reaction solution was isolated from the resulting precipitate and charcoal *via* cannula filtration to a second purged Schlenk flask. Solvent and residual diphosgene were removed under reduced pressure and capture using a liquid nitrogen-cooled pre-trap to yield a pale brown solid. Recrystallisation from dry tetrahydrofuran and pentanes gave fine white crystals which were isolated by removal of the supernatant *via* cannula filtration to a freshly dried, purged Schlenk flask. Crystals were dried under reduced pressure before being identified as the title compound (3.11 g, 10.66 mmol, 47%).

¹H NMR (400 MHz, CDCl₃) δ 5.26 (s, 1H, *H*^d), 4.80 (s, 2H, *H*^g), 3.36 (d, *J* = 26.8 Hz, 1H, *H*^{6a}), 3.31 (d, *J* = 26.7 Hz, 1H, *H*^{6b}).

¹³C NMR (101 MHz, CDCl₃) δ 166.88 (s, *C*⁷), 166.35 (s, *C*⁵), 148.03 (s, *C*²), 93.90 (s, *C*¹⁰), 74.96 (s, *C*^d), 74.86 (s, *C*^g), 34.28 (s, *C*⁶).

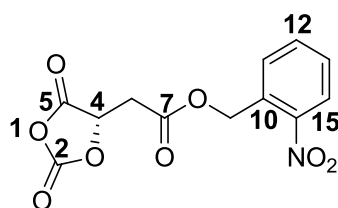
HR-MS: Calculated for C₇H₅Cl₃NaO₆ (M+Na⁺, 3x³⁵Cl) 312.9049, Found 312.9048 (M+Na⁺, 3x³⁵Cl) m/z.

Elemental Analysis: Calculated for $C_7H_5Cl_3O_6$ C = 28.85, H = 1.73, Cl = 36.49; Found C = 29.01, H = 1.78, Cl = 35.73

$[\alpha]_D^{22} = -8.57$ (0.112 g.ml⁻¹ in CHCl₃)

Melting Point = 47.8 °C (Degrades)

6.3.9 (S)-2-Nitrobenzyl 2-(2,5-dioxo-1,3-dioxolan-4-yl)acetate



To a dried Schlenk flask was added dicyclohexylammonium (S)-2-hydroxy-4-(2-nitrobenzyloxy)-4-oxobutanoate (4.94 g, 10.96 mmol, 1.0 eq.), the flask was sealed and the atmosphere exchanged for nitrogen *via* repeated evacuation and refill cycles. Dry tetrahydrofuran (250 mL) was added *via* cannula and the stirring solution cooled to 0 °C before the careful addition of diphosgene (1.6 mL, 13.16 mmol, 1.2 eq.). Activated charcoal (approx. 1 g) was added and the flask resealed and the reaction mixture allowed to stir at room temperature overnight. The yellow reaction solution was isolated from the resulting precipitate and charcoal *via* cannula filtration to a second purged Schlenk flask. Solvent and residual diphosgene were removed under reduced pressure and capture using a liquid nitrogen-cooled pre-trap to yield a pale yellow solid. Recrystallisation from dry tetrahydrofuran and pentanes gave fine white crystals which were isolated by removal of the supernatant *via* cannula filtration to a freshly dried, purged Schlenk flask. Crystals were dried under reduced pressure before being identified as the title compound (1.81 g, 6.14 mmol, 56%).

¹H NMR (400 MHz, CDCl₃) δ 8.14 (d, J = 8.1 Hz, 1H, H¹⁴), 7.69 (t, J = 7.5 Hz, 1H, H¹²), 7.55 (dd, J = 10.0, 8.1 Hz, 2H, H¹¹ & ¹³), 5.58 (d, J = 14.6 Hz, 2H, H⁹), 5.20 (t, J = 3.2 Hz, 1H, H⁴), 3.29 (dd, J = 18.6, 3.6 Hz, 1H, H^{6a}), 3.23 (dd, J = 18.6, 3.1 Hz, 1H, H^{6b}).

¹³C NMR (101 MHz, CDCl₃) δ 168.30 (s, C⁷), 168.02 (s, C⁵), 148.60 (s, C¹⁵), 134.11 (s, C¹⁴), 130.4 (s, C¹⁰), 129.95 (s, C¹²), 129.78 (s, C¹¹), 125.52 (s, C¹³), 74.96 (s, C⁴), 64.90 (s, C⁹), 34.50 (s, C⁵).

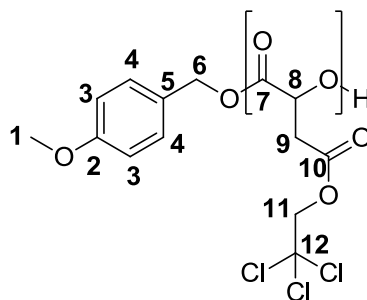
HR-MS: Calculated for C₁₂H₉NNaO₈ (M+Na⁺) 318.0226, Found 318.0224 (M+Na⁺) m/z

Elemental Analysis: Calculated for C₁₂H₉NO₈ C = 48.82, H = 3.07, N = 4.74; Found C = 48.76, H = 3.08, N = 4.59

$[\alpha]_D^{22} = -9.83$ (0.084 g.ml⁻¹ in CHCl₃)

Melting Point = 53.2 °C (Degrades)

6.3.10 General procedure for the polymerisation of (S)-2,2,2-Trichloroethyl 2-(2,5-dioxo-1,3-dioxolan-4-yl)acetate



Within a glovebox, (S)-2,2,2-Trichloroethyl 2-(2,5-dioxo-1,3-dioxolan-4-yl)acetate (36.24 mg, 125.0 μmol, 20 eq.) was dissolved in deuterated chloroform (485 μl) before the addition of 4-methoxybenzyl alcohol (8.63 μL of a 100 mg.mL⁻¹ CDCl₃ solution; 6.25 μmol, 1.0 eq.) and 4-methoxypyridine (6.82 μL of a 100 mg.mL⁻¹ CDCl₃ solution; 6.25 μmol, 1.0 eq.). The

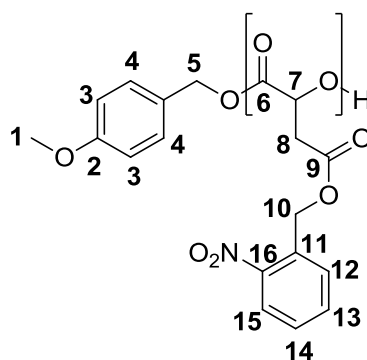
reaction solution was transferred to a Young's tap NMR tube and monitored *via* ^1H NMR spectroscopy. Once conversion reached equilibrium the reaction was stopped terminated by precipitation from hexanes, the precipitate was isolated and dissolved in dichloromethane (0.5 mL) and washed with 1 M aqueous hydrochloric acid (3×1 mL), dried with anhydrous magnesium sulphate and filtered before being reprecipitated from hexanes and dried under reduced pressure to yield a viscous clear oil (22.2 mg, 72%).

^1H NMR (400 MHz, CDCl_3) δ 7.25 (d, $J = 5.1$ Hz, H^4), 6.89 (d, $J = 8.6$ Hz, H^3), 5.68 – 5.60 (m, H^8), 5.12 (q, $J = 11.8$ Hz, H^6), 4.85 – 4.75 (m, H^{11}), 3.81 (s, H^1), 3.28 – 3.06 (m, H^9).

^{13}C NMR (101 MHz, CDCl_3) δ 167.08 (s, C^{10}), 166.63 (s, C^7), 130.64 (s, C^4), 124.97 (s, C^5), 114.28 (s, C^3), 94.52 (s, C^{12}), 74.51 (s, C^{11}), 68.89 (s, C^8), 67.04 (s, C^6), 55.45 (s, C^1), 35.56 (s, C^9).

GPC (CHCl_3 ; RI): M_n (D_M) = $2516 \text{ g}\cdot\text{mol}^{-1}$ (1.32)

6.3.11 General procedure for the polymerisation of (*S*)-2-Nitrobenzyl 2-(2,5-dioxo-1,3-dioxolan-4-yl)acetate



Within a glovebox, (*S*)-2-Nitrobenzyl 2-(2,5-dioxo-1,3-dioxolan-4-yl)acetate (36.24 mg, 125.0 μmol , 20 eq.) was dissolved in deuterated dichloromethane (485 μl) before the addition of 4-methoxybenzyl alcohol (8.63 μL of a $100 \text{ mg}\cdot\text{mL}^{-1}$ D_2 -DCM solution; 6.25

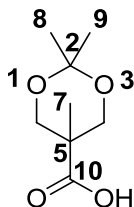
μmol , 1.0 eq.) and 4-methoxypyridine (6.82 μL of a 100 $\text{mg}\cdot\text{mL}^{-1}$ $\text{D}_2\text{-DCM}$ solution; 6.25 μmol , 1.0 eq.). The reaction solution was transferred to a Young's tap NMR tube and monitored *via* ^1H NMR spectroscopy. Once conversion reached equilibrium the reaction was stopped terminated by precipitation from hexanes, the precipitate was isolated and dissolved in dichloromethane (0.5 mL) and washed with 1 M aqueous hydrochloric acid (3×1 mL), dried with anhydrous magnesium sulphate and filtered before being reprecipitated from hexanes and dried under reduced pressure to yield a viscous clear oil (24.5 mg, 78%).

^1H NMR (400 MHz, CDCl_3) δ 8.10 – 7.96 (m, H^{15}), 7.61 (d, $J = 7.3$ Hz, H^{13}), 7.54 (d, $J = 7.6$ Hz, H^{12}), 7.50 – 7.38 (m, H^{14}), 7.22 (s, H^4), 6.84 (s, H^3), 5.57 (d, $J = 20.4$ Hz, H^7), 5.48 (s, H^{10}), 5.08 (s, H^5) 3.76 (s, H^1), 3.08 (dd, $J = 31.6, 10.6$ Hz, H^8).

GPC (CHCl_3 ; RI): M_n (D_M) = 2371 $\text{g}\cdot\text{mol}^{-1}$ (1.38)

6.4 Experimental Details for Chapter 3

6.4.1 2,2,5-Trimethyl-1,3-dioxane-5-carboxylic acid



To a dried Shlenk flask was added 2,2-*bis*-(hydroxymethyl)propionic acid (50.79 g, 378.66 mmol, 1.0 eq.), the atmosphere was exchanged for nitrogen *via* repeated evacuation and refill cycles before the addition of acetone (250 mL). To the stirring solution was added 2,2-dimethoxypropane (69.84 mL, 567.99 mmol, 1.5 eq.) and *p*-toluenesulfonic acid monohydrate (3.60 g, 18.93 mmol, 0.05 eq.). The flask was sealed and the reaction stirred overnight at room temperature before being neutralised by the careful addition of saturated aqueous ammonium hydroxide. The quenched reaction mixture was stirred vigorously with dichloromethane (500 mL) for 1 hour before being washed repeatedly with deionised water (3 × 300 mL). The dichloromethane layer was isolated, dried over anhydrous magnesium sulfate, filtered and concentrated under reduced pressure to yield a white solid (20.40 g, 117.00 mmol, 30%). Characterisation data in agreement with those reported in literature.⁷⁵

¹H NMR (400 MHz, CDCl₃) δ 4.17 (d, *J* = 11.8 Hz, 1H, *H*^{4a & 6a}), 3.64 (d, *J* = 11.8 Hz, 1H, *H*^{4b & 6b}), 1.42 (s, 3H, *H*⁸), 1.39 (s, 3H, *H*⁹), 1.19 (s, 3H, *H*⁷).

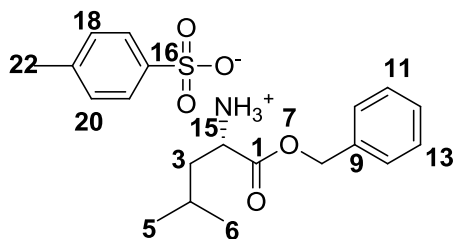
¹³C NMR (101 MHz, CDCl₃) δ 180.42 (s, *C*¹⁰), 98.41 (s, *C*²), 65.88 (s, *C*^{4 & 6}), 41.83 (s, *C*⁵), 25.09 (s, *C*⁸), 22.22 (s, *C*⁹), 18.53 (s, *C*⁷).

IR (ν_{max} / cm⁻¹) 2955, 1744, 1609, 1529, 1274, 1213, 1169, 1124 1036, 1011, 814.

HR-MS: Calculated for C₈H₁₅O₄ (M+H⁺) 175.0970, Found 175.0973 (M+H⁺) m/z;
Calculated for C₈H₁₄NaO₄ (M+Na⁺) 197.0790, Found 197.0787 (M+Na⁺) m/z.

Melting Point = 119.6 °C

6.4.2 (S)-1-(Benzyloxy)-4-methyl-1-oxopentan-2-aminium 4-methylbenzene sulfonate



To a dried round-bottomed flask was added *L*-leucine (49.95 g, 380.80 mmol, 1.0 eq.) and *p*-toluenesulfonic acid monohydrate (76.06 g, 399.84 mmol, 1.05 eq.) which were suspended in toluene (1 L) before the addition of benzyl alcohol (78.8 mL, 766.61 mmol, 2.0 eq.). The flask was fitted with a Dean-Stark condenser and the stirring reaction mixture heated to reflux for 18 hours with the continual removal of any isolated water. The reaction was stopped and diluted with diethyl ether before being cooled to room temperature, leading to a large quantity of white precipitate which was isolated *via* filtration and washed with further diethyl ether. The isolated solid was dried under reduced pressure to give a light, white powder (125.70 g, 319.87 mmol, 84%).

¹H NMR (400 MHz, CDCl₃) δ 8.26 (d, *J* = 3.8 Hz, 3H, *H*¹⁵), 7.75 (d, *J* = 8.1 Hz, 2H, *H*^{17&21}), 7.26 (m, 5H, *H*¹⁰⁻¹⁴), 7.07 (d, *J* = 8.1 Hz, 2H, *H*^{18&20}), 5.13 (d, *J* = 12.3 Hz, 1H, *H*^{8a}), 5.05 (d, *J* = 12.3 Hz, 1H, *H*^{8b}), 3.97 (dd, *J* = 11.6, 5.9 Hz, 1H, *H*²), 2.30 (s, 3H, *H*²²), 1.75 – 1.54 (m, 3H, *H*^{3&4}), 0.74 (t, *J* = 6.0 Hz, 6H, *H*^{5,6}).

¹³C NMR (101 MHz, CDCl₃) δ 169.98 (s, *C*¹), 141.77 (s, *C*¹⁶), 140.48 (*C*²¹), 135.14 (s, *C*⁹), 129.04 (s, *C*^{18&20}), 128.73 (s, *C*^{11&13}), 128.57 (s, *C*¹²), 128.49 (s, *C*^{10&14}), 126.41 (s, *C*^{17&21}), 67.94 (s, *C*⁸), 51.99 (s, *C*²), 39.51 (s, *C*³), 24.40 (s, *C*⁴), 22.23 (s, *C*⁵), 22.14 (s, *C*⁶), 21.53 (s, *C*²²).

IR (ν_{\max} / cm^{-1}) 2983, 1743, 1515, 1204, 1174, 1123, 1036, 1011, 815.

HR-MS: Anion – Calculated for $\text{C}_7\text{H}_7\text{O}_3\text{S}^-$ (M^-) 171.0121, Found 171.0125 m/z (M^-);

Cation – Calculated for $\text{C}_{13}\text{H}_{20}\text{NO}_2^+$ (M^+) 222.1489, Found 222.1487 (M^+) m/z .

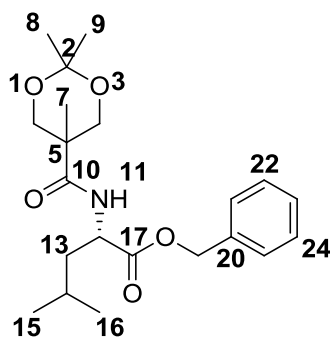
Elemental Analysis: Calculated for $\text{C}_{20}\text{H}_{27}\text{NO}_5\text{S}$ C = 61.05, H = 6.92, N = 3.56, S = 8.15;

Found C = 61.05, H = 6.90, N = 3.50, S = 7.67.

$[\alpha]_D^{22} = -2.75$ (0.043 $\text{g}\cdot\text{mL}^{-1}$ in CHCl_3)

Melting Point = 148.4 °C

6.4.3 (S)-Benzyl 4-methyl-2-(2,2,5-trimethyl-1,3-dioxane-5-carboxamido)pentanoate



To a dried Schlenk flask were added 2,2,5-trimethyl-1,3-dioxane-5-carboxylic acid (10.36 g, 59.48 mmol, 1.0 eq.), (S)-1-(benzyloxy)-4-methyl-1-oxopentan-2-aminium 4-methylbenzenesulfonate (24.70 g, 62.45 mmol, 1.05 eq.) and 4-dimethylaminopyridine (8.36 g, 68.40 mmol, 1.15 eq.). The atmosphere was exchanged *via* repeated evacuation and back-filling with nitrogen before the addition of anhydrous dichloromethane (300 mL) which led to full dissolution. The stirring solution was cooled to 0 °C before the careful addition of *N*-(3-dimethylaminopropyl)-*N'*-ethylcarbodiimide hydrochloride (12.54 g, 65.42 mmol, 1.1 eq.) in anhydrous dichloromethane (200 mL). The reaction was sealed and allowed to warm slowly to room temperature overnight, after which the reaction was stopped and the pink

dichloromethane solution was washed repeatedly with deionised water (4 × 150 mL). The dichloromethane layer was isolated, dried over anhydrous magnesium sulfate, filtered and concentrated under reduced pressure to yield a pale yellow oil. The crude oil was purified *via* column chromatography (Dichloromethane/1% Methanol, $R_f = 0.52$) to afford the title compound (10.77 g, 28.50 mmol, 48%).

^1H NMR (400 MHz, CDCl_3) δ 7.51 (d, $J = 7.8$ Hz, 1H, H^{11}), 7.42 – 7.27 (m, 5H, H^{21-25}), 5.19 (d, $J = 12.3$ Hz, 1H, H^{19a}), 5.14 (d, $J = 12.3$ Hz, 1H, H^{19b}), 4.73 (tt, $J = 10.7, 5.4$ Hz, 1H, H^{12}), 3.96 – 3.87 (m, 2H, H^{4a} & $6a$), 3.77 (dd, $J = 12.3, 1.6$ Hz, 2H, H^{4b} & $6b$), 1.76 – 1.64 (m, 2H, H^{13a} & 14), 1.64 – 1.56 (m, 1H, H^{13b}), 1.47 (s, 3H, H^8), 1.45 (s, 3H, H^9), 1.00 (s, 3H, H^7), 0.93 (d, $J = 6.0$ Hz, 3H, H^{15}), 0.93 (d, $J = 6.2$ Hz, 3H, H^{16}).

^{13}C NMR (101 MHz, CDCl_3) δ 174.60 (s, C^{10}), 172.82 (s, C^{17}), 135.57 (s, C^{20}), 128.55 (s, $C^{22\&24}$), 128.30 (s, C^{23}), 128.22 (s, $C^{22\&25}$), 98.54 (s, C^2), 67.18 (s, C^{19}), 66.91 (s, C^4), 66.87 (s, C^6), 50.90 (s, C^{12}), 41.70 (s, C^{13}), 40.15 (s, C^5), 28.68 (s, C^7), 24.87 (s, C^{14}), 22.83 (s, C^{16}), 22.04 (s, C^{15}), 18.37 (s, C^8), 17.73 (s, C^9).

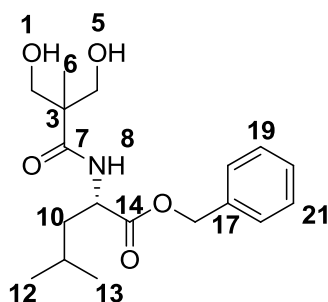
IR ($\nu_{\text{max}} / \text{cm}^{-1}$) 3378, 2966, 1746, 1662, 1526, 1378, 1197, 1148, 1081, 827.

HR-MS: Calculated for $\text{C}_{21}\text{H}_{32}\text{NO}_5$ ($\text{M}+\text{H}^+$) 378.2280, Found 378.2281 ($\text{M}+\text{H}^+$) m/z .

Elemental Analysis: Calculated for $\text{C}_{21}\text{H}_{31}\text{NO}_5$ C = 66.82, H = 8.28, N = 3.71; Found C = 66.36, H = 8.33, N = 3.61.

$[\alpha]_D^{22} = -12.09$ (0.072 $\text{g}\cdot\text{mL}^{-1}$ in CHCl_3)

6.4.4 (S)-Benzyl 2-(3-hydroxy-2-(hydroxymethyl)-2-methylpropanamido)-4-methylpentanoate



To a dried round-bottomed flask was added (*S*)-benzyl 4-methyl-2-(2,2,5-trimethyl-1,3-dioxane-5-carboxamido)pentanoate (10.95 g, 29.01 mmol), this was dissolved in methanol (450 mL) before the addition of pre-washed DOWEX HCR-W2 (33.0 g). The reaction was sealed and stirred at room temperature for 48 hours before the DOWEX resin was removed *via* filtration and the solvent removed under reduced pressure to yield a clear, colourless oil which was purified *via* column chromatography (Dichloromethane/3% Methanol, $R_f = 0.47$) to yield a clear colourless oil which crystallised upon standing (8.14 g, 27.44 mmol, 83%).

$^1\text{H NMR}$ (400 MHz, CDCl_3) δ 7.45 (d, $J = 7.8$ Hz, 1H, H^8), 7.40 – 7.29 (m, 5H, H^{18-22}), 5.21 (d, $J = 12.3$ Hz, 1H, H^{16a}), 5.12 (d, $J = 12.2$ Hz, 1H, H^{16b}), 4.69 – 4.54 (m, 1H, H^9), 3.82 (t, $J = 10.9$ Hz, 2H, H^{2a} & $4a$), 3.77 – 3.64 (m, 2H, H^{2b} & $4b$), 3.38 (d, $J = 14.5$ Hz, 2H, H^1 & 5), 1.75 – 1.64 (m, 2H, H^{10a} & 11), 1.64 – 1.53 (m, 1H, H^{10b}), 1.06 (s, 3H, H^6), 0.93 (d, $J = 6.0$ Hz, 3H, H^{12}), 0.92 (d, $J = 5.9$ Hz, 3H, H^{13}).

$^{13}\text{C NMR}$ (101 MHz, CDCl_3) δ 176.77 (s, C^7), 173.57 (s, C^{14}), 135.38 (s, C^{17}), 128.71 (s, C^{19} & 21), 128.56 (s, C^{20}), 128.34 (s, C^{18} & 22), 68.94 (s, C^4), 68.19 (s, C^2), 67.38 (s, C^{16}), 51.25 (s, C^9), 47.80 (s, C^3), 40.62 (s, C^{10}), 25.14 (s, C^{11}), 22.94 (s, C^{12}), 21.85 (s, C^{13}), 17.52 (s, C^6).

IR (ν_{max} / cm^{-1}) 3321, 2962, 1741, 1646, 1537, 1457, 1154, 1044, 741.

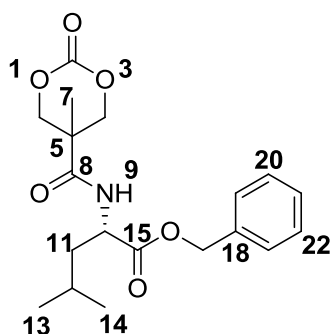
HR-MS: Calculated for $\text{C}_{18}\text{H}_{27}\text{NNaO}_5$ ($\text{M}+\text{Na}^+$) 360.1787, Found 360.1782 ($\text{M}+\text{Na}^+$) m/z .

Elemental Analysis: Calculated for $C_{18}H_{27}NO_5$ C = 64.07, H = 8.07, N = 4.15; Found C = 62.54, H = 8.18, N = 4.08.

$[\alpha]_D^{22} = -19.75$ (0.064 g.mL⁻¹ in CHCl₃)

Melting Point = 44.1 °C

6.4.5 (S)-Benzyl 4-methyl-2-(5-methyl-2-oxo-1,3-dioxane-5-carboxamido)pentanoate



To a dried Schlenk flask was added (*S*)-benzyl 2-(3-hydroxy-2-(hydroxymethyl)-2-methylpropanamido)-4-methylpentanoate (4.17 g, 12.32 mmol, 1.0 eq.), the atmosphere was exchanged for nitrogen *via* repeated evacuation and back-filling with nitrogen before the addition of dry tetrahydrofuran (300 mL) and pyridine (11.96 g, 147.84 mmol, 12.0 eq.). The stirring solution was cooled to 0 °C before the slow addition of triphosgene (3.66 g, 12.32 mmol, 1.0 eq.) in anhydrous tetrahydrofuran (100 mL). Once addition was complete the reaction solution was allowed to warm to room temperature and stirred overnight. The resulting precipitate was removed *via* filtration before the filtrate was concentrated under reduced pressure to yield a clear, colourless oil. This crude oil was redissolved in dichloromethane (500 mL) before being repeatedly washed with deionised water (4 x 250 mL) and brine (250 mL). The dichloromethane layer was isolated, dried over anhydrous magnesium sulfate, filtered and concentrated under reduced pressure to yield a clear, orange

oil. This was purified *via* column chromatography (4:1 Ethyl Acetate/*n*-Hexane, $R_f = 0.63$) to yield a clear colourless oil, crystallised from diethyl ether (2.06 g, 5.67 mmol, 46%).

$^1\text{H NMR}$ (400 MHz, CDCl_3) δ 7.41 – 7.30 (m, 5H, H^{19-23}), 6.28 (d, $J = 8.0$ Hz, 1H, H^9), 5.19 (d, $J = 12.2$ Hz, 1H, H^{17a}), 5.14 (d, $J = 12.2$ Hz, 1H, H^{17b}), 4.71 – 4.60 (m, 3H, $H^{4a,6a \text{ \& } 10}$), 4.25 – 4.14 (m, 2H, $H^{4b,6b}$), 1.74 – 1.64 (m, 1H, H^{11a}), 1.63 – 1.52 (m, 2H, $H^{11b \text{ \& } 12}$), 1.34 (s, 3H, H^7), 0.92 (d, $J = 1.7$ Hz, 3H, H^{13}), 0.91 (d, $J = 1.8$ Hz, 3H, H^{14}).

$^{13}\text{C NMR}$ (101 MHz, CDCl_3) δ 172.42 (s, C^8), 170.09 (s, C^{15}), 151.62 (s, C^2), 135.25 (s, C^{18}), 128.81 (s, $C^{20 \text{ \& } 22}$), 128.73 (s, C^{21}), 128.49 (s, $C^{19 \text{ \& } 23}$), 73.94 (s, C^4), 73.61 (s, C^6), 67.56 (s, C^{17}), 51.40 (s, C^{10}), 41.20 (s, C^5), 40.07 (s, C^{11}), 25.11 (s, C^{12}), 22.89 (s, C^{13}), 21.98 (s, C^{14}), 17.81 (s, C^7).

IR ($\nu_{\text{max}} / \text{cm}^{-1}$) 3359, 2957, 1739, 1665, 1523, 1373, 1199, 1152, 1078, 825.

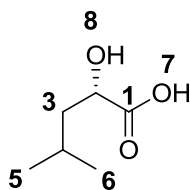
HR-MS: Calculated for $\text{C}_{19}\text{H}_{25}\text{NNaO}_6$ ($\text{M}+\text{Na}^+$) 386.1580, Found 386.1574 ($\text{M}+\text{Na}^+$) m/z .

Elemental Analysis: Calculated for $\text{C}_{19}\text{H}_{25}\text{NO}_6$ C = 62.80, H = 6.93, N = 3.85; Found C = 62.77, H = 6.92, N = 3.88.

$[\alpha]_D^{22} = -11.72$ (0.027 $\text{g}\cdot\text{mL}^{-1}$ in CHCl_3)

Melting Point = 74.5-76.1 (75.2) $^\circ\text{C}$

6.4.6 (S)-2-hydroxy-4-methylpentanoic acid



To a round-bottomed flask was added *L*-leucine (50.05 g, 381.6 mmol, 1.0 eq.) and this was dissolved in 1.25 M sulfuric acid (610.5 mL, 763.1 mmol, 2.0 eq.). The stirring solution was cooled to 0 °C and the cooling maintained during the slow addition of an aqueous sodium nitrite solution (157.96 g in 1 L, 2289.4 mmol, 6.0 eq.). The reaction was allowed to slowly warm to room temperature overnight before being extracted repeatedly with diethyl ether (10 × 250 mL). The organic layers were combined, dried over anhydrous magnesium sulfate, filtered and the solvent removed under reduced pressure to give a clear, colourless oil that crystallised upon standing. The resulting white crystals were isolated *via* filtration, washed with hexanes and dried under reduced pressure (35.88 g, 271.5 mmol, 71%). Characterisation data in agreement with those reported in literature.⁹⁵

¹H NMR (400 MHz, D₆-DMSO) δ 3.93 (dd, *J* = 8.6, 4.9 Hz, 1H, *H*²), 1.75 (tt, *J* = 13.2, 6.6 Hz, 1H, *H*⁴), 1.48 – 1.35 (m, 1H, *H*³), 0.87 (t, *J* = 6.3 Hz, 1H, *H*^{5 & 6}).

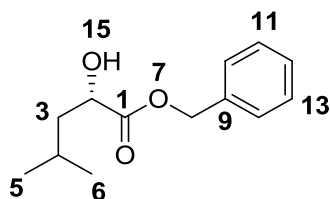
¹³C NMR (101 MHz, D₆-DMSO) δ 176.35 (s, *C*¹), 68.20 (s, *C*²), 42.96 (s, *C*³), 23.94 (s, *C*⁴), 23.20 (s, *C*⁶), 21.53 (s, *C*⁵).

HR-MS: Calculated for C₆H₁₂NaO₃ (M+Na⁺) 155.0684, Found 155.0679 (M+Na⁺) m/z.

$[\alpha]_D^{22} = -15.71$ (0.164 g·ml⁻¹ in DMSO)

Melting Point = 65.9 °C

6.4.7 (S)-Benzyl 2-hydroxy-4-methylpentanoate



To a dried Schlenk flask was added (*S*)-2-hydroxy-4-methylpentanoic acid (10.07 g, 76.24 mmol, 1.0 eq.) and the atmosphere exchanged for nitrogen. Acetone (350 mL) was added and stirred until full dissolution occurred, after which triethylamine (21.19 mL, 152.48 mmol, 2.0 eq.) was added and the stirring solution cooled to 0 °C. Benzyl bromide (10.88 mL, 91.49 mmol, 1.2 eq.) was added carefully before the flask was sealed and the reaction allowed to warm to room temperature whilst stirring overnight. The resulting white precipitate was removed *via* filtration and the clear colourless filtrate was concentrated under reduced pressure to yield a pale yellow oil. This crude oil was redissolved in dichloromethane (300 mL) before being washed repeatedly with deionised water (5 × 100 mL). The dichloromethane layer was isolated, dried over anhydrous magnesium sulfate, filtered and the solvent removed under reduced pressure to give a clear, colourless oil (13.17 g, 59.23 mmol, 77%). Characterisation data in agreement with those reported in literature.¹²¹

¹H NMR (400 MHz, CDCl₃) δ 7.42 – 7.31 (m, 5H, *H*¹⁰⁻¹⁴), 5.21 (s, 2H, *H*⁸), 4.32 – 4.16 (m, 1H, *H*²), 2.68 (s, 1H, *H*¹⁵), 1.96 – 1.77 (m, 1H, *H*⁴), 1.65 – 1.48 (m, 2H, *H*³), 0.95 (d, *J* = 4.4 Hz, 1H, *H*⁵), 0.93 (d, *J* = 4.5 Hz, 1H, *H*⁶).

¹³C NMR (101 MHz, CDCl₃) δ 175.87 (s, *C*¹), 135.36 (s, *C*⁹), 128.79 (s, *C*^{11 & 13}), 128.68 (s, *C*¹²), 128.45 (s, *C*^{10 & 14}), 69.30 (s, *C*²), 67.41 (s, *C*⁸), 43.54 (s, *C*³), 24.55 (s, *C*⁴), 23.37 (s, *C*⁶), 21.68 (s, *C*⁵).

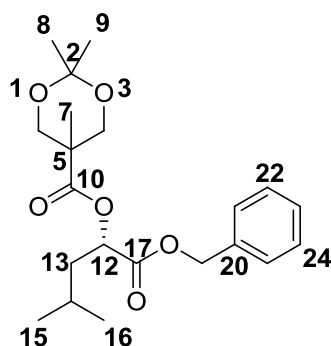
IR (*v*_{max} / cm⁻¹) 3492, 2958, 1734, 1457, 1271, 1200, 1140, 1087, 1006, 750, 697.

HR-MS: Calculated for C₁₃H₁₈NaO₃ (M+Na⁺) 245.1154, Found 245.1148 (M+Na⁺) m/z.

Elemental Analysis: Calculated for C₁₃H₁₈O₃ C = 70.24, H = 8.16; Found C = 69.32, H = 8.04.

$[\alpha]_D^{22} = -13.91$ (0.076 g.mL⁻¹ in CHCl₃)

6.4.8 (S)-1-(Benzyloxy)-4-methyl-1-oxopentan-2-yl 2,2,5-trimethyl-1,3-dioxane-5-carboxylate



To a dried Schlenk flask was added (*S*)-benzyl 2-hydroxy-4-methylpentanoate (11.61 g, 52.21 mmol, 1.0 eq.), 2,2,5-trimethyl-1,3-dioxane-5-carboxylic acid (9.55 g, 54.83 mmol, 1.05 eq.) and 4-dimethylaminopyridine (957 mg, 7.83 mmol, 0.15 eq.) and the atmosphere exchanged for nitrogen before the addition of anhydrous dichloromethane (250 mL). The stirring solution was cooled to 0 °C before the addition of *N*-(3-dimethylaminopropyl)-*N'*-ethylcarbodiimide hydrochloride (11.01 g, 57.44 mmol, 1.1 eq.) in anhydrous dichloromethane (150 mL). The reaction was allowed to warm to room temperature and stirred overnight before being washed with deionised water (3 × 300 mL). The dichloromethane layer was isolated, dried over anhydrous magnesium sulphate, filtered and the solvent removed under reduced pressure to yield a pale yellow oil. The crude product was purified *via* column chromatography (4:1 *n*-Hexane:Ethyl Acetate, $R_f = 0.37$) to afford a clear colourless oil (11.25 g, 29.76 mmol, 57%).

$^1\text{H NMR}$ (400 MHz, CDCl_3) δ 7.42 – 7.29 (m, 5H, H^{21-25}), 5.16 (q, $J = 12.2$ Hz, 2H, H^{19}), 5.17 – 5.14 (m, 1H, H^{12}), 4.20 (d, $J = 4.4$ Hz, 1H, H^{4a}), 4.17 (d, $J = 4.1$ Hz, 1H, H^{6a}), 3.68 – 3.57 (m, 2H, H^{4b} & $6b$), 1.95 – 1.80 (m, 1H, H^{13a}), 1.77 (ddd, $J = 13.0, 6.5, 1.5$ Hz, 1H, H^{14}), 1.73 – 1.62 (m, 1H, H^{13b}), 1.42 (s, 3H, H^8), 1.36 (s, 3H, H^9), 1.21 (s, 3H, H^7), 0.94 (d, $J = 6.4$ Hz, 3H, H^{15}), 0.92 (d, $J = 6.5$ Hz, 3H, H^{16}).

^{13}C NMR (101 MHz, CDCl_3) δ 173.91 (s, C^{10}), 170.47 (s, C^{17}), 135.38 (s, C^{20}), 128.73 (s, C^{22} & C^{24}), 128.58 (s, C^{23}), 128.44 (s, C^{21} & C^{25}), 98.21 (s, C^2), 71.19 (s, C^{12}), 67.17 (s, C^{19}), 66.06 (s, C^4), 65.91 (s, C^6), 41.92 (s, C^5), 39.57 (s, C^{13}), 24.80 (s, C^{15}), 24.32 (s, C^{16}), 23.21 (s, C^8), 21.48 (s, C^9), 18.51 (s, C^7).

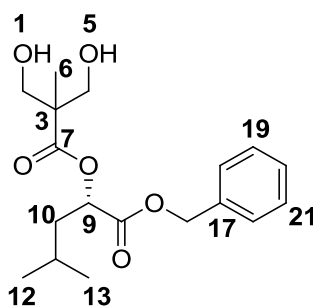
IR (ν_{max} / cm^{-1}) 2963, 1735, 1456, 1370, 1260, 1200, 1122, 1083, 832, 752.

HR-MS: Calculated for $\text{C}_{21}\text{H}_{30}\text{NaO}_6$ ($\text{M}+\text{Na}^+$) 401.1940, Found 401.1940 ($\text{M}+\text{Na}^+$) m/z.

Elemental Analysis: Calculated for $\text{C}_{21}\text{H}_{30}\text{O}_6$ C = 66.65, H = 7.99; Found C = 66.93, H = 8.15.

$[\alpha]_D^{22} = -26.12$ ($0.026 \text{ g}\cdot\text{mL}^{-1}$ in CHCl_3)

6.4.9 (S)-Benzyl 2-(3-hydroxy-2-(hydroxymethyl)-2-methylpropanoyloxy)-4-methylpentanoate



To a dried round-bottomed flask was added (S)-1-(benzyloxy)-4-methyl-1-oxopentan-2-yl 2,2,5-trimethyl-1,3-dioxane-5-carboxylate (34.54 g, 91.33 mmol), this was dissolved in methanol (400 mL) before the addition of pre-washed DOWEX HCR-W2 (70.0 g). Reaction was stirred at room temperature for 48 hours before the DOWEX was removed *via* filtration and the filtrate concentrated under reduced pressure to yield a clear, colourless oil which required no further purification (28.54 g, 84.39 mmol, 92%).

¹H NMR (400 MHz, CDCl₃) δ 7.41 – 7.31 (m, 1H, *H*¹⁸⁻²²), 5.24 (dd, *J* = 9.8, 3.5 Hz, 2H, *H*¹⁶), 5.18 (dd, *J* = 32.8, 12.2 Hz, 1H, *H*⁹), 3.90 (td, *J* = 12.6, 4.2 Hz, 1H, *H*^{3a & 4a}), 3.69 (ddd, *J* = 19.5, 11.3, 7.6 Hz, 2H, *H*^{3b & 4b}), 2.99 – 2.91 (m, 1H, *H*¹), 2.82 (t, *J* = 6.3 Hz, 1H, *H*⁵), 1.88 – 1.79 (m, 2H, *H*^{10a & 11}), 1.72 (dtd, *J* = 12.3, 8.3, 4.9 Hz, 1H, *H*^{10b}), 1.16 (s, 3H, *H*⁶), 0.93 (t, *J* = 6.1 Hz, 6H, *H*^{12 & 13}).

¹³C NMR (101 MHz, CDCl₃) δ 175.45 (s, *C*⁷), 171.48 (s, *C*¹⁴), 134.99 (s, *C*¹⁷), 128.81 (s, *C*^{19 & 21}), 128.56 (s, *C*^{18,20 & 22}), 71.05 (s, *C*⁹), 67.75 (s, *C*⁴), 67.69 (s, *C*²), 67.38 (s, *C*¹⁶), 50.25 (s, *C*³), 39.48 (s, *C*¹⁰), 24.93 (s, *C*¹¹), 23.15 (s, *C*¹³), 21.58 (s, *C*¹²), 16.92 (s, *C*⁶).

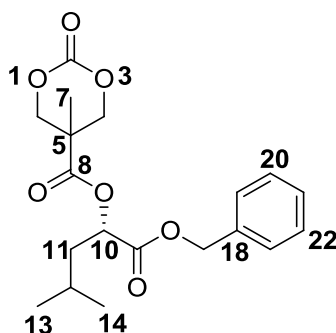
IR (*v*_{max} / cm⁻¹) 3470, 2954, 1728, 1458, 1383, 1197, 1118, 1036, 754.

HR-MS: Calculated for C₁₈H₂₇O₆ (M+H⁺) 339.1808, Found 339.1798 (M+H⁺) m/z.

Elemental Analysis: Calculated for C₁₈H₂₆O₆ C = 63.89, H = 7.74; Found C = 62.62, H = 7.70.

$[\alpha]_D^{22} = -0.62$ (0.064 g.mL⁻¹ in CHCl₃)

6.4.10 (S)-1-(Benzyloxy)-4-methyl-1-oxopentan-2-yl 5-methyl-2-oxo-1,3-dioxane-5-carboxylate



To a dried Schlenk flask was added (*S*)-benzyl 2-(3-hydroxy-2-(hydroxymethyl)-2-methylpropanoyloxy)-4-methylpentanoate (5.50 g, 16.25 mmol, 1.0 eq.) and the atmosphere

exchanged *via* repeatedly evacuating and back-filling with nitrogen before the addition of anhydrous tetrahydrofuran (250 mL) and pyridine (15.77 mL, 195.04 mmol, 12.0 eq.). The stirring solution was cooled to 0 °C and cooling maintained during the careful addition of triphosgene (4.82 g, 16.25 mmol, 1.0 eq.) as an anhydrous tetrahydrofuran solution (50 mL). The reaction was allowed to warm to room temperature and stirred overnight. The resulting precipitate was removed *via* filtration and the filtrate concentrated under reduced pressure to yield a clear, colourless oil which was redissolved in dichloromethane (400 mL) before being washed with 2M aqueous hydrochloric acid (2 × 250 mL) and saturated aqueous ammonium chloride (250 mL). The dichloromethane layer was isolated, dried over anhydrous magnesium sulfate, filtered and concentrated under reduced pressure to yield a pale yellow oil which crystallised on standing. The product was purified by recrystallisation from diethyl ether (3.73 g, 10.24 mmol, 63%).

¹H NMR (400 MHz, CDCl₃) δ 7.41 – 7.30 (m, 5H, *H*¹⁹⁻²³), 5.20 (d, *J* = 12.1 Hz, 1H, *H*^{17a}), 5.18 (dd, *J* = 8.9, 4.3 Hz, 1H, *H*¹⁰), 5.13 (d, *J* = 12.1 Hz, 1H, *H*^{17b}), 4.69 (dd, *J* = 5.5, 1.9 Hz, 1H, *H*^{4a}), 4.66 (dd, *J* = 5.5, 1.9 Hz, 1H, *H*^{6a}), 4.19 (dd, *J* = 10.8, 5.4 Hz, 2H, *H*^{4b & 6b}), 1.89 – 1.78 (m, 1H, *H*^{11a}), 1.78 – 1.66 (m, 2H, *H*^{11b & 12}), 1.34 (s, 3H, *H*⁷), 0.94 (d, *J* = 6.2 Hz, 3H, *H*¹³), 0.91 (d, *J* = 6.1 Hz, 3H, *H*¹⁴).

¹³C NMR (101 MHz, CDCl₃) δ 170.88 (s, *C*⁸), 169.68 (s, *C*¹⁵), 147.40 (s, *C*²), 135.10 (s, *C*¹⁸), 128.81 (s, *C*^{20 & 22}), 128.60 (s, *C*^{19,21 & 23}), 73.05 (s, *C*¹⁰), 72.76 (s, *C*⁴), 72.42 (s, *C*⁶), 67.56 (s, *C*¹⁷), 39.37 (s, *C*¹¹), 24.89 (s, *C*¹²), 23.10 (s, *C*¹⁴), 21.56 (s, *C*¹³), 17.60 (s, *C*⁷).

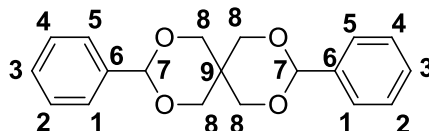
HR-MS: Calculated for C₁₉H₂₅O₇ (M+H⁺) 365.1600, Found 365.1594 (M+H⁺) m/z.

Elemental Analysis: Calculated for C₁₉H₂₄O₇ C = 62.63, H = 6.64; Found C = 62.33, H = 6.77.

$[\alpha]_D^{22} = -0.76$ (0.083 g.mL⁻¹ in CHCl₃)

Melting Point = 85.1 °C

6.4.11 3,9-Diphenyl-2,4,8,10-tetraoxaspiro[5.5]undecane



To a round-bottomed flask was added pentaerythritol (20.17 g, 148.15 mmol, 1.0 eq.) and *p*-toluenesulfonic acid monohydrate (2.82 g, 14.82 mmol, 0.1 eq.) and these were suspended in toluene (500 mL) before the addition of benzaldehyde (75.3 mL, 740.73 mmol, 5.0 eq.). The reaction was fitted with a Dean-Stark condenser and heated to reflux before being allowed to stir overnight with the continual removal of water. The reaction was stopped and cooled to room temperature before the removal of solvent under reduced pressure to yield a brown solution from which crystals developed when allowed to stand overnight. The resulting pale brown crystals were isolated *via* filtration before being sequentially rinsed with copious amounts of *n*-hexane and ethanol to yield fine white needles. Finally these needles were dried under reduced pressure (38.84 g, 124.40 mmol, 84%). Characterisation data in agreement with those reported in the literature.¹²²

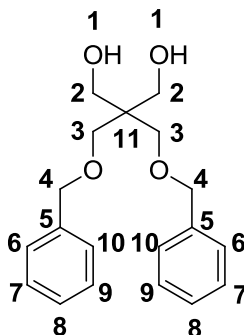
¹H NMR (400 MHz, CDCl₃) δ 7.49 (td, *J* = 7.7, 3.5 Hz, 4H, *H*^{1 & 5}), 7.42 – 7.32 (m, 6H, *H*²⁻⁴), 5.47 (s, 2H, *H*⁷), 4.89 (dd, *J* = 11.5, 2.3 Hz, 2H, *H*⁸), 3.86 (d, *J* = 11.6 Hz, 2H, *H*⁸), 3.84 (dd, *J* = 11.6, 2.6 Hz, 2H, *H*⁸), 3.67 (d, *J* = 11.6 Hz, 2H, *H*⁸).

¹³C NMR (101 MHz, CDCl₃) δ 138.07 (s, *C*⁷), 129.25 (s, *C*^{2 & 4}), 128.49 (s, *C*³), 126.20 (s, *C*^{1 & 5}), 102.43 (s, *C*⁷), 71.22 (s, *C*⁸), 70.76 (s, *C*⁸), 32.64 (s, *C*⁹).

HR-MS: Calculated for C₁₉H₂₁O₄ (M+H⁺) 313.1440, Found 313.1445 (M+H⁺) m/z.

Melting Point = 159.6 °C

6.4.12 2,2-bis((Benzyloxy)methyl)propane-1,3-diol



To a dried Schlenk flask was added 3,9-diphenyl-2,4,8,10-tetraoxaspiro[5.5]undecane (9.99 g, 31.99 mmol, 1.0 eq.) and the atmosphere exchanged *via* repeatedly evacuating and back-filling with nitrogen before the addition of anhydrous dichloromethane (200 mL). The stirring solution was cooled to 0 °C before the dropwise addition of a 1.0 M solution of diisobutylaluminum hydride in hexanes (96.0 mL, 96.00 mmol, 3.0 eq.). Once addition was complete the reaction was allowed to warm to room temperature before being left to stir for 14 hours. The reaction solution was again cooled to 0 °C before being quenched by the careful addition of methanol (50 mL) and further addition of a 10% aqueous sodium hydroxide solution (200 mL). Reaction was warmed to room temperature before being allowed to stir vigorously for a further 8 hours. The reaction was stopped, the layers separated and the aqueous layer repeatedly washed with diethyl ether (3 × 300 mL). The ether and dichloromethane portions were combined and dried over anhydrous magnesium sulfate before being filtered and the solvent removed under reduced pressure to yield a white solid. Crude product was crystallised from 1:1 water ethanol, the resulting crystals were isolated and dried under reduced pressure (9.01 g, 28.47 mmol, 89%).¹²³

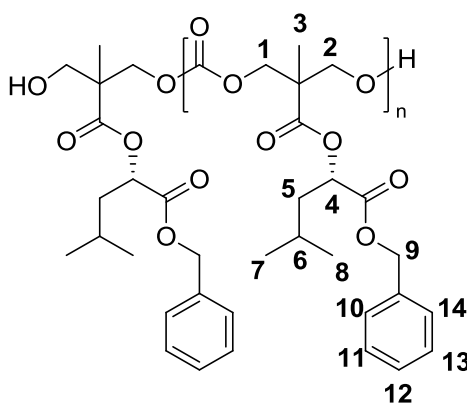
¹H NMR (400 MHz, CDCl₃) δ 7.40 – 7.26 (m, 10H, *H*⁶⁻¹⁰), 4.50 (s, 4H, *H*⁴), 3.70 (s, 4H, *H*³), 3.57 (s, 4H, *H*²), 2.69 (s, 2H, *H*¹).

^{13}C NMR (101 MHz, CDCl_3) δ 137.99 (s, C^{10}), 128.58 (s, $\text{C}^{7 \& 9}$), 127.90 (s, C^8), 127.67 (s, $\text{C}^6 \& 10$), 73.82 (s, C^3), 72.01 (s, C^4), 65.02 (s, C^2), 45.06 (s, C^{11}).

HR-MS: Calculated for $\text{C}_{19}\text{H}_{24}\text{NaO}_4$ ($\text{M}+\text{Na}^+$) 339.1572, Found 339.1572 ($\text{M}+\text{Na}^+$) m/z.

Melting Point = 71.3 °C

6.4.13 General procedure for the polymerisation of (*S*)-1-(benzyloxy)-4-methyl-1-oxopentan-2-yl 5-methyl-2-oxo-1,3-dioxane-5-carboxylate ($[M]_0/[I]_0 = 20$)



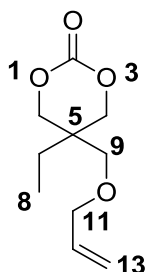
Within a glovebox, (*S*)-1-(benzyloxy)-4-methyl-1-oxopentan-2-yl 5-methyl-2-oxo-1,3-dioxane-5-carboxylate (45.5 mg, 124.87 μmol , 20 eq.) was dissolved in deuterated chloroform (472 μL) before the addition of 4-methoxybenzyl alcohol (8.63 μL of a 100 $\text{mg}\cdot\text{mL}^{-1}$ CDCl_3 solution; 6.24 μmol , 1.0 eq.) and 1,8-diazabicyclo[5.4.0]undec-7-ene (19.01 μL of a 100 $\text{mg}\cdot\text{mL}^{-1}$ CDCl_3 solution; 12.48 μmol , 2.0 eq.). The reaction solution was transferred to a Young's tap NMR tube and monitored *via* ^1H NMR spectroscopy. Once conversion reached equilibrium the reaction was stopped and the DBU catalyst removed *via* stirring with Amberlyst 15 acidic resin in dichloromethane solution before filtration. The solvent was removed under reduced pressure before being redissolved in dichloromethane (0.5 mL) and precipitated into cooled n-hexane (20 mL). The polymer was isolated and dried under reduced pressure to yield a viscous clear oil (30.1 mg, 66%).

^1H NMR (400 MHz, CDCl_3) δ 7.39 – 7.27 (m, H^{10-14}), 5.22 – 5.06 (m, $H^4 \ \& \ 9$), 4.36 – 4.22 (m, $H^1 \ \& \ 2$), 1.85 – 1.74 (m, H^{5a}), 1.73 – 1.57 (m, $H^{5b \ \& \ 6}$), 1.24 (s, H^3), 0.97 – 0.79 (m, $H^7 \ \& \ 8$).

GPC (CHCl_3 ; RI): M_n (\mathcal{D}) = 4911 $\text{g}\cdot\text{mol}^{-1}$ (1.11)

6.5 Experimental Details for Chapter 4

6.5.1 5-((Allyloxy)methyl)-5-ethyl-1,3-dioxan-2-one



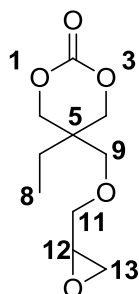
To a round-bottomed flask was added trimethylolpropane allyl ether (100.34 g, 576.24 mmol, 1.0 eq.) and this was dissolved in anhydrous tetrahydrofuran (900 mL) before the addition of ethyl chloroformate (110.19 mL, 1152.47 mmol, 2.0 eq.). The stirring reaction mixture was cooled to 0 °C and cooling maintained throughout the slow addition of triethylamine (160.63 mL, 1152.47 mmol 2.0 eq.) in anhydrous tetrahydrofuran (500 mL). Once addition was complete, the reaction was allowed to stir overnight at room temperature. The reaction was stopped and the resulting white precipitate removed *via* filtration and the filtrate concentrated under reduced pressure to yield a clear, pale brown oil. This crude oil was redissolved in dichloromethane (500 mL) before being sequentially washed with 1 M aqueous hydrochloric acid solution (2 × 250 mL) and deionised water (250 mL). The dichloromethane layer was isolated, dried over anhydrous magnesium sulfate and filtered before the filtrate was concentrated under reduced pressure to yield a pale brown oil. This crude mixture was purified *via* distillation under reduced pressure (140 °C, 0.3 Torr) to yield a clear, colourless oil (65.72 g, 328.44 mmol, 57%). Characterisation data in agreement with those reported in literature.⁹⁹

¹H NMR (400 MHz, CDCl₃) δ 5.84 (ddd, *J* = 22.8, 10.8, 5.6 Hz, 1H, *H*¹²), 5.28 – 5.15 (m, 2H, *H*¹³), 4.32 (d, *J* = 10.9 Hz, 2H, *H*^{4a} & ^{6a}), 4.12 (d, *J* = 10.9 Hz, 2H, *H*^{4b} & ^{6b}), 3.96 (d, *J* = 5.6 Hz, 2H, *H*¹¹), 3.38 (s, 2H, *H*⁹), 1.51 (q, *J* = 7.6 Hz, 2H, *H*⁷), 0.90 (t, *J* = 7.6 Hz, 3H, *H*⁸).

¹³C NMR (101 MHz, CDCl₃) δ 148.64 (s, *C*²), 134.08 (s, *C*¹²), 117.63 (s, *C*¹³), 72.89 (s, *C*⁴ & ⁶), 72.54 (s, *C*¹¹), 68.31 (s, *C*⁹), 35.56 (s, *C*⁵), 23.43 (s, *C*⁷), 7.47 (s, *C*⁸).

HR-MS: Calculated for C₁₀H₁₆NaO₄ (M+Na⁺) 223.0946, Found 223.0949 (M+Na⁺) m/z.

6.5.2 5-Ethyl-5-((oxiran-2-ylmethoxy)methyl)-1,3-dioxan-2-one



To a round-bottomed flask was added *m*-chloroperoxybenzoic acid (70 wt.%, 15.84 g, 64.24 mmol, 1.4 eq.) and this was dissolved in dichloromethane (300 mL) before the addition of 5-((allyloxy)methyl)-5-ethyl-1,3-dioxan-2-one (9.18 g, 45.89 mmol, 1.0 eq.) in dichloromethane solution (100 mL). The reaction was allowed to stir at room temperature overnight before being quenched by the addition of solid potassium carbonate (9 g), leading to the production of a large quantity of white precipitate. The quenched reaction mixture was washed sequentially with 10 wt.% aqueous sodium hydrogen carbonate solution (3 × 150 mL) and saturated brine (150 mL). The dichloromethane layer was isolated, dried over anhydrous magnesium sulfate and filtered before the filtrate was concentrated under reduced pressure to yield a clear, colourless oil. The crude oil was purified *via* column

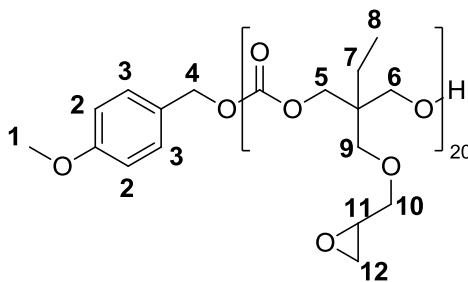
chromatography (Diethyl ether, $R_f = 0.34$) to yield a clear, colourless oil (8.64 g, 22.11 mmol, 48%). Characterisation data in agreement with those reported in literature.⁹⁹

¹H NMR (400 MHz, CDCl₃) δ 4.36 – 4.28 (m, 2H, H^{4a} & $6a$), 4.13 (dd, $J = 10.8, 1.9$ Hz, 2H, H^{4b} & $6b$), 3.80 (dd, $J = 11.8, 2.5$ Hz, 1H, H^{11a}), 3.53 (d, $J = 9.7$ Hz, 1H, H^{9a}), 3.45 (d, $J = 9.7$ Hz, 1H, H^{9b}), 3.33 (dd, $J = 11.8, 6.1$ Hz, 1H, H^{11b}), 3.11 (td, $J = 6.4, 2.7$ Hz, 1H, H^{12}), 2.79 (t, $J = 4.6$ Hz, 1H, H^{13a}), 2.57 (dd, $J = 4.9, 2.7$ Hz, 1H, H^{13b}), 1.52 (q, $J = 7.5$ Hz, 2H, H^7), 0.91 (t, $J = 7.6$ Hz, 3H, H^8).

¹³C NMR (101 MHz, CDCl₃) δ 148.60 (s, C^2), 72.84 (s, C^4), 72.77 (s, C^6), 72.40 (s, C^{11}), 69.88 (s, C^9), 50.77 (s, C^{12}), 43.93 (s, C^{13}), 35.72 (s, C^5), 23.48 (s, C^7), 7.52 (s, C^8).

HR-MS: Calculated for C₁₀H₁₇O₅ (M+H⁺) 217.1076, Found 217.1074 (M+H⁺) m/z; Calculated for C₁₀H₁₆NaO₅ (M+Na⁺) 239.0895, Found 239.0891 (M+Na⁺) m/z.

6.5.3 General procedure for the polymerisation of Ethyl-5-((oxiran-2-ylmethoxy)methyl)-1,3-dioxan-2-one ([M]₀/[I]₀ = 20)



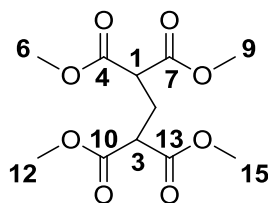
Within a glovebox, 5-ethyl-5-((oxiran-2-ylmethoxy)methyl)-1,3-dioxan-2-one (109.0 mg, 504.33 μ mol, 1.0 eq.) was dissolved in deuterated chloroform (395 μ L) before the addition of 4-methoxybenzyl alcohol (34.8 μ L of a 100 mg.mL⁻¹ CDCl₃ solution; 25.22 μ mol, 0.05 eq.) and 1,5,7-triazabicyclo[4.4.0]dec-5-ene (70.2 μ L of a 10 mg.mL⁻¹ CDCl₃ solution; 5.04 μ mol, 0.01 eq.). The reaction solution was transferred to a Young's tap NMR tube and

monitored *via* ^1H NMR spectroscopy. Once conversion reached equilibrium (72.2% after 20 minutes) the reaction was stopped by removal of TBD catalyst *via* elution through a short silica column using diethyl ether to removal residual monomer (20 mL) and subsequent elution with ethyl acetate (10 mL) to yield poly(ethyl-5-((oxiran-2-ylmethoxy)methyl)-1,3-dioxan-2-one)₂₀ as a viscous liquid (67.6 mg, 62%)

^1H NMR (400 MHz, CDCl_3) δ 7.33 – 7.30 (m, H^3), 6.89 – 6.86 (m, H^2), 5.07 (s, H^4), 4.09 (s, $J = 3.9$ Hz, H^5 & 6), 3.72 – 3.66 (m, H^{10a}), 3.49 – 3.41 (m, H^{9a}), 3.38 – 3.30 (m, H^{9b} & $10b$), 3.08 (ddt, $J = 5.7, 4.0, 2.8$ Hz, H^{11}), 2.77 – 2.73 (m, H^{12a}), 2.56 (dd, $J = 5.0, 2.7$ Hz, H^{12b}), 1.47 (q, $J = 7.5$ Hz, H^7), 0.87 (t, $J = 7.5$ Hz, H^8).

GPC (CHCl_3 ; RI): M_n (D) = 4058 $\text{g}\cdot\text{mol}^{-1}$ (1.17)

6.5.4 Tetramethyl propane-1,1,3,3-tetracarboxylate



To a round-bottomed flask was added dimethyl malonate (494.97 g, 3746.51 mmol, 4.0 eq.) and paraformaldehyde (28.13 g, 936.63 mmol, 1.0 eq.). This suspension was heated to 60 °C before the addition of a 10 wt.% solution of potassium hydroxide in ethanol (8 mL, 14.06 mmol, 0.015 eq.). The reaction flask was fitted with a condenser before being heated to 95 °C overnight. Reaction was stopped and excess dimethyl malonate was removed under reduced pressure before the addition of dichloromethane (1 L). The resulting precipitate was removed *via* filtration and the filtrate concentrated under reduced pressure to yield a clear, colourless oil which crystallised upon standing to yield a crystalline white solid (215.13 g, 778.71 mmol, 83%). Characterisation data in agreement with those reported in literature.⁹⁴

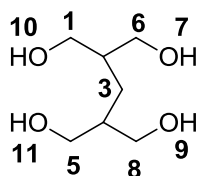
$^1\text{H NMR}$ (400 MHz, CDCl_3) δ 3.64 (s, 12H, $H^{6,9,12 \text{ \& } 15}$), 3.40 (t, $J = 7.4$ Hz, 2H, $H^1 \text{ \& } 3$), 2.36 (t, $J = 7.4$ Hz, 2H, H^2).

$^{13}\text{C NMR}$ (101 MHz, CDCl_3) δ 168.80 (s, $C^{4,7,10,13}$), 52.60 (s, $C^{6,9,12 \text{ \& } 15}$), 48.89 (s, $C^1 \text{ \& } 3$), 27.27 (s, C^2).

HR-MS: Calculated for $\text{C}_{11}\text{H}_{16}\text{NaO}_8$ ($\text{M}+\text{Na}^+$) 299.0743, Found 299.0738 ($\text{M}+\text{Na}^+$) m/z.

Melting Point = 44.9 °C

6.5.5 2,4-Bis(hydroxymethyl)pentane-1,5-diol



A three-neck round-bottomed flask was purged with nitrogen before the addition of lithium aluminium hydride (30.08 g, 796.24 mmol, 4.0 eq.). This was cooled to 0 °C and cooling was maintained throughout the addition of anhydrous tetrahydrofuran (800 mL) *via* cannula - vigorous stirring was required to maintain a free-flowing suspension. Once addition was complete, a similarly prepared solution of tetramethyl propane-1,1,3,3-tetracarboxylate (54.74 g, 198.16 mmol, 1.0 eq.) in anhydrous tetrahydrofuran (200 mL) was added dropwise *via* cannula, cooling was again maintained throughout addition. Upon complete addition, the reaction mixture was fitted with a condenser and heated to reflux overnight. The reaction was then stopped and cooled to 0 °C before careful quenching by slow sequential addition of deionised water (27 mL), 15 wt.% aqueous sodium hydroxide solution (27 mL) and further deionised water (54 mL). The resulting mixture was filtered under reduced pressure and rinsed sparingly with cold tetrahydrofuran to yield a white solid. This crude mixture was extracted overnight *via* a Soxhlet apparatus using tetrahydrofuran (800 mL).

Extraction was stopped and cooled to room temperature before removal of the solvent under reduced pressure to yield a white solid. This was rinsed with further cold tetrahydrofuran before being dried overnight under reduced pressure (16.74 g, 101.95 mmol, 51%). Characterisation data in agreement with those reported in literature.⁹⁴

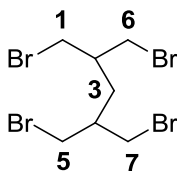
¹H NMR (400 MHz, MeOD) δ 3.57 (d, $J = 5.7$ Hz, 8H, $H^{1,5,6 \& 8}$), 1.81 – 1.66 (m, 2H, $H^{2 \& 3}$), 1.29 (t, $J = 6.9$ Hz, 2H, H^3).

¹³C NMR (101 MHz, MeOD) δ 64.00 (s, $C^{1,5,6 \& 8}$), 41.83 (s, $C^{2 \& 3}$), 27.41 (s, C^3).

HR-MS: Calculated for C₇H₁₆NaO₄ (M+Na⁺) 187.0946, Found 187.0939 (M+Na⁺) m/z.

Melting Point = 129.4 - 131.7 °C (130.1 °C)

6.5.6 1,5-Dibromo-2,4-bis(bromomethyl)pentane



To a dried round-bottomed flask was added 2,4-bis(hydroxymethyl)pentane-1,5-diol (18.71 g, 113.95 mmol, 1.0 eq.) and this was placed under a nitrogen atmosphere and fitted with an aqueous sodium hydroxide bubbler on the gas exhaust. The stirring solid was heated to 80 °C before the careful dropwise addition of phosphorous tribromide (21.42 mL, 227.89 mmol, 2.0 eq.) - this led to the vigorous production of hydrogen bromide vapours. The orange reaction mixture was heated to 100 °C and allowed to stir overnight before cooling to room temperature. The cooled reaction mixture was quenched by the careful addition of deionised water (90 mL) before extraction with dichloromethane (3 × 200 mL). The dichloromethane layers were combined, dried over anhydrous magnesium sulfate, filtered and solvent

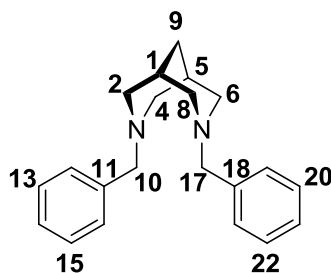
removed under reduced pressure to yield a clear colourless oil which crystallised on standing. The crude product was purified *via* column chromatography (Dichloromethane, $R_f = 0.96$) to yield a white crystalline solid (7.67 g, 18.46 mmol, 16%). Characterisation data in agreement with those reported in literature.⁹⁴

$^1\text{H NMR}$ (400 MHz, CDCl_3) δ 3.61 (dd, $J = 10.5, 4.0$ Hz, 4H, $H^{1a,5a,6a \ \& \ 7a}$), 3.46 (dd, $J = 10.5, 6.2$ Hz, 4H, $H^{1b,5b,6b \ \& \ 7b}$), 2.13 – 2.03 (m, 2H, $H^2 \ \& \ 4$), 1.64 (t, $J = 7.0$ Hz, 2H, H^3).

$^{13}\text{C NMR}$ (101 MHz, CDCl_3) δ 38.99 (s, $C^2 \ \& \ 4$), 35.59 (s, $C^{1,5,6 \ \& \ 7}$), 33.69 (s, C^3).

Melting Point = 41.7 °C

6.5.7 (1S,5S)-3,7-Dibenzyl-3,7-diazabicyclo[3.3.1]nonane



To a dried ampoule was added 1,5-dibromo-2,4-bis(bromomethyl)pentane (7.76 g, 18.66 mmol, 1.0 eq.) and the atmosphere exchanged for nitrogen before the addition of anhydrous toluene (60 mL) and benzylamine (12.22 mL, 111.98 mmol, 6.0 eq.). The ampoule was sealed and the stirring solution heated to reflux (120 °C) before being allowed to stir for three days. The reaction was stopped, the toluene washed with 15 wt.% aqueous sodium hydroxide solution (100 mL) before the aqueous layer was re-extracted with fresh toluene (3 \times 100 mL). The organic phases were combined, dried over anhydrous magnesium sulfate, filtered and concentrated under reduced pressure to yield a pale yellow oil. The crude product was purified *via* column chromatography using dichloromethane with 10%

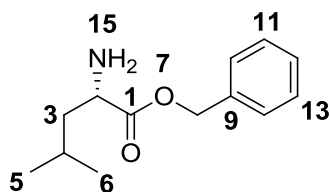
methanol as eluent to remove impurities before elution of the desired pure product using dichloromethane with 10% methanol and 10% triethylamine. Removal of the solvent under reduced pressure gave a clear colourless oil (1.66 g, 5.41 mmol, 29%). Characterisation data in agreement with those reported in literature.⁹⁴

¹H NMR (400 MHz, CDCl₃) δ 7.46 (d, *J* = 7.5 Hz, 4H, *H*^{12,16,19 & 23}), 7.34 (t, *J* = 7.5 Hz, 4H, *H*^{13,15,20 & 22}), 7.26 (t, *J* = 7.2 Hz, 2H, *H*^{14 & 21}), 3.50 (s, 4H, *H*^{10 & 17}), 2.82 (d, *J* = 10.7 Hz, 4H, *H*^{2a,4a,6a & 8a}), 2.36 (dd, *J* = 10.8, 4.0 Hz, 4H, *H*^{2b,4b,6b & 8b}), 1.91 (m, 2H, *H*^{1 & 5}), 1.57 (t, *J* = 2.9 Hz, 2H, *H*⁹).

¹³C NMR (101 MHz, CDCl₃) δ 139.99 (s, *C*^{11 & 18}), 128.99 (s, *C*^{12,16,19 & 23}), 128.18 (s, *C*^{13,15,20 & 22}), 126.64 (s, *C*^{14 & 21}), 63.51 (s, *C*^{10 & 17}), 58.08 (s, *C*^{2,4,6 & 8}), 31.11 (s, *C*⁹), 30.01 (s, *C*^{1 & 5}).

HR-MS: Calculated for C₂₁H₂₇N₇ (M+H⁺) 307.2174, Found 307.2167 (M+H⁺) m/z.

6.5.8 (S)-benzyl 2-amino-4-methylpentanoate



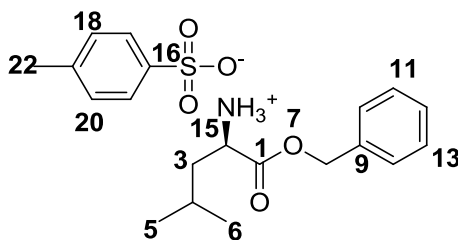
To a round-bottomed flask was added (S)-1-(benzyloxy)-4-methyl-1-oxopentan-2-aminium 4-methylbenzenesulfonate (10.08 g, 45.55 mmol, 1.0 eq.) and this was dissolved in 1.0 M aqueous sodium carbonate solution (250 mL) and allowed to stir for 1 hour before being stopped and washed with ethyl acetate (3 × 150 mL). The ethyl acetate portions were isolated and combined before being washed with deionised water (2 × 100 mL). The ethyl acetate layer was again isolated, dried over anhydrous magnesium sulfate, filtered and the

the solvent removed under reduced pressure to yield a clear colourless oil (7.35 g, 33.25 mmol, 73%).

$^1\text{H NMR}$ (400 MHz, CDCl_3) δ 7.40 – 7.30 (m, 5H, H^{10-14}), 5.14 (s, 2H, H^8), 3.50 (dd, $J = 8.6, 5.7$ Hz, 1H, H^2), 1.82 – 1.66 (m, 3H, H^4 & 15), 1.58 (ddd, $J = 13.7, 8.1, 5.7$ Hz, 1H, H^{3a}), 1.48 – 1.38 (m, 1H, H^{3b}), 0.92 (d, $J = 8.3$ Hz, 3H, H^6), 0.90 (d, $J = 8.2$ Hz, 3H, H^5).

$^{13}\text{C NMR}$ (101 MHz, CDCl_3) δ 176.53 (s, C^1), 135.85 (s, C^9), 128.68 (s, C^{10} & 14), 128.42 (s, C^{12}), 128.32 (s, C^{11} & 13), 66.68 (s, C^8), 53.00 (s, C^2), 44.04 (s, C^3), 24.82 (s, C^4), 23.03 (s, C^6), 21.92 (s, C^5).

6.5.9 (*R*)-1-(benzyloxy)-4-methyl-1-oxopentane-2-aminium 4-methylbenzene sulfonate



To a round-bottomed flask was added *D*-leucine (25.65 g, 195.55 mmol, 1.0 eq.), *p*-toluenesulfonic acid monohydrate (39.06 g, 205.33 mmol, 1.05 eq.) and these were suspended in toluene (800 mL) before the addition of benzyl alcohol (40.47 mL, 391.10 mmol, 2.0 eq.). The flask was fitted with a Dean-Stark condenser and the stirring reaction mixture heated to reflux for 18 hours with the continual removal of isolated water. The reaction was stopped and diluted with diethyl ether before being cooled to room temperature, leading to a large quantity of white precipitate which was isolated *via* filtration and washed with further diethyl ether. The isolated solid was dried under reduced pressure to give a light, white powder (72.70 g, 184.79 mmol, 94%).

¹H NMR (400 MHz, D₆-DMSO) δ 8.37 (s, 2H, *H*¹⁵), 7.50 (d, *J* = 8.1 Hz, 2H, *H*^{17 & 21}), 7.44 – 7.30 (m, 5H, *H*¹⁰⁻¹⁴), 7.12 (d, *J* = 8.0 Hz, 2H, *H*¹⁸⁻²⁰), 5.23 (s, 2H, *H*⁸), 4.06 (t, *J* = 7.0 Hz, 1H, *H*²), 2.29 (s, 3H, *H*²²), 1.77 – 1.55 (m, 3H, *H*^{3 & 4}), 0.86 (d, *J* = 6.2 Hz, 6H, *H*^{5 & 6}).

¹³C NMR (101 MHz, D₆-DMSO) δ 169.79 (s, *C*¹), 145.46 (s, *C*¹⁶), 137.79 (s, *C*²¹), 135.12 (s, *C*⁹), 128.52 (s, *C*^{18 & 20}), 128.43 (s, *C*^{11 & 13}), 128.25 (s, *C*¹²), 128.10 (s, *C*^{10 & 14}), 125.50 (s, *C*^{17 & 21}), 67.14 (s, *C*⁸), 50.64 (s, *C*²), 39.15 (s, *C*³), 23.72 (s, *C*⁴), 22.03 (s, *C*⁵), 21.98 (s, *C*⁶), 20.79 (s, *C*²²).

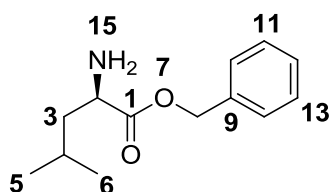
HR-MS: Anion – Calculated for C₇H₇O₃S⁻ (M⁻) 171.0121, Found 171.0122 m/z (M⁻);

Cation – Calculated for C₁₃H₂₀NO₂⁺ (M⁺) 222.1489, Found 222.1488 (M⁺) m/z.

[α]_D²² = -0.84 (95.2 mg.mL⁻¹ in MeOH)

Melting Point = 157.3 °C

6.5.10 (*R*)-benzyl 2-amino-4-methylpentanoate



To a round-bottomed flask was added (*R*)-1-(benzyloxy)-4-methyl-1-oxopentan-2-aminium 4-methylbenzenesulfonate (10.38 g, 46.90 mmol, 1.0 eq.) and this was dissolved in 1.0 M aqueous sodium carbonate solution (250 mL) and allowed to stir for 1 hour before being stopped and washed with ethyl acetate (3 × 150 mL). The ethyl acetate portions were isolated and combined before being washed with deionised water (2 × 100 mL). The ethyl acetate was again isolated, dried over anhydrous magnesium sulfate, filtered and the the

solvent removed under reduced pressure to yield a clear colourless oil (8.09 g, 36.58 mmol, 78%).

¹H NMR (400 MHz, CDCl₃) δ 7.40 – 7.32 (m, 5H, *H*¹⁰⁻¹⁴), 5.14 (s, 2H, *H*⁸), 3.50 (dd, *J* = 8.6, 5.7 Hz, 1H, *H*²), 1.81 – 1.70 (m, 1H, *H*⁴), 1.66 (s, 2H, *H*¹⁵), 1.58 (ddd, *J* = 13.7, 8.1, 5.7 Hz, 1H, *H*^{3a}), 1.47 – 1.39 (m, 1H, *H*^{3b}), 0.92 (d, *J* = 6.7 Hz, 3H, *H*⁶), 0.90 (d, *J* = 6.6 Hz, 3H, *H*⁵).

¹³C NMR (101 MHz, CDCl₃) δ 176.57 (s, *C*¹), 135.87 (s, *C*⁹), 128.69 (s, *C*^{10 & 14}), 128.42 (s, *C*¹²), 128.33 (s, *C*^{11 & 13}), 66.68 (s, *C*⁸), 53.03 (s, *C*²), 44.07 (s, *C*³), 24.83 (s, *C*⁴), 23.05 (s, *C*⁶), 21.93 (s, *C*⁵).

Chapter 7

References

-
- (1) Hayashi, T. *Progress in Polymer Science* **1994**, *19*, 663.
 - (2) Amass, W.; Amass, A.; Tighe, B. *Polymer International* **1998**, *47*, 89.
 - (3) Middleton, J. C.; Tipton, A. J. *Biomaterials* **2000**, *21*, 2335.
 - (4) Sinclair, R. G. *Journal of Macromolecular Science, Part A* **1996**, *33*, 585.
 - (5) Lourenço, A. V. *Ann. Chim. Phys.* **1863**, *67*.
 - (6) Carothers, W. H. *Journal of the American Chemical Society* **1929**, *51*, 2548.
 - (7) Carothers, W. H. *J. Am. Chem. Soc.* **1929**, *51*, 2560.
 - (8) Zhong, Z.; Ankoné, M. J. K.; Dijkstra, P. J.; Birg, C.; Westerhausen, M.; Feijen, J. *Polymer Bulletin* **2001**, *46*, 51.
 - (9) Kricheldorf, H. R.; Boettcher, C. *Die Makromolekulare Chemie* **1993**, *194*, 1665.
 - (10) Bero, M.; Dobrzyński, P.; Kasperczyk, J. *Journal of Polymer Science Part A: Polymer Chemistry* **1999**, *37*, 4038.
 - (11) Kasperczyk, J.; Bero, M. *Polymer* **2000**, *41*, 391.
 - (12) Kricheldorf, H. R.; Lee, S.-R. *Polymer* **1995**, *36*, 2995.
 - (13) Dumitrescu, A.; Martin-Vaca, B.; Gornitzka, H.; Cazaux, J.-B.; Bourissou, D.; Bertrand, G. *European Journal of Inorganic Chemistry* **2002**, *2002*, 1948.
 - (14) Finne, A.; Reema; Albertsson, A.-C. *Journal of Polymer Science Part A: Polymer Chemistry* **2003**, *41*, 3074.
 - (15) Kricheldorf, H. R.; Boettcher, C. *Journal of Macromolecular Science, Part A* **1993**, *30*, 441.
 - (16) Hsieh, K.-C.; Lee, W.-Y.; Hsueh, L.-F.; Lee, H. M.; Huang, J.-H. *European Journal of Inorganic Chemistry* **2006**, *2006*, 2306.
 - (17) Frederick, M. O.; Mulder, J. A.; Tracey, M. R.; Hsung, R. P.; Huang, J.; Kurtz, K. C. M.; Shen, L.; Douglas, C. J. *J. Am. Chem. Soc.* **2003**, *125*, 2368.
 - (18) Chamberlain, B. M.; Sun, Y.; Hagadorn, J. R.; Hemmesch, E. W.; Young, V. G.; Pink, M.; Hillmyer, M. A.; Tolman, W. B. *Macromolecules* **1999**, *32*, 2400.
 - (19) Zhang, J.; Gan, Z.; Zhong, Z.; Jing, X. *Polymer International* **1998**, *45*, 60.
 - (20) Zhang, L.; Shen, Z.; Yu, C.; Fan, L. *Polymer International* **2004**, *53*, 1013.
 - (21) Coulembier, O.; Dove, A. P.; Pratt, R. C.; Sentman, A. C.; Culkin, D. A.; Mespouille, L.; Dubois, P.; Waymouth, R. M.; Hedrick, J. L. *Angewandte Chemie International Edition* **2005**, *44*, 4964.
 - (22) Connor, E. F.; Nyce, G. W.; Myers, M.; Möck, A.; Hedrick, J. L. *Journal of the American Chemical Society* **2002**, *124*, 914.
 - (23) Pratt, R. C.; Lohmeijer, B. G. G.; Long, D. A.; Lundberg, P. N. P.; Dove, A. P.; Li, H.; Wade, C. G.; Waymouth, R. M.; Hedrick, J. L. *Macromolecules* **2006**, *39*, 7863.
-

-
- (24) Pratt, R. C.; Lohmeijer, B. G. G.; Long, D. A.; Waymouth, R. M.; Hedrick, J. L. *Journal of the American Chemical Society* **2006**, *128*, 4556.
- (25) Dove, A. P.; Pratt, R. C.; Lohmeijer, B. G. G.; Waymouth, R. M.; Hedrick, J. L. *Journal of the American Chemical Society* **2005**, *127*, 13798.
- (26) Carothers, W. H.; Van Natta, F. J. *J. Am. Chem. Soc.* **1929**, *52*, 314.
- (27) Gross, S. M.; Flowers, D.; Roberts, G.; Kiserow, D. J.; DeSimone, J. M. *Macromolecules* **1999**, *32*, 3167.
- (28) Inoue, S.; Koinuma, H.; Tsuruta, T. *Journal of Polymer Science Part B: Polymer Letters* **1969**, *7*, 287.
- (29) Kember, M. R.; Buchard, A.; Williams, C. K. *Chemical Communications* **2011**, 47, 141.
- (30) Darensbourg, D. J.; Moncada, A. I.; Choi, W.; Reibenspies, J. H. *Journal of the American Chemical Society* **2008**, *130*, 6523.
- (31) Koinuma, H.; Hirai, H. *Makromol. Chem.* **1977**, *178*, 241.
- (32) Baba, A.; Kashiwagi, H.; Matsuda, H. *Organometallics* **1987**, *6*, 137.
- (33) Chen, X.; Gross, R. A. *Macromolecules* **1998**, *32*, 308.
- (34) Kricheldorf, H. R.; Damrau, D.-O. *Macromolecular Chemistry and Physics* **1997**, *198*, 1767.
- (35) Kamber, N. E.; Jeong, W.; Waymouth, R. M.; Pratt, R. C.; Lohmeijer, B. G. G.; Hedrick, J. L. *Chemical Reviews* **2007**, *107*, 5813.
- (36) Myers, M.; Connor, E. F.; Glauser, T.; Möck, A.; Nyce, G.; Hedrick, J. L. *Journal of Polymer Science Part A: Polymer Chemistry* **2002**, *40*, 844.
- (37) Nederberg, F.; Connor, E. F.; Möller, M.; Glauser, T.; Hedrick, J. L. *Angewandte Chemie International Edition* **2001**, *40*, 2712.
- (38) Nederberg, F.; Connor, E. F.; Glauser, T.; Hedrick, J. L. *Chemical Communications* **2001**, 2066.
- (39) Morinaga, H.; Ochiai, B.; Mori, H.; Endo, T. *Journal of Polymer Science Part A: Polymer Chemistry* **2006**, *44*, 1985.
- (40) Morinaga, H.; Ochiai, B.; Endo, T. *Journal of Polymer Science Part A: Polymer Chemistry* **2006**, *44*, 6633.
- (41) Dubois, P.; Coulembier, O.; Raquez, J.-M. *Handbook of Ring-Opening Polymerization*; Wiley-VCH: Weinheim, 2009.
- (42) Lohmeijer, B. G. G.; Pratt, R. C.; Leibfarth, F.; Logan, J. W.; Long, D. A.; Dove, A. P.; Nederberg, F.; Choi, J.; Wade, C.; Waymouth, R. M.; Hedrick, J. L. *Macromolecules* **2006**, *39*, 8574.
-

-
- (43) Nederberg, F.; Lohmeijer, B. G. G.; Leibfarth, F.; Pratt, R. C.; Choi, J.; Dove, A. P.; Waymouth, R. M.; Hedrick, J. L. *Biomacromolecules* **2006**, *8*, 153.
- (44) Bourissou, D.; Martin-Vaca, B.; Dumitrescu, A.; Graullier, M.; Lacombe, F. *Macromolecules* **2005**, *38*, 9993.
- (45) Sanda, F.; Sanada, H.; Shibasaki, Y.; Endo, T. *Macromolecules* **2001**, *35*, 680.
- (46) Casas, J.; Persson, P. V.; Iversen, T.; Córdova, A. *Advanced Synthesis & Catalysis* **2004**, *346*, 1087.
- (47) Persson, P. V.; Schröder, J.; Wickholm, K.; Hedenström, E.; Iversen, T. *Macromolecules* **2004**, *37*, 5889.
- (48) Liu, J.; Liu, L. *Macromolecules* **2004**, *37*, 2674.
- (49) Albertson, A.-C.; Sjoling, M. *Journal of Macromolecular Science, Part A* **1992**, *29*, 43.
- (50) Ariga, T.; Takata, T.; Endo, T. *Macromolecules* **1997**, *30*, 737.
- (51) Movassaghi, M.; Schmidt, M. A. *Organic Letters* **2005**, *7*, 2453.
- (52) Lai, C.-L.; Lee, H. M.; Hu, C.-H. *Tetrahedron Letters* **2005**, *46*, 6265.
- (53) Culkin, D. A.; Jeong, W.; Csihony, S.; Gomez, E. D.; Balsara, N. P.; Hedrick, J. L.; Waymouth, R. M. *Angewandte Chemie International Edition* **2007**, *46*, 2627.
- (54) Numata, K.; Srivastava, R. K.; Finne-Wistrand, A.; Albertsson, A.-C.; Doi, Y.; Abe, H. *Biomacromolecules* **2007**, *8*, 3115.
- (55) Matsumura, S.; Mabuchi, K.; Toshima, K. *Macromolecular Rapid Communications* **1997**, *18*, 477.
- (56) Gross, R. A.; Kumar, A.; Kalra, B. *Chemical Reviews* **2001**, *101*, 2097.
- (57) Kumar, R.; Gao, W.; Gross, R. A. *Macromolecules* **2002**, *35*, 6835.
- (58) Fiore, G. L.; Jing, F.; Young, J. V. G.; Cramer, C. J.; Hillmyer, M. A. *Polymer Chemistry* **2010**, *1*, 870.
- (59) Yin, M.; Baker, G. L. *Macromolecules* **1999**, *32*, 7711.
- (60) Simmons, T. L.; Baker, G. L. *Biomacromolecules* **2001**, *2*, 658.
- (61) Gerhardt, W. W.; Noga, D. E.; Hardcastle, K. I.; García, A. J.; Collard, D. M.; Weck, M. *Biomacromolecules* **2006**, *7*, 1735.
- (62) Jing, F.; Hillmyer, M. A. *Journal of the American Chemical Society* **2008**, *130*, 13826.
- (63) Kricheldorf, H.; Jonté, J. M. *Polymer Bulletin* **1983**, *9*, 276.
- (64) Thillaye du Boullay, O.; Marchal, E.; Martin-Vaca, B.; Cossío, F. P.; Bourissou, D. *Journal of the American Chemical Society* **2006**, *128*, 16442.
- (65) Thillaye du Boullay, O.; Bonduelle, C.; Martin-Vaca, B.; Bourissou, D. *Chemical Communications* **2008**, 1786.
-

-
- (66) Dibenedetto, A.; Aresta, M.; Giannoccaro, P.; Pastore, C.; Pápai, I.; Schubert, G. *European Journal of Inorganic Chemistry* **2006**, 2006, 908.
- (67) Bonduelle, C.; Martín-Vaca, B.; Cossío, F. P.; Bourissou, D. *Chemistry – A European Journal* **2008**, 14, 5304.
- (68) Yin, Q.; Tong, R.; Xu, Y.; Baek, K.; Dobrucki, L. W.; Fan, T. M.; Cheng, J. *Biomacromolecules* **2013**, 14, 920.
- (69) Xie, Z.; Lu, C.; Chen, X.; Chen, L.; Wang, Y.; Hu, X.; Shi, Q.; Jing, X. *Journal of Polymer Science Part A: Polymer Chemistry* **2007**, 45, 1737.
- (70) Parzuchowski, P. G.; Jaroch, M.; Tryznowski, M.; Rokicki, G. *Macromolecules* **2008**, 41, 3859.
- (71) He, F.; Wang, Y.-P.; Liu, G.; Jia, H.-L.; Feng, J.; Zhuo, R.-X. *Polymer* **2008**, 49, 1185.
- (72) Chen, W.; Yang, H.; Wang, R.; Cheng, R.; Meng, F.; Wei, W.; Zhong, Z. *Macromolecules* **2009**, 43, 201.
- (73) Miyagawa, T.; Shimizu, M.; Sanda, F.; Endo, T. *Macromolecules* **2005**, 38, 7944.
- (74) Tempelaar, S.; Mespouille, L.; Coulembier, O.; Dubois, P.; Dove, A. P. *Chemical Society Reviews* **2013**, 42, 1312.
- (75) Ihre, H.; Hult, A.; Fréchet, J. M. J.; Gitsov, I. *Macromolecules* **1998**, 31, 4061.
- (76) Early, n.; Kuran, W. *J. Macromol. Sci., Rev. Macromol. Chem.* **1981**, C21, 135.
- (77) Weilandt, K. D.; Keul, H.; Höcker, H. *Macromolecular Chemistry and Physics* **1996**, 197, 3851.
- (78) Pratt, R. C.; Nederberg, F.; Waymouth, R. M.; Hedrick, J. L. *Chemical Communications* **2008**, 114.
- (79) Sanders, D. P.; Fukushima, K.; Coady, D. J.; Nelson, A.; Fujiwara, M.; Yasumoto, M.; Hedrick, J. L. *Journal of the American Chemical Society* **2010**, 132, 14724.
- (80) Darensbourg, D. J.; Holtcamp, M. W.; Reibenspies, J. H. *Polyhedron* **1996**, 15, 2341.
- (81) Venkataraman, S.; Veronica, N.; Voo, Z. X.; Hedrick, J. L.; Yang, Y. Y. *Polymer Chemistry* **2013**, 4, 2945.
- (82) Pounder, R. J., University of Warwick, 2010.
- (83) Neises, B.; Steglich, W. *Angewandte Chemie International Edition in English* **1978**, 17, 522.
- (84) Katakai, R.; Iizuka, Y. *The Journal of Organic Chemistry* **1985**, 50, 715.
- (85) Du Boullay, O. T.; Marchal, E.; Martín-Vaca, B.; Cossío, F. P.; Bourissou, D. *J. Am. Chem. Soc.* **2006**, 128, 16442.
-

-
- (86) Pounder, R. J.; Fox, D. J.; Barker, I. A.; Bennison, M. J.; Dove, A. P. *Polymer Chemistry* **2011**, *2*, 2204.
- (87) Seebach, D.; Naef, R.; Calderari, G. *Tetrahedron* **1984**, *40*, 1313.
- (88) Suriano, F.; Pratt, R.; Tan, J. P. K.; Wiradharma, N.; Nelson, A.; Yang, Y.-Y.; Dubois, P.; Hedrick, J. L. *Biomaterials* **2010**, *31*, 2637.
- (89) Sanda, F.; Kamatani, J.; Endo, T. *Macromolecules* **2001**, *34*, 1564.
- (90) Hu, X.; Chen, X.; Xie, Z.; Cheng, H.; Jing, X. *Journal of Polymer Science Part A: Polymer Chemistry* **2008**, *46*, 7022.
- (91) Nederberg, F.; Trang, V.; Pratt, R. C.; Kim, S.-H.; Colson, J.; Nelson, A.; Frank, C. W.; Hedrick, J. L.; Dubois, P.; Mespouille, L. *Soft Matter* **2010**, *6*, 2006.
- (92) Zhang, X.; Cai, M.; Zhong, Z.; Zhuo, R. *Macromolecular Rapid Communications* **2012**, *33*, 693.
- (93) Wang, H.-F.; Su, W.; Zhang, C.; Luo, X.-h.; Feng, J. *Biomacromolecules* **2010**, *11*, 2550.
- (94) Todd, R.; Rubio, G.; Hall, D. J.; Tempelaar, S.; Dove, A. P. *Chemical Science* **2013**, *4*, 1092.
- (95) McLaren, K. L. *The Journal of Organic Chemistry* **1995**, *60*, 6082.
- (96) Bruckner, R. *Organic Mechanisms: Reactions, Stereochemistry and Synthesis*; Springer-Verlag: Berlin Heidelberg, 2010.
- (97) Delcroix, D.; Martín-Vaca, B.; Bourissou, D.; Navarro, C. *Macromolecules* **2010**, *43*, 8828.
- (98) Campos, J. M.; Ribeiro, M. R.; Ribeiro, M. F.; Deffieux, A.; Peruch, F. *Macromolecular Chemistry and Physics* **2013**, *214*, 85.
- (99) He, Y.; Keul, H.; Möller, M. *Reactive and Functional Polymers* **2011**, *71*, 175.
- (100) Cañamero, P. F.; de la Fuente, J. L.; Madruga, E. L.; Fernández-García, M. *Macromolecular Chemistry and Physics* **2004**, *205*, 2221.
- (101) Mangold, C.; Wurm, F.; Frey, H. *Polymer Chemistry* **2012**, *3*, 1714.
- (102) Darensbourg, D. J. *Chemical Reviews* **2007**, *107*, 2388.
- (103) Coates, G. W.; Moore, D. R. *Angewandte Chemie International Edition* **2004**, *43*, 6618.
- (104) Riva, R.; Lenoir, S.; Jérôme, R.; Lecomte, P. *Polymer* **2005**, *46*, 8511.
- (105) Michalak, M.; Kawalec, M.; Kurcok, P. *Polymer Degradation and Stability* **2012**, *97*, 1861.
- (106) Zhou, J.; Wang, W.; Villarroya, S.; Thurecht, K. J.; Howdle, S. M. *Chemical Communications* **2008**, 5806.
-

-
- (107) Burfield, D. R.; Gan, S.-n.; Smithers, R. H. *Journal of the Chemical Society, Perkin Transactions 1* **1977**, 666.
- (108) Tong, K.; Tu, J.; Qi, X.; Wang, M.; Wang, Y.; Fu, H.; Pittman Jr, C. U.; Zhou, A. *Tetrahedron* **2013**, *69*, 2369.
- (109) Chakraborti, A. K.; Kondaskar, A. *Tetrahedron Letters* **2003**, *44*, 8315.
- (110) Placzek, A. T.; Donelson, J. L.; Trivedi, R.; Gibbs, R. A.; De, S. K. *Tetrahedron Letters* **2005**, *46*, 9029.
- (111) Fujiwara, M.; Imada, M.; Bab, A.; Matsuda, H. *Tetrahedron Letters* **1989**, *30*, 739.
- (112) Bhanushali, M. J.; Nandurkar, N. S.; Bhor, M. D.; Bhanage, B. M. *Tetrahedron Letters* **2008**, *49*, 3672.
- (113) Fu, X.-L.; Wu, S.-H. *Synthetic Communications* **1997**, *27*, 1677.
- (114) Kamal, A.; Ramu, R.; Azhar, M. A.; Khanna, G. B. R. *Tetrahedron Letters* **2005**, *46*, 2675.
- (115) Cepanec, I.; Litvić, M.; Mikuldaš, H.; Bartolinčić, A.; Vinković, V. *Tetrahedron* **2003**, *59*, 2435.
- (116) Chakraborti, Asit K.; Rudrawar, S.; Kondaskar, A. *European Journal of Organic Chemistry* **2004**, *2004*, 3597.
- (117) Tundo, P.; Rossi, L.; Loris, A. *The Journal of Organic Chemistry* **2005**, *70*, 2219.
- (118) De Faveri, G.; Ilyashenko, G.; Watkinson, M. *Chemical Society Reviews* **2011**, *40*, 1722.
- (119) Still, W. C.; Kahn, M.; Mitra, A. *The Journal of Organic Chemistry* **1978**, *43*, 2923.
- (120) Denmark, S. E.; Yang, S.-M. *J. Am. Chem. Soc.* **2004**, *126*, 12432.
- (121) Degerbeck, F.; Fransson, B.; Grehn, L.; Ragnarsson, U. *Journal of the Chemical Society, Perkin Transactions 1* **1993**, *0*, 11.
- (122) Chen, C.-T.; Weng, S.-S.; Kao, J.-Q.; Lin, C.-C.; Jan, M.-D. *Organic Letters* **2005**, *7*, 3343.
- (123) Lizarzaburu, M. E.; Jones, R. M.; Nantz, M. H.; Kurth, M. J. *Organic Preparations and Procedures International* **1999**, *31*, 440.
-